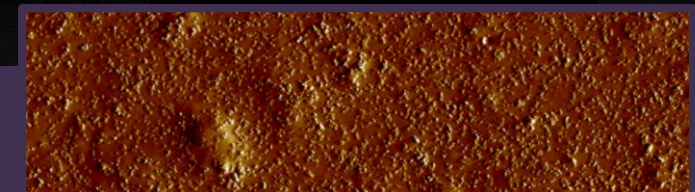# Alternatives to insecticides:
Bio-inspired coatings and sprays to tackle insect pests

Aurélie Féat

Aurélie Féat

Propositions

1. Poorly durable coatings can be used as insect-repellent solutions in buildings.
   (this thesis)

2. Emulsions based on linseed oil reduce insect damage to leaves.
   (this thesis)

3. Integrated pest management, use of genetically modified crops and meat consumption reduction will help decrease crop loss to address global food demand.

4. The development of fully eco-friendly paints is hindered by the cost-ineffectiveness of bio-based binders.

5. Hearing about climate change too frequently can lead to environmental numbness.
   (R. Gifford, Am. Psychol., 2011, 66(4):290-302)

6. To effectively reduce CO_2 emissions, governments should ban short haul flights, tax aviation fuel and introduce a rationing system for passengers.

7. The gender gap in all STEM (Science, Technology, Engineering and Math) careers is unlikely to be filled not only due to cultural barriers and stereotypes, but also as women tend to be more people-oriented.

8. The resilience in the face of failure among PhD candidates could be increased through video games.

Propositions belonging to the thesis entitled:

Alternatives to insecticides:
Bio-inspired coatings and sprays to tackle insect pests
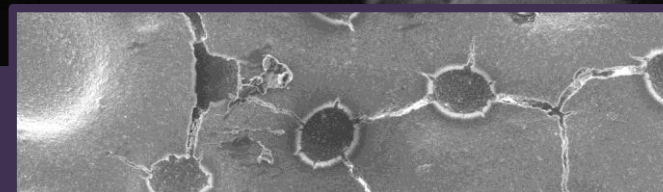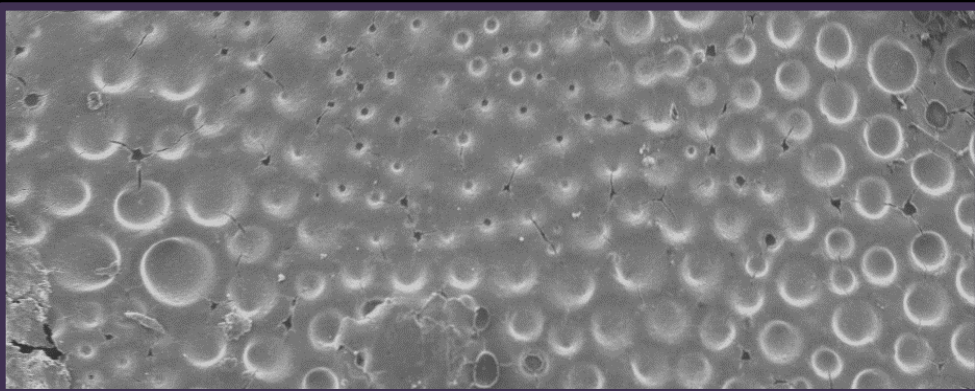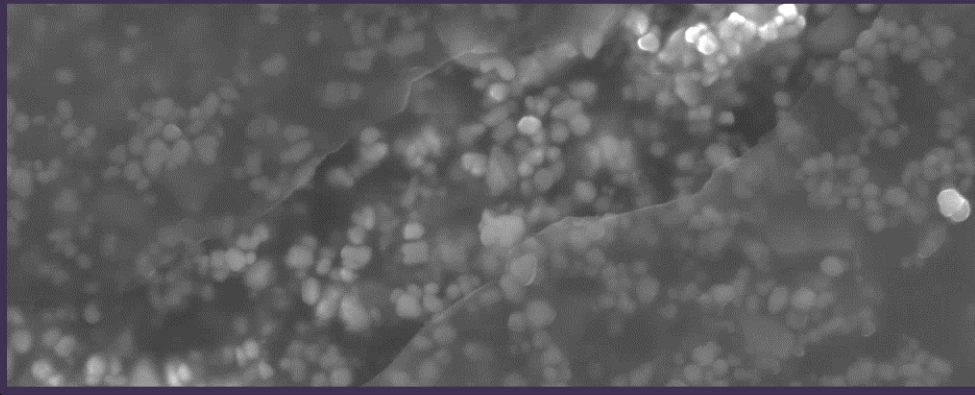
Aurélie Féat

Wageningen, 7th October 2019

Alternatives to insecticides:

Bio-inspired coatings and sprays to tackle insect pests

Aurélie Féat

Alternatives to insecticides:

Bio-inspired coatings and sprays to tackle insect pests

Aurélie Féat

Thesis

submitted in fulfilment of the requirements for the degree of doctor

at Wageningen University

by the authority of the Rector Magnificus,

Prof. Dr. A. P. J. Mol,

in the presence of the

Thesis Committee appointed by the Academic Board

to be defended in public

on Monday 7 October 2019

at 1.30 P.M. in the Aula.

Contents

5   Slippery paints: how tuning polymer and pigment size can prevent ants from walking on walls   **127**

6   Linseed oil-based emulsions to protect plants against thrips   **157**

7   General discussion   **185**

1

General introduction

1.1   Motivation

In this thesis, we describe bio-inspired pest control measures to tackle insect pests in agriculture (emulsion sprays which protect crops against *Frankliniella occidentalis* thrips) and in buildings (paints slippery to *Atta cephalotes* leaf-cutting ants) (Figure 1.1).

To date, only 20% of insect species have been discovered, accounting for about one million species [1]. Many insects are beneficial to ecosystems as crop pollinators, seed dispersers, shredders and antagonists in biological pest control [2–5]. Insects present a strong potential to sustain food demands in the next future [6]. They are used in the food, dying and textile industries (e.g. meal, cochineal and silk) [7].

However, insects can also have adverse effects. Insect pests in agriculture need to be controlled to avoid crop diseases or damage as they harm or contaminate crops either in the field or during storage [8, 9]. Common storage insect pests include moths, mites, cockroaches and beetles. Worldwide, about 14% of crops are lost to insect pests [10–12].

Insects, most notably termites, cockroaches and ants, are detrimental to buildings, furniture, can cause visual discomfort or affect hygiene and human health [13, 14]. Termites, despite being of ecological importance [15–17], cause serious damage to homes, building materials, dams and

Slippery to insects   Sticky to insects

Figure 1.1: Strategies employed in this thesis as alternatives to insecticides: paints slippery to insects (**Chapters 3-5**) and crop protective emulsion sprays which are sticky to insects (**Chapter 6**).

so forth, sometimes leading to villagers abandoning their homes. Termite damage was estimated to be between \$2-\$40 billion p.a. [18–20]. Moreover, ants enter buildings in search of food or can cause structural damage as they establish their nests close to heat sources [21, 22].

Given these issues, the need to eliminate insect pests becomes clear. Pest control methods are used to reduce the presence of insects, and mainly consist in insecticides. Most insecticides are composed of neuroactive chemicals, such as chlorinated hydrocarbons (e.g. DDT), organophosphates or carbamates and present human health and environment issues [23]. Every year, the use of pesticides, including insecticides, leads to 26 million cases of non-fatal poisonings, of which 3 million cases are hospitalised and cause approximately 220 000 deaths [24–26].

Insecticides may harm, or even kill non-target organisms (such as organisms that recycle soil nutrients, pollinate crops, and prey on pest species) and reduce and/or contaminate food supplies for animals which feed on them (higher trophic levels) [27]. Reduction of pollination also occurs due to honeybee colony loss [24]. Many pests have responded to insecticides by developing resistance mechanisms based on mutations in insecticide target sites or detoxification

processes [28–30].

This underlines the need for more efficient, eco-friendlier and, where possible, more selective pest control methods (**Chapter 2**). Alternatives to "traditional" insecticides include, but are not limited to: (1) in the building and coating industries: plant-based insect-repellent coatings [31], slippery surfaces [32–34]; (2) in agriculture, biological control, where an insect pest population is reduced by introducing its antagonists in the area [5]; and the use of inert materials (particle film technology) [35, 36]. The slippery and particle films are repellent to insects in a purely mechanical way, inert materials leading to their death by dehydration after contact of particles with their pads.

Other methods of interest could find their source in nature: plants are deterrent to herbivores by chemical (e.g. feeding inhibitors or toxins) and physical means (spines, sticky trichomes, waxy surfaces) [3, 7, 37]. Surfaces inspired from the inner walls of pitcher plants demonstrate great anti-adhesive properties to many biological objects, including insects [38]. We first describe how emulsion sprays and paints and coatings can be prepared to be used as bio-inspired alternatives to insecticides in agriculture and buildings, respectively.

1.2   Paints and Coatings

Coatings are materials, generally prepared from liquids, which form a film after drying or curing once applied to substrates. They are used in a wide range of applications for their decorative, protective and/or functional purposes [39]. These properties are typically associated with specific parts of a coating system (Figure 1.2). The global market for coatings was valued at about $29 billion in 2018 [40]. Paints are composed of four major ingredients:

- The solvent,

- The polymer binder,

- The pigment, and,

- The additives.

The solvent, or carrier, allows the coating to be applied on a substrate and then evaporates. Because of emission of volatile organic compounds (VOCs) in the atmosphere, the amount of solvent should be limited, by either formulating high solids paints (low-solvent), eliminating solvents completely (solvent-free technology), or replacing it with water (waterborne) [41, 42].
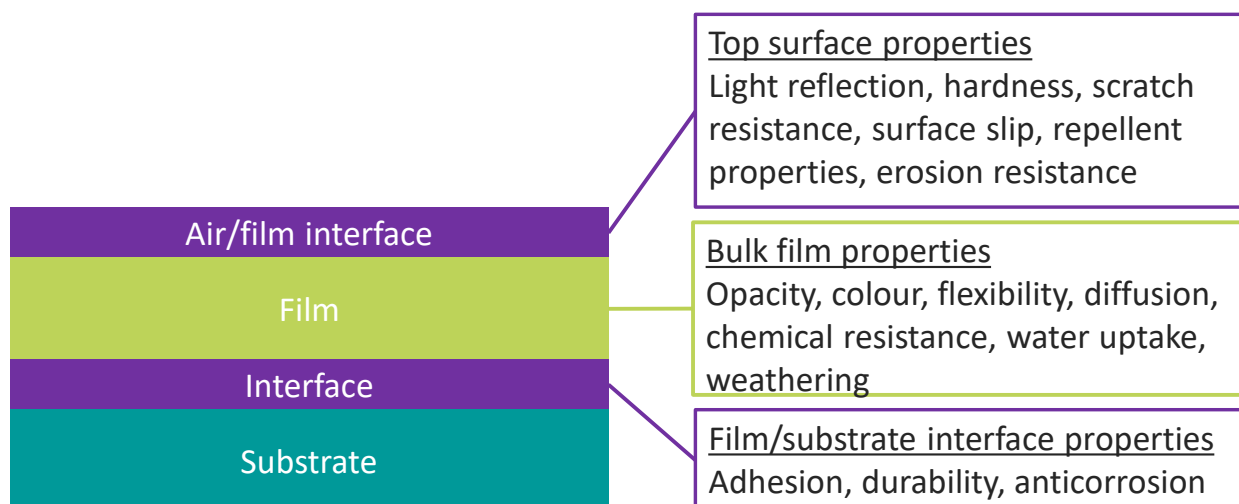
Figure 1.2: Topological classification of coating properties (reproduced from [39]).

The binders (also called resins or simply, polymers) used in waterborne coatings are generally emulsion polymers, or latexes. They are dispersions of small spherical particles sized between 50 to 1000 nm [43]. The film forming properties of a latex are essential to form a homogeneous coating. The film formation process has been widely studied (see e.g. [44]) and can be briefly described in the following three stages after application on a substrate: (1) the solvent evaporates, which brings the latex particles into close contact; (2) a very close packing is obtained as the particles are deformed by capillary forces; and (3) particles form a polyhedron-shaped network and the particle boundaries are lost by particle-particle coalescence. The last stage is only achieved if the drying temperature is above the latex minimum film formation temperature (MFFT).

The film formation process can be aided by adding coalescing agents, usually organic solvents with high boiling points (e.g. ethylene glycol derivatives). They act as plasticisers to lower the polymer's MFFT as well as the glass transition temperature (T_g) and aid the polymer diffusion across particle-particle interfaces in the film. Properties, such as adhesion or mechanical rigidity and strength, are determined by the appropriate selection of the polymer(s), e.g. acrylics or polyurethanes [41, 43].

The pigments (and extenders, to a lesser extent) provide opacity and colour to the film. Despite its high carbon footprint, the most widely used pigment remains titanium dioxide; more than 6 million tons were produced in 2016 [45]. Extender (or fillers), such as calcium carbonate or silica, improve the spacing of pigment particles to improve the opacity of a paint

film [46]. They can give extra properties to the paint coating, such as flame retardancy, and also affect the mechanical properties [43]. Minor paint components are called additives and are present in a small amount (generally less than 1%). Common additives are pigment dispersants, defoamers and biocides and these are typically used to improve the paint stability, drying or adhesion properties [41].

A key parameter of a paint formulation is the volume ratio between the binder, pigments and extenders, stated as the Pigment Volume Concentration (PVC):

$$PVC = \frac{Volume\ of\ pigments}{Volume\ of\ pigments + volume\ of\ binder} \tag{1.1}$$

The paints properties dramatically change at a point called the critical PVC (CPVC), above which there isn't sufficient binder to fill the voids between solid particles [47]. Below CPVC, coatings have high gloss, low porosity, low dirt pick-up, high elongation-to-break, are flexible and have low water permeability [43]. Above CPVC they display low gloss, high porosity, high dirt-pick-up, low elongation-to-break, are brittle and have high water permeability [43].

Waterborne paints are easy to apply on large areas, are cheap, durable and non-toxic, and are hence good candidates for insect-repellency purposes. The working mechanism of existing insect-repellent surfaces are based on insecticides, essential oils, lubricants or topography [31, 34, 38, 48]. They either pose regeneration, lack of efficiency, scaling-up or cost issues. We investigate in **Chapters 3-5** the use of coatings which are slippery to leaf-cutting ants (*A. cephalotes*) and which can be applied to buildings to protect them against insect pests. They are directly inspired from the inner wall surfaces of pitcher plants [49]. To reduce the use of insecticides in agriculture, we also investigated novel oil-in-water emulsions to protect crops from insect pests.

1.3 Emulsions in crop protection

Emulsions are metastable colloidal systems prepared by dispersing one fluid into an immiscible second fluid [50]. They are typically biphasic systems: oil-in-water (o/w), *i.e.* the continuous phase is water, or water-in-oil (w/o) if the oil, or hydrophobic fluid, is the continuous phase (Figure 1.3). Emulsions are ubiquitous as they are present in cosmetics, bitumen, food, medicines, etc. The use of stabilisers (e.g. emulsifiers or texture modifiers) improves the stability of

emulsions. Emulsifiers are amphiphilic surfactants which form a stabilising layer around the dispersed droplets to prevent them from aggregating. In case of poor stabilisation, emulsions are subject to different mechanisms of instability, such as droplet flocculation, aggregation, coalescence, Ostwald ripening, as well as phase separation (creaming or sedimentation) or phase inversion [50].

Sprays of petroleum oil-based emulsions have long been used in pest control as alternatives to traditional insecticides [51]. The oil and water phases are violently mixed in the absence of stabiliser, producing an emulsion that exhibits fast phase-breaking upon spraying on the plant. Damages to plants have often been observed, such as leaf tissue death, leaf dropping or damage to wood and fruits with oils rich in unsaturated hydrocarbons [51]. Environmental concerns resulted in a growing demand for emulsions based on vegetable oils as they offer a renewable feedstock [52, 53]. Besides being more toxic to insects, the high fatty acid content of vegetable oils is also less detrimental to plants than petroleum-based sprays [51]. Botanical oil sprays also show some repellency but for short periods of time, requiring frequent applications [54].

Plant surfaces made sticky using vegetable oil beads which could retain insects might present better alternatives to petroleum sprays by reducing environmental impact and providing better efficiency. In **Chapter 6**, we describe sprays of linseed oil-in-water emulsions which, once applied on surfaces, form beads which are sticky to thrips. The concept is bio-inspired from the adhesive trichomes present at the surface of plants. This also avoids the issue of improving chemical resistance by insect pests.
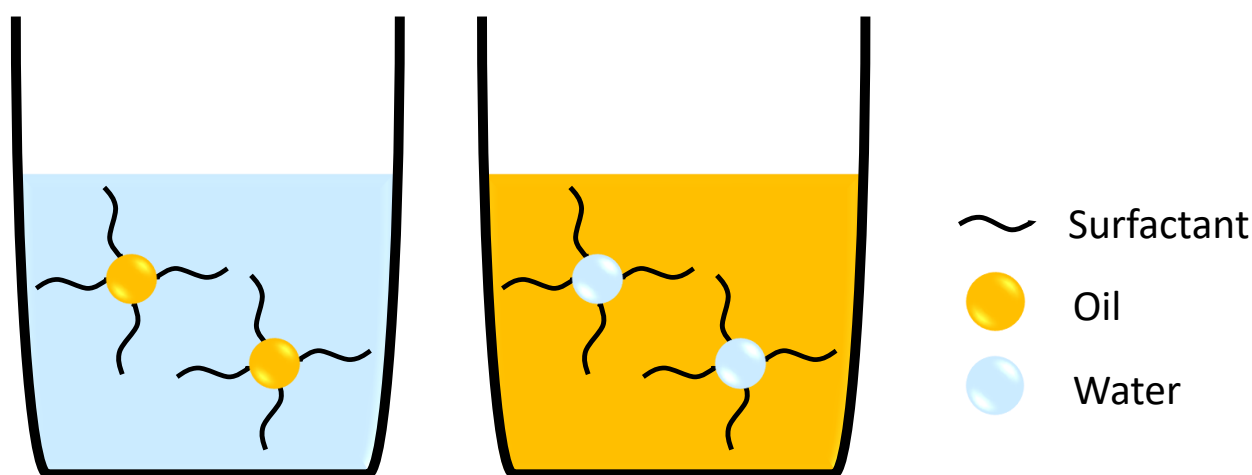
Figure 1.3: Schematic oil-in-water and water-in-oil emulsions (not drawn to scale).

1.4 Outline

This thesis explores eco-friendly pest control measures to tackle insect pests in buildings and agriculture. We address the following questions: what formulating parameters are important to produce (1) wall paints slippery to *A. cephalotes* ants? (**Chapters 2-5**); and (2) spray emulsions sticky to *F. occidentalis* thrips on plants? (**Chapter 6**).

Chapter 2 summarises the wide literature describing issues brought by insect pests and the use of insecticides to tackle them (health and environment, agriculture). Special emphasis is given to coatings solutions as alternatives to traditional insecticides. This serves as an introduction to other chapters, especially to **Chapters 3-5**.

In **Chapter 3**, we investigate how paint coatings can be rendered slippery to insects (*A. cephalotes* ants). We find that coatings can be formulated such that pigment particles transfer from the coating to the adhesive pads of insects. The process is based upon using the right balance of polymer and pigment. We also show that once the loose particles are removed from the coating, the increased coating roughness then reduces insect adhesion, similarly to the inner wall surface of the carnivorous plant *Nepenthes alata* [49].

In **Chapter 4**, we study the feasibility of JKR-type adhesion experiments using PDMS lenses to measure the particle transfer properties of the coatings as a potential replacement test for the insect climbing experiments. We do not reach our goal completely. However, we open the way for future research to use this test in adhesion experiments when the use of AFM (mechanical analysis) is not possible.

In **Chapter 5**, we optimise the anti-adhesive properties of the paints described in **Chapter 3** by tuning the polymer binder size and the pigment diameter. We report that porous paints allow absorption of the adhesive fluid of insects [55] and that pigments sized between 1 μm and 10 μm are more efficient at impeding *A. cephalotes* locomotion, hence improving the anti-adhesive properties of the paints.

Chapter 6 explores the use of sprayable linseed oil-in-water emulsions as an alternative to insecticides used in agriculture. We show that when sufficiently crosslinked, the linseed oil forms sticky beads, to which insects (*F. occidentalis* thrips) stick, immobilising them and hence preventing them from producing further damage to leaves.

In **Chapter 7**, the final chapter of this thesis, we reflect on the previous chapters and

discuss the further work that can be done to improve the alternatives to insecticides described in **Chapters 3**, **5** and **6**. Ultimately, it provides useful formulation guidelines to improve the paints and spray emulsions discussed in other chapters.

References

[1] Stork, N. E. (2018) How Many Species of Insects and Other Terrestrial Arthropods Are There on Earth?. *Annu. Rev. Entomol.,* **63**(1), 31–45.

[2] Free, J. (1993) Insect pollination of crops., Academic Press, London, UK.

[3] Whitney, H. M. and Federle, W. (2013) Biomechanics of plant-insect interactions. *Curr. Opin. Plant Biol.,* **16**(1), 105–111.

[4] Graça, M. A. (2001) The Role of Invertebrates on Leaf Litter Decomposition in Streams - a Review. *Int. Rev. Hydrobiol.,* **86**(4-5), 383–393.

[5] DeBach, P. (1964) Biological control of insect pests and weeds, Chapman & Hall, London, UK.

[6] Yen, A. L. (2009) Edible insects: Traditional knowledge or western phobia?. *Entomol. Res.,* **39**(5), 289–298.

[7] Loxdale, H. D. (2016) Insect science - a vulnerable discipline?. *Entomol. Exp. Appl.,* **159**(2), 121–134.

[8] Hill, D. S. (2008) Pest damage to crop plants, Springer, Dordrecht.

[9] Sallam, M. N. Insect Damage: Post-harvest Operations. `http://www.fao.org/in-action/inpho/crop-compendium/pests/en/` (1999) (accessed 27.07.2018).

[10] Oerke, E.-C. (2006) Crop losses to pests. *J. Agric. Sci.,* **144**, 31–43.

[11] Cramer, H. H. (1967) Plant protection and world crop production, Bayer, Leverkusen.

[12] Dhaliwal, G. S., Jindal, V., and Dhawan, A. K. (2010) Insect pest problems and crop losses: changing trends. *Indian J. Ecol.,* **37**(1), 1–7.

[13] Lee, C. Y. (2002) Tropical household ants: pest status, species diversity, foraging behavior and baiting studies. *Proc. Fourth Int. Conf. Urban Pests,* pp. 3–18.

[14] Bonnefoy, X., Kampen, H., and Sweene, K. (2008) Public health significance of urban pests, World Health Organization, Copenhagen.

[15] Donovan, S. E., Eggleton, P., Dubbin, W. E., Batchelder, M., and Dibog, L. (2001) The effect of a soil-feeding termite, *Cubitermes fungifaber* (Isoptera: Termitidae) on soil properties: termites may be an important source of soil microhabitat heterogeneity in tropical forests. *Pedobiologia,* **45**(1), 1–11.

[16] Black, H. and Okwakol, M. (1997) Agricultural intensification, soil biodiversity and agroecosystem function in the tropics: the role of termites. *Appl. Soil Ecol.,* **6**(1), 37–53.

[17] Dawes, T. Z. (2010) Reestablishment of ecological functioning by mulching and termite invasion in a degraded soil in an Australian savanna. *Soil Biol. Biochem.,* **42**(10), 1825–1834.

[18] Su, N.-Y. and Scheffrahn, R. H. (2000) Termites as Pests of Buildings, Springer Netherlands, Dordrecht.

[19] Mahapatro, G. K. and Chatterjee, D. (2018) Termites as Structural Pest: Status in Indian Scenario. *Proc. Natl. Acad. Sci. India Sect. B Biol. Sci.,* **88**(3), 977–994.

[20] Ghaly, A. and Edwards, S. (2011) Termite Damage to Buildings: Nature of Attacks and Preventive Construction Methods. *Am. J. Eng. Appl. Sci.,* **4**(2), 187–200.

[21] Birkemoe, T. (2002) Structural infestations of ants (Hymenoptera, Formicidae) in southern Norway. **49**(2), 139–142.

[22] Oi, D. H., Vail, K. M., Williams, D. F., and Bieman, D. N. (1994) Indoor and Outdoor Foraging Locations of Pharaoh Ants (Hymenoptera: Formicidae) and Control Strategies Using Bait Stations. *Florida Entomol.,* **77**(1), 85.

[23] Casida, J. E. and Quistad, G. B. (1998) Golden age of insecticide research: past, present, or future?. *Annu. Rev. Entomol.,* **43**(1), 1–16.

[24] Pimentel, D. (2005) Environmental and economic costs of the application of pesticides primarily in the United States. *Environ. Dev. Sustain.,* **7**(2), 229–252.

[25] Richter, E. (2002) Acute human pesticide poisonings, Dekker, New York.

[26] Jeyaratnam, J. (1990) Acute Pesticide Poisoning: a Major Global Health Problem. *World Heal. Stat Q.,* **43**(3), 139–144.

[27] Devine, G. J. and Furlong, M. J. (2007) Insecticide use: Contexts and ecological consequences. *Agric. Human Values,* **24**(3), 281–306.

[28] Freebairn, K., Yen, J. L., and McKenzie, J. A. (1996) Environmental and genetic effects on the asymmetry pnenotype: Diazinon resistance in the Australian sheep blowfly, *Lucilia cuprina. Genetics,* **144**(1), 229–239.

[29] Foster, S. P., Tomiczek, M., Thompson, R., Denholm, I., Poppy, G., Kraaijeveld, A. R., and Powell, W. (2007) Behavioural side-effects of insecticide resistance in aphids increase their vulnerability to parasitoid attack. *Anim. Behav.,* **74**(3), 621–632.

[30] Sparks, T. C. and Nauen, R. (2015) IRAC: Mode of action classification and insecticide resistance management. *Pestic. Biochem. Physiol.,* **121**, 122–128.

[31] Overman, G. R. Method for admixing plant essential oils to coatings for the purpose of repelling insects. (2009) US Patent 20090155394.

[32] Chen, J. (2007) Advancement on techniques for the separation and maintenance of the red imported fire ant colonies. *Insect Sci.,* **14**(1), 1–4.

[33] Zhou, Y. (2015) Insect adhesion on rough surfaces and properties of insect repellent surfaces (PhD thesis), University of Cambridge, Cambridge.

[34] Graf, C., Kesel, A. B., Gorb, E. V., Gorb, S. N., and Dirks, J.-H. H. (2018) Investigating the efficiency of a bio-inspired insect repellent surface structure. *Bioinspir. Biomim.,* **13**(5), 56010.

[35] Boiteau, G., Pelletier, Y., Misener, G. C., and Bernard, G. (1994) Development and Evaluation of a Plastic Trench Barrier for Protection of Potato from Walking Adult Colorado Potato Beetles (Coleoptera: Chrysomelidae). *J. Econ. Entomol.,* **87**(5), 1325–1331.

[36] Glenn, D. M. and Puterka, G. J. (2010) Particle films: a new technology for agriculture, Vol. 31, John Wiley & Sons, Inc., .

[37] Barthlott, W., Mail, M., Bhushan, B., and Koch, K. (2017) Plant Surfaces: Structures and Functions for Biomimetic Innovations. *Nano-Micro Lett.,* **9**(2), 23.

[38] Wong, T.-S., Kang, S. H., Tang, S. K. Y., Smythe, E. J., Hatton, B. D., Grinthal, A., and Aizenberg, J. (2011) Bioinspired self-repairing slippery surfaces with pressure-stable omniphobicity. *Nature,* **477**(7365), 443–447.

[39] Ghosh, S. K. (2006) Functional Coatings and Microencapsulation: A General Perspective, Wiley-VCH Verlag GmbH & Co. KGaA, Weinheim, FRG.

[40] Research and Markets Coating Resins Market by Resin Type (Acrylic, Alkyd, Polyurethane, Vinyl, Epoxy), Technology (Waterborne, Solventborne, Powder, High Solids), Application (Architectural, General Industrial, Automotive), and Region - Global Forecast to 2023. (2019).

[41] Scholz, W. (1993) Paint Additives, Springer Science+Business Media, Dordrecht.

[42] Hansen, M. K., Larsen, M., and Cohr, K.-H. (1987) Waterborne paints: A review of their chemistry and toxicology and the results of determinations made during their use. *Scand. J. Work. Environ. Health,* **13**(6), 473–485.

[43] Otterstedt, J.-E. and Brandreth, D. A. (1998) Various applications of small particles, Springer US, New York.

[44] Keddie, J. L. (1997) Film formation of latex. *Mater. Sci. Eng. R Reports,* **21**(3), 101–170.

[45] Research and Markets Titanium Dioxide (TiO$_2$) - A Global Market Overview. (2016).

[46] Dietz, P. F. (2003) Spacing for better effects. *Eur. Coatings J.,* **49**, 14–20.

[47] Asbeck, W. K. and Loo, M. V. (1949) Critical Pigment Volume Relationships.. *Ind. Eng. Chem.,* **41**(7), 1470–1475.

[48] Mosqueira, B., Chabi, J., Chandre, F., Akogbeto, M., Hougard, J.-M., Carnevale, P., and Mas-Coma, S. (2010) Efficacy of an insecticide paint against malaria vectors and nuisance in West Africa - Part 2: Field evaluation. *Malar. J.,* **9**(1), 341.

[49] Gorb, E., Haas, K., Henrich, A., Enders, S., Barbakadze, N., and Gorb, S. (2005) Composite structure of the crystalline epicuticular wax layer of the slippery zone in the pitchers of the carnivorous plant *Nepenthes alata* and its effect on insect attachment. *J. Exp. Biol.,* **208**(24), 4651–4662.

[50] McClements, D. J. (2015) Food Emulsions, CRC Press, Boca Raton.

[51] DeOng, E. R., Knight, H., and Chamberlin, J. C. (1927) A preliminary study of petroleum oil as an insecticide for citrus trees. *Hilgardia,* **2**(9), 351–386.

[52] Agnello, A. M. (2002) Petroleum-derived spray oils: chemistry, history, refining and formulation, University of Western Sydney, .

[53] Shogren, R. L., Petrovic, Z., Liu, Z., and Erhan, S. Z. (2004) Biodegradation behavior of some vegetable oil-based polymers. *J. Polym. Environ.,* **12**(3), 173–178.

[54] Puri, S., Butler, G. J., and Henneberry, T. (1991) Plant-derived oils and soap solutions as control agents

for the whitefly on cotton. *J. Appl. Zool. Res.,* **2**(1), 1–5.

[55] Gorb, E. V., Hosoda, N., Miksch, C., and Gorb, S. N. (2010) Slippery pores: anti-adhesive effect of nanoporous substrates on the beetle attachment system. *J. R. Soc. Interface,* **7**(52), 1571–1579.

2

Coatings preventing insect adhesion

Insect pests cause considerable damage worldwide to plants, buildings and human health. This review explores how controlling insect adhesion to coatings might mitigate these problems. We summarise the current knowledge of the mechanisms of insect adhesion on natural and synthetic surfaces and natural examples of non-adhesive and slippery surfaces. Biomimetic, multi-scaled rough and particle-transferring surfaces provide an efficient method to reduce adhesion of crawling insects.

Aurélie Féat[a,b], Walter Federle[c], Marleen Kamperman[b,d] and Jasper van der Gucht[b]

[a]AkzoNobel Decorative Paints, Wexham Road, Slough, SL2 5DS, United Kingdom

[b]Physical Chemistry and Soft Matter, Wageningen University, Stippeneng 4, 6708 WE, Wageningen, The Netherlands

[c]Department of Zoology, University of Cambridge, Cambridge, CB2 3EJ, United Kingdom

[d]Zernike Institute for Advanced Materials, University of Groningen, Nijenborgh 4, 9747 AG Groningen, The Netherlands

2.1 Introduction

2.1.1 Coatings: definition and applications

Coatings are materials prepared, generally, from liquids which form a film after drying or curing once applied to substrates. Their use has become ubiquitous in the past decades for decorative, protective and functional applications [1]. Important functional and protective properties include antibacterial, self-healing, self-cleaning, antifouling, anti-corrosive, hydrophobic, oleophobic, or ice-repellency and flame-retardancy. Such coatings should be durable, easy-to-apply, inexpensive and environmentally friendly [1, 2].

As well as the important aesthetic and barrier properties that coatings deliver, they are being applied to a wide range of substrates for their specialised functional properties, e.g. fruits, textiles and solar cells [3–5]. Nature shows the control of the surfaces of the coatings is important to access these functional effects, as demonstrated in the well-known examples of e.g. self-cleaning lotus leaves, shark skin or butterfly wings [6–8]. For example, lotus leaves (*Nelumbo nucifera*) are highly hierarchical rough structures made of hydrophobic, three dimensional epicuticular wax crystals, allowing for water to roll off the surface and to self-clean [6]. Bio-inspired strategies from the so-called Lotus-effect gave rise to extensive research in self-cleaning coatings, such as the self-cleaning outdoor Lotusan paints [9].

Insects interact with the surfaces of coatings when they land, crawl or climb on them. Whilst insects, such as pollinators and seed dispersers, are essential for most land ecosystems, many insects are considered pests, because they pose a serious threat to agriculture, forestry, buildings and human health. Possible strategies to tackle insect pests include insecticides, insect-repellent and low insect adhesion coatings [10–15]. The former however are harmful to the environment and alternative strategies are preferred [10]. This chapter reviews the threats caused by insects, their mechanism of adhering to surfaces and the possible formulating strategies related to protective building and agricultural coatings.

2.1.2 Insect damage to crops

Insect pests in agriculture need to be controlled to avoid crop diseases or damage. Crops can be harmed or contaminated in the field or during storage [16, 17]. Insect pests damage plants and crops *via* feeding, sap-sucking or infesting different parts of the plant: leaves, buds, flowers, stems, fruits and seeds, roots, tubers and bulbs; as well as seedlings and sown seeds [16]. Fruits, nectar and sap are rich in sugars, which are of particular importance in some insects' diet, such as Hemiptera [18]. Invading pests include gall insects, thrips or aphids. Generally, these attacks will result in notches, irregular margins, scarification and holes in leaves, flowers or other parts of the plant. Damages to plants are not only aesthetic, but can reduce the plant's growth, photosynthesis and disturb the plant's water and nutrient balances [19].

During storage, insects can harm crops by feeding, leading to a population exponential growth, and hence contaminate the products [16, 17]. Common storage insect pests include moths, mites, cockroaches and beetles.

Oerke reported the worldwide losses of various crops due to animal pests (insects, birds, snails, etc.), which widely depend on the type of crop and region [20, 21]. About 8% for wheat, 15% for rice, 10% for maize, 11% for potatoes, 9% for soybeans and 12% for cotton are lost to animal pests. The losses in the Mediterranean basin, where approximately 98% of the world's olive trees are harvested, olive fruit loss to insect pests is at least 15% of production, equivalent to $800 million loss [22–24]. Overall, the global crop production was reduced by about 14% due to insect pests [20, 25, 26].

Another major economical example of the non-control of pests is the loss of $46 million in 1999 in a Californian vineyard, where the grapes were contaminated with Pierce's disease, which prevents the fruits from growing, and was transmitted by leafhoppers [27].

Many other examples of crop diseases and defects caused by insect pests are reported elsewhere [21, 25, 28, 29].

2.1.3 Transmission of diseases by insects

Insects transmitting diseases are referred to as either biological or mechanical vectors, depending on where in the insect the pathogen developed, which affect several billions of people every year [30, 31].

Biological vectors carry pathogens within their bodies, which are transmitted to humans or animals through bites by blood-feeding insects, such as lice, mosquitoes or fleas. Mechanical vectors, for instance flies, carry infectious agents at the surface of their bodies (legs or mouthparts) and hosts become infected by simple physical contact [30, 31]. Although not responsible for transmitting diseases, stings (due to Hymenoptera, e.g. honeybees, hornets or wasps) may also be accountable for allergies, which can range from discomfort and local swelling to life-threatening anaphylaxis [32].

Upon physical contact or blood-feeding on their hosts, insects can transmit pathogens developed within their bodies our mouthparts, and toxins or potential allergens through their saliva [30]. Some species of ticks for instance, carry some toxins in their saliva which can cause paralysis of the host, allergic reactions and transmit a broad range of viral, bacterial and protozoan pathogens [33, 34]. Examples of transmitted diseases to humans include malaria, with about 2 billion people at risk and causing approximately one million deaths per year [30, 35]; or dengue, which affects 50 to 100 million people and causing about 20,000 deaths annually [30, 36, 37].

Insect pests also caused considerable losses to livestock, which are mainly due to reduction of milk and meat production through both transmitted diseases and stress owed to bites [30]. A dramatic example is the tsetse flies: they caused about \$4.5 billion losses by infecting cattle in Africa with trypanosomiasis [38]. Ticks, mites, stable and horn flies were reported to cause the loss of approximately cumulative \$5 billion on overall US livestock [39–41].

2.1.4   Insect damage to buildings

About 2,300 termite species have been discovered, of which 183 species are accounted for damaging buildings [42]. Termites are mostly present in Asia (mainly in India, Malaysia, China, Japan), Australia, Africa and in the USA. Termites are however of ecological importance: they raise soil quality by improving pH, organic carbon content, water content and porosity for soil aeration [43–45].

Termites feed primarily on cellulose, present in various sources e.g. wood, lichen, grass or soil, and are considered pests as soon as they start damaging man-made structures [44]. Wood-feeding termites can cause serious damage to buildings, sometimes causing them to collapse or villagers to abandon their houses. The precise economical cost of termite damage is difficult

to assess due to the lack of data in underdeveloped countries, but has been estimated to be between and \$2 and \$40 billion per year, with about \$1-1.5 billion p.a. in the USA alone [42, 46, 47].

When entering buildings, insect pests can further infest or damage objects or furniture made of wood, wool, linen, etc., or even pieces of art or books if entering museums and libraries [48].

In the next sections, we first review the current knowledge about insect biomechanics and insect adhesion to natural surfaces. Methods to repel or reduce insect adhesion to surfaces are discussed. Emphasis is given on paints and coatings which can reduce insect attachment to buildings and plants without using insecticides.

2.2 Insect adhesion and slippery plant surfaces

2.2.1 Biomechanics of insects

Insect climbing mechanisms

Adhesion is defined as the force required to dissociate two surfaces from one another. To describe friction, Coulomb distinguished static friction from dynamic friction: static friction is the friction between two objects in contact that are not moving relative to each other; while dynamic friction is the force which is necessary to slide a surface on one another. Insects can climb on a surface by means of interlocking or by adhesion forces. Their pads generate both adhesion and friction forces [49, 50]. Surface roughness tends to reduce adhesion as asperities reduce contact area, yet insects and geckos can adhere to smooth as well as rough substrates [49, 51, 52]. Alternatively, body hairs have also been reported to provide adhesion, as observed in honeybees, which carry lubricated pollen particles from flowers to hives [53, 54].

Claws and spines on the tarsus (insect foot) can interlock with substrate asperities [55, 56]. The stiffness and morphology of the claws, especially the sharpness of the claw tip, impact their performances to cling to asperities [57]. On a soft surface, a stiff claw may be able to dig into the surface and find grip for locomotion [58]. On a rigid rough surface, a claw can grip on surface protrusions that are larger than approximately the diameter of the claw tip [59, 60].
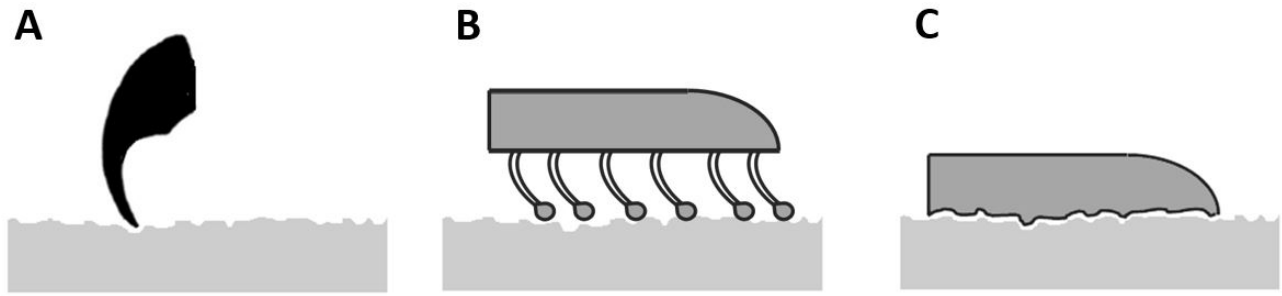
Figure 2.1: Schematic representation of (A) claw, (B) hairy pad and (C) smooth pad in contact with a rough substrate.

On smooth surfaces with insufficient grip for their claws, insects use their adhesive pads, which fall into two categories: hairy (or fibrillar) and smooth pads. Both types of pads increase the contact area with substrates to improve attachment to rough surfaces [61, 62] (Figure 2.1).

The movement of insect legs occurs through attachment and detachment of the pads, *via* a peeling mechanism, similar to pressure adhesive tapes [63]. When pulling the pad towards the insect's body, adhesion is enhanced ('attachment'); while moving the pad in a distal direction (away from the insect's body), when no adhesion is required, pulls off the pad from the surface ('detachment') [49, 64].

Hairy adhesive pads are composed of densely packed arrays of fine and flexible fibers, the setae, generally tipped with triangular or circular end-plates [63, 65, 66]. They are found in many insects, such as beetles, bugs and flies, with widths ranging from ca. 100 nm in spiders and geckos to more than 5 μm in beetles [63]. These long and flexible hair arrays provide low elastic modulus, which are hence able to balance the surface roughness by bending and allow rapid attachment and detachment from a surface by pushing/pulling mechanisms [61]. The latter is aided by the distal orientation of the hairs as well as easy, rapid and simultaneous setae peeling off from the surface [67]. The maximum adhesive force was found to increase with the number of adhesive setae in leaf beetles [68]. Adhesion force differences in males and females have been reported in beetles, due to different seta tips for mating purposes [61, 69, 70].

Smooth pads are found in many insects, such as ants, bees, stick insects, grasshoppers and cockroaches (Figure 2.2). A smooth pad consists of a very soft cuticular sac between the tarsal claws. Surface protrusions causes the soft pad to deform, hence maximising contact area on rough substrates [62, 71]. The adhesive pad is referred to as arolium in many insects [55, 72]. Arolia can be retractable and fluid-filled (e.g. in Hymenopteran insects) or non-retractable (e.g.
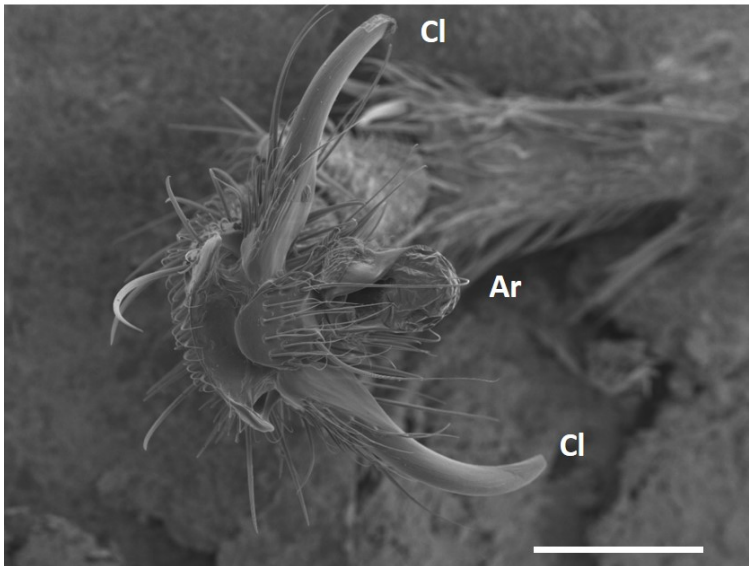
Figure 2.2: Scanning electron microscopy image of *Atta cephalotes* ant tarsus showing the claws (Cl) and arolium (Ar). Scale bar: 100 μm.

in cockroaches) [56, 72–74]. A synthetic attachment device inspired from an insect pad/claw system was described in [75]. These artificial adhesive pads and claws were reported to increase adhesion synergistically on steel spheres.

Many insects of orders such as Hymenoptera, Blattodea or Phasmatodea possess several attachment pads on the same leg [76]. The function of each individual pad has been investigated in e.g. stick insects (*Carausius morosus*) [77] and cockroaches (*Gromphadorhina portentosa*) [78] where the results suggested arolia serve as adhesion pads ("toe" pads) and tarsal pads (euplantulae or "heel" pads) are friction pads, hence providing little adhesion, in these types of insects [50]. This indicates the pads can passively and energy-efficiently control the adhesion and friction forces during locomotion.

Adhesion in insect pads is mediated by an adhesive secretion: this fluid maximises adhesion to rough substrates by filling protrusions between the pad and the surface [57, 67, 71, 78]. The composition and nature of this fluid however remain unclear, due to the variations between insect species and the low volume secreted by pads [57, 79–81]. For many insects possessing smooth pads (e.g. ants, cockroaches or certain mites), the secretion has been found to be a water-in-oil emulsion mainly containing hydrocarbons, fatty acids, alcohols, amino acids, etc. It was suggested that in smooth pads, the thin films of fluid rheologically behave like shear-thinning Bingham fluids with a yield stress [57, 79], while the secretion was found to be a Newtonian fluid in beetles and flies (hairy pads) [80, 82].

In insects possessing smooth pads, the thickness of the adhesive fluid was reported to be about 100 nm, making its investigation challenging [57, 83]. On smooth surfaces, insects should

minimise the secretion of fluid to increase capillary adhesion (wet adhesion situation), whose viscosity could also impede locomotion speed and pad re-usability [62, 84]. Interestingly, the adhesion in dry and wet conditions (absence and presence of adhesive secretion, respectively) has been reported to be similar by Labonte and Federle [84]. The fluid's viscous forces were found not to improve adhesion significantly and the pad retraction speed was not correlated to the amount of fluid. The fluid layer may not only help to increase adhesion on rough surfaces, but it could at the same time act as a lubricant to ease fast detachment from surfaces [78, 84].

Effect of surface roughness on insect climbing

The locomotory behaviour of insects depends on both the insect type and the nature of the surface. Many plants use surface roughness to reduce insect adhesion, as further discussed in the section 2.2.2 Slippery plant surfaces. Although not demonstrated formally, some insects, such as ants and cockroaches, are suspected to use their antennae to investigate surface asperities before walking on a substrate [12, 85]. Antennae can indeed perceive the ant's environment, such as airflow, chemical signalling, and detect mechanical fragilities; and were suggested to counterbalance poor vision [86].

Both types of pads can comply with surface asperities to maximise attachment forces to surfaces [61, 62] (Figure 2.1). They secrete adhesive fluid to improve surface contact as it compensates the surface asperities, hence increasing adhesion to rough surfaces [57, 67, 71, 78]. Ants, which possess smooth pads and extensible adhesive pads [73], have been reported to passively deploy their arolia after mechanical claw slipping on the surface [56, 73].

Hairy pads, as found in beetles, do not provide sufficient adhesion on micro-rough surfaces. The setae are suspected to make incomplete contact with the surface asperities, leading to a reduction of the contact area [60, 69]. Adhesion forces generated by insects were reported to be larger on surfaces displaying surface asperity size smaller than 300 nm ('smooth', pad adhesion, Figure 2.1B) or larger than 3 μm ('rough', claw interlocking, Figure 2.1A) [60, 68, 70, 87]. Specifically, surfaces with asperity diameters between 50 nm and 1.0 μm led to the lowest attachment forces, as large seta tips cannot interlock with small surface protrusions [60, 61, 69]. Similar roughness effects have been described in insects possessing smooth pads [88, 89]. In particular, Scholz *et al.* [89] modelled that the *Nepenthes alata* pitcher plant inner wall should possess a pore size of 1 μm to minimise the adhesion of insects.
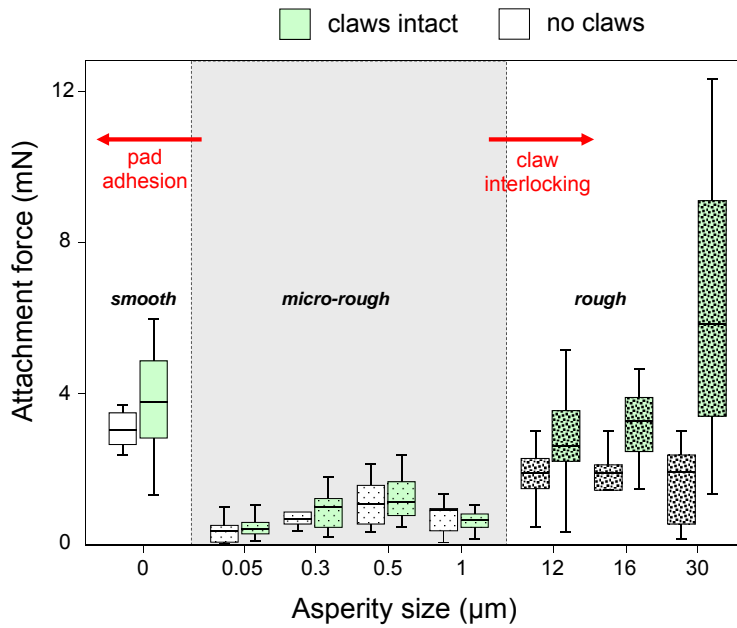
Figure 2.3: Centrifuge measurements of whole-body detachment forces of male *G. viridula* on epoxy substrates of varying roughness. Asperity size is approximate and corresponds to the average nominal particle size of the original sandpaper (redrawn from [60]).

The roughness ranges can be defined as (1) ca. 0 nm ('smooth', pad adhesion), (2) 50 nm-1.0 μm ('nano/micro-rough') and (3) larger than 3 μm ('rough', claw interlocking) [60, 70]. In the 'nano/micro-rough' range (50 nm-1.0 μm), both adhesive pads and claw interlocking are inefficient for climbing (Figure 2.3).

Zhou *et al.* have studied insect adhesion on various rough substrates produced by lithography and displaying different pillar spacings (3-22 μm) and heights (0.5 and 1.4 μm) [90]. They studied cockroaches and beetles (smooth and hairy pads, respectively), which were found to make partial contact on dense array of pillars, while full contact was obtained for large spacing (above 4 μm) and smaller pillars (0.5 μm).

Self-cleaning mechanisms

The accumulation of particles on the body or tacky adhesive pads of insects lead to a loss of adhesion [57] and possibly to locomotion problems [91, 92]. Fouling particles must be removed from crawling insects' pads to maintain their adhesive properties, or from the body of flying insects for controlled flight. Figure 2.4 shows *Atta cephalotes* ant tarsi after being contaminated with 300 nm titanium dioxide particles.

Fouling particles can be removed through self-cleaning, *via* grooming, brushing using cleaning structures, and supposedly when bringing them into contact with a surface with greater attraction forces to these contaminating particles through scratching, rolling and sliding movements [52, 93–95]. The adhesive secretion of insects has also been suggested to aid the self-
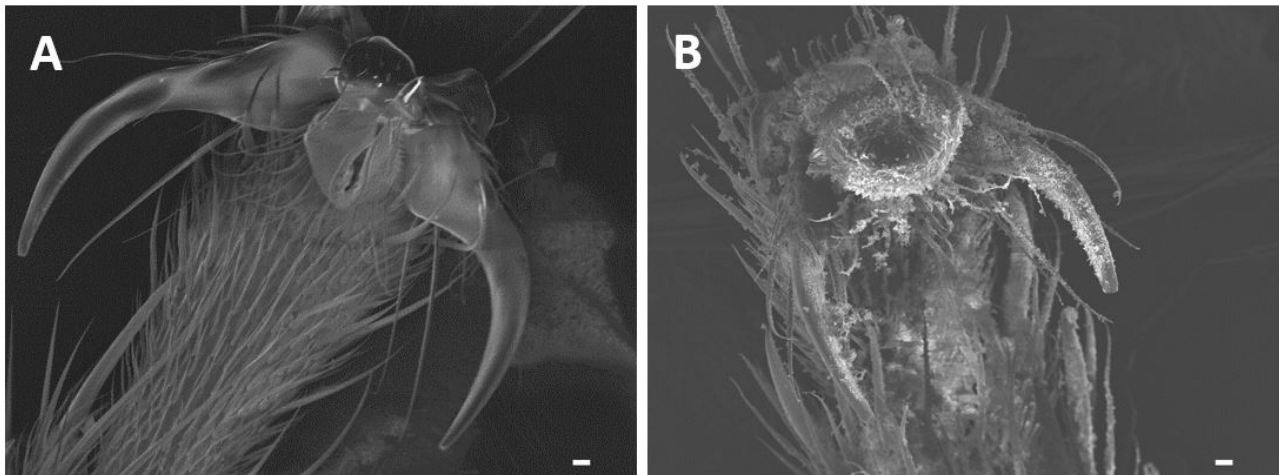
Figure 2.4: Scanning electron microscopy images of (A) uncontaminated and (B) contaminated tarsi of *Atta cephalotes* ants after free roaming on 300 nm titanium dioxide particles. Scale bars: 10 μm.

cleaning process by washing off particles [94].

In practice, self-cleaning is achieved in just a few steps on smooth surfaces, as observed in ants [93], stick insects and beetles [94], or even geckos [96]. On rough surfaces, on which claws are mainly used, the pad/surface contact area is assumed to be too low to efficiently remove particles from the pad [94, 97]. Particles were found to be removed more easily from hairy pads: in smooth pads, the presence of shear was necessary, while pull-off movements only could efficiently remove particles of hairy pads [93, 94]. The low surface energy of the setae might also aid the self-cleaning process [94].

The fouling particle size has been demonstrated to significantly impact self-cleaning of the pads of ants, Coccinellids and dock beetles, but surprisingly did not significantly affect stick insects [93, 94]. 1 μm and larger than 45 μm particles were easily removed from insect pads, whereas 10-20 μm particles needed more steps to be removed through self-cleaning [93, 94, 97]. For hairy pads, large particles cannot fit in between fibrillar setae, leading to rapid particle removal [94, 95, 97]. Interestingly, no pad fouling has been observed on ants' smooth pads using contaminating particles larger than 100 μm, suggesting the particles need to be smaller than the claw basal spacing to adhere to the arolium [85].

2.2.2 Slippery plant surfaces

Pitcher plants families Cephalotaceae, Nepenthaceae, and Sarraceniaceae have been long known for capturing and digesting insects, mainly ants, which are attracted by the nectar the plants secrete [89, 99, 100]. They then fall into the pitcher, with barely any chance to escape, and get
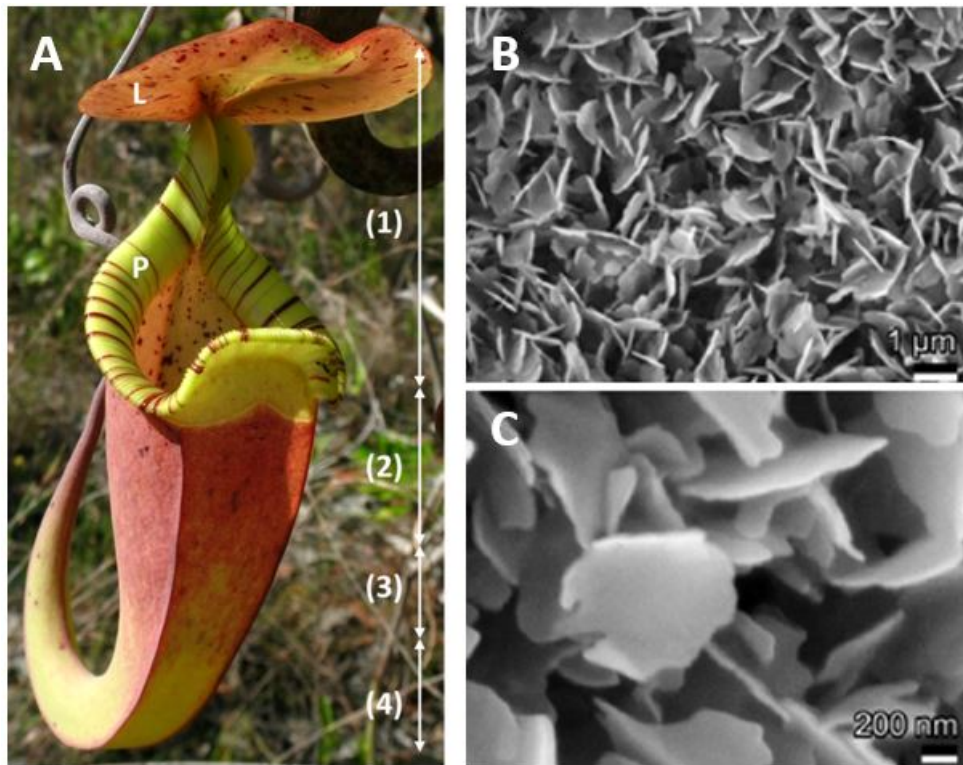
Figure 2.5: (A) *Nepenthes* pitcher plant morphology with four functional zones: (1) the lid (L) and peristome (P), (2) the slippery zone, (3) the transitional zone, and (4) the digestive zone. Scanning electron microscopy of the waxy zone: (B) the upper wax layer and (C) wax crystals of the upper wax layer. Adapted with kind permission from [98]. Scale bars: (B) 1 μm and (C) 200 nm.

digested by pitcher fluid. Some species of the genus *Nepenthes* possess an insect-slippery waxy surface, like the widely studied *N. alata* [89, 98, 100], while some others (e.g. *N. bicalcarata*) only become slippery when wet [99].

Nepenthes pitchers consist of several zones: (1) the lid and peristome, (2) the slippery zone, (3) the transitional zone, and (4) the digestive zone [101] (Figure 2.5A). The sections below describe these two main slippery mechanisms in species of the genus *Nepenthes*.

Slippery wax-covered plant surfaces

Many plants are known to possess a superhydrophobic surface, such as the lotus leaf, rose petals or the inner pitcher walls of *Nepenthes* pitcher plants [6, 100, 102]. The latter is superhydrophobic due to the combination of roughness and hydrophobicity of its epicuticular crystals present at its top surface. Superhydrophobic substrates exhibit water contact angles greater than 150° and contact angle hysteresis lower than 10° [103]. The combination of cutin biopolymer and lipids protects plants from water loss [9]. Climbing of insects on epicuticular wax-covered pitcher plant surfaces has been widely studied, see e.g. [89, 98, 100].

Gorb *et al.* studied the epicuticular wax coverage in *N. alata*, which consists of two different layers (Figure 2.5B/C) and display different structures, chemical compositions, mechanical properties and different insect anti-adhesion mechanisms [98]. The lower wax layer shows a foam-like structure and is composed of platelet-shaped wax crystals coming off the surface at sharp angles [98]. The upper layer wax displays closed-packed platelets perpendicularly oriented to the lower layer. Both waxy layers are mainly composed of alkanes, aldehydes, primary alcohols, free fatty acids, esters and triterpenoids expressed in different proportions in the two layers, with predominant aldehydes and alcohols, which are likely to co-crystallise [98, 104].

Insects slip into the pitcher *via* a two-fold mechanism relying on (1) pad contamination and (2) surface roughness. (1) Upon contact with insect feet, crystals of the upper wax layer break off and contaminate the adhesive pads of insects. They are also too small and too fragile for claw interlocking [98]. (2) In laboratory conditions where the upper epicuticular lipid layer was removed, the rough lower wax layer reduces the real contact area of insects' feet with the plant surface as pads cannot comply well with the surface protrusions [89, 98]. In similar experimental conditions, the upper wax layer has interestingly been found to be non-recoverable, suggesting that when all crystals have detached from the upper layer, the micro-roughness of the lower wax layer would be efficient at preventing insects from climbing the walls of the inner pitcher's surface [101].

Additional anti-adhesive properties hypotheses to (1) and (2) were proposed by Gorb and Gorb [105, 106]: (3) the wax-dissolution hypothesis: the insects' adhesive fluid may cause epicuticular wax crystals to dissolve, covering the surface in a thick layer of lubricating, slippery fluid; and (4) the epicuticular wax crystals may absorb the secretion, hence reducing the attachment forces of insects (fluid absorption hypothesis).

Slippery when wet plant surfaces

Unlike epicuticular wax-covered surfaces, some other plant surfaces, such as the peristomes of *N. bicalcarata* pitcher plants, only become slippery to insects when wet, in the presence of dew or rain [99]. The pitcher rim, or peristome, possesses ridges oriented toward the inside of the pitcher [99, 107] (Figure 2.5A). These surfaces are superhydrophilic (fully wettable), thereby

stabilising thin lubricating water films between the insect foot and the surface so that insects slip *via* aquaplaning [99].

When insects climb on the wet peristome, they fall into the pitcher with barely any chance to escape. In contrast to this, dry peristomes are not slippery to insects [100]. In the lower part of the pitcher plant, specialised glands secrete a digestive fluid to absorb nutrients obtained from the insects [89]. In some species, this fluid has non-Newtonian properties and particularly a high extensional viscosity, so that it sticks to the insect's legs, which helps to retain them in the pitcher [108, 109].

Due to surface tension forces, getting a grip on the pitcher wall becomes difficult. The pitcher fluid indeed needs to be removed from the insects' adhesive pads to make full contact with the wall, which may be a long process if the fluid is viscous [99]. Friction forces of weaver ants (*Oecophylla smaragdina*) were measured on the peristome surface [99]. The slipperiness of peristomes is a combination between water lubrication and surface topography, which is effective against different attachment structures of the insect tarsus [99, 107]. Water films on pitcher rims only prevent adhesion for soft adhesive pads but not for claws, while surface roughness creates friction only for the claws but not for pads [99].

Interestingly, some insects have evolved counteradaptations to climb on slippery plant surfaces, including ants capable of overcoming aquaplaning in *Nepenthes* pitcher plants and "waxrunning" ant partners of *Macaranga* ant-plants with slippery waxy stems [88, 99, 109–111]. In these obligate ant-plant mutualisms, it is both in the ants' and the host plants' interest to isolate the ant partners from predators and competitors, promoting the development of such specific adaptations [109, 111].

The knowledge of insect locomotion and naturally slippery surfaces could be used to formulate products preventing crawling insects from entering buildings or adhering to plant surfaces, a reduction in the use of insecticides and the issues they can cause.

2.3   Coating strategies to minimise insect adhesion

Possible strategies to repel insects or reduce the adhesion of crawling insects to coatings (applied to e.g. buildings or plants) are summarised herein, special attention has been given to the development of substrates bio-inspired by plant surfaces. These approaches might not be suitable for all insects due to the attachment and friction forces discrepancies observed across

gender [61, 70], pad type and species [12, 88, 90, 99]. With regards to the biomimetic strategies described, the adhesive performance of both types of pad is however very similar [67], and substrates known to be slippery for one type are also slippery for the other [107, 112].

2.3.1 Insecticides and insecticidal coatings

Insect pests are currently controlled mainly by insecticides, which present health and environmental issues, and are summarised in this section.

In the United States only, insects destroy 13% of crops [10]. Hence, one can see the need to eliminate them. Between 2006 and 2007, more than 400 million kilograms insecticides were produced worldwide; while 70% of insecticides were used in agriculture in the United States [113]. Over the 2008-2012 time period, this number however decreased to 57%, due to an increase of use by private individuals (home and garden) at a similar production level [114].

Since the introduction of synthetic organic insecticides in the 1940s, four major classes of 'conventional' insecticides have emerged: (1) organophosphates, (2) carbamates, (3) synthetic pyrethroids and (4) neonicotinoids [115, 116]. Neurochemical insecticides affect the insects' nerve–muscle system and account for 85% of sales [117]. Otherwise, insecticides target respiratory organs (4%) and limit the growth and development of insects (9%), for instance by inhibiting the biosynthesis of chitin or by mimicking juvenile hormones [116, 117].

Although beneficial to agriculture, conventional insecticides and pesticides are detrimental to the environment and may affect human and animal health [10, 118]. When sprayed, most of the insecticide is lost to the air during application and depending on its persistence and volatility, disperses globally or bioaccumulates in food chains [118–121].

According to Pimentel [122], pesticide use in the United States returns about $4 per $1 invested for pest control. These costs however do not take into account the side economic consequences on health and environment [10]. They were estimated in the USA to be: public health, $1.1 billion per year; pesticide resistance in pests, $1.5 billion; crop losses caused by pesticides, $1.4 billion; bird losses due to pesticides, $2.2 billion; and groundwater contamination, $2.0 billion [10].

Every year, the use of pesticides, including insecticides, leads to 26 million cases of non-fatal poisonings, of which 3 million cases are hospitalised and cause approximately 220 000 deaths [10, 123, 124]. Insecticides are indeed well-known carcinogen compounds and can cause chronic

illnesses, such as neurological damage [10, 125]. In addition to humans, insecticides also harm domestic animals.

Upon exposure to insecticides, mutations in insecticide target sites or detoxification processes may occur, resulting in increased resistance to the chemicals [126]. This has been for instance observed in the Australian sheep blowfly, which developed an insecticide-resistant allele [127]. Some insect pests such as the diamondback moth, Colorado potato beetle and cotton aphid have developed resistance to at least 50 insecticides [117].

Insecticides may harm, or even kill non-target organisms (such as organisms that recycle soil nutrients, pollinate crops, and prey on pest species) and reduce and/or contaminate food supplies for animals which feed on them due to bioaccumulation in the food chain [120, 121, 128]. Using the example of Brazilian tomatoes, insecticides were reported to eliminate more parasitoid natural predators than the targeted tomato pests, due to an increase of their chemical resistance [129], which hence led to a pest population increase. Reduction of pollination also occurs due to honeybee colonies loss [10, 128].

It should however be noted that new insecticides with lower health and ecological impact are being developed [128, 130], as well as alternatives to lower the amount of insecticides used, e.g. biological control as part of integrated pest management, see e.g. [29].

Novel insecticides based on nanotechnologies and inert materials have arisen to replace the aforementioned conventional insecticides [130, 131]. Nanoparticles are particles having at least one dimension smaller than 100 nm; they have grown in attention for the past two decades as their use as encapsulants allows the controlled release of insecticides or pesticides [131, 132]. They offer advantages including a higher surface area, higher solubility, higher mobility and lower toxicity due to elimination of organic solvents [119].

Inert materials include diatomaceous earths, zeolites and kaolin, and present a lower environmental impact than conventional insecticides due to their inert nature [130]. Their size is generally comprised between 0.5 μm and 100 μm, improved insecticidal effect has been obtained for particles smaller than 45 μm [130, 133, 134]. The death of insects is caused by desiccation as these abrasive particles adhere to their cuticle, which normally protects them from water loss [130, 133, 135]. The particle film technology is a hydrophilic kaolin particle-based coating applied to plants and trees. Particle films were shown to reduce oviposition and adult settling

of various pest species on pears and apples [136–138], potatoes [139], olives [140, 141] and others [142]. They are however to be used in sunny, dry weather as the hydrophilic and porous particle films are easily washed off by rain [140].

Including insecticides in interior and exterior coatings of buildings (houses, hospitals, restaurants, etc.) can be effective to avoid the presence of insects by repelling, killing or preventing infestation [143–145]. As previously described, the use of insecticides should be limited due to health and environmental concerns [10], although their environmental impact once incorporated in coatings hasn't been assessed in the authors' knowledge. The rest of this section will focus on alternatives to insecticides to reduce the presence of insects in buildings by repelling them or minimising their adhesion to walls using functional coatings.

2.3.2 Insect-repellent coatings using natural products

Essential oils (e.g. eucalyptus or citronella oils) and plant extracts (branches or leaves) consist in an effective natural method to repel insects and present the advantage that they can readily be added to formulated paints [146, 147]. Many plants contain chemicals to prevent insects feeding on them, which can be classified in five groups: (1) nitrogen compounds (primarily alkaloids), (2) terpenoids, (3) phenolics, (4) proteinase inhibitors and (5) growth regulators [148]. Most essential oils contain terpenoids, which affect insects in many ways: repellency, acute toxicity, fumigant activity, reproductive toxicity, and neurotoxicity depending on the target site in the insect [149, 150]. The efficiency of many essential oils in laboratory conditions, however, lasts only for a few hours [151, 152]. Encapsulation allows the slow release of active ingredients and once incorporated into coatings, essential oils repel insects for at least a year [146].

While essential oils and plant extracts can cause contact and airborne allergies (provoking e.g. eczema and asthma) [153, 154], their effect once incorporated in paint coatings hasn't been tested to the best of our knowledge, but is expected to be negligible due to encapsulation.

2.3.3 Biomimetic strategies

In this section, we first review the general methods to produce plant bio-inspired properties using synthetic materials, such as superhydrophobicity, like the well-known lotus effect [6], or slipperiness as observed in *Nepenthes* [98, 99] and how they can be used to reduce insect adhesion to surface coatings.

Surface functionalisation and asperities

A superhydrophobic surface displays a water contact angle greater than 15° and contact angle hysteresis lower than 10° [103]. It is commonly accepted that superhydrophobicity in synthetic surfaces can be achieved by a combination of (1) hydrophobic treatment and (2) surface roughness according to the well-known Wenzel and Cassie models [155, 156]. In the Wenzel model (homogeneous wetting), the surface roughness increases the available surface area of the solid [155]. The Cassie model (composite wetting) states that the superhydrophobic nature of a rough surface is caused by microscopic pockets of air remaining trapped underneath a liquid droplet, leading to a composite interface (solid-air-liquid) (Figure 2.6) [156].

It has been known for decades that surfaces can be rendered hydrophobic by coating them with techniques such as perfluorination or silanisation, and such surfaces have been extensively described in literature [103, 157]. The corresponding chemicals indeed bring low surface energy to the top coating. High water contact angles (about 160°) have been measured on functionalised, roughened surfaces [158].

Hydrophobicity properties can be further enhanced by roughening the surface. Methods include nanoparticle functionalisation, which can be e.g. nanosilicas, silicone nanofilaments, carbon nanotubes, plasma treatment, etching, and by producing hierarchical surface structures similar to the asperities found in plants [103, 157, 159]. The latter can be done using (1) top-down and (2) bottom-up techniques [100]. In (1), the surface to reproduce is replicated by moulding. In (2), structured materials are obtained by chemical self-assembly, from molecular level up to micron scale. These approaches have been extensively described in the literature, see e.g. [157, 160, 161].
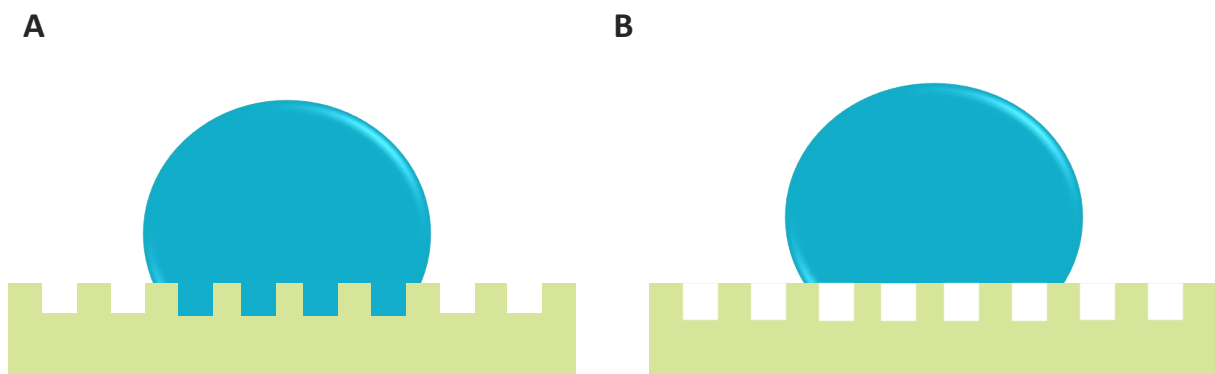

Figure 2.6: Schematic (A) Wenzel and (B) Cassie-Baxter wetting models.

For example, Meredith and coworkers have developed an easy process to create micropatterns bio-inspired from pollen receptive surfaces using blends of commercial polymers [53]. They are formed through demixing of the polymers, and the surface roughness simply increases with the polymer molecular weight. The authors suggest that pollen and stigma surfaces could be used as biomimetic model systems for the design of microparticles [162, 163].

Slippery surfaces

Given the importance of surface roughness on insect locomotion (see section 2.2.1 Biomechanics of insects), nano/micro-rough surfaces may provide a mechanical way to control insects [69, 98], rather than using potentially harmful chemicals to kill or repel crawling insects.

Several studies suggest that insect attachment on surfaces can be reduced by structuring surfaces with asperities ("peaks" and "valleys") [69, 90]. Graf *et al.* [12] designed insect-repellent surfaces by tailoring their topographies following the work of Zhou *et al.* (presented in the 2.2.1 Effect of surface roughness on insect climbing section) [90]. The surfaces could reduce the escape rate of cockroach (smooth pads) from a cage by 44%. Interestingly, the adhesion of beetles (hairy pads) was barely affected, probably as the roughness (ca. 45 μm) was in the 'rough' domain, where claw interlocking predominates (Figure 2.3). As observed in pitcher plants, a low 'capture rate' could be beneficial to some applications, as scouts recruit more ants to the pitcher [164].

Prototypes of paints made slippery through surface asperities have been studied by Zhou [112]. By tailoring the quantity and size of solid particles at the paint surface, called pigment and extender, paints were produced where insects were unable to find grip. As the solid particles were loosely bound to the paint surfaces (low polymer binder amount), it is also possible that contamination of the pads occurs through transfer of the loose particles to the insect feet. This however hasn't been studied by the author. Another study showed the importance of pigment particle size to render surfaces slippery: when the particles were smaller than 500 nm, the coatings were very slippery to fire ants as their adhesion was reduced [165].

Tilt

Porous surface
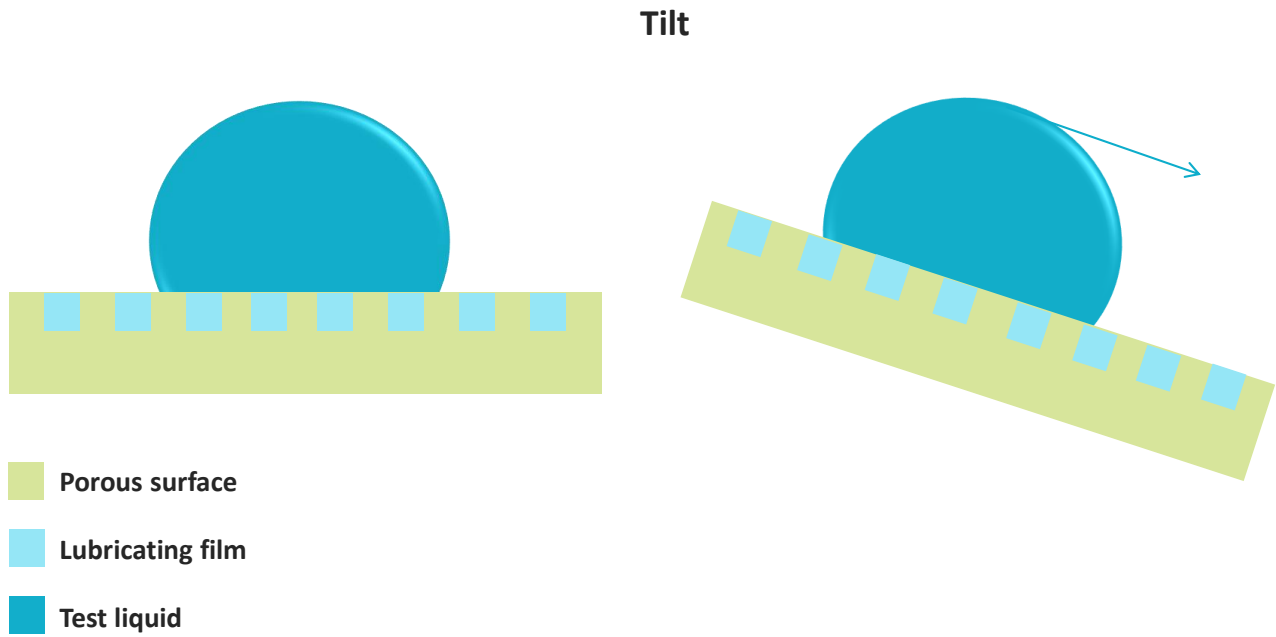
Lubricating film

Test liquid

Figure 2.7: Schematic Slippery Liquid-Infused Porous Surface (SLIPS) fabrication.

Addition of an extra coating layer (overcoat or overlayer) allows the reduction of properties such as adhesion, fouling or wettability. This is for example done on ship hulls or aircrafts to minimise adhesion of marine organisms and insects, respectively, allowing to reduce drag, and hence, fuel consumption [7, 166, 167]. The addition of silicones and waxes has been found to improve surface slip by reducing the friction on coating surfaces [168], hence one could imagine this strategy can be efficient to reduce insect adhesion to coatings. The use of low surface energy particles is extremely efficient to do so: in insect colonies, waterborne polytetrafluoroethylene (PTFE, Fluon or Teflon) coatings are used to prevent insects from escaping their cages as Fluon-coated walls are very slippery to insects [13, 169]. The surface roughness has however been found to predominantly affect insect adhesion rather than surface energy [87].

Slippery liquid infused porous surfaces (SLIPS) have been developed by Aizenberg and coworkers (see e.g. [14, 170, 171]) and is a similar approach to the overcoating one. Inspired by the combination of the liquid film found on the *Nepenthes* pitcher plant peristome and its multi-scaled structure, the SLIPS technology involves a porous solid infused by a lubricant (Figure 2.7). This lubricating film fills the voids of the substrate, is incompressible and must be immiscible with the test liquid in order to repel it.

The porous substrate is nanostructured, for example made of nanofibres of e.g. epoxy or PTFE. To prepare the SLIPS, the surfaces are first rendered more hydrophobic by silanisa-

tion. The perfluorinated lubricant is then added to the substrates to form a liquid overcoat [14]. SLIPS surfaces are stable under high pressure, omniphobic, mechanically robust and self-repairing. Besides repelling many liquids and ice, they can interestingly prevent the adhesion of many biological objects, such as bacteria, fungi and insects.

Particle transfer strategies

Similarly to epicuticular wax crystals detaching from *Nepenthes* plant surfaces to make insects slip, another strategy to minimise insect adhesion to coatings could include the transfer of particles as contaminating particles present on insects' pads or body impede their locomotion [57, 91, 92].

As discussed in the 2.2.1 Self-cleaning mechanisms section, the fouling particle size has been demonstrated to significantly impact self-cleaning of the pads of ants, Coccinellids and dock beetles, but did not affect stick insects [93, 94]. Particle diameters of 1 μm and larger than 45 μm were easily cleaned from insect pads, but particle diameters of 10-20 μm needed more time to be removed [93, 94, 97]. The surface energy of the contaminating particles was found to have little influence on loss of adhesion [85]. Interestingly, the recovery of adhesion was shown to be influenced by the fouling particles' surface energy in ants (smooth pads), but not in Coccinellids (hairy pads) [93]. Low surface energy substrates also slowed down the regain of adhesion of contaminated hairy pads [93].

Hackmann *et al.* [91] have studied the removal of fouling particles by antenna cleaner in *Camponotus rufifemur* ants. They report that small particles (< 25 μm) are harder to clean for insects, as they can interlock and remain longer on their antennae, hence impeding their locomotion [12, 85]. Anyon *et al.* approximated the arolium-particle adhesive force, F_{pa}, to be [85, 172]:

$$F_{pa} = 4\pi\gamma R \tag{2.1}$$

With γ the surface tension of the fluid secretion, R the radius of the particle asperity in contact with the arolium and corresponding to the particle diameter for spherical particles. For spherical particles typically sized between 1 μm-100 μm and considering $\gamma \approx 30$ mN/m [83], insect pads would approximately need to generate adhesion forces in the range of 0.38 μN-38

μN to detach them from a loose particle coating, in line with the attachment forces measured for climbing insects [49, 59].

This suggests that coatings made of loose particles, formulated with different particle sizes and surface energies, could for instance only repel one type of insect. In practise, this could be achieved in e.g. paints containing low binder amount (matte paints) or no solvent (powder coatings) [168]. Loose particle barriers have for instance been shown to be effective both in the lab and field conditions to protect potatoes from Colorado potato beetles [15].

2.4 Conclusions

We have reviewed the problems caused by insect pests and strategies to control them. The use of insecticides has detrimental effects, not only for the environment, but also for human and animal health. Informed by the mechanisms of insect adhesion to various surfaces, surfaces are being developed that are slippery for insects, providing an alternative strategy to control pest insects in an environmentally friendlier way. Several parameters have been identified as critical for minimising insect adhesion, including surface energy, surface roughness, and the force required to detach particles from the coatings.

Coatings inspired by slippery plant surfaces may provide an alternative to toxic insecticides. To become commercially feasible, the coating should be inexpensive, easy to make and apply.

Acknowledgements

References

[1] Ghosh, S. K. (2006) Functional Coatings and Microencapsulation: A General Perspective, Wiley-VCH Verlag GmbH & Co. KGaA, Weinheim, FRG.

[2] Hansen, M. K., Larsen, M., and Cohr, K.-H. (1987) Waterborne paints: A review of their chemistry and toxicology and the results of determinations made during their use. *Scand. J. Work. Environ. Health,* **13**(6), 473–485.

[3] Devlieghere, F., Vermeulen, A., and Debevere, J. (2004) Chitosan: antimicrobial activity, interactions with food components and applicability as a coating on fruit and vegetables. *Food Microbiol.,* **21**(6), 703–714.

[4] Yuranova, T., Mosteo, R., Bandara, J., Laub, D., and Kiwi, J. (2006) Self-cleaning cotton textiles surfaces modified by photoactive SiO_2/TiO_2 coating. *J. Mol. Catal. A Chem.,* **244**(1-2), 160–167.

[5] Forberich, K., Dennler, G., Scharber, M. C., Hingerl, K., Fromherz, T., and Brabec, C. J. (2008) Performance improvement of organic solar cells with moth eye anti-reflection coating. *Thin Solid Films,* **516**(20), 7167–7170.

[6] Barthlott, W. and Neinhuis, C. (1997) Purity of the sacred lotus, or escape from contamination in biological surfaces. *Planta,* **202**(1), 1–8.

[7] Bixler, G. D. and Bhushan, B. (2012) Biofouling: lessons from nature. *Philos. Trans. R. Soc. A,* **370**(1967), 2381–2417.

[8] Nishimoto, S. and Bhushan, B. (2013) Bioinspired self-cleaning surfaces with superhydrophobicity, superoleophobicity, and superhydrophilicity. *RSC Adv.,* **3**, 671–690.

[9] Solga, A., Cerman, Z., Striffler, B. F., Spaeth, M., and Barthlott, W. (2007) The dream of staying clean: Lotus and biomimetic surfaces. *Bioinspir. Biomim.,* **2**(4), S126—-S134.

[10] Pimentel, D. (2005) Environmental and economic costs of the application of pesticides primarily in the United States. *Environ. Dev. Sustain.,* **7**(2), 229–252.

[11] Glenn, D. M., Puterka, G. J., VanderZwet, T., Byers, R. E., and Feldhake, C. (1999) Hydrophobic particle films: a new paradigm for suppression of arthropod pests and plant diseases. *J. Econ. Entomol.,* **92**(4), 759–771.

[12] Graf, C., Kesel, A. B., Gorb, E. V., Gorb, S. N., and Dirks, J.-H. H. (2018) Investigating the efficiency of a bio-inspired insect repellent surface structure. *Bioinspir. Biomim.,* **13**(5), 56010.

[13] Radinovsky, S. and Krantz, G. W. (1962) The use of Fluon to prevent the escape of stored-product insects from glass containers. *J. Econ. Entomol.,* **55**(5), 815–816.

[14] Wong, T.-S., Kang, S. H., Tang, S. K. Y., Smythe, E. J., Hatton, B. D., Grinthal, A., and Aizenberg, J. (2011) Bioinspired self-repairing slippery surfaces with pressure-stable omniphobicity. *Nature,* **477**(7365), 443–447.

[15] Boiteau, G., Pelletier, Y., Misener, G. C., and Bernard, G. (1994) Development and Evaluation of a Plastic Trench Barrier for Protection of Potato from Walking Adult Colorado Potato Beetles (Coleoptera: Chrysomelidae). *J. Econ. Entomol.,* **87**(5), 1325–1331.

[16] Hill, D. S. (2008) Pest damage to crop plants, Springer, Dordrecht.

[17] Sallam, M. N. Insect Damage: Post-harvest Operations. `http://www.fao.org/in-action/inpho/crop-compendium/pests/en/` (1999) (accessed 27.07.2018).

[18] Douglas, A. E. (2006) Phloem-sap feeding by animals: problems and solutions. *J. Exp. Bot.,* **57**(4), 747–754.

[19] Boote, K. J., Jones, J. W., Mishoe, J. W., and Berger, R. D. (1983) Coupling pests to crop growth

simulators to predict yield reductions. *Phytopathology,* **73**(11), 1581–1587.

[20] Oerke, E.-C. (2006) Crop losses to pests. *J. Agric. Sci.,* **144**, 31–43.

[21] Sharma, S., Kooner, R., and Arora, R. (2017) Insect Pests and Crop Losses, Springer, Singapore.

[22] Bueno, A. M. and Jones, O. (2001) Alternative methods for controlling the olive fly,. *IOBC wprs Bull.,* **25**(9), 1–11.

[23] Hepdurgun, B., Turanli, T., and Zümreoğlu, A. (2009) Control of the olive fruit fly, *Bactrocera oleae,* (Diptera: Tephritidae) through mass trapping and mass releases of the parasitoid *Psyttalia concolor* (Hymenoptera: Braconidae) reared on irradiated mediterranean fruit fly. *Biocontrol Sci. Technol.,* **19**, 211–224.

[24] Hoelmer, K. A., Kirk, A. A., Pickett, C. H., Daane, K. M., Johnson, W., Hoelmer, K. A., Kirk, A. A., Pickett, C. H., and Daane, K. M. (2011) Prospects for improving biological control of olive fruit fly, *Bactrocera oleae* (Diptera: Tephritidae), with introduced parasitoids (Hymenoptera). *Biocontrol Sci. Technol.,* **21**(9), 1005–1025.

[25] Cramer, H. H. (1967) Plant protection and world crop production, Bayer, Leverkusen.

[26] Dhaliwal, G. S., Jindal, V., and Dhawan, A. K. (2010) Insect pest problems and crop losses: changing trends. *Indian J. Ecol.,* **37**(1), 1–7.

[27] Brown, C., Lynch, L., and Zilberman, D. (2002) The economics of controlling insect-transmitted plant diseases. *Amer. J. Agr. Econ.,* **84**(2), 279–291.

[28] Gratwick, M. (1992) Crop Pests in the UK, Springer Netherlands, Dordrecht.

[29] Meissle, M., Mouron, P., Musa, T., Bigler, F., Pons, X., Vasileiadis, V. P., Otto, S., Antichi, D., Kiss, J., J.; Pálinkás, Z., Dorner, Z., van der Weide, R., Groten, J., Czembor, E., Adamczyk, J., Thibord, J.-B., Melander, B., Cordsen Nielsen, G., Poulsen, R. T., Zimmermann, O., Verschwele, A., and Oldenburg, E. (2010) Pests, pesticide use and alternative options in European maize production: current status and future prospects. *J. Appl. Entomol.,* **134**, 357–375.

[30] Lehane, M. J. (2005) The Biology of Blood-Sucking in Insects, Cambridge University Press, Cambridge 2nd edition.

[31] Sarwar, M. (2015) Insect vectors involving in mechanical transmission of human pathogens for serious diseases. *Int. J. Bioinforma. Biomed. Eng.,* **1**(3), 300–306.

[32] Volcheck, G. W. (2008) Stinging Insect Allergy, Mayo Foundation for Medical Education and Research, Rochester.

[33] Parola, P. and Raoult, D. (2001) Ticks and tickborne bacterial diseases in humans: an emerging infectious threat. *Clin. Infect. Dis.,* **32**(6), 897–928.

[34] Estrada-Peña, A. and Jongejan, F. (1999) Ticks feeding on humans: a review of records on human-biting Ixodoidea with special reference to pathogen transmission. *Exp. Appl. Acarol.,* **23**(9), 685–715.

[35] Greenwood, B. M., Fidock, D. A., Kyle, D. E., Kappe, S. H. I., Alonso, P. L., Collins, F. H., and Duffy, P. E. (2008) Malaria: progress, perils, and prospects for eradication. *J. Clin. Invest.,* **118**(4), 1266–1276.

[36] Fredericks, A. C. and Fernandez-Sesma, A. (2014) The burden of dengue and Chikungunya worldwide:

Implications for the Southern United States and California. *Ann. Glob. Heal.,* **80**(6), 466–475.

[37] Stanaway, J. D., Shepard, D. S., Undurraga, E. A., Halasa, Y. A., Coffeng, L. E., Brady, O. J., Hay, S. I., Bedi, N., Bensenor, I. M., Castañeda-Orjuela, C. A., Chuang, T.-W., Gibney, K. B., Memish, Z. A., Rafay, A., Ukwaja, K. N., Yonemoto, N., and Murray, C. J. L. (2016) The global durden of dengue: an analysis from the Global Burden of Disease Study 2013. *Lancet Infect. Dis.,* **16**(6), 712–723.

[38] Budd, L. T. (1999) DFID-funded tsetse and trypanosome research and development since 1980. *Econ. Anal.,* **123**(2).

[39] Geden, C. J. and Hoqsette, J. (1994) Research and extension needs for integrated pest management for arthropods of veterinary importance. In *Proc. a Work. Lincoln, Nebraska, April 12-14, 1994.*

[40] Kunz, S. E., Murrell, K. D., Lambert, G., James, L. F., and Terrill, C. E. (1991) Estimated losses of livestock to pests, CRC Press, Boca Raton, Florida.

[41] Taylor, D. B., Moon, R. D., and M., D. R. (2012) Economic Impact of Stable Flies (Diptera: Muscidae) on Dairy and Beef Cattle Production. *J. Med. Entomol.,* **49**(1), 198–209.

[42] Su, N.-Y. and Scheffrahn, R. H. (2000) Termites as Pests of Buildings, Springer Netherlands, Dordrecht.

[43] Donovan, S. E., Eggleton, P., Dubbin, W. E., Batchelder, M., and Dibog, L. (2001) The effect of a soil-feeding termite, *Cubitermes fungifaber* (Isoptera: Termitidae) on soil properties: termites may be an important source of soil microhabitat heterogeneity in tropical forests. *Pedobiologia,* **45**(1), 1–11.

[44] Black, H. and Okwakol, M. (1997) Agricultural intensification, soil biodiversity and agroecosystem function in the tropics: the role of termites. *Appl. Soil Ecol.,* **6**(1), 37–53.

[45] Dawes, T. Z. (2010) Reestablishment of ecological functioning by mulching and termite invasion in a degraded soil in an Australian savanna. *Soil Biol. Biochem.,* **42**(10), 1825–1834.

[46] Mahapatro, G. K. and Chatterjee, D. (2018) Termites as Structural Pest: Status in Indian Scenario. *Proc. Natl. Acad. Sci. India Sect. B Biol. Sci.,* **88**(3), 977–994.

[47] Ghaly, A. and Edwards, S. (2011) Termite Damage to Buildings: Nature of Attacks and Preventive Construction Methods. *Am. J. Eng. Appl. Sci.,* **4**(2), 187–200.

[48] Trematerra, P. and Pinniger, D. (2018) Museum Pests-Cultural Heritage Pests, Springer, Berlin, Heidelberg.

[49] Endlein, T. and Federle, W. (2015) On heels and toes: How ants climb with adhesive pads and tarsal friction hair arrays. *PLoS One,* **10**(11), e0141269.

[50] Labonte, D., Williams, J. A., and Federle, W. (2014) Surface contact and design of fibrillar 'friction pads' in stick insects (*Carausius morosus*): Mechanisms for large friction coefficients and negligible adhesion. *J. R. Soc. Interface,* **11**, 20140034.

[51] Fuller, K. N. G. and Tabor, D. (1975) The effect of surface roughness on the adhesion of elastic solids. *Proc. R. Soc. Lond. A,* **345**(1642), 327–342.

[52] Persson, B. N. J. (2007) Biological Adhesion for Locomotion on Rough Surfaces: Basic Principles and A Theorist's View. *MRS Bull.,* **32**(6), 486–490.

[53] Lin, H., Qu, Z., and Meredith, J. C. (2016) Pressure sensitive microparticle adhesion through biomimicry

of the pollen-stigma interaction. *Soft Matter,* **12**, 2965–2975.

[54] Amador, G. J., Matherne, M., Waller, D., Mathews, M., Gorb, S. N., and Hu, D. L. (2017) Honey bee hairs and pollenkitt are essential for pollen capture and removal. *Bioinspiration and Biomimetics,* **12**(2), 26015.

[55] Gorb, S. N. (2002) Attachment Devices of Insect Cuticle, Kluwer Academic Publishers, Dordrecht.

[56] Endlein, T. and Federle, W. (2008) Walking on smooth or rough ground: Passive control of pretarsal attachment in ants. *J. Comp. Physiol. A,* **194**(1), 49–60.

[57] Dirks, J.-H. and Federle, W. (2011) Fluid-based adhesion in insects - principles and challenges. *Soft Matter,* **7**(23), 11047.

[58] Goetzke, H. H., Pattrick, J. G., and Federle, W. (2019) Froghoppers jump from smooth plant surfaces by piercing them with sharp spines. *Proc. Natl. Acad. Sci.,* **116**(8), 3012–3017.

[59] Dai, Z., Gorb, S. N., and Schwarz, U. (2002) Roughness-dependent friction force of the tarsal claw system in the beetle *Pachnoda marginata* (Coleoptera, Scarabaeidae). *J. Exp. Biol.,* **205**, 2479–2488.

[60] Bullock, J. M. R. and Federle, W. (2011) The effect of surface roughness on claw and adhesive hair performance in the dock beetle *Gastrophysa viridula*. *Insect Sci.,* **18**(3), 298–304.

[61] Bullock, J. M. R. and Federle, W. (2009) Division of labour and sex differences between fibrillar, tarsal adhesive pads in beetles: effective elastic modulus and attachment performance. *J. Exp. Biol.,* **212**(12), 1876–1888.

[62] Dirks, J. H. (2014) Physical principles of fluid-mediated insect attachment - Shouldn't insects slip?. *Beilstein J. Nanotechnol.,* **5**(1), 1160–1166.

[63] Federle, W. (2006) Why are so many adhesive pads hairy?. *J. Exp. Biol.,* **209**(14), 2611–2621.

[64] Clemente, C. J. and Federle, W. (2008) Pushing versus pulling: Division of labour between tarsal attachment pads in cockroaches. *Proc. R. Soc. B,* **275**(1640), 1329–1336.

[65] Haas, F. and Gorb, S. (2004) Evolution of locomotory attachment pads in the Dermaptera (Insecta). *Arthropod Struct. Dev.,* **33**(1), 45–66.

[66] Langer, M. G., Ruppersberg, J. P., and Gorb, S. (2004) Adhesion forces measured at the level of a terminal plate of the fly's seta. *Proc. R. Soc. B Biol. Sci.,* **271**(1554), 2209–2215.

[67] Bullock, J. M. R., Drechsler, P., and Federle, W. (2008) Comparison of smooth and hairy attachment pads in insects: friction, adhesion and mechanisms for direction-dependence. *J. Exp. Biol.,* **211**(20), 3333–3343.

[68] Stork, N. E. (1980) Experimental analysis of adhesion of *Chrysolina polita* (Chrysomelidae: Coleoptera) on a variety of surfaces. *J. Exp. Biol.,* **88**, 91–107.

[69] Gorb, E. V., Hosoda, N., Miksch, C., and Gorb, S. N. (2010) Slippery pores: anti-adhesive effect of nanoporous substrates on the beetle attachment system. *J. R. Soc. Interface,* **7**(52), 1571–1579.

[70] Voigt, D., Schuppert, J. M., Dattinger, S., and Gorb, S. N. (2008) Sexual dimorphism in the attachment ability of the Colorado potato beetle *Leptinotarsa decemlineata* (Coleoptera: Chrysomelidae) to rough substrates. *J. Insect Physiol.,* **54**(5), 765–776.

[71] Drechsler, P. and Federle, W. (2006) Biomechanics of smooth adhesive pads in insects: Influence of tarsal

secretion on attachment performance. *J. Comp. Physiol. A,* **192**(11), 1213–1222.

[72] Gladun, D., Gorb, S., and Frantsevich, L. I. (2009) Alternative Tasks of the Insect Arolium with Special Reference to Hymenoptera, Springer, Dordrecht.

[73] Federle, W., Brainerd, E. L., McMahon, T. A., and Hölldobler, B. (2001) Biomechanics of the movable pretarsal adhesive organ in ants and bees. *Proc. Natl. Acad. Sci.,* **98**(11), 6215–6220.

[74] Frantsevich, L. and Gorb, S. (2002) Arcus as a tensegrity structure in the arolium of wasps (Hymenoptera: Vespidae). *Zoology,* **105**(3), 225–237.

[75] Song, Y., Dai, Z., Wang, Z., Ji, A., and Gorb, S. N. (2016) The synergy between the insect-inspired claws and adhesive pads increases the attachment ability on various rough surfaces. *Sci. Rep.,* **6**, 26219.

[76] Beutel, R. G. and Gorb, S. N. (2001) Ultrastructure of attachment specializations of hexapods (Arthropoda): Evolutionary patterns inferred from a revised ordinal phylogeny. *J. Zool. Syst. Evol. Res.,* **39**(4), 177–207.

[77] Labonte, D. and Federle, W. (2013) Functionally different pads on the same foot allow control of attachment: Stick insects have load-sensitive "heel" pads for friction and shear-sensitive "toe" pads for adhesion. *PLoS One,* **8**(12), e81943.

[78] Betz, O., Frenzel, M., Steiner, M., Vogt, M., Kleemeier, M., Hartwig, A., Sampalla, B., Rupp, F., Boley, M., and Schmitt, C. (2017) Adhesion and friction of the smooth attachment system of the cockroach *Gromphadorhina portentosa* and the influence of the application of fluid adhesives. *Biol. Open,* **6**(5), 589–601.

[79] Dirks, J.-H., Clemente, C. J., and Federle, W. (2010) Insect tricks: two-phasic foot pad secretion prevents slipping.. *J. R. Soc. Interface,* **7**, 587–593.

[80] Peisker, H., Heepe, L., Kovalev, A. E., and Gorb, S. N. (2014) Comparative study of the fluid viscosity in tarsal hairy attachment systems of flies and beetles. *J. R. Soc. Interface,* **11**(99), 20140752.

[81] Reitz, M., Gerhardt, H., Schmitt, C., Betz, O., Albert, K., and Lammerhofer, M. (2015) Analysis of chemical profiles of insect adhesion secretions by gas chromatography-mass spectrometry. *Anal. Chim. Acta,* **854**, 47–60.

[82] Abou, B., Gay, C., Laurent, B., Cardoso, O., Voigt, D., Peisker, H., and Gorb, S. (2010) Extensive collection of femtolitre pad secretion droplets in the beetle *Leptinotarsa decemlineata* allows nanolitre microrheology. *J. R. Soc. Interface,* **7**(53), 1745–1752.

[83] Federle, W., Riehle, M., Curtis, A. S., and Full, R. J. (2002) An integrative study of insect adhesion: mechanics and wet adhesion of pretarsal pads in ants. *Integr. Comp. Biol.,* **42**(6), 1100–1106.

[84] Labonte, D. and Federle, W. (2015) Rate-dependence of 'wet' biological adhesives and the function of the pad secretion in insects. *Soft Matter,* **11**(44), 8661–8673.

[85] Anyon, M. J., Orchard, M. J., Buzza, D. M. A., Humphries, S., and Kohonen, M. M. (2012) Effect of particulate contamination on adhesive ability and repellence in two species of ant (Hymenoptera; Formicidae). *J. Exp. Biol.,* **215**(4), 605–616.

[86] Bernadou, A. and Fourcassié, V. (2008) Does substrate coarseness matter for foraging ants? An experi-

ment with *Lasius niger* (Hymenoptera; Formicidae). *J. Insect Physiol.,* **54**(3), 534–542.

[87] England, M. W., Sato, T., Yagihashi, M., Hozumi, A., Gorb, S. N., and Gorb, E. V. (2016) Surface roughness rather than surface chemistry essentially affects insect adhesion. *Beilstein J. Nanotechnol.,* **7**(1), 1471–1479.

[88] Federle, W. and Bruening, T. (2006) Ecology and Biomechanics of Slippery Wax Barriers and Wax Running in Macaranga-Ant Mutualisms, CRC Press, Boca Raton, Florida.

[89] Scholz, I., Buckins, M., Dolge, L., Erlinghagen, T., Weth, A., Hischen, F., Mayer, J., Hoffmann, S., Riederer, M., Riedel, M., and Baumgartner, W. (2010) Slippery surfaces of pitcher plants: *Nepenthes* wax crystals minimize insect attachment *via* microscopic surface roughness. *J. Exp. Biol.,* **213**(7), 1115–1125.

[90] Zhou, Y., Robinson, A., Steiner, U., and Federle, W. (2014) Insect adhesion on rough surfaces: analysis of adhesive contact of smooth and hairy pads on transparent microstructured substrates. *J. R. Soc. Interface,* **11**(98), 20140499.

[91] Hackmann, A., Delacave, H., Robinson, A., Labonte, D., and Federle, W. (2015) Functional morphology and efficiency of the antenna cleaner in *Camponotus rufifemur ants*. *R. Soc. Open Sci.,* **2**(7), 150129.

[92] Amador, G. J. and Hu, D. L. (2015) Cleanliness is next to godliness: mechanisms for staying clean. *J. Exp. Biol.,* **218**(20), 3164–3174.

[93] Orchard, M. J., Kohonen, M., and Humphries, S. (2012) The influence of surface energy on the self-cleaning of insect adhesive devices. *J. Exp. Biol.,* **215**(2), 279–286.

[94] Clemente, C. J., Bullock, J. M. R., Beale, A., and Federle, W. (2010) Evidence for self-cleaning in fluid-based smooth and hairy adhesive systems of insects. *J. Exp. Biol.,* **213**(4), 635–642.

[95] Mengüç, Y., Röhrig, M., Abusomwan, U., Hölscher, H., and Sitti, M. (2014) Staying sticky: contact self-cleaning of gecko-inspired adhesives. *J. R. Soc. Interface,* **11**(94), 20131205–20131205.

[96] Hansen, W. R. and Autumn, K. (2005) Evidence for self-cleaning in gecko setae. *Proc. Natl. Acad. Sci.,* **102**(2), 385–389.

[97] Amador, G. J., Endlein, T., and Sitti, M. (2017) Soiled adhesive pads shear clean by slipping: a robust self-cleaning mechanism in climbing beetles. *J. R. Soc. Interface,* **14**(131), 20170134.

[98] Gorb, E., Haas, K., Henrich, A., Enders, S., Barbakadze, N., and Gorb, S. (2005) Composite structure of the crystalline epicuticular wax layer of the slippery zone in the pitchers of the carnivorous plant *Nepenthes alata* and its effect on insect attachment. *J. Exp. Biol.,* **208**(24), 4651–4662.

[99] Bohn, H. F. and Federle, W. (2004) Insect aquaplaning: *Nepenthes* pitcher plants capture prey with the peristome, a fully wettable water-lubricated anisotropic surface. *Proc. Natl. Acad. Sci.,* **101**(39), 14138–14143.

[100] Koch, K., Bhushan, B., and Barthlott, W. (2010) Multifunctional plant surfaces and smart materials, Springer, Würzburg.

[101] Gorb, E. V., Baum, M. J., and Gorb, S. N. (2013) Development and regeneration ability of the wax coverage in *Nepenthes alata* pitchers: a cryo-SEM approach. *Sci. Rep.,* **3**.

[102] Wang, G., Guo, Z., and Liu, W. (2014) Interfacial effects of superhydrophobic plant surfaces: A review. *J. Bionic Eng.,* **11**(3), 325–345.

[103] Chu, Z. and Seeger, S. (2014) Superamphiphobic surfaces. *Chem. Soc. Rev.,* **43**(8), 2784–2798.

[104] Riedel, M., Eichner, A., Meimberg, H., and Jetter, R. (2007) Chemical composition of epicuticular wax crystals on the slippery zone in pitchers of five *Nepenthes* species and hybrids. *Planta,* **225**(6), 1517–1534.

[105] Gorb, E. and Gorb, S. (2002) Attachment ability of the beetle *Chrysolina fastuosa* on various plant surfaces. *Entomol. Exp. Appl.,* **105**(1), 13–28.

[106] Gorb, S. N. (2010) Biological and biologically inspired attachment systems, Springer Berlin Heidelberg, Berlin, Heidelberg.

[107] Bauer, U. and Federle, W. (2009) The insect-trapping rim of *Nepenthes* pitchers. *Plant Signal. Behav.,* **4**(11), 1019–1023.

[108] Gaume, L. and Forterre, Y. (2007) A viscoelastic deadly fluid in carnivorous pitcher plants. *PLoS One,* **2**(11), e1185.

[109] Whitney, H. M. and Federle, W. (2013) Biomechanics of plant-insect interactions. *Curr. Opin. Plant Biol.,* **16**(1), 105–111.

[110] Federle, W., Maschwitz, U., Fiala, B., Riederer, M., and Hölldobler, B. (1997) Slippery ant-plants and skilful climbers: selection and protection of specific ant partners by epicuticular wax blooms in *Macaranga* (Euphorbiaceae). *Oecologia,* **112**(2), 217–224.

[111] Bohn, H. F., Thornham, D. G., and Federle, W. (2012) Ants swimming in pitcher plants: kinematics of aquatic and terrestrial locomotion in *Camponotus schmitzi*. *J. Comp. Physiol. A,* **198**(6), 465–476.

[112] Zhou, Y. (2015) Insect adhesion on rough surfaces and properties of insect repellent surfaces (PhD thesis), University of Cambridge, Cambridge.

[113] Grube, A., Donaldson, D., Kiely, T., Wu, L., and Kiely, T. Pesticides Industry Sales and Usage: 2006 and 2007 Market Estimates. (2011).

[114] Atwood, D. and Paisley-Jones, C. Pesticides industry sales and usage: 2008-2012 Market Estimates. (2017).

[115] Casida, J. E. and Quistad, G. B. (1998) Golden age of insecticide research: past, present, or future?. *Annu. Rev. Entomol.,* **43**(1), 1–16.

[116] Nauen, R. (2006) Insecticide mode of action: return of the ryanodine receptor. *Pest Manag. Sci.,* **62**(8), 690–692.

[117] Sparks, T. C. and Nauen, R. (2015) IRAC: Mode of action classification and insecticide resistance management. *Pestic. Biochem. Physiol.,* **121**, 122–128.

[118] Tilman, D., Fargione, J., Wolff, B., D'Antonio, C., Dobson, A., Howarth, R., Schindler, D., Schlesinger, W. H., Simberloff, D., and Swackhamer, D. (2001) Forecasting agriculturally driven global environmental change. *Science,* **292**(5515), 281–284.

[119] Ghormade, V., Deshpande, M. V., and Paknikar, K. M. (2011) Perspectives for nano-biotechnology enabled protection and nutrition of plants. *Biotechnol. Adv.,* **29**(6), 792–803.

[120] Walker, C. (1990) Persistent pollutants in fish-eating sea birds - bioaccumulation, metabolism and effects. *Aquat. Toxicol.,* **17**(4), 293–324.

[121] Naqvi, S. M. and Vaishnavi, C. (1993) Bioaccumulative potential and toxicity of endosulfan insecticide to non-target animals. *Comp. Biochem. Physiol. Part C Comp. Pharmacol.,* **105**(3), 347–361.

[122] Pimentel, D. (1997) Pest management in agriculture, John Wiley & Sons, Chichester, UK.

[123] Richter, E. (2002) Acute human pesticide poisonings, Dekker, New York.

[124] Jeyaratnam, J. (1990) Acute Pesticide Poisoning: a Major Global Health Problem. *World Heal. Stat Q.,* **43**(3), 139–144.

[125] National Research Council (1987) Estimates of dietary oncogenic risks, The National Academy Press, Washington, DC.

[126] Foster, S. P., Tomiczek, M., Thompson, R., Denholm, I., Poppy, G., Kraaijeveld, A. R., and Powell, W. (2007) Behavioural side-effects of insecticide resistance in aphids increase their vulnerability to parasitoid attack. *Anim. Behav.,* **74**(3), 621–632.

[127] Freebairn, K., Yen, J. L., and McKenzie, J. A. (1996) Environmental and genetic effects on the asymmetry pnenotype: Diazinon resistance in the Australian sheep blowfly, *Lucilia cuprina. Genetics,* **144**(1), 229–239.

[128] Devine, G. J. and Furlong, M. J. (2007) Insecticide use: Contexts and ecological consequences. *Agric. Human Values,* **24**(3), 281–306.

[129] Cônsoli, F. L., Parra, J. R. P., and Hassan, S. A. (1998) Side-effects of insecticides used in tomato fields on the egg parasitoid *Trichogramma pretiosum* Riley (Hym., Trichogrammatidae), a natural enemy of *Tuta absoluta* (Meyrick) (Lep., Gelechiidae). *J. Appl. Entomol.,* **122**(1-5), 43–47.

[130] Athanassiou, C. G. and Arthur, F. H. (2018) Bacterial Insecticides and Inert Materials, Springer, Berlin, Heidelberg.

[131] Prasad, R., Kumar, V., and Prasad, K. S. (2014) Nanotechnology in sustainable agriculture: Present concerns and future aspects. *African J. Biotechnol.,* **13**(6), 705–713.

[132] Bhattacharyya, A., Bhaumik, A., Rani, P., Mandal, S., and Epidi, T. (2010) Nano-particles - A recent approach to insect pest control. *African J. Biotechnol.,* **9**(24), 3489–3493.

[133] Alexander, P., Kitchener, J. A., and Briscoe, H. V. A. (1944) Inert dust insecticides: Part I. Mechanism of action. *Ann. Appl. Biol.,* **31**(2), 143–149.

[134] Kavallieratos, N. G., Athanassiou, C. G., Korunic, Z., and Mikeli, N. H. (2015) Evaluation of three novel diatomaceous earths against three stored-grain beetle species on wheat and maize. *Crop Prot.,* **75**, 132–138.

[135] Ebeling, W. (1961) Physicochemical mechanisms for the removal of insect wax by means of finely divided powders. *Hilgardia,* **30**(18), 531–564.

[136] Telford, A. M., Easton, C. D., Hawkett, B. S., and Neto, C. (2016) Waterborne, all-polymeric, colloidal 'raspberry' particles with controllable hydrophobicity and water droplet adhesion properties. *Thin Solid Films,* **603**, 69–74.

[137] Unruh, T. R., Knight, A. L., Upton, J., Glenn, D. M., and Puterka, G. J. (2000) Particle films for suppression of the codling moth (Lepidoptera: Tortricidae) in apple and pear orchards. *J. Econ. Entomol.,* **93**(3), 737–743.

[138] Puterka, G. J., Glenn, D. M., and Pluta, R. C. (2005) Action of particle films on the biology and behavior of pear psylla (Homoptera: Psyllidae). *J. Econ. Entomol.,* **98**(6), 2079–2088.

[139] Peng, L., Trumble, J. T., Munyaneza, J. E., and Liu, T.-X. (2011) Repellency of a kaolin particle film to potato psyllid, *Bactericera cockerelli* (Hemiptera: Psyllidae), on tomato under laboratory and field conditions. *Pest Manag. Sci.,* **67**(7), 815–824.

[140] Saour, G. and Makee, H. (2004) A kaolin-based particle film for suppression of the olive fruit fly *Bactrocera oleae* Gmelin (Dip., Tephritidae) in olive groves. *J. Appl. Entomol.,* **128**(1), 28–31.

[141] Pascual, S., Cobos, G., Seris, E., and González-Núñez, M. (2010) Effects of processed kaolin on pests and non-target arthropods in a Spanish olive grove. *J. Pest Sci. (2004).,* **83**(2), 121–133.

[142] Glenn, D. M. and Puterka, G. J. (2010) Particle films: a new technology for agriculture, Vol. 31, John Wiley & Sons, Inc., .

[143] Maloney, K. M., Ancca-Juarez, J., Salazar, R., Borrini-Mayori, K., Niemierko, M., Yukich, J. O., Naquira, C., Keating, J. A., and Levy, M. Z. (2013) Comparison of insecticidal paint and deltamethrin against *Triatoma infestans* (Hemiptera: Reduviidae) feeding and mortality in simulated natural conditions. *J. Vector Ecol.,* **38**(1), 6–11.

[144] Gorla, D. E., Vargas Ortiz, R., and Catalá, S. S. (2015) Control of rural house infestation by *Triatoma infestans* in the Bolivian Chaco using a microencapsulated insecticide formulation. *Parasit. Vectors,* **8**(1), 255.

[145] Mosqueira, B., Chabi, J., Chandre, F., Akogbeto, M., Hougard, J.-M., Carnevale, P., and Mas-Coma, S. (2010) Efficacy of an insecticide paint against malaria vectors and nuisance in West Africa - Part 2: Field evaluation. *Malar. J.,* **9**(1), 341.

[146] Overman, G. R. Method for admixing plant essential oils to coatings for the purpose of repelling insects. (2009) US Patent 20090155394.

[147] Tomioka, T. Insect repellent coating and industrial product using the same. (2006) US Patent 2006177472.

[148] Maia, M. and Moore, S. J. (2011) Plant-based insect repellents: a review of their efficacy, development and testing. *Malar. J.,* **10**.

[149] Coats, J. R., Karr, L. L., and Drewes, C. D. (1991) Toxicity and neurotoxic effects of monoterpenoids: in insects and earthworms, American Chemical Society, .

[150] Lee, S.-E., Lee, B.-H., Choi, W.-S., Park, B.-S., Kim, J.-G., and Campbell, B. C. (2001) Fumigant toxicity of volatile natural products from Korean spices and medicinal plants towards the rice weevil, *Sitophilus oryzae* (L). *Pest Manag. Sci.,* **57**(6), 548–553.

[151] Yang, P. and Ma, Y. (2005) Repellent effect of plant essential oils against *Aedes albopictus*. *J. Vector Ecol.,* **30**(2), 231–234.

[152] Scialdone, M. A. Formulations containing insect repellent compounds. (2014) US Patent 8748477.

[153] Schaller, M. and Korting, H. (1995) Allergie airborne contact dermatitis from essential oils used in aromatherapy. *Clin. Exp. Dermatol.,* **20**(2), 143–145.

[154] Trattner, A., David, M., and Lazarov, A. (2008) Occupational contact dermatitis due to essential oils. *Contact Dermatitis,* **58**(5), 282–284.

[155] Wenzel, R. N. (1936) Resistance of solid surfaces to wetting by water. *Ind. Eng. Chem.,* **28**(8), 988–994.

[156] Cassie, A. B. D. and Baxter, S. (1944) Wettability of porous surfaces. *Trans. Faraday Soc.,* **40**(5), 546–551.

[157] Roach, P., Shirtcliffe, N. J., and Newton, M. I. (2008) Progess in superhydrophobic surface development. *Soft Matter,* **4**(2), 224–240.

[158] Tuteja, A., Choi, W., Ma, M., Mabry, J. M., Mazzella, S. a., Rutledge, G. C., McKinley, G. H., and Cohen, R. E. (2007) Designing superoleophobic surfaces. *Science,* **318**(5856), 1618–1622.

[159] Koch, K., Dommisse, A., Barthlott, W., and Gorb, S. N. (2007) The use of plant waxes as templates for micro- and nanopatterning of surfaces. *Acta Biomater.,* **3**(6), 905–909.

[160] Zhang, S. (2003) Fabrication of novel biomaterials through molecular self-assembly. *Nat. Biotechnol.,* **21**(10), 1171–1178.

[161] Hawker, C. J. and Russell, T. P. (2005) Block copolymer lithography: Merging "bottom-up"with "top-down" processes. *MRS Bull.,* **30**(12), 952–966.

[162] Goodwin, W. B., Shin, D., Sabo, D., Hwang, S., Zhang, Z. J., Meredith, J. C., and Sandhage, K. H. (2017) Tunable multimodal adhesion of 3D, nanocrystalline $CoFe_2O_4$ pollen replicas. *Bioinspir. Biomim.,* **12**(6), 066009.

[163] Johnstone, L. R., Gomez, I. J., Lin, H., Fadiran, O. O., Chen, V. W., Meredith, J. C., and Perry, J. W. (2017) Adhesion Enhancements and Surface-Enhanced Raman Scattering Activity of Ag and $Ag@SiO_2$ Nanoparticle Decorated Ragweed Pollen Microparticle Sensor. *ACS Appl. Mater. Interfaces,* **9**(29), 24804–24811.

[164] Bauer, U., Bohn, H. F., and Federle, W. (2008) Harmless nectar source or deadly trap: *Nepenthes* pitchers are activated by rain, condensation and nectar. *Proc. R. Soc. B Biol. Sci.,* **275**(1632), 259–265.

[165] Long, R. H. Surfaces upon which insects can not climb or alight and methods and means for their establishment. (1996) US Patent 5561941.

[166] Kok, M. and Young, T. M. (2014) The evaluation of hierarchical structured superhydrophobic coatings for the alleviation of insect residue to aircraft laminar flow surfaces. *Appl. Surf. Sci.,* **314**, 1053–1062.

[167] Wohl, C. J., Smith, J. G., Penner, R. K., Lorenzi, T. M., Lovell, C. S., and Siochi, E. J. (2013) Evaluation of commercially available materials to mitigate insect residue adhesion on wing leading edge surfaces. *Prog. Org. Coatings,* **76**(1), 42–50.

[168] Scholz, W. (1993) Paint Additives, Springer Science+Business Media, Dordrecht.

[169] Chen, J. and Wei, X. (2007) Coated containers with reduced concentrations of Fluon to prevent ant escape. *J. Entomol. Sci.,* **42**(1), 119–121.

[170] Epstein, A. K., Wong, T.-S., Belisle, R. A., Boggs, E. M., and Aizenberg, J. (2012) Liquid-infused structured surfaces with exceptional anti-biofouling performance. *Proc. Natl. Acad. Sci.,* **109**(33), 13182–

13187.

[171] Wilson, P. W., Lu, W., Xu, H., Kim, P., Kreder, M. J., Alvarenga, J., and Aizenberg, J. (2013) Inhibition of ice nucleation by slippery liquid-infused porous surfaces (SLIPS). *Phys. Chem. Chem. Phys.,* **15**(2), 581–585.

[172] Butt, H.-J., Barnes, W. J. P., del Campo, A., Kappl, M., and Schönfeld, F. (2010) Capillary forces between soft, elastic spheres. *Soft Matter,* **6**(23), 5930–5936.

3

Slippery paints: eco-friendly coatings that cause ants to slip

Many insects are considered to be pests and can be serious threats to buildings. Insecticides represent an effective way to control pest insects but are harmful to the environment. As an eco-friendlier alternative, we have formulated waterborne, organic paints which provided a slippery physical barrier for leafcutter ants (Atta cephalotes) *on vertical surfaces. Different paints were produced by varying the Pigment Volume Concentration (PVC) and amount of TiO_2 and $CaCO_3$ particles, and characterised in terms of contact angles, surface roughness and scrub resistance. The paints' slipperiness for* A. cephalotes *ants was evaluated in climbing tests on vertical paint panels (by recording the percentage of fallen ants). Two main factors reduced the insects' attachment to vertical paint surfaces: (1) the PVC: in paints above a critical PVC, more loose particles detach from the coating and thereby reduce insect attachment; and (2) the type, dimensions and shape of solid particles: $CaCO_3$ particles detach more easily from the paint than TiO_2, probably due to their larger size and platelet shape. Paints formulated at PVC 70 and containing 20 wt% $CaCO_3$ showed the best performance in terms of slipperiness, as well as providing good scrub resistance.*

Aurélie Féat[a,b], Walter Federle[c], Marleen Kamperman[b,d], Martin W. Murray[a], Jasper van der Gucht[b] and Philip L. Taylor[a]

[a]AkzoNobel Decorative Paints, Wexham Road, Slough, SL2 5DS, United Kingdom

[b]Physical Chemistry and Soft Matter, Wageningen University, Stippeneng 4, 6708 WE, Wageningen, The Netherlands

[c]Department of Zoology, University of Cambridge, Cambridge, CB2 3EJ, United Kingdom

[d]Zernike Institute for Advanced Materials, University of Groningen, Nijenborgh 4, 9747 AG Groningen, The Netherlands

3.1   Introduction

3.1.1   Motivation and existing methods to tackle insect pests

Many insects are considered pests, because they pose serious threat to agriculture, forestry, buildings and human health (see e.g. [1–3]). Many crawling insects, most notably termites, cockroaches and ants, cause damages to buildings and furniture, or can affect hygiene and human health [4, 5]. About 2,300 termite species have been discovered, of which 183 species were accounted for damaged buildings as they feed primarily on wood, mostly in Asia, Australia, Africa and in the USA, causing annual damages between \$2 and \$40 billion [6–8]. Many cockroach species are significant indoor pests worldwide, and can increase domestic exposure to allergens associated with asthma [5]. About 0.5% of ant species are considered pests, such as fire ants and Pharaoh ants, and have been acknowledged to be the most difficult pests to eliminate [4, 9, 10]. Ants enter buildings in search of food or cause structural damage as they establish their nests close to heat sources, especially in cooler climates [9, 10]. Thus, it is essential to prevent pest insects from entering buildings. Existing methods to do so will be briefly reviewed in this section.

Chemical treatments are widely used to tackle insect pests and include insecticide sprays, groomable coatings, baits, soil termiticide injection, and chemical fumigation [4, 10, 11]. These methods rely on insecticides, which are an effective way to control pests but cause environmental and health damage. In the United States only, the impact of pesticides (including insecticides) on health and environment were estimated in 2005 to cost more than \$8 billion annually [12], and the serious worldwide decline of insects may be partly based on the widespread use of insecticides [13].

Physical barriers can be used to prevent crawling insects from entering buildings [11]. They rely on concrete slabs, graded particles with specific sizes or sheets made of metal or plastic, and are non-toxic [14, 15]. However, such barriers do not protect buildings from drywood termites [15]. Other physical methods of combatting pest insects include heat, freezing, electricity, and microwaves, but are impractical to use in large areas [11].

Slippery paints and coatings may provide superior alternatives to the above methods as they are easy to apply, cheap, and durable, and combine aesthetic appearance with insect-repellent

properties [16]. Using environmentally-friendly essential oils and plant extracts in paint coatings is an effective alternative way to repel insects from buildings [17]. The efficacy of such coatings, however, needs to be improved, as essential oils have been reported to repel insects for only up to a few hours [11, 18], and can be increased to up to one year once incorporated into coatings [19]. Nanoparticles such as calcium carbonate and diatomaceous earths, both of which are commonly found in paints, showed insecticidal activity as insects die by desiccation after contact with these abrasive particles [20–22]. The commonly used titanium dioxide particles are genotoxic to some insect species [23]. Dispersions made of calcium carbonate particles in gelatine were also found to prevent wood infestation by termites for two years, and up to five years when combined with zinc oxide particles [24], but such dispersions cannot be readily used as exterior coatings as they would not resist e.g. weathering.

Both ants and termites are of high ecological importance as many species increase soil quality and aeration [25–28], an eco-friendlier alternative strategy to toxic insecticides is to develop coatings that prevent crawling insects from adhering to the surface by making it slippery. To this end, understanding insect locomotion and how to reduce their attachment to surfaces is of major importance.

3.1.2 Insect locomotion on surfaces

In nature, insects climb plant surfaces by sickle-shaped claws and adhesive pads that release an adhesion-mediating fluid [29–32]. Insect adhesive pads can conform to surface asperities, thereby increasing adhesion on rough substrates [32, 33]. Two categories of adhesive pads can be found in different insect orders: smooth and hairy pads [29, 34, 35]. Both types of pad secrete fluids, which can fill out surface irregularities, and thereby increase the contact area and adhesion to rough surfaces [36–38]. Fluid-mediated wet adhesion in insects occurs through van der Waals, capillary and viscous forces (Stefan adhesion) [30, 39, 40]. Second, the claws enable the insects to interlock with the substrate's protrusions [41, 42].

The oily phase of the adhesive secretion allows insects to adhere to a wide variety of substrates [29, 43, 44]. The effect of surface chemistry or surface hydrophobicity on fluid-mediated insect attachment has been studied on both natural and synthetic surfaces, and only weak or no effects were observed [45–47]. Substrate roughness has been found to dominate insect attachment forces over surface chemistry [46–48]. One interesting exception where surface chemistry

plays an important role is the underwater attachment of dock beetles *Gastrophysa viridula* De Geer (Coleoptera, Chrysomelidae); here, adhesion forces were strongly reduced on hydrophilic substrates [49].

The effect of surface roughness on insect attachment has been investigated in many studies on hairy and smooth pads. It was shown that insects produce stronger attachment forces both on 'smooth' and coarse 'rough' substrates, but their attachment is reduced on micro-rough surfaces (0.05-1 μm asperity size) [30, 46, 50–53]. The function of micro-rough surfaces in reducing insect attachment is explained by its effect on both claws and adhesive pads. The roughness of these surfaces reduces the contact area for adhesive pads, but the asperities are too small to allow interlocking of the claws [50, 51, 53].

Inspiration from nature can improve the functionality of coatings, as demonstrated by the well-known example of self-cleaning paints inspired by the surface of lotus leaves (*Nelumbo nucifera*, Gaertn., Nelumbonaceae) [54, 55]. The superhydrophobicity of lotus leaves mediated by hierarchically arranged surface structures causes water to roll off the surface and wash away particles [54]. This so-called Lotus-effect has given rise to extensive research in anti-adhesive, self-cleaning coatings, such as the exterior Lotusan paint [55].

In nature, many plant surfaces are known to be slippery to insects, in particular insect-trapping surfaces of plants covered with nano- to micrometre-sized epicuticular wax crystals, such as those found in *Nepenthes* pitcher plants, which mostly feed on ants as they fall in their traps [30, 56–59]. Both the small size and likely brittleness of wax crystals reduce their suitability for the interlocking of insect claws, and the surfaces they form are too rough for insect adhesive pads to develop sufficient contact area [50, 53, 60, 61]. Most epicuticular wax crystals also break off easily under mechanical load, leading to pad contamination, and a loss of adhesion [56, 61] (Figure 3.1).
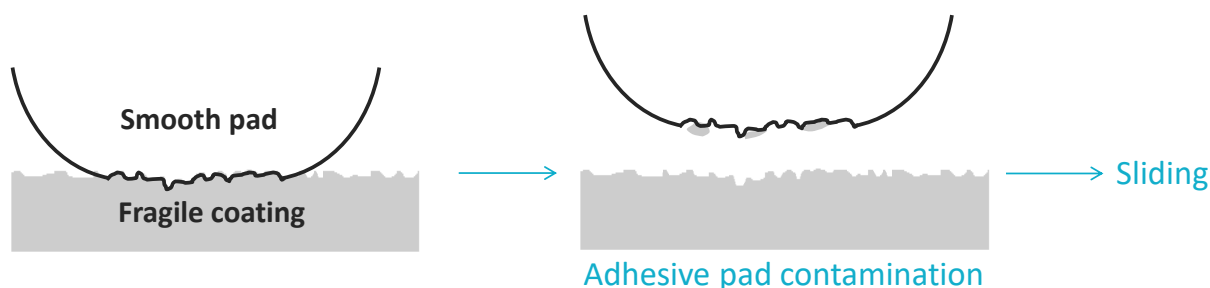

Figure 3.1: Schematic showing the contamination mechanism of smooth adhesive pads on slippery, fragile surfaces.

From a biological and biomimetic perspective, it is of interest to understand to what extent (1) particle detachment, (2) surface roughness and (3) surface lubrication contribute to reducing insect attachment on surfaces [62]. The bioinspired, slippery SLIPS surfaces developed by Aizenberg and co-workers combine surface roughness, lubrication and porosity [63–65]. The perfluorinated lubricants, however, are harmful to the environment and deplete after a certain number of uses [66]. Eco-friendlier, non-fluorinated and more durable lubricant solutions are hence being investigated [66, 67].

Zhou *et al.* studied insect attachment on various micro-structured substrates produced by photolithography and nanoimprinting with different pillar spacings (3-22 μm) and heights (0.5 and 1.4 μm) [68]. Adhesive pads on the feet of cockroaches (*Nauphoeta cinerea* Olivier (Blattodea, Blaberidae) smooth pads) and dock beetles (*G. viridula*, hairy pads) were found to make only partial contact on dense arrays of micropillars, whereas full contact was observed for wider pillar spacing (> 4 μm) and shorter pillars (0.5 μm).

The recent work of Graf *et al.* [69] achieved some reduction of insect attachment to polymer films with a dual-scale rough surface, where the larger-scale asperities had a spacing of 2 μm and asperity height of 0.9 μm. In containers covered with the polymer film, the escape rate of cockroaches (*N. cinerea*, smooth pads) was reduced by 44%, but no effect was found for beetles (*G. viridula*, hairy pads) [69]. These results suggest that surfaces can be selective for particular insects, which would have potential applications, such as allowing access to beneficial insects but not pest insect species. However, the result may also be explained by the fact that *N. cinerea* cockroaches are generally 'poorer' climbers than *G. viridula* beetles on various surfaces, including polymer films [69, 70].

In insect rearings, waterborne polytetrafluoroethylene dispersions (PTFE, Fluon or Teflon) are used to prevent insects from escaping their cages [71, 72]. Fluon-coated walls are very slippery to insects, as aggregates of PTFE particles detach from the surfaces and adhere to their pads (Figure 3.2). However, climbing ants can remove Fluon coatings from the walls of their nest containers (A.F. & W.F., personal observation), and the coatings are significantly less slippery under high humidity conditions [28].
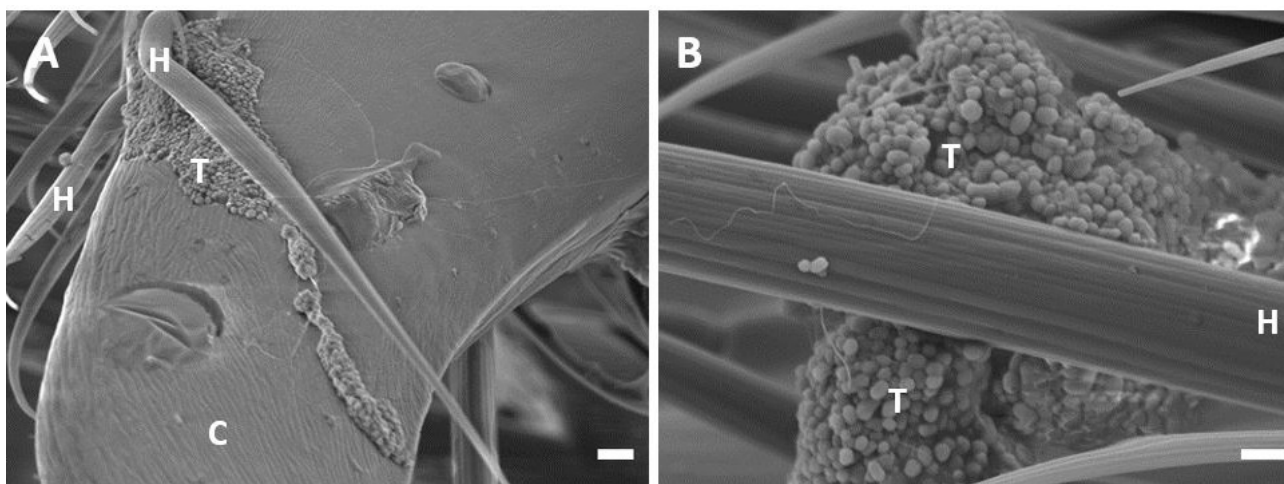
Figure 3.2: SEM images of *Atta cephalotes* tarsi after walking on a wall painted with Fluon coating (Blades Biological Ltd, Edenbridge, UK). Fluon is a slippery coating used to retain insects in their nest containers. Some areas of (A) claws and (B) tarsus' hairs are covered in PTFE particles. Labels: H: hairs, T: PTFE, C: claw. Scale bars: 1 μm.

3.1.3 Formulation of paints slippery to ants

As an eco-friendlier alternative to insecticidal coatings, we have formulated model waterborne, organic paints which provide a slippery physical barrier for crawling insects on vertical surfaces. The different paint components were systematically varied to investigate the effect of wettability, surface roughness and scrub resistance, and their slipperiness for *Atta cephalotes* L. ant workers (Hymenoptera, Formicidae) using climbing tests. The working principle of the inner wall of pitcher plant traps, causing insects to slip on a surface covered by wax crystals, inspired the paint components used in this study.

Paints are made of four major ingredients: (1) the solvent, most often water for improved health and environmental impact [73, 74]; (2) the pigment which brings opacity to the coating, e.g. TiO$_2$; (3) the polymer binder, or latex, which wets the solid particles and forms a film *via* coalescence once applied to a substrate [75, 76]; and (4), the additives, such as dispersing and biocide agents [77]. Although the monomers used in the present study are typically found in market-available coatings, our organic paints represent an eco-friendlier insect-repellent alternative owing to the absence of volatile insecticide. One of the key paint formulation parameters is the Pigment Volume Concentration (PVC), which refers to the volume of pigment with regard to the volume of binder [78, 79]:

$$PVC = \frac{Volume\ of\ pigments}{Volume\ of\ pigments + volume\ of\ binder} \tag{3.1}$$

Above a threshold value stated as the Critical Pigment Volume Concentration (CPVC), there is not enough binder to wet the pigment particles, leading to a dramatic decrease of most paint properties (e.g. gloss, durability), as well as a fragile and non-coherent coating. The CPVC of a pigment-binder system is affected by many parameters. The CPVC was found to depend on the functional monomers used and size of the polymer binder [80, 81]. The presence of certain additives such as thickeners can contribute to binding as well. The CPVC is also lower for waterborne polymers than for their solventborne counterparts [81].

3.2 Materials and methods

3.2.1 Materials

Methyl methacrylate (MMA), butyl acrylate (BA), acrylic acid (AA), sodium bicarbonate, tert-Butyl hydroperoxide (t-BHP), sodium persulfate (NaPS), sodium dodecylbenzenesulfonate and AMP 95 were obtained from Sigma-Aldrich (Gillingham, UK) and used as received. Sodium dodecyl sulphate (SDS, CMC = 7.9 mM, surface tension measurement) was used both as a stabiliser in the latex synthesis and a dispersant in the paints and was supplied by VWR (Lutterworth, UK). Bruggolite FF6 was purchased from Brueggemann (Heilbronn, Germany). Texanol was added as a coalescent and was bought from Eastman (Kingsport, TN, USA). The titanium dioxide pigment used, Tiona 595, was supplied by Cristal (Grimsby, UK) and is an aluminate- and zirconia-coated rutile with a density of 4.1 g/cm^3 and a mean particle size of 300 nm (Figure 3.3A).

The extender was a ground calcium carbonate from Omya (Orgon, France), Omyacoat 850-OG, with a density of 2.7 g/cm^3 and a mean particle size of 1 μm (Figure 3.3B). In the present work, the number of ingredients was restricted as much as possible to limit the number of possible interactions between the paint components. The model paint systems were therefore composed of only latex (polymer binder), dispersant, pigment, extender and coalescing agent and did not contain supplementary additives found in paints, such as anti-foaming agents, thickeners or biocides.

3.2.2 Latex synthesis and characterisation

Latexes, or polymer binders, are one of the main ingredients in paints, as the paint coating is formed *via* coalescence and evaporation of water. Since they bind the solid particles together, their physical properties are of major importance to understand the paint coating's properties. Acrylic binders are widely used in the coating industry given their dirt pick-up resistance, durability, UV stability, etc. [74].

An approximately 40 wt% poly(methyl methacrylate-*co*-butyl acrylate-*co*-acrylic acid) (P(MMA/BA/AA)) (52/45/3) latex was prepared by seeded semi-batch emulsion polymerisation following a conventional procedure, see e.g. [74, 81, 82]. These monomers are typically found in binders used in the coating industry. SDS, sodium bicarbonate and demineralised water were first pre-heated in a 1L-reactor to 70°C and stirred at 200 rpm. The seed was composed of 10 wt% of total monomers and 20 wt% of total initiator (sodium persulfate (NaPS)) and was prepared by batch emulsion polymerisation after adding them to the reactor. The remaining monomers and initiator (feed) were then added over the course of three hours at 75°C to grow the latex particles (Table 3.1). After cooling to 70°C and 60°C, 0.05 wt% *t*-BHP and 0.05 wt% Bruggolite FF6 were respectively injected to react with the potentially remaining unreacted monomers and reduce the Volatile Organic Components (VOC) [83]. The latex was filtered after being cooled down to 30°C.

Table 3.1: Formulation of the poly(methyl methacrylate-*co*-butyl acrylate-*co*-acrylic acid) latex used in this study. In short, it was prepared by emulsion polymerisation by feeding monomers (MMA, BA and AA) and initiator at 75°C to a pre-emulsion (seed) made of monomers stabilised by SDS. *t*-BHP and Bruggolite FF6 were added once the feed was complete to react with potentially unreacted monomers. The final latex was obtained after filtering it at 30°C.

Ingredient	Function	Initial volume (g)	Seed (g)	Feed (g)	Reducing feed (g)
Water	Solvent	464.9	20.0	80.0	16.7
SDS	Surfactant	11.8			
NaHCO$_3$	pH buffer	2.5			
MMA	Monomer		20.8	187.2	
BA	Monomer		18.0	162.0	
AA	Monomer		1.2	10.8	
NaPS	Initiator		0.6	2.4	
t-BHP	Initiator				0.5
Bruggolite FF6	Reducing agent				0.5

Table 3.2: Physical properties of the P(MMA/BA/AA) latex used in this study. M_w, T_g and MFFT refer to the polymer's molecular weight, glass transition temperature and minimum film formation temperature, respectively. The solid content and M_w were measured on samples of wet latex, while temperature transitions were measured on dried samples of polymer. The water contact angle was measured on a glass panel coated with polymer. The values are expressed as mean ± standard deviation (SD).

Particle size (nm)	Solid content (%)	M_w (kDa)	T_g (°C)	MFFT (°C)	Water contact angle (°)
68 ± 1 ($n = 10$)	41.9 ± 1.0 ($n = 3$)	633 ($n = 1$)	28.0 ± 0.8 ($n = 3$)	13.0 ± 0.6 ($n = 3$)	26.8 ± 1.6 ($n = 4$)

The physical properties of the P(MMA/BA/AA) latex are shown in Table 3.2. The particle size was determined by Dynamic Light Scattering (Delsa Nano C from Beckman Coulter, Brea, CA, USA) and was about 70 nm (68 nm ± 1 nm, $n = 10$). The 41.9% ± 1.0% ($n = 3$) solids content was measured by gravimetric analysis. To measure the molecular weight (M_w) *via* Gel Permeation Chromatography (GPC), the latex was first diluted in 4% acetic acid in tetrahydrofuran (THF) and filtered through a 0.2 μm PTFE membrane. The results were relative to a polystyrene calibration over the molecular weight range 580-8500000 g/mol (Viscotek TDA 305, Malvern, Worcestershire, UK).

The glass transition temperature (T_g) of the latex was determined to be 28.0°C ± 0.8°C ($n = 3$), which was obtained by Differential Scanning Calorimetry (DSC, Q2000, TA Instruments, Elstree, UK), after drying the latex for 24 hours at room temperature. The minimum film formation temperature (MFFT) was measured using a temperature bar (Rhopoint MFFT, Bexhill, UK) and corresponds to the lowest temperature at which a clear and coherent latex film is formed, which was 13.0°C ± 0.6°C ($n = 3$). 100 μm latex films were applied to glass panels using a film applicator (TQC Sheen, Rotterdam, The Netherlands) and dried for 24 hours. The dry latex film showed high wettability, with a water contact angle of 26.8° ± 1.6° ($n = 4$).

3.2.3   Waterborne model paint systems and characterisation

Paint preparation

45 waterborne paints were prepared as follows: 70 wt% TiO_2 and 75 wt% $CaCO_3$ slurries were prepared by dispersing the solids in water at about 2000 rpm using a Dispermat high speed disperser blade (VMA–Getzmann, Reichshof, Germany) with 0.4 wt% and 0.3 wt% SDS,
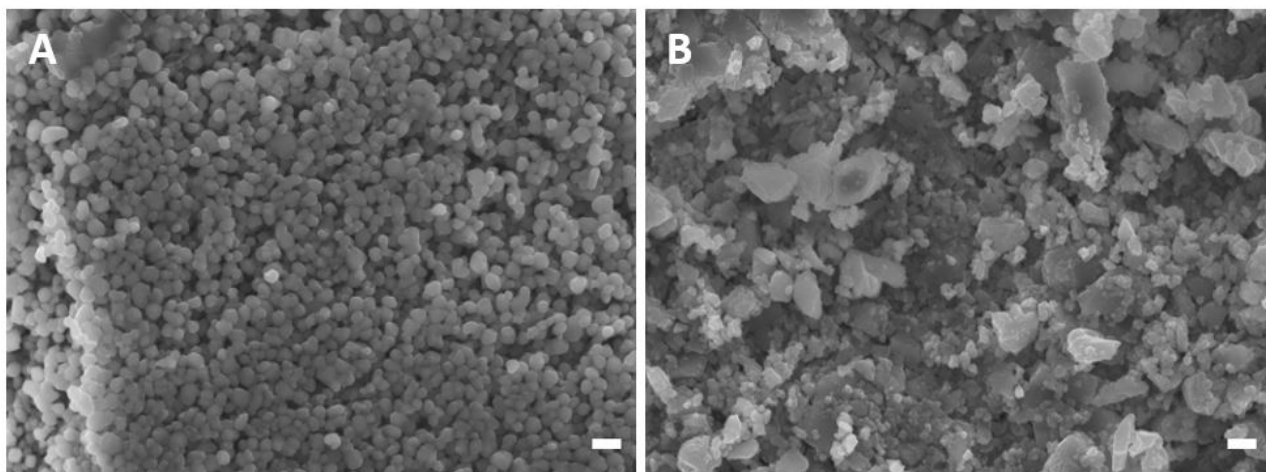
Figure 3.3: SEM images of the (A) titanium dioxide (Tiona 595, spherical shape, mean diameter: 300 nm) and (B) calcium carbonate (Omyacoat 850-OG, platelet shape, mean diameter: 1 μm) grades used in this study. Scale bars: 1 μm.

respectively. The optimum amount of surfactant was determined by the minimum viscosity dispersant demand method [84, 85]. Various TiO_2 and $CaCO_3$ quantities (0, 10, 20, 30 wt% and 0, 6.6, 13, 20 wt%, respectively) were combined at three different PVCs (50, 60 and 70) by adding the corresponding amount of neutralised latex.

These pigment and extender quantities are typically found in high PVC commercial paints. 3 wt% Texanol, based on the total formulation, was added to each paint formulation to aid the latex coalescence process and limit the formation of cracks. The pH of the paints was brought to 8-8.5 by adding, if necessary, AMP 95. These pH values are typically used in the coating industry, as (1) the effect of Texanol has been found to be optimised at alkaline pH [86] and (2) ensures that the anionic surfactants that stabilise the latexes and pigments are fully ionised.

Paint characterisation

The paints were applied on metal panels (10.5 cm × 8.5 cm) using a square film applicator (TQC Sheen, Rotterdam, The Netherlands) with a wet thickness of 100 μm and dried 24 hours at 21.5 ± 0.4°C and 49 ± 1.9%RH. The panels were 0.15 mm thick steel sheets from Ernst Sauter AG (Reinach, Switzerland) and possessed a surface roughness of 0.9 μm ± 0.2 μm.

Contact angle measurements were performed with an OCA 50 from DataPhysics (Filderstadt, Germany) using 5 μL droplets of Milli-Q water at 20.5 ± 0.5°C and 38 ± 2.0%RH. Four measurements were carried out at different locations on the panel.

The surface roughness of paint coatings was measured using NanoFocus μScan Explorer

(Oberhausen, Germany). Six measurements of 1 mm × 1 mm area (500 nm XY-resolution, 15 nm Z-resolution, 1001 pixels × 1001 pixels) were performed on the panels. The average roughness (R_a) profiles were analysed with μsoft analysis. A 'peak' was defined as any protruding region larger than 5% of the highest asperity relative to the midline, enabling access to the maximum peak height and peak density from the roughness profiles.

Scanning electron microscopy (SEM) images were obtained with JSM7001F from JEOL (Tokyo, Japan) by prior sample coating with a 30-nm carbon layer using Q150T ES (Quorum Technologies, Laughton, UK). The images were recorded at an acceleration voltage of 10.0 kV.

The scrub resistance of PVC 70 coatings was determined by abrasion weight loss tests according to the ASTM D4213-96 standard method. The paints (wet thickness = 400 μm) were applied to PVC scrub panels and dried for 7 days at 40°C ± 1°C. The coated panels were then scrubbed to either 200 or 2000 cycles at a speed of 36 cycles/min with a nylon-silicon carbide abrasive pad (40 mm × 94 mm, R_a = 30.0 ± 16.9 μm, Scotch-Brite, 3M, St. Paul, MN, USA). A force of 2.4 N was applied onto the pads in a surfactant-based scrub medium (2.5 g/L sodium dodecylbenzenesulfonate). The scrub resistance is measured as follows:

$$Scrub\ resistance\ (mg/cm^2) = \frac{weight\ loss}{scrubbed\ area} \tag{3.2}$$

When PVC > CPVC, there is not enough binder to fully wet the pigment particles, leading to a dramatic decrease of most paint properties (e.g. gloss, durability). The approximate CPVC values of the paint systems were between 54-63% as calculated using the oil absorptions provided by the suppliers (Table A3.1, Appendix) [78]:

$$CPVC(\%) = \frac{100}{1 + \dfrac{pigment\ density \times oil\ absorption}{linseed\ oil\ density}} \tag{3.3}$$

with linseed oil density = 0.93 kg/L. In the coating industry, the oil absorption of binders is estimated from the required amount of linseed oil to saturate 100 grams of pigment or extender (volume of linseed oil adsorbed per unit volume of pigment) [78]. As it reflects how much binder will be needed to fully wet the solid particles, high PVC coatings containing particles with high oil absorption values are likely to be mechanically fragile.

Insect climbing experiments

In order to select model climbing insects, we conducted preliminary tests on paint substrates on several insect species with smooth pads (weaver ants, *Oecophylla smaragdina* Fab., Hymenoptera, Formicidae); leaf cutting ants, *A. cephalotes*; stick insects, *Carausius morosus*, Sinéty; Phasmatodea, Phasmatidae; and cockroaches, *N. cinerea*), as well as hairy pads (flies, *Calliphora vicina* Robineau-Desvoidy, Diptera, Calliphoridae; and dock beetles, *G. viridula*) [70]. While there are differences in adhesive forces between different insect species, the performance of both types of pad is very similar [36], and substrates slippery for one type are also slippery for the other [70, 87]. As leaf cutting ants (*A. cephalotes*) are motivated climbers, we selected them for the climbing experiments as representatives of insects with smooth adhesive pads. Adult workers were taken from a large, 5-year-old laboratory colony kept at 24°C and fed on bramble leaves.

The ant workers first had their pads cleaned by allowing them to walk on soft tissue paper (Tork, Dunstable, UK) and were then placed on a paint-free starting platform (1 cm^2 of 201E masking tape, 3M, St. Paul, MN, USA) located in the middle of the vertically oriented paint panel (100 μm thickness). Once 4 (out of 6) legs had left the starting platform, the time needed to reach the edge of the paint panel was measured. The test was discarded if the insect slipped from the surface within less than three seconds after placing it on the starting platform. The insect was considered "unsuccessful" if it slipped or did not reach the edge of the panel within two minutes. Ants that reached the edge of the paint panel by walking were considered "successful". Ten ants were tested on each paint panel; each ant was not used more than three times per day to avoid any adaptive or learning effects [88]. The paint slipperiness was calculated as follows:

$$Paint\ slipperiness\ (\%) = \frac{100 \times number\ of\ unsuccessful\ ants}{number\ of\ tested\ ants} \tag{3.4}$$

Non-painted, smooth metal sheets were used as controls; all ants could climb up these surfaces without any difficulty.

To assess the long-term durability of the paint and its slipperiness following intense exposure to ants attempting to climb on them (termed here 'long-term slipperiness'), paint panels were

placed vertically on the walls inside the ants' nest container and were left there for five months. The slipperiness of these panels was measured approximately bimonthly, by the proportion of unsuccessful ants. Ants which walked on the panel for less than three seconds were discarded from the test.

To observe ant adhesive pads (referred to as arolia) under the SEM, samples were prepared as follows: immediately after climbing on paint surfaces, the ant's legs were cut off and mounted on SEM stubs using conductive carbon double-sided adhesive tape. The samples were frozen for 48 hours to limit arolium deflation and facilitate the observation of particles [89]. Samples were then coated with a 30-nm carbon layer. Control ant samples which had not climbed the paints were observed under SEM to verify that the contaminants present on pads only came from the coatings. Images were recorded at an acceleration voltage of 5.0 kV. ImageJ (Version 1.51r, National Institutes of Health, Bethesda, MD, USA) was used to measure the claw tip radius and the spacing between the two claws from the micrographs.

3.2.4   Statistics

When values with distributions are given in the text, they are expressed as mean $\pm$ standard deviation (SD). All data were tested for normal distribution. Mann–Whitney tests (U-tests) were used for non-normally distributed unpaired data; paired and independent t-tests were used otherwise. All the performed tests were two-tailed; P-values below $\alpha = 0.05$ were interpreted as significant differences. Multi-way ANOVA (type II) and Principal Component Regression (PCR) analyses were performed was performed using R v3.4.4 (Vienna, Austria) [90]. Since the slipperiness data were not normally distributed, they were arcsine-transformed to achieve a homogeneous distribution of the variances of the residuals resulting from ANOVA analysis. Student's t-tests were carried out in Microsoft Excel 2016 (Microsoft Office, Redmond, WA, USA). Mann-Whitney U-tests and Spearman's rank test were done using Social Science Statistics (`https://www.socscistatistics.com`).

3.3 Results and discussion

3.3.1 Latex and paint characterisation

To study the effect of the paint composition on leafcutter ant attachment, we investigated the systematic variation of the amount of TiO_2 and $CaCO_3$, as described in the Materials and methods section, hereby modifying the PVC values. Paints were formulated at three different PVC values, 50%, 60% and 70%, by varying the amount of pigment and extender with regards to the quantity of latex. At PVCs 60 and 70, the paints were above their CPVC (ca. 55%), so that there was not enough binder to completely wet the particles (Figure 3.4). One can see that paints formulated above their CPVC (Figure 3.4B and C) lack polymer to bind efficiently all particles and tend to be porous [80, 91].

The pigment and the extender present different sizes and shapes: the TiO_2 spherical particles have a diameter of about 300 nm (280 ± 60 nm, $n = 39$), while the $CaCO_3$ particles are platelet-shaped and about 1 μm in length (941 nm $\pm$ 156 nm, $n = 20$, both measured by SEM) (Figure 3.3). Results for surface roughness, peak density, wettability and slipperiness of 13 formulated paints are shown in Table 3.3. The full set of data (45 paints) is given in Table A3.1. Figure 3.5A shows surface slipperiness as a function of PVC.
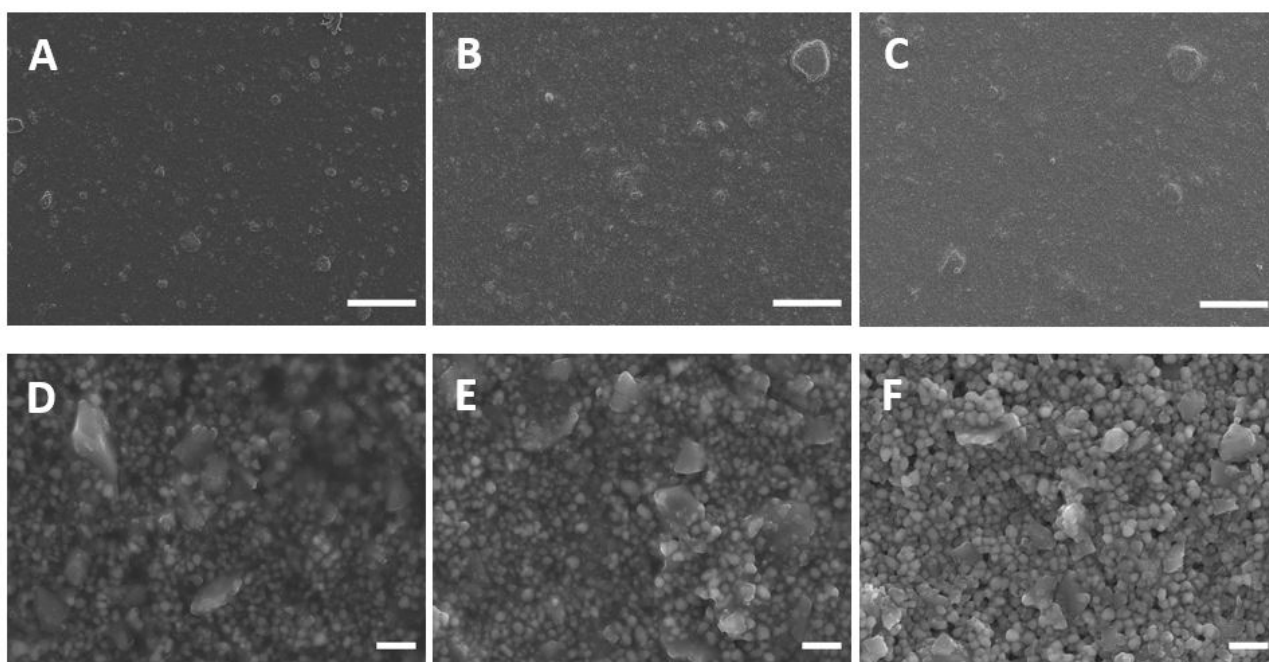

Figure 3.4: SEM images of 30 wt% TiO_2, 20 wt% $CaCO_3$ paint surfaces with varying PVC: (A, D) PVC 50, (B, E) PVC 60 and (C, F) PVC 70. Paints shown in (B, E) and (C, F) are formulated above their CPVC. Scale bars: (A-C) 100 μm and (D-F) 1 μm.
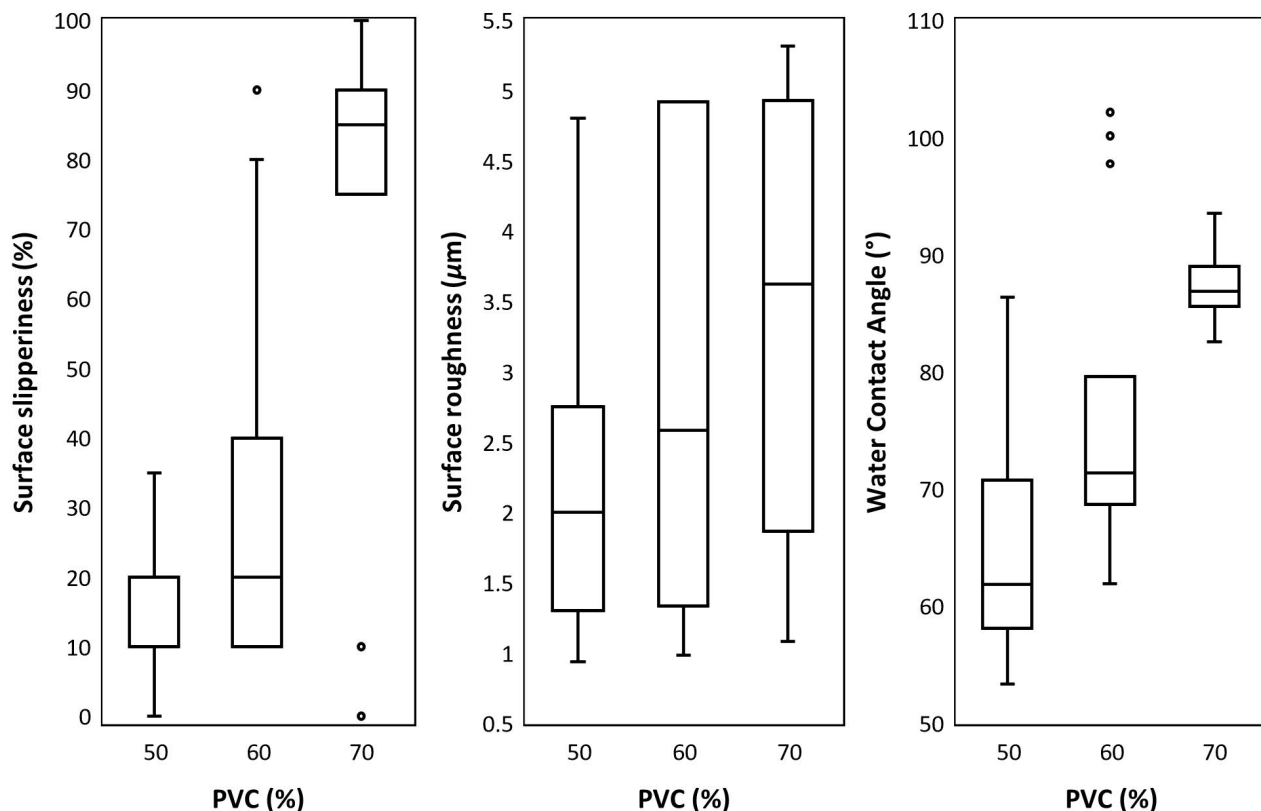
Figure 3.5: Boxplots showing (A) surface slipperiness (percentage of unsuccessful ants in climbing tests), (B) surface roughness average (R_a) and (C) water contact angle measured for the full set of paints formulated at different PVC values. In (B), three outliers ($R_a > 10$ μm) were not shown for more clarity. Centre lines and boxes represent the median within the 25th and 75th percentiles, whiskers show the 10th and 90th percentiles and circles indicate outliers.

For the overall set of paints (1-45, Table A3.1), the slipperiness for ants greatly increased with the PVC (Table 3.4, Spearman's rank test $r_s = 0.59$, $n = 45$, $P < 0.001$). The slipperiness increased strongly with the PVC for the paints containing only $CaCO_3$ (paints 10-18, $r_s = 0.80$, $n = 9$, $P = 0.010$), unlike TiO_2-paints (paints 1-9, $r_s = -0.62$, $n = 9$, $P = 0.074$). For some paints containing only TiO_2 (paints 4-6, Table 3.3), the reverse trend was observed: the higher the PVC, the lower the slipperiness. Unlike other coatings, TiO_2 paints tend to form cracks despite the presence of coalescent. This is likely due to the fact that TiO_2-only paints are further above their CPVC at PVCs 60 and 70 than the $CaCO_3$-only paints (54% vs. 63%).

The number of cracks was found to increase with the PVC under SEM, as the amount of polymer binder is reduced. These cracks most likely provide good grip to insect claws: claw interlocking with surface asperities is possible if the asperity size is larger than the claw tip radius [41, 50], which is for *A. cephalotes* 5.0 ± 1.7 μm ($n = 31$). The cracks present larger dimensions (at least 10 μm in width) and one can imagine that once the claws get into contact

with the paint, the cracks may expand due to the coating stiffness. Image examples of the cracks are given in Figure A3.1 (A and B, Appendix).

The paints containing only $CaCO_3$ were found to be more slippery for ants than TiO_2-only paints, at PVC 70 in particular (Table A3.1). Neither the amounts of TiO_2 nor $CaCO_3$ were found to significantly influence slipperiness (slipperiness $\times$ TiO_2: r_s = -0.12, n = 45, P = 0.449; slipperiness $\times$ $CaCO_3$: r_s = 0.09, n = 45, P = 0.572). Although non-significant at α = 0.05, the slipperiness results obtained in the PVC 70 paint series may suggest an impact of the $CaCO_3$ amount on the slipperiness (r_s = -0.49, n = 27, P = 0.064, Table A3.1). This suggests that both particle size and shape influence insect attachment to surfaces.

Optimum paint formulations that maximise the slipperiness for *A. cephalotes* ants included 20 wt% TiO_2 and 20 wt% $CaCO_3$. In these conditions, it is important to note that our surfaces achieved high slipperiness on vertical paints (90% of ants fallen, PVC 70), while only 44% cockroaches could not escape 60° tilted surfaces coated with insect-repellent polymers prepared by Graf *et al.* [69].

Table 3.3: Composition, CPVC, PVC, surface roughness, peak density, wettability and slipperiness values of 13 custom-made waterborne paints applied on metal sheets. The CPVC was approximated from Eq. 3.3. Both R_a and peak density were measured *via* optical profilometry. The slipperiness to *A. cephalotes* ants refers to the number of unsuccessful ants in climbing tests. The values are expressed as mean ± standard deviation (SD). See section Materials and Methods for further explanations.

Paint	[TiO$_2$] (wt%)	[CaCO$_3$] (wt%)	Approximate CPVC (%)	PVC (%)	R_a (μm) (n = 6)	Peak density (peaks/mm^2) (n = 6)	Water contact angle (°) (n = 4)	Slipperiness (%) (n = 20)
2	10	0	54	60	2.7 ± 0.2	339 ± 101	98 ± 3	90 ± 10
4	20	0	54	50	2.2 ± 0.7	374 ± 134	79 ± 8	20 ± 10
5	20	0	54	60	1.9 ± 0.4	42 ± 3	102 ± 8	10 ± 10
6	20	0	54	70	5.3 ± 1.0	20 ± 6	86 ± 5	0 ± 10
8	30	0	54	60	2.6 ± 0.3	30 ± 15	100 ± 3	40 ± 10
11	0	6.6	63	60	26.7 ± 4.5	304 ± 51	62 ± 3	30 ± 10
14	0	13	63	60	13.0 ± 4.6	394 ± 59	73 ± 1	30 ± 10
17	0	20	63	60	30.0 ± 10.2	49 ± 12	71 ± 1	20 ± 20
39	30	6.6	56	70	1.3 ± 0.4	299 ± 136	86 ± 5	87 ± 12
42	30	13	58	70	4.8 ± 0.1	1156 ± 41	94 ± 1	90 ± 10
43	30	20	59	50	4.8 ± 0.1	1136 ± 33	53 ± 2	10 ± 10
44	30	20	59	60	4.9 ± 0.1	1110 ± 88	66 ± 1	10 ± 10
45	30	20	59	70	4.6 ± 0.1	1140 ± 46	89 ± 3	90 ± 10

Based on our observations, we further investigated three hypotheses to explain why both high PVC and $CaCO_3$ paints are slippery to ants: (1) surface roughness, (2) surface wettability, and (3) particle detachment. It should be noted that because of the similar design and performance of insect adhesive pads, the observed slipperiness trends may possibly apply to many other insects [36, 70, 87].

Table 3.4: Correlation between test variables, correlation coefficient r_s and P-values obtained by Spearman's rank test for the following parameters: paint PVC, slipperiness, roughness average R_a, water contact angle and peak density for all paints, paints segregated by PVC and paint type. Only correlations with P-values indicating significant correlations (below $\alpha = 0.05$) have been indicated for more clarity.

	Variable 1	Variable 2	Correlation coefficient r_s	P-value
All paints ($n = 45$)	PVC	Slipperiness	0.60	< 0.001
	PVC	Water contact angle	0.74	0
	Water contact angle	Slipperiness	0.54	< 0.001
	[$CaCO_3$]	Water contact angle	-0.37	0.011
	[$CaCO_3$]	Peak density	0.51	< 0.001
PVC 50 paints ($n = 15$)	[$CaCO_3$]	Water contact angle	0.71	0.003
	Peak density	Water contact angle	-0.65	0.008
	Water contact angle	Slipperiness	0.54	0.036
PVC 60 paints ($n = 15$)	[TiO_2]	R_a	-0.53	0.043
	[$CaCO_3$]	Water contact angle	-0.63	0.013
PVC 70 paints ($n = 15$)	[TiO_2]	Water contact angle	0.68	0.006
	[$CaCO_3$]	Peak density	0.58	0.025
TiO_2-only paints ($n = 9$)	PVC	R_a	0.86	0.003
	PVC	Peak density	-0.79	0.011
	Peak density	Slipperiness	0.67	0.050
$CaCO_3$-only paints ($n = 9$)	PVC	Slipperiness	0.80	0.010
	PVC	Water contact angle	0.85	0.003
	Water contact angle	Slipperiness	0.71	0.003
TiO_2/$CaCO_3$ paints ($n = 27$)	PVC	Slipperiness	0.89	0
	PVC	Water contact angle	0.90	0
	Water contact angle	Slipperiness	0.90	0
	R_a	Peak density	0.42	0.029

3.3.2 Effect of surface roughness

The surface roughness of the paint coatings is based on both the presence of large particles at the surface and the formation of clusters formed by self-aggregation of extender and pigment [92–94]. It is worth mentioning that small calcium carbonate grades can reduce TiO_2 self-aggregation, which is referred to as the spacing effect of $CaCO_3$ [95], and can be driven by the opposite surface zeta potentials between TiO_2 and $CaCO_3$ [96]. However, our SDS-stabilised TiO_2 and $CaCO_3$ particles both displayed negative zeta potential values (data not shown), indicating that the formation of aggregates should be hindered by electrostatic repulsion [92].

Figure 3.5B shows that the R_a values ranged from 1.0 μm to 5.5 μm, the median values slightly increased with the PVC, with similar data distributions between the three PVC series. Paints 11, 14 and 17 exhibited large roughness values ($R_a > 10$ μm, Table 3.3) and are hence not shown in Figure 3.5B for more clarity. These are 60% PVC $CaCO_3$-only paints which reached their CPVC at PVC 60, leading to very rough surfaces [91]. Even when removing these outliers, R_a did not significantly increased with PVC at $\alpha = 0.05$, but it is commonly accepted that paint formulated with increasing PVC lead to rougher coatings ($r_s = 0.30$, $n = 42$, $P = 0.053$) [80, 81, 92].

It has been suggested that insect attachment forces are decreased on micro-rough surfaces (0.3-1.0 μm asperity size) [50, 51], as well as paints [70], because the small asperities reduce the contact area for the adhesive pads but do not allow the claws to interlock. Despite the wide range of slipperiness values (0-100% unsuccessful ants), we did not observe any effect of roughness average R_a on slipperiness (Figure 3.6, $r_s = 0.14$, $n = 45$, $P = 0.358$), suggesting that other mechanisms explain the reduction in ant attachment to paint coatings.

It has been shown in the literature that insect attachment forces to surfaces are minimised for asperity sizes in the submicron range (0.05-1 μm asperity size) [46, 50–53, 97]. We obtained a broad range of slipperiness values, despite our pigment particles being in the same size range as the surface asperities used in the various studies (ca. 300 nm TiO_2 and 1 μm $CaCO_3$ particles). However, the slipperiness of surfaces is not only based on roughness average R_a, but also on the lateral dimensions of surface roughness (e.g. asperity spacing and slope). Optical profilometry has a limited XY-resolution (ca. 500 nm) for capturing the lateral length scale of surface roughness. Measuring surface roughness *via* AFM proved difficult due to the large
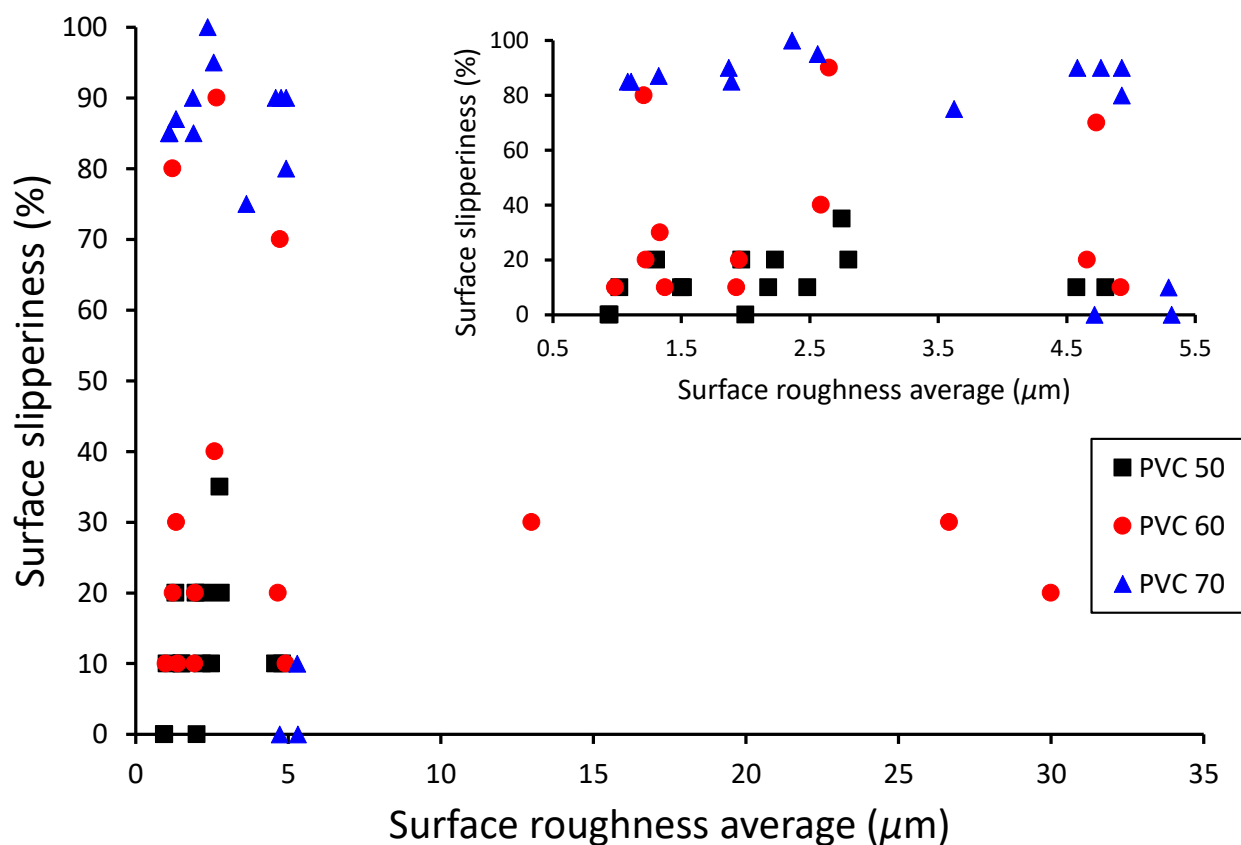
Figure 3.6: Surface slipperiness (percentage of unsuccessful ants) of model paints formulated at different PVCs vs. surface roughness average R_a for PVCs 50, 60 and 70; inset: detail of 0.5-5.5 μm roughness. It can be seen that an effect of R_a on slipperiness cannot directly be concluded from this graph. Error bars are not included for more clarity.

height differences of some coatings.

Defining peaks as any protruding regions greater than 5% of the largest asperity (relative to the midline), we measured the peak density by profilometry in 1 mm $\times$ 1 mm areas (Table A3.1). 'Low' values (< 300 peaks/mm^2) were generally due to the formation of large aggregates at the surface. 'Large' values indicate that many narrow peaks were formed. Although there is no linear correlation between the peak density and the slipperiness ($r_s = 0.15$, $n = 45$, $P = 0.327$), the peak density seems to slightly influence the slipperiness for CaCO$_3$-only paints and TiO$_2$/CaCO$_3$ paints. For these two series, the slipperiness decreases until reaching the approximate threshold values of 200 and 600 peaks/mm^2, respectively (Figure A3.2, Appendix, dashed lines), from which the slipperiness increases with the density. This suggests that 200 peaks/mm^2 and 600 peaks/mm^2 are the peak densities at which ants' adhesive pads can make full contact with the surface asperities for CaCO$_3$-only paints and TiO$_2$/CaCO$_3$ paints, respectively. We propose that the slipperiness in TiO$_2$-only paints is mainly driven by the cracks, and hence does not depend on the number of peaks.

One can imagine that rigid surface asperities may damage or destroy the smooth adhesive pad (arolium) of the ant, hence reducing contact between the pad and the substrate [98]. Wear damage would result in stiffening of the pad after several days. This cannot be readily observed by direct visual means as *A. cephalotes* ants possess retractable adhesive pads [89], and no apparent pad damage could be observed under SEM. Our results have not clearly demonstrated an influence of R_a on slipperiness; hence, other factors such as surface hydrophobicity or particle detachment must be considered.

3.3.3 Effect of surface wettability

As a high surface hydrophobicity or low surface energy of various surfaces has been found to affect attachment forces of beetles to some extent, we investigated the effect of the water contact angle on the slipperiness [45–47].

All water contact angles of the paint coatings were between 50° and 105°, with TiO_2- and $CaCO_3$-only paints displaying higher contact angles. The three outlier data points correspond to paints 2, 5, and 8 (Table 3.3), which are PVC 60 TiO_2-only paints reaching their CPVC and hence showing large contact angles [91]. The water contact angle greatly increased with the PVC (Table 3.4, $r_s = 0.74$, $n = 45$, $P = 0$).

Figure 3.7 shows the effect of paint wettability on slipperiness for $TiO_2/CaCO_3$ paints. One can see in Table 3.4 that paint slipperiness was significantly correlated to both PVC ($r_s = 0.59$, $n = 45$, $P < 0.001$) and paint wettability ($r_s = 0.54$, $n = 45$, $P < 0.001$).
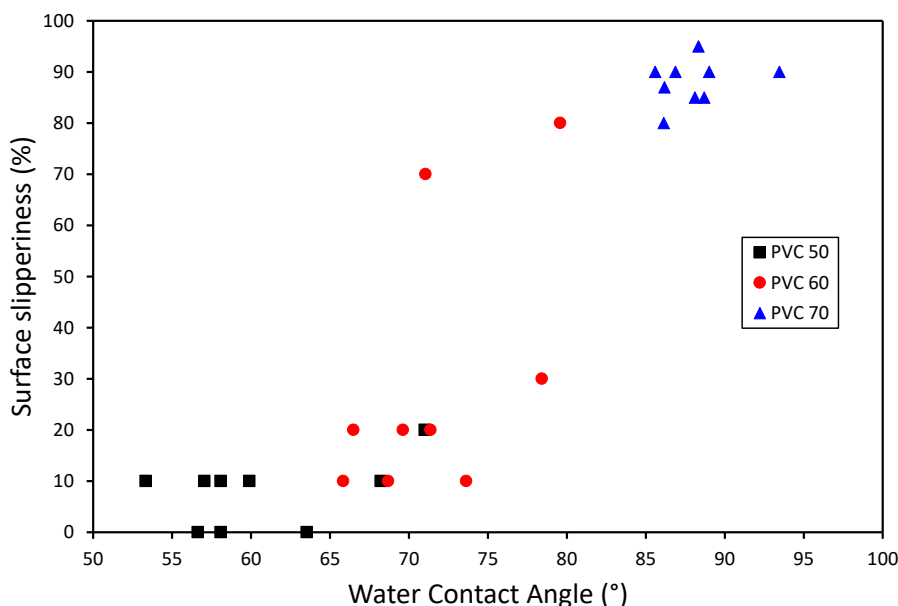

Figure 3.7: Contact angle of water on paint surface vs. slipperiness (portion of unsuccessful ants) and PVC. One can see that both slipperiness and water contact angle increased with PVC. Data points corresponding to TiO_2- and $CaCO_3$-only paints and error bars were not included for more clarity.

Fluid-mediated wet adhesion in insects occurs through van der Waals, capillary and viscous forces [30, 39, 40]. The biphasic fluid secreted by insects has been shown to decrease adhesion and friction forces on smooth surfaces, as well as increasing attachment forces on rough substrates by filling asperities [37, 99]. The secretion is mainly oily and therefore wets most substrates [43], including rough surfaces [100]. The adhesive fluid's oily phase has been suggested to aid attachment on both hydrophilic and hydrophobic substrates [43, 44, 100]. However, the slipperiness to ants increased with a reduced wettability (for water) of the paint coatings. It is unlikely that this effect is based on insufficient wetting by the adhesive fluid; instead, slipperiness and water contact angle are both influenced by the PVC, rather than directly correlated.

An ANOVA test was performed to assess which parameters influenced the slipperiness the most. To this end, the slipperiness data were arcsine-transformed to achieve a homogeneous distribution of the variances of the residuals. To avoid artefacts resulting from the ordering of factors in unbalanced datasets, we conducted an ANOVA based on Type II sums of squares. By minimising the model to the most relevant parameters (PVC, R_a, contact angle and peak density), the minimal model contained several significant interactions that involved all the factors (Table A3.2, Appendix). The parameters affecting significantly the slipperiness were the PVC ($F_{1,38} = 12.93$, $P < 0.001$), the peak density ($F_{1,38} = 5.22$, $P = 0.028$) and interactions between the parameters (interaction wettability $\times$ peak density, $F_{1,38} = 13.87$, $P < 0.001$; interaction $R_a \times$ PVC, $F_{1,38} = 17.21$, $P < 0.001$).

The explanatory variables of this analysis are correlated with each other, in particular water contact angle and PVC (Table 3.4). We conducted a Principal Component Regression (PCR) to decorrelate the explanatory factors. The explanatory variables could be reduced to three principal components (PCs) that explained 95% of the variation (Eq. 3.5, Appendix). Slipperiness depended most strongly on PC1, which was mainly associated with PVC and water contact angle (Table A3.3).

3.3.4   Particle/aggregate detachment from the paint surfaces

As an alternative explanation as to why high PVC paints are slippery, we considered the hypothesis of detachment of particles from the paints. Particle detachment can lead to contamination of insect tarsal adhesive pads [62, 101]. After climbing paint surfaces, the legs of *A. cephalotes*

ants were removed and observed under the SEM (Figure 3.8). We found that the arolium and hairs were contaminated by aggregates coming from the paint surfaces. In particular, the contamination level appeared to increase with the PVC. Quantification of the contaminating particles was challenging as individual particles could not always be distinguished due to the presence of polymer binder 'gluing' the particles together. From the SEM micrographs given in Figure 3.8, we estimated that one pad detached approximately 51 and 203 particles from the PVC 60 and 70 paints containing 30 wt% TiO_2, 20 wt% $CaCO_3$, respectively. This confirms that particles detach more easily from paints with a higher PVC.

Our results suggest that similarly to some pitcher plant surfaces, in which epicuticular wax crystals detach [56, 57, 60], aggregates detach from the paint surfaces and adhere to the tacky pads of leaf cutter ants. Particle detachment is based on the small amount of polymer, which results in incomplete wetting of the solid particles when paints are formulated above their CPVC.

We propose that the slipperiness is also based on insect pad contamination, leading to reduction or loss of contact area between the pad and the surface's irregularities.

The forces generated to detach pigment and extender particles should be stronger than the hydrogen and electrostatic bonding between the polymer binder and the particles [102] and should also fracture the polymer adsorbed onto the surface of particles [103]. Anyon *et al.* suggested the adhesive force necessary for particles to contaminate arolia increases with both the particle's radius and the surface tension of the insect's adhesive secretion [101, 104]. When contaminating particles are present on insect pads, they can be removed through self-cleaning, which, during locomotion, occurs when the arolium is subject to shear forces that help remove the fouling particles [103, 105]. The insects' adhesive fluid was found to aid the process by filling the gaps between the particles, then increasing the contact area and hence, the adhesion and friction forces [106]. The self-cleaning time depends on the insect species and hence, pad type, as well as the size, nature and surface energy of the fouling particles [106–108]. In beetles, 1 μm and larger than 45 μm fouling particles were found to be removed in a few steps, unlike 10-20 μm particles, which fit in between the hairs of the beetles' pads and hence needed more steps to be removed [105, 107, 108].
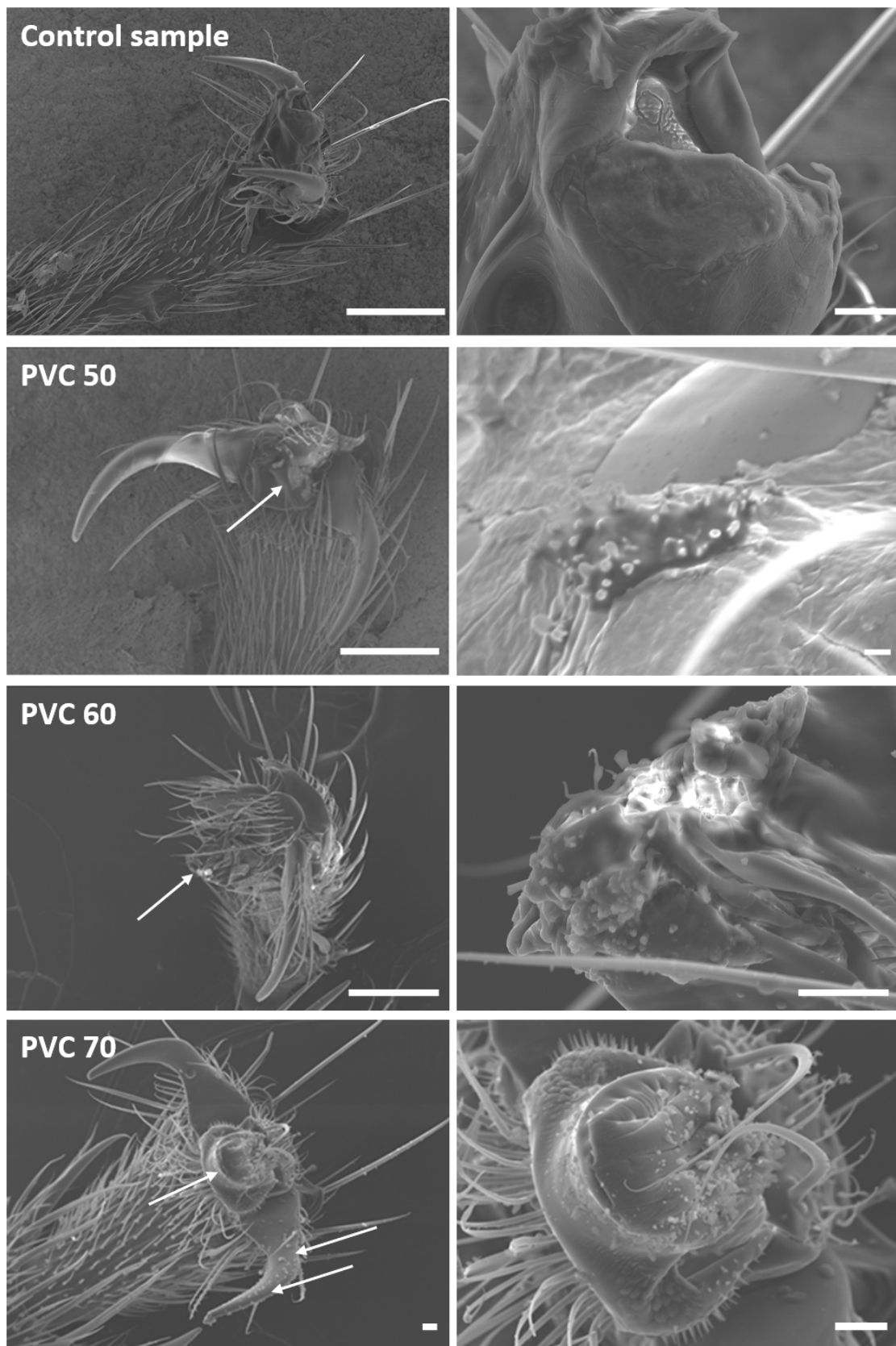
Figure 3.8: SEM images of *A. cephalotes* ant tarsi contamination after climbing 30 wt% TiO_2, 20 wt% $CaCO_3$ paint surfaces formulated at PVC 50, 60 and 70. Control sample: ants which did not climb on paint, no contaminant could be observed. Scale bars: 100 μm (left) and 10 μm (right). PVC 50: only a few contaminating particles could be observed on the arolium; scale bars: 100 μm (left) and 1 μm (right). PVC 60: the arolium tip was fouled by paint particles. Scale bars: 100 μm (left) and 10 μm (right). PVC 70: the arolium and claws were heavily contaminated by particles, mostly $CaCO_3$. Arrows show where contaminating particles were observed. Scale bars: 10 μm (left) and 10 μm (right).

To further test our hypothesis that paint surfaces are slippery through the detachment of particles, we allowed ants that had been climbed on 30 wt% TiO_2, 20 wt% $CaCO_3$ paints (43-45, Table 3.3) to climb on clean glass using a simple double-vial set-up (Figure 3.9). At PVC 50, the ants could climb up the glass immediately after falling off from the surface of the painted vial, while they needed 5 minutes and 55 minutes to climb up glass again for the PVC 60 and 70 paints, respectively. These results support the argument that slipperiness is mainly due to pad contamination. They also allow us to estimate the self-cleaning time of *A. cephalotes* ants, which corresponds to the time needed to remove contaminating particles from their pads [106, 108].

Paints containing only $CaCO_3$ were found to show greater slipperiness than TiO_2-only paints, at PVC 70 in particular, as shown in Table A3.1. We tentatively explain this by an easier detachment of $CaCO_3$ particles from the paint surface, as $CaCO_3$ particles are larger than TiO_2 particles (ca. 1 μm vs. 300 nm) and as their irregular shape (platelet vs. spherical particles) prevents strong attachment. Liquid calcium carbonate-based dispersions have already been shown to be efficient against termites to prevent wood infestation [24]. Although one could expect that some pigment particles may segregate to the bottom of the surface in the absence of thickener [93, 94], SEM micrographs show that both types of particle were present at the surface (Figure 3.4).

The TiO_2 and $CaCO_3$ particles had similar oil absorption values (19 and 20 g per 100 g, respectively), which indicate how much binder is needed to fully cover the particles. Oil absorption was therefore not considered a significant parameter explaining why the $CaCO_3$ detached more easily than TiO_2 particles. It is possible that either insect pads have greater affinity for $CaCO_3$ particles, or that TiO_2 particles are more tightly bound to the acrylic polymer film. The latter hypothesis should be tested in further work using polymer-pigment adsorption isotherms [102].

Figure 3.9: Double-vial set-up to test the particle detachment hypothesis after contamination of feet of *A. cephalotes* ants: the top vial was painted with test paint and the bottom vial was clean glass.

It is noteworthy to mention that the paints, depending on the TiO_2/$CaCO_3$ combination, present slight variations in their CPVC (54-63%, Table A3.1). For smaller CPVC values (e.g. TiO_2-only paints), it is expected that the particles should detach more easily at PVC 60 and 70, as these PVC values are well above the CPVC. However, this was generally not observed, in particular for the TiO_2-only paints which showed low slipperiness values, and the optimised formulations containing 20 wt% TiO_2, 20 wt% $CaCO_3$, *i.e.* presenting an approximate CPVC value of 59%. The effect of the type, size and shape of the extender particles on the paint slipperiness will be explored in further studies. It is expected that particles larger than the spacing between the two claws, approximately 69 $\pm$ 11 μm ($n = 25$) for *A. cephalotes* as measured by SEM, cannot contaminate the ants' arolia [101]. For particles showing wide size distributions, only the smaller particles could foul arolia. Contamination may be enhanced by the capillary adhesion between the ants' fluid and the particles, similar to that observed between polymer binder and pigment particles [102].

3.3.5 Long-term slipperiness and paint durability

Since particles detach from the paints, it is important to assess both the mechanical stability, or durability, and the long-term slipperiness of the coatings. The scrub resistance test simulates how paints cope with wear over time. Coatings were rubbed with a scrubbing pad and an abrasive surfactant solution (2.5 g/L sodium dodecylbenzenesulfonate) for either 200 or 2000 cycles at a speed of 36 cycles/min by applying a force of 2.4 N.

We randomly selected three PVC 70 paints from our sample set, which were scrubbed to 200 cycles (Table 3.5). All coatings showed good durability, in particular paint 33 (20 wt% TiO_2, 13 wt% $CaCO_3$), which was further scrubbed for 2000 cycles. Ant climbing tests were performed on these scrubbed panels.

After scrubbing (200 and 2000 cycles), high slipperiness values were observed for the three coatings. We found that after being scrubbed, the paint surfaces exposed more loose particles at their top surface, and one can clearly see that the ants' pads were heavily fouled (Figure 3.10), in particular with $CaCO_3$ particles, supporting the earlier assumption that either their pads present greater affinity for $CaCO_3$ than TiO_2 particles, or that TiO_2 particles are more tightly bound to the coating. The surface roughness values suggest that ants used their claws to cling to surface asperities, but particles were also found on their arolia.

Table 3.5: Slipperiness and roughness average (R_a) comparison of scrubs panels before and after scrubbing the paints (200 or 2000 cycles). The values are expressed as mean ± standard deviation (SD).

Paint	[TiO$_2$] (wt%)	[CaCO$_3$] (wt%)	Scrub resistance (mg/cm^2) (number of cycles) ($n = 2$)	Slipperiness before scrubs (%) ($n = 20$)	Slipperiness after scrubs (%) ($n = 20$)	R_a before scrubs (μm) ($n = 6$)	R_a after scrubs (μm) ($n = 6$)
24	10	13	0.38 ± 0.08 (200)	90 ± 5	100 ± 10	6.0 ± 3.4	9.4 ± 7.2
39	30	6.6	0.23 ± 0.05 (2000)	87 ± 12	100 ± 10	5.9 ± 4.3	6.8 ±4.3
33	20	13	0.75 ± 0.17 (2000)	85 ± 5	100 ± 10	4.4 ± 3.5	11.8 ± 6.3

This further suggests that particle detachment is the main mechanism which prevents leaf cutting ant workers from climbing on PVC 70 paints.

To measure the long-term slipperiness of the paints, we placed paints of the 30 wt% TiO$_2$ series, with varying CaCO$_3$ concentrations (paints 39, 42 and 45, Table 3.3) on the walls at the bottom of the cage containing a large *A. cephalotes* colony so that the ants had direct access to the panels, and recorded the slipperiness over five months. Figure 3.11 illustrates that the slipperiness gradually decreased over time, and that surfaces were more slippery when the paints contained more CaCO$_3$. After five months, the 30 wt% TiO$_2$, 20 wt% CaCO$_3$ paint still displayed approximately 70% slipperiness (significant difference between t = 0 and t = 5 months, paired *t*-test, $T_2 = 5.29$, $P = 0.034$).
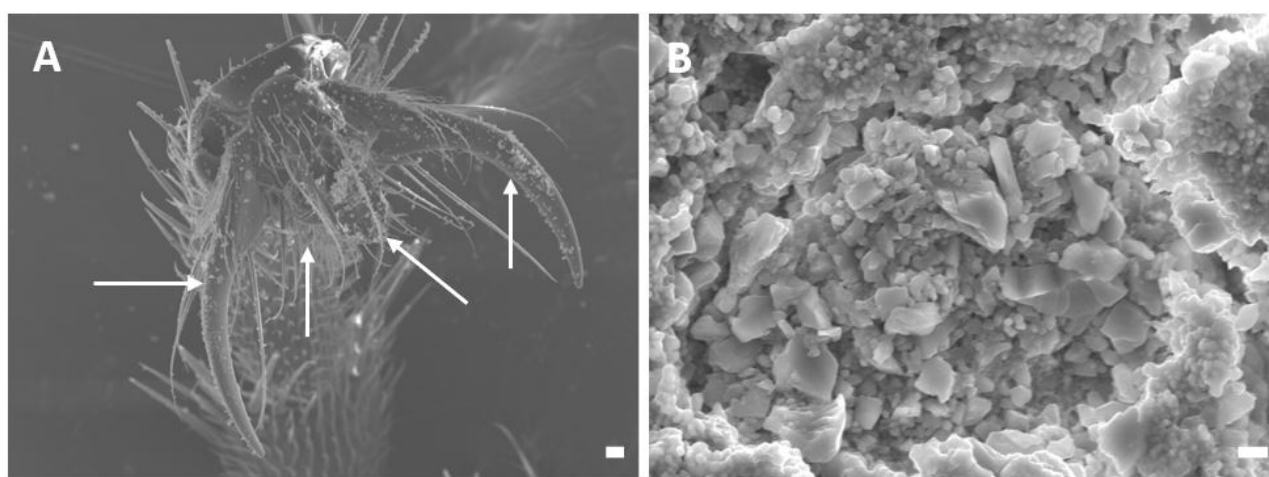

Figure 3.10: SEM images of (A) contaminated *A. cephalotes* tarsus after climbing a scrubbed paint panel. Arrows show contaminating particles. (B) exposed "craters" rich in loose particles after the coating was scrubbed for 2000 cycles. Scale bars: (A) 10 μm and (B) 1 μm.
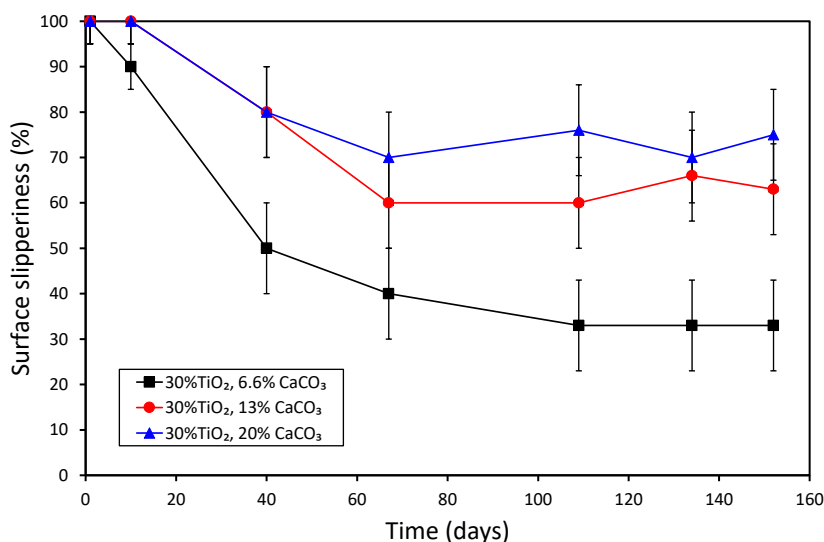
Figure 3.11: Long-term slipperiness test: slipperiness (portion of unsuccessful ants) measured as a function of time during 5 months by leaving the painted panels (30 wt% TiO$_2$, variable concentration of CaCO$_3$) in the *A. cephalotes* colony's rearing. A slipperiness plateau was reached within ca. 2 months for the three paints, which suggests that thereafter, insect attachment forces were reduced through surface roughness.

Interestingly, the slipperiness first gradually decreased over the first two months of testing, and then reached a plateau at about 33%, 60% and 70% slipperiness for paints containing 6.6 wt%, 13 wt% and 20 wt% CaCO$_3$, respectively. These results suggest that *A. cephalotes* ants removed most of the loose, detachable particles within the first two months and thereafter, their attachment was mainly reduced due to the surface asperities. As particles still detached from all tested scrubbed paint panels to the ant's arolia, the particle detachment forces produced by the ants' feet may be at least as strong as those in the scrub test.

A similar effect has been proposed for N. alata pitcher plants, where the slippery surface is composed of two layers of epicuticular wax crystals [56, 57, 60]. The crystals of the upper layer detach upon contact with insect tarsi and do not regenerate [58]. Mechanical removal of the whole upper layer using dental wax lift-off left behind a rough bottom layer that still reduced insect adhesion [53, 56]. Assuming that the upper layer also becomes fully removed by insect pads, the surface roughness of the bottom layer alone could reduce insect attachment. However, it is unclear to what extent the upper layer is removed by insect feet under natural conditions, and if the remaining surface is comparable to that obtained *via* experimental lift-off. The SEM of ant pads after climbing the paints, after being placed for five months in the colony cage, showed that there were no more particles attached to their arolia (Figure A3.3).

The profilometry measurements of the paint panels showed the roughness average R_a had dramatically increased due to pigment removal, by 330% on average, and was significantly different for paints 39 (Mann-Whitney $U_{10,6} = 0$, $P = 0.001$) and 45 ($U_{10,6} = 0$, $P = 0.001$), but not for 42 ($U_{10,6} = 18$, $P = 0.211$) between t = 0 months and t = 5 months (Table A3.4).

It is important to note that the number of climbing ants decreased over time as a result of behavioural adaptations (A.F., personal observation). In real-life conditions, it is assumed that after a few climbing trials, insects would forage or nest elsewhere [88, 109]. From our results, we estimate that ten ants try to climb the paints per minute, *i.e.* about 14,000 insects per day assuming constant activity. From ant pads analysed by SEM after climbing paint 45 (Figure 3.8, PVC 70), about 200 particles were removed by one pad, which is low compared to the approximate number of 2.9×10^{12} particles contained in the paint film (Eq. 3.9, Appendix). Based on their shape, most fouling particles seemed to be $CaCO_3$ particles. An estimate of the removed particle weight was not possible as the ants had left trail secretions on the panels, possibly to mark their territory [110]. Assuming that 14,000 ants removed 200 particles per pad daily for two months, then about a billion particles would be removed, *i.e.* about 3.4% of the total amount of particles contained in the paint film. Considering these rough orders of magnitude, this suggests that the fraction of loose pigment and extender particles in the coating is relatively low as they were removed in about two months by the ants.

It is known that high PVC paints generally present low mechanical stability and low gloss, in particular when formulated above their CPVC [93]. However, our model paints showed good durability (Table 3.5), likely due to the absence of hydrophilic compounds, which tend to decrease the durability (scrub resistance) of coatings. Our $CaCO_3$-only and $TiO_2/CaCO_3$ PVC 70 paints showed a good balance between mechanical properties and long-term, high slipperiness. However, it must be noted that these coatings are unlikely to withstand outdoor conditions, e.g. weathering or rain, due to the absence of adequate additives.

3.4   Conclusions

Insect-slippery model paints were prepared using an acrylic polymer binder, 300 nm TiO_2 and 1 μm $CaCO_3$ particles. Our findings show that ant workers (*A. cephalotes*) could not adhere to the vertical surfaces of some paints mainly due to particle detachment, in combination with surface roughness. A long-term insect exposure experiment showed that even after detachment of most loose particles, the paints remained slippery for insects, likely due to their surface roughness. Insect attachment to paint surfaces was mainly related to the following paint formulation parameters:

1. Paint PVC (Pigment Volume Concentration): when above the Critical Pigment Volume Concentration (CPVC), loose particles will detach from the coating and adhere to ant pads, leading to a loss of contact.

2. The type, dimensions and shape of solid particles: $CaCO_3$ particles were found to detach more easily from the paint than TiO_2 particles, possibly due to their larger size (ca. 1 μm vs. 300 nm, Figure 3.3) and shape (platelet vs. spherical) which may facilitate interlocking of claws and pads. Indeed, high PVC TiO_2-only paints were not slippery. Paints containing 20 wt% $CaCO_3$ showed the best combination of slipperiness and mechanical (scrub) resistance.

The stiffness and yield strength of the coatings has not been tested here but may be important, as insect claws or spines can dig into soft substrates to get a grip [111]. The influence of the latex type (chemistry, particle diameter and temperature properties) as well as the extender (chemistry, size and geometry) will be further investigated. Finally, it will be important to verify our findings with tests on other insect species. Because of the similar effects of slippery substrates on insect adhesive pads [37, 70, 87], the observed trends may apply to all climbing insects.

Acknowledgements

References

[1] Oerke, E.-C. (2006) Crop losses to pests. *J. Agric. Sci.,* **144**, 31–43.

[2] Greenwood, B. M., Fidock, D. A., Kyle, D. E., Kappe, S. H. I., Alonso, P. L., Collins, F. H., and Duffy, P. E. (2008) Malaria: progress, perils, and prospects for eradication. *J. Clin. Invest.,* **118**(4), 1266–1276.

[3] Dhaliwal, G. S., Jindal, V., and Dhawan, A. K. (2010) Insect pest problems and crop losses: changing trends. *Indian J. Ecol.,* **37**(1), 1–7.

[4] Lee, C. Y. (2002) Tropical household ants: pest status, species diversity, foraging behavior and baiting studies. *Proc. Fourth Int. Conf. Urban Pests,* pp. 3–18.

[5] Bonnefoy, X., Kampen, H., and Sweene, K. (2008) Public health significance of urban pests, World Health Organization, Copenhagen.

[6] Su, N.-Y. and Scheffrahn, R. H. (2000) Termites as Pests of Buildings, Springer Netherlands, Dordrecht.

[7] Ghaly, A. and Edwards, S. (2011) Termite Damage to Buildings: Nature of Attacks and Preventive Construction Methods. *Am. J. Eng. Appl. Sci.,* **4**(2), 187–200.

[8] Mahapatro, G. K. and Chatterjee, D. (2018) Termites as Structural Pest: Status in Indian Scenario. *Proc. Natl. Acad. Sci. India Sect. B Biol. Sci.,* **88**(3), 977–994.

[9] Birkemoe, T. (2002) Structural infestations of ants (Hymenoptera, Formicidae) in southern Norway. **49**(2), 139–142.

[10] Oi, D. H., Vail, K. M., Williams, D. F., and Bieman, D. N. (1994) Indoor and Outdoor Foraging Locations of Pharaoh Ants (Hymenoptera: Formicidae) and Control Strategies Using Bait Stations. *Florida Entomol.,* **77**(1), 85.

[11] Verma, M., Sharma, S., and Prasad, R. (2009) Biological alternatives for termite control: A review. *Int. Biodeterior. Biodegradation,* **63**(8), 959–972.

[12] Pimentel, D. (2005) Environmental and economic costs of the application of pesticides primarily in the United States. *Environ. Dev. Sustain.,* **7**(2), 229–252.

[13] Sánchez-Bayo, F. and Wyckhuys, K. A. (2019) Worldwide decline of the entomofauna: A review of its drivers. *Biol. Conserv.,* **232**, 8–27.

[14] Lenz, M., Schafer, B., Runko, S., and Glossop, L. (1997) The concrete slab as part of a termite barrier system: response of Australian subterranean termites to cracks of different width in concrete. *Sociobiology,* **30**, 103–118.

[15] Programme, U. N. E. Finding alternatives to persistent organic pollutants (POPS) for termite management. (2000).

[16] Ghosh, S. K. (2006) Functional Coatings and Microencapsulation: A General Perspective, Wiley-VCH Verlag GmbH & Co. KGaA, Weinheim, FRG.

[17] Whalon, M. and Malloy, G. Insect Repellent Coatings. (1998) US Patent 5843215.

[18] Maia, M. and Moore, S. J. (2011) Plant-based insect repellents: a review of their efficacy, development and testing. *Malar. J.,* **10**.

[19] Overman, G. R. Method for admixing plant essential oils to coatings for the purpose of repelling insects. (2009) US Patent 20090155394.

[20] Alexander, P., Kitchener, J. A., and Briscoe, H. V. A. (1944) Inert dust insecticides: Part I. Mechanism of action. *Ann. Appl. Biol.,* **31**(2), 143–149.

[21] Glenn, D. M. and Puterka, G. J. (2010) Particle films: a new technology for agriculture, Vol. 31, John Wiley & Sons, Inc., .

[22] Athanassiou, C. G. and Arthur, F. H. (2018) Bacterial Insecticides and Inert Materials, Springer, Berlin,

Heidelberg.

[23] Shahzad, K. and Manzoor, F. (2019) Nanoformulations and their mode of action in insects: a review of biological interactions. *Drug Chem. Toxicol.,* pp. 1–11.

[24] Roomi, M. W., Shah, A. H., Anwarullah, M., and Hussain, M. (1990) Studies on the control of subterranean termites by inorganic pesticides. *Anzeiger für Schädlingskunde Pflanzenschutz Umweltschutz,* **63**(3), 50–52.

[25] Donovan, S. E., Eggleton, P., Dubbin, W. E., Batchelder, M., and Dibog, L. (2001) The effect of a soil-feeding termite, *Cubitermes fungifaber* (Isoptera: Termitidae) on soil properties: termites may be an important source of soil microhabitat heterogeneity in tropical forests. *Pedobiologia,* **45**(1), 1–11.

[26] Black, H. and Okwakol, M. (1997) Agricultural intensification, soil biodiversity and agroecosystem function in the tropics: the role of termites. *Appl. Soil Ecol.,* **6**(1), 37–53.

[27] Dawes, T. Z. (2010) Reestablishment of ecological functioning by mulching and termite invasion in a degraded soil in an Australian savanna. *Soil Biol. Biochem.,* **42**(10), 1825–1834.

[28] Hölldobler, B. and Wilson, E. (1990) The Ants, Harvard University Press, Cambridge.

[29] Gorb, S. N. (2002) Attachment Devices of Insect Cuticle, Kluwer Academic Publishers, Dordrecht.

[30] Gorb, S. N. (2010) Biological and biologically inspired attachment systems, Springer Berlin Heidelberg, Berlin, Heidelberg.

[31] Endlein, T. and Federle, W. (2015) On heels and toes: How ants climb with adhesive pads and tarsal friction hair arrays. *PLoS One,* **10**(11), e0141269.

[32] Dirks, J. H. (2014) Physical principles of fluid-mediated insect attachment - Shouldn't insects slip?. *Beilstein J. Nanotechnol.,* **5**(1), 1160–1166.

[33] Bullock, J. M. R. and Federle, W. (2009) Division of labour and sex differences between fibrillar, tarsal adhesive pads in beetles: effective elastic modulus and attachment performance. *J. Exp. Biol.,* **212**(12), 1876–1888.

[34] Gladun, D., Gorb, S., and Frantsevich, L. I. (2009) Alternative Tasks of the Insect Arolium with Special Reference to Hymenoptera, Springer, Dordrecht.

[35] Crosland, M. W. J., Su, N.-Y., and Scheffrahn, R. H. (2005) Arolia in termites (Isoptera): functional significance and evolutionary loss. *Insectes Soc.,* **52**(1), 63–66.

[36] Bullock, J. M. R., Drechsler, P., and Federle, W. (2008) Comparison of smooth and hairy attachment pads in insects: friction, adhesion and mechanisms for direction-dependence. *J. Exp. Biol.,* **211**(20), 3333–3343.

[37] Drechsler, P. and Federle, W. (2006) Biomechanics of smooth adhesive pads in insects: Influence of tarsal secretion on attachment performance. *J. Comp. Physiol. A,* **192**(11), 1213–1222.

[38] Dirks, J.-H. and Federle, W. (2011) Fluid-based adhesion in insects - principles and challenges. *Soft Matter,* **7**(23), 11047.

[39] Dixon, A. F. G., Croghan, P. C., and Gowing, R. P. (1990) The mechanism by which aphids adhere to smooth surfaces. *J. Exp. Biol.,* **152**(1), 243–253.

[40] Stork, N. E. (1980) Experimental analysis of adhesion of *Chrysolina polita* (Chrysomelidae: Coleoptera)

on a variety of surfaces. *J. Exp. Biol.,* **88**, 91–107.

[41] Dai, Z., Gorb, S. N., and Schwarz, U. (2002) Roughness-dependent friction force of the tarsal claw system in the beetle *Pachnoda marginata* (Coleoptera, Scarabaeidae). *J. Exp. Biol.,* **205**, 2479–2488.

[42] Endlein, T. and Federle, W. (2008) Walking on smooth or rough ground: Passive control of pretarsal attachment in ants. *J. Comp. Physiol. A,* **194**(1), 49–60.

[43] Dirks, J.-H., Clemente, C. J., and Federle, W. (2010) Insect tricks: two-phasic foot pad secretion prevents slipping.. *J. R. Soc. Interface,* **7**, 587–593.

[44] Gorb, S. N. (2007) Smooth Attachment Devices in Insects: Functional Morphology and Biomechanics, Vol. 34, , .

[45] Grohmann, C., Blankenstein, A., Koops, S., and Gorb, S. N. (2014) Attachment of *Galerucella nymphaeae* (Coleoptera, Chrysomelidae) to surfaces with different surface energy. *J. Exp. Biol.,* **217**(23), 4213–4220.

[46] England, M. W., Sato, T., Yagihashi, M., Hozumi, A., Gorb, S. N., and Gorb, E. V. (2016) Surface roughness rather than surface chemistry essentially affects insect adhesion. *Beilstein J. Nanotechnol.,* **7**(1), 1471–1479.

[47] Prüm, B., Florian Bohn, H., Seidel, R., Rubach, S., and Speck, T. (2013) Plant surfaces with cuticular folds and their replicas: Influence of microstructuring and surface chemistry on the attachment of a leaf beetle. *Acta Biomater.,* **9**(5), 6360–6368.

[48] Gorb, E. and Gorb, S. (2009) Effects of surface topography and chemistry of *Rumex obtusifolius* leaves on the attachment of the beetle *Gastrophysa viridula*. *Entomol. Exp. Appl.,* **130**(3), 222–228.

[49] Hosoda, N. and Gorb, S. N. (2012) Underwater locomotion in a terrestrial beetle: combination of surface de-wetting and capillary forces. *Proc. R. Soc. B Biol. Sci.,* **279**(1745), 4236–4242.

[50] Bullock, J. M. R. and Federle, W. (2011) The effect of surface roughness on claw and adhesive hair performance in the dock beetle *Gastrophysa viridula*. *Insect Sci.,* **18**(3), 298–304.

[51] Voigt, D., Schuppert, J. M., Dattinger, S., and Gorb, S. N. (2008) Sexual dimorphism in the attachment ability of the Colorado potato beetle *Leptinotarsa decemlineata* (Coleoptera: Chrysomelidae) to rough substrates. *J. Insect Physiol.,* **54**(5), 765–776.

[52] Federle, W. and Bruening, T. (2006) Ecology and Biomechanics of Slippery Wax Barriers and Wax Running in Macaranga-Ant Mutualisms, CRC Press, Boca Raton, Florida.

[53] Scholz, I., Buckins, M., Dolge, L., Erlinghagen, T., Weth, A., Hischen, F., Mayer, J., Hoffmann, S., Riederer, M., Riedel, M., and Baumgartner, W. (2010) Slippery surfaces of pitcher plants: *Nepenthes* wax crystals minimize insect attachment *via* microscopic surface roughness. *J. Exp. Biol.,* **213**(7), 1115–1125.

[54] Barthlott, W. and Neinhuis, C. (1997) Purity of the sacred lotus, or escape from contamination in biological surfaces. *Planta,* **202**(1), 1–8.

[55] Solga, A., Cerman, Z., Striffler, B. F., Spaeth, M., and Barthlott, W. (2007) The dream of staying clean: Lotus and biomimetic surfaces. *Bioinspir. Biomim.,* **2**(4), S126—-S134.

[56] Gorb, E., Haas, K., Henrich, A., Enders, S., Barbakadze, N., and Gorb, S. (2005) Composite structure

of the crystalline epicuticular wax layer of the slippery zone in the pitchers of the carnivorous plant *Nepenthes alata* and its effect on insect attachment. *J. Exp. Biol.,* **208**(24), 4651–4662.

[57] Koch, K., Bhushan, B., and Barthlott, W. (2010) Multifunctional plant surfaces and smart materials, Springer, Würzburg.

[58] Gorb, E. V., Baum, M. J., and Gorb, S. N. (2013) Development and regeneration ability of the wax coverage in *Nepenthes alata* pitchers: a cryo-SEM approach. *Sci. Rep.,* **3**.

[59] Bohn, H. F. and Federle, W. (2004) Insect aquaplaning: *Nepenthes* pitcher plants capture prey with the peristome, a fully wettable water-lubricated anisotropic surface. *Proc. Natl. Acad. Sci.,* **101**(39), 14138–14143.

[60] Gaume, L., Perret, P., Gorb, E., Gorb, S., Labat, J.-J., and Rowe, N. (2004) How do plant waxes cause flies to slide? Experimental tests of wax-based trapping mechanisms in three pitfall carnivorous plants. *Arthropod Struct. Dev.,* **33**(1), 103–111.

[61] Gorb, E. V. and Gorb, S. N. (2017) Anti-adhesive effects of plant wax coverage on insect attachment. *J. Exp. Bot.,* **68**(19), 5323–5337.

[62] Gorb, E. and Gorb, S. (2002) Attachment ability of the beetle *Chrysolina fastuosa* on various plant surfaces. *Entomol. Exp. Appl.,* **105**(1), 13–28.

[63] Wong, T.-S., Kang, S. H., Tang, S. K. Y., Smythe, E. J., Hatton, B. D., Grinthal, A., and Aizenberg, J. (2011) Bioinspired self-repairing slippery surfaces with pressure-stable omniphobicity. *Nature,* **477**(7365), 443–447.

[64] Epstein, A. K., Wong, T.-S., Belisle, R. A., Boggs, E. M., and Aizenberg, J. (2012) Liquid-infused structured surfaces with exceptional anti-biofouling performance. *Proc. Natl. Acad. Sci.,* **109**(33), 13182–13187.

[65] Aizenberg, J., Aizenberg, M., Kang, S. H., Wong, T. S., and Kim, P. Lubricated slippery surfaces with high pressure stability, optical transparency, and self-healing characteristics. US Patent 9121307.

[66] Coady, M. J., Wood, M., Wallace, G. Q., Nielsen, K. E., Kietzig, A.-M., Lagugné-Labarthet, F., and Ragogna, P. J. (2018) Icephobic behavior of UV-cured polymer networks incorporated into slippery lubricant-infused porous surfaces: Improving SLIPS durability. *ACS Appl. Mater. Interfaces,* **10**(3), 2890–2896.

[67] Bittner, R. W., Bica, K., and Hoffmann, H. (2017) Fluorine-free, liquid-repellent surfaces made from ionic liquid-infused nanostructured silicon. *Monatshefte für Chemie,* **148**(1), 167–177.

[68] Zhou, Y., Robinson, A., Steiner, U., and Federle, W. (2014) Insect adhesion on rough surfaces: analysis of adhesive contact of smooth and hairy pads on transparent microstructured substrates. *J. R. Soc. Interface,* **11**(98), 20140499.

[69] Graf, C., Kesel, A. B., Gorb, E. V., Gorb, S. N., and Dirks, J.-H. H. (2018) Investigating the efficiency of a bio-inspired insect repellent surface structure. *Bioinspir. Biomim.,* **13**(5), 56010.

[70] Zhou, Y. (2015) Insect adhesion on rough surfaces and properties of insect repellent surfaces (PhD thesis), University of Cambridge, Cambridge.

[71] Radinovsky, S. and Krantz, G. W. (1962) The use of Fluon to prevent the escape of stored-product insects

from glass containers. *J. Econ. Entomol.,* **55**(5), 815–816.

[72] Chen, J. (2007) Advancement on techniques for the separation and maintenance of the red imported fire ant colonies. *Insect Sci.,* **14**(1), 1–4.

[73] Hansen, M. K., Larsen, M., and Cohr, K.-H. (1987) Waterborne paints: A review of their chemistry and toxicology and the results of determinations made during their use. *Scand. J. Work. Environ. Health,* **13**(6), 473–485.

[74] Mariz, I. d. F. A., Millichamp, I. S., de la Cal, J. C., and Leiza, J. R. (2010) High performance water-borne paints with high volume solids based on bimodal latexes. *Prog. Org. Coatings,* **68**(3), 225–233.

[75] Sperry, P. R., Snyder, B. S., O'Dowd, M. L., and Lesko, P. M. (1994) Role of water in particle deformation and compaction in latex film formation. *Langmuir,* **10**(8), 2619–2628.

[76] Steward, P. A., Hearn, J., and Wilkinson, M. C. (2000) An overview of polymer latex film formation and properties. *Adv. Colloid Interface Sci.,* **86**(3), 195–267.

[77] Scholz, W. (1993) Paint Additives, Springer Science+Business Media, Dordrecht.

[78] Asbeck, W. K. and Loo, M. V. (1949) Critical Pigment Volume Relationships.. *Ind. Eng. Chem.,* **41**(7), 1470–1475.

[79] Müller, B. and Poth, U. (2010) Paint formulation, Vincentz, Hanover.

[80] del Rio, G. and Rudin, A. (1996) Latex particle size and CPVC. *Prog. Org. Coatings,* **28**(4), 259–270.

[81] Alvarez, V. and Paulis, M. (2017) Effect of acrylic binder type and calcium carbonate filler amount on the properties of paint-like blends. *Prog. Org. Coatings,* **112**, 210–218.

[82] Ding, T., Daniels, E. S., El-Aasser, M. S., and Klein, A. (2005) Film Formation from Pigmented Latex Systems: Mechanical and Surface Properties of Ground Calcium Carbonate/Functionalized Poly (*n*-butyl methacrylate-*co-n*-butyl acrylate) Latex Blend Films. *J. Appl. Polym. Sci.,* **100**(6), 4550–4560.

[83] Daniels, Christian Leonard Gruber, B. High solids pigmented latex compositions. US Patent 20120234490.

[84] Davies, J. and Binner, J. G. P. (2000) The role of ammonium polyacrylate in dispersing concentrated alumina suspensions. *J. Eur. Ceram. Soc.,* **20**(10), 1539–1553.

[85] Baklouti, S., Romdhane, M. R. B., Boufi, S., Pagnoux, C., Chartier, T., and Baumard, J. F. (2003) Effect of copolymer dispersant structure on the properties of alumina suspensions. *J. Eur. Ceram. Soc.,* **23**(6), 905–911.

[86] Lohmeijer, B., Balk, R., and Baumstark, R. (2012) Preferred partitioning: the influence of coalescents on the build-up of mechanical properties in acrylic core-shell particles (I). *J. Coatings Technol. Res.,* **9**(4), 399–409.

[87] Bauer, U. and Federle, W. (2009) The insect-trapping rim of *Nepenthes* pitchers. *Plant Signal. Behav.,* **4**(11), 1019–1023.

[88] Dukas, R. (2008) Evolutionary Biology of Insect Learning. *Annu. Rev. Entomol.,* **53**(1), 145–160.

[89] Federle, W., Brainerd, E. L., McMahon, T. A., and Hölldobler, B. (2001) Biomechanics of the movable pretarsal adhesive organ in ants and bees. *Proc. Natl. Acad. Sci.,* **98**(11), 6215–6220.

[90] R Development Core Team R: A language and environment for statistical computing. `https://www.`

r-project.org/ (2018).

[91] Wang, J., Xu, H., Battocchi, D., and Bierwagen, G. (2014) The determination of critical pigment volume concentration (CPVC) in organic coatings with fluorescence microscopy. *Prog. Org. Coatings,* **77**(12), 2147–2154.

[92] Tang, J., Daniels, E. S., Dimonie, V. L., Klein, A., and El-Aasser, M. S. (2002) Influence of particle surface properties on film formation from precipitated calcium carbonate/latex blends. *J. Appl. Polym. Sci.,* **86**(4), 891–900.

[93] Tiarks, F., Frechen, T., Kirsch, S., Leuninger, J., Melan, M., Pfau, A., Richter, F., Schuler, B., and Zhao, C.-L. (2003) Formulation effects on the distribution of pigment particles in paints. *Prog. Org. Coatings,* **48**(2-4), 140–152.

[94] Farrokhpay, S., Morris, G. E., and Fornasiero, D. (2006) Titania pigment particles dispersion in water-based paint films. *J. Coatings Technol. Res.,* **3**(4), 275–283.

[95] Dietz, P. F. (2003) Spacing for better effects. *Eur. Coatings J.,* **49**, 14–20.

[96] Karakaş, F. and Çelik, M. (2012) Effect of quantity and size distribution of calcite filler on the quality of water borne paints. *Prog. Org. Coatings,* **74**(3), 555–563.

[97] Gorb, E. V., Hosoda, N., Miksch, C., and Gorb, S. N. (2010) Slippery pores: anti-adhesive effect of nanoporous substrates on the beetle attachment system. *J. R. Soc. Interface,* **7**(52), 1571–1579.

[98] Zhou, Y., Robinson, A., Viney, C., and Federle, W. (2015) Effect of shear forces and ageing on the compliance of adhesive pads in adult cockroaches. *J. Exp. Biol.,* **218**(17), 2775–2781.

[99] Betz, O., Frenzel, M., Steiner, M., Vogt, M., Kleemeier, M., Hartwig, A., Sampalla, B., Rupp, F., Boley, M., and Schmitt, C. (2017) Adhesion and friction of the smooth attachment system of the cockroach *Gromphadorhina portentosa* and the influence of the application of fluid adhesives. *Biol. Open,* **6**(5), 589–601.

[100] Kovalev, A. E., Filippov, A. E., and Gorb, S. N. (2012) Insect wet steps: loss of fluid from insect feet adhering to a substrate. *J. R. Soc. Interface,* **10**(78), 20120639–20120639.

[101] Anyon, M. J., Orchard, M. J., Buzza, D. M. A., Humphries, S., and Kohonen, M. M. (2012) Effect of particulate contamination on adhesive ability and repellence in two species of ant (Hymenoptera; Formicidae). *J. Exp. Biol.,* **215**(4), 605–616.

[102] Farrokhpay, S., Morris, G. E., Fornasiero, D., and Self, P. (2004) Effects of chemical functional groups on the polymer adsorption behavior onto titania pigment particles. *J. Colloid Interface Sci.,* **274**(1), 33–40.

[103] Persson, B. N. J. (2007) Biological Adhesion for Locomotion on Rough Surfaces: Basic Principles and A Theorist's View. *MRS Bull.,* **32**(6), 486–490.

[104] Butt, H.-J., Barnes, W. J. P., del Campo, A., Kappl, M., and Schönfeld, F. (2010) Capillary forces between soft, elastic spheres. *Soft Matter,* **6**(23), 5930–5936.

[105] Clemente, C. J., Bullock, J. M. R., Beale, A., and Federle, W. (2010) Evidence for self-cleaning in fluid-based smooth and hairy adhesive systems of insects. *J. Exp. Biol.,* **213**(4), 635–642.

[106] Clemente, C. J. and Federle, W. (2012) Mechanisms of self-cleaning in fluid-based smooth adhesive pads

of insects. *Bioinspir. Biomim.,* **7**(4), 46001.

[107] Amador, G. J., Endlein, T., and Sitti, M. (2017) Soiled adhesive pads shear clean by slipping: a robust self-cleaning mechanism in climbing beetles. *J. R. Soc. Interface,* **14**(131), 20170134.

[108] Orchard, M. J., Kohonen, M., and Humphries, S. (2012) The influence of surface energy on the self-cleaning of insect adhesive devices. *J. Exp. Biol.,* **215**(2), 279–286.

[109] Tomioka, T. Insect repellent coating and industrial product using the same. (2006) US Patent 2006177472.

[110] Jaffé, K., Bazire-Benazét, M., and Howse, P. E. (1979) An integumentary pheromone-secreting gland in *Atta* sp: Territorial marking with a colonyspecific pheromone in *Atta cephalotes*. *J. Insect Physiol.,* **25**(10), 833–839.

[111] Goetzke, H. H., Pattrick, J. G., and Federle, W. (2019) Froghoppers jump from smooth plant surfaces by piercing them with sharp spines. *Proc. Natl. Acad. Sci.,* **116**(8), 3012–3017.

Appendix

A3.1 Paint formulation

Table A3.1: Composition, CPVC, PVC, surface roughness (R_a), peak density, wettability and slipperiness values of the full set of waterborne paints (45 paints) applied on metal sheets. The CPVC was approximated from Eq. 3.3. Both R_a and peak density were measured *via* optical profilometry. The slipperiness to *A. cephalotes* ants refers to the number of unsuccessful ants in climbing experiments. The values are expressed as mean $\pm$ standard deviation (SD). See section Materials and Methods for further explanations.

Paint	[TiO$_2$] (wt%)	[CaCO$_3$] (wt%)	Approximate CPVC (%) (Eq. 3.3)	PVC (%)	R_a (μm) ($n = 6$)	Peak density (peaks/mm^2) ($n = 6$)	Water contact angle (°) ($n = 4$)	Slipperiness (%) ($n = 20$)
1	10	0	54	50	2.8 $\pm$ 0.4	56 $\pm$ 6	64 $\pm$ 7	20 $\pm$ 10
2	10	0	54	60	2.7 $\pm$ 0.2	339 $\pm$ 101	98 $\pm$ 3	90 $\pm$ 10
3	10	0	54	70	4.7 $\pm$ 1.8	23 $\pm$ 8	89 $\pm$ 6	0 $\pm$ 10
4	20	0	54	50	2.2 $\pm$ 0.7	374 $\pm$ 134	79 $\pm$ 8	20 $\pm$ 10
5	20	0	54	60	1.9 $\pm$ 0.4	42 $\pm$ 3	102 $\pm$ 8	10 $\pm$ 10
6	20	0	54	70	5.3 $\pm$ 1.0	20 $\pm$ 6	86 $\pm$ 5	0 $\pm$ 10
7	30	0	54	50	1.3 $\pm$ 0.5	46 $\pm$ 14	86 $\pm$ 3	20 $\pm$ 10
8	30	0	54	60	2.6 $\pm$ 0.3	30 $\pm$ 15	100 $\pm$ 3	40 $\pm$ 10
9	30	0	54	70	5.3 $\pm$ 0.5	39 $\pm$ 12	94 $\pm$ 3	10 $\pm$ 10
10	0	6.6	63	50	2.5 $\pm$ 0.2	118 $\pm$ 33	71 $\pm$ 1	10 $\pm$ 10
11	0	6.6	63	60	26.7 $\pm$ 4.5	304 $\pm$ 51	62 $\pm$ 3	30 $\pm$ 10
12	0	6.6	63	70	1.1 $\pm$ 0.3	150 $\pm$ 72	83 $\pm$ 2	85 $\pm$ 15
13	0	13	63	50	2.2 $\pm$ 0.3	91 $\pm$ 24	59 $\pm$ 2	10 $\pm$ 10
14	0	13	63	60	13.0 $\pm$ 4.6	394 $\pm$ 59	73 $\pm$ 1	30 $\pm$ 10
15	0	13	63	70	2.4 $\pm$ 0.3	67 $\pm$ 30	84 $\pm$ 4	100 $\pm$ 5
16	0	20	63	50	2.8 $\pm$ 0.7	83 $\pm$ 11	62 $\pm$ 1	35 $\pm$ 5
17	0	20	63	60	30.0 $\pm$ 10.2	49 $\pm$ 12	71 $\pm$ 1	20 $\pm$ 20
18	0	20	63	70	3.6 $\pm$ 1.8	626 $\pm$ 157	84 $\pm$ 2	75 $\pm$ 5
19	10	0	54	60	2.7 $\pm$ 0.2	339 $\pm$ 101	98 $\pm$ 3	90 $\pm$ 10
20	10	6.6	59	60	1.2 $\pm$ 0.5	291 $\pm$ 70	70 $\pm$ 3	20 $\pm$ 10

Table A3.1: (continued).

Paint	[TiO$_2$] (wt%)	[CaCO$_3$] (wt%)	Approximate CPVC (%) (Eq. 3.3)	PVC (%)	R_a (μm) ($n = 6$)	Peak density (peaks/mm^2) ($n = 6$)	Water contact angle (°) ($n = 4$)	Slipperiness (%) ($n = 20$)
21	10	6.6	59	70	4.9 ± 0.1	1130 ± 45	86 ± 1	80 ± 5
22	10	13	60	50	1.5 ± 0.1	1158 ± 17	57 ± 3	10 ± 10
23	10	13	60	60	4.7 ± 0.1	1163 ± 39	71 ± 3	20 ± 10
24	10	13	60	70	4.9 ± 0.1	1156 ± 15	86 ± 5	90 ± 5
25	10	20	61	50	4.6 ± 0.1	1167 ± 46	58 ± 1	10 ± 10
26	10	20	61	60	4.7 ± 0.1	1122 ± 42	71 ± 1	70 ± 10
27	10	20	61	70	1.9 ± 0.4	80 ± 14	89 ± 1	85 ± 5
28	20	6.6	57	50	2.0 ± 0.6	149 ± 52	71 ± 2	20 ± 10
29	20	6.6	57	60	1.2 ± 0.1	774 ± 53	80 ± 1	80 ± 5
30	20	6.6	57	70	2.6 ± 1.2	21 ± 13	88 ± 1	95 ± 5
31	20	13	59	50	1.5 ± 0.4	282 ± 37	60 ± 5	10 ± 10
32	20	13	59	60	1.0 ± 0.1	313 ± 58	74 ± 3	10 ± 10
33	20	13	59	70	1.1 ± 0.3	381 ± 159	88 ± 6	85 ± 5
34	20	20	59	50	0.9 ± 0.2	547 ± 104	58 ± 2	0 ± 10
35	20	20	59	60	1.4 ± 0.1	438 ± 105	69 ± 1	10 ± 10
36	20	20	59	70	1.9 ± 0.4	363 ± 77	87 ± 2	90 ± 5
37	30	6.6	56	50	1.0 ± 0.1	270 ± 88	68 ± 4	10 ± 10
38	30	6.6	56	60	1.3 ± 0.2	61 ± 13	78 ± 1	30 ± 10
39	30	6.6	56	70	1.3 ± 0.4	299 ± 136	86 ± 5	87 ± 12
40	30	13	58	50	2.0 ± 0.4	39 ± 34	64 ± 1	0 ± 10
41	30	13	58	60	2.0 ± 0.8	196 ± 93	67 ± 1	20 ± 10
42	30	13	58	70	4.8 ± 0.1	1156 ± 41	94 ± 1	90 ± 10
43	30	20	59	50	4.8 ± 0.1	1136 ± 33	53 ± 2	10 ± 10
44	30	20	59	60	4.9 ± 0.1	1110 ± 88	66 ± 1	10 ± 10
45	30	20	59	70	4.6 ± 0.1	1140 ± 46	89 ± 3	90 ± 10

A3.2 Example of TiO$_2$-only paints displaying cracks and their CaCO$_3$-only counterpart paints
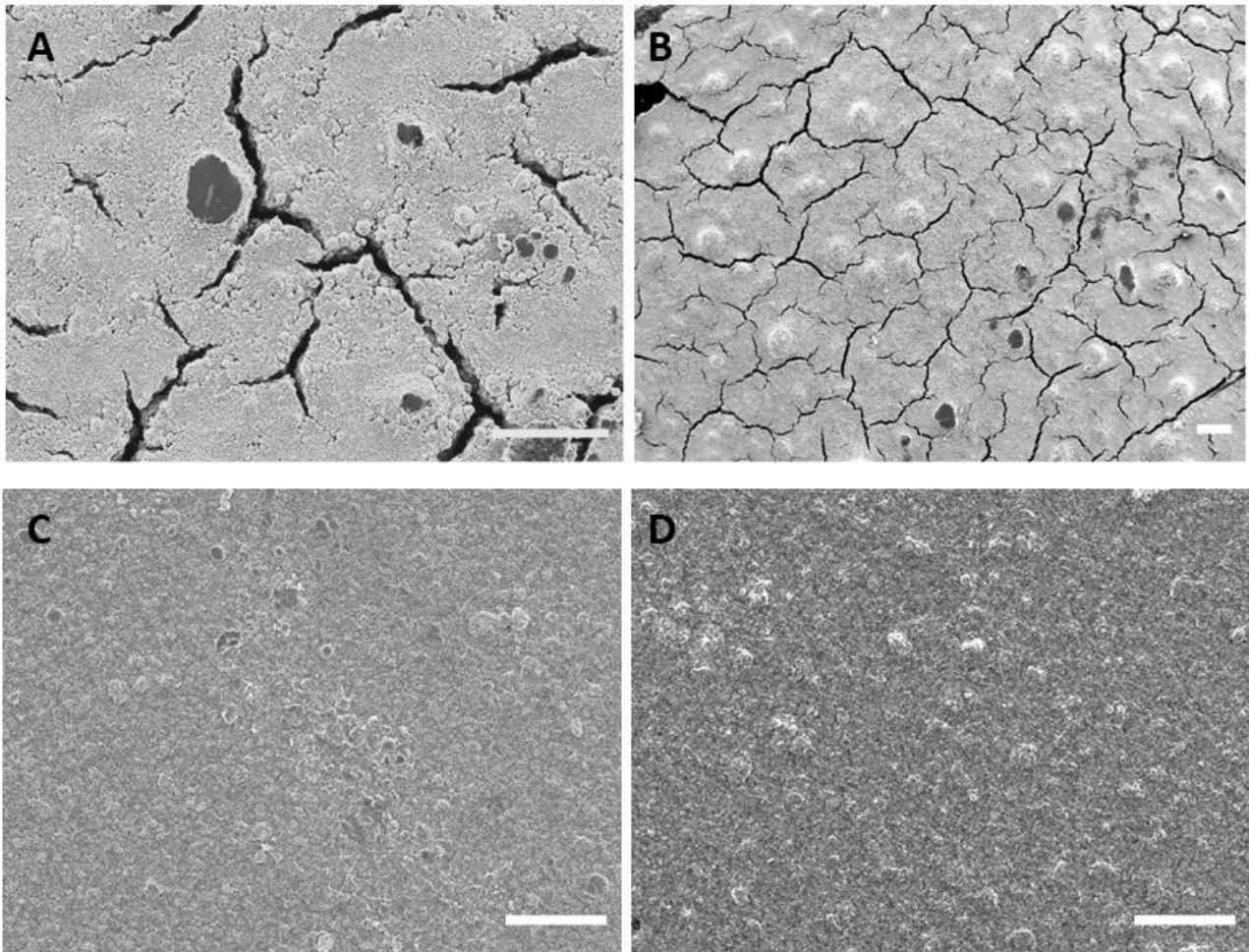

Figure A3.1: SEM images of 20 wt% TiO$_2$ paints formulated at (A) PVC 60 and (B) PVC 70. The number of cracks increases with the PVC, which are likely to expand upon contact with the stiff claws of *A. cephalotes* ants if the coatings are too soft. SEM images of 13 wt% CaCO$_3$ paints formulated at (C) PVC 60 and (D) PVC 70. These paints did not show any cracks. Scale bars: 100 μm.

A3.3   Effect of peak density
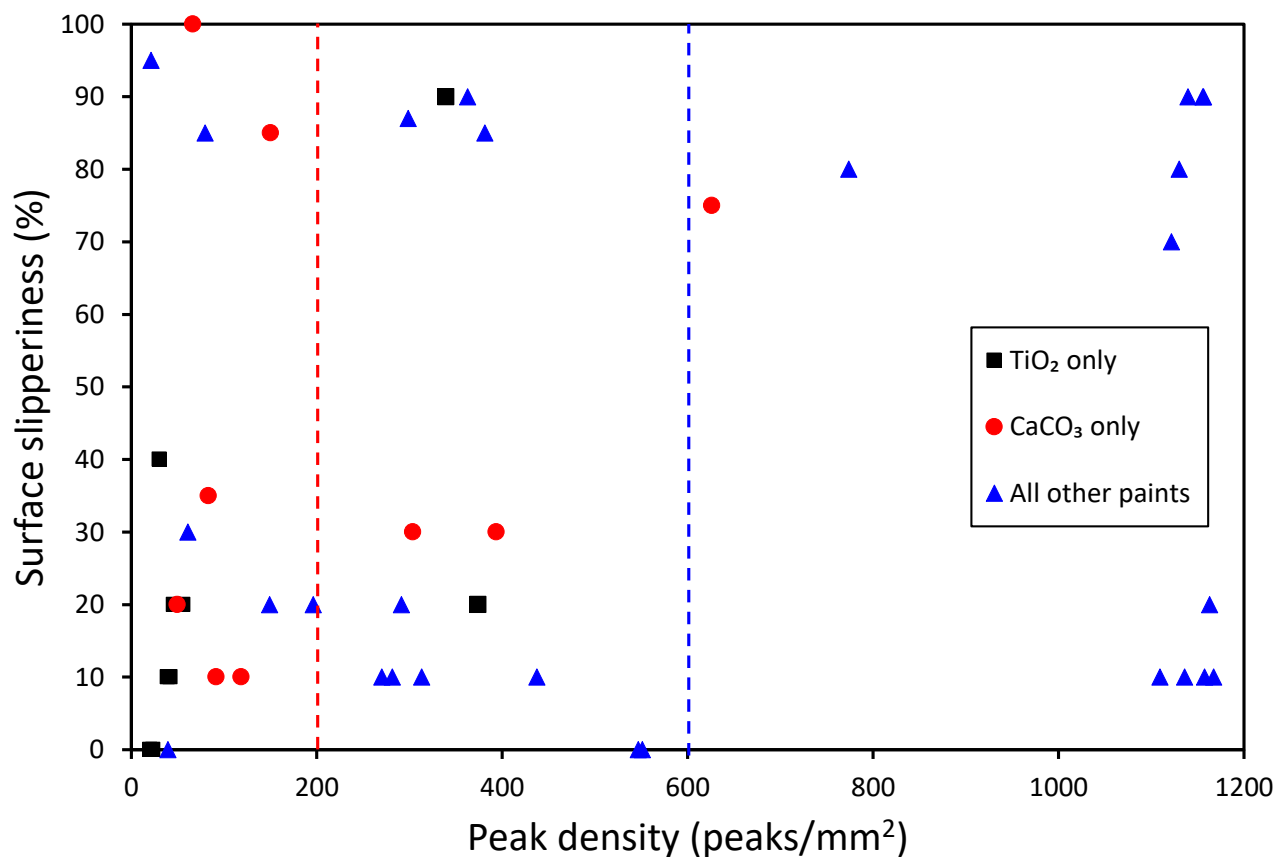
Figure A3.2: Surface slipperiness (percentage of unsuccessful ants) vs. peak density. For $CaCO_3$-only paints (red circles) and $TiO_2/CaCO_3$ solid paints (blue triangles), the slipperiness decreased until reaching approximate threshold values of 200 and 600 peaks/mm^2, respectively (dashed lines). The slipperiness in TiO_2-only paints (black squares) appeared mainly driven by cracks; hence, the slipperiness increased with peak density as the number of cracks decreased. Error bars were not included for more clarity.

A3.4 ANOVA (type II) and Principal Component Regression (PCR) of the slipperiness data for the 45 paints

To avoid artefacts resulting from the ordering of factors in unbalanced datasets, we conducted an ANOVA based on Type II sums of squares. We considered PVC, water contact angle, R_a and peak density as explanatory variables that influence slipperiness. The minimal model contained several significant interactions that involved all the factors. A correlation matrix revealed that the explanatory variables of this analysis are correlated with each other, in particular water contact angle and PVC.

As the explanatory variables were correlated with each other, we conducted a principal component regression analysis on them, and obtained the following eigenvalues and loadings:

Table A3.2: Results of the ANOVA (type II) analysis performed on the minimised dataset involving PVC, water contact angle, R_a and peak density as explanatory variables. A correlation matrix shows these explanatory variables are correlated with each other. Values in bold indicate either significant impact on slipperiness or correlation between factors.

	Sum of squares	Degrees of freedom	F-value	P-value
R_a	0.13063	1	1.81	0.187
Wettability	0.25783	1	3.57	0.066
Peak density	**0.37667**	**1**	**5.22**	**0.028**
PVC	**0.93406**	**1**	**12.94**	**< 0.001**
Wettability $\times$ peak density	**1.00106**	**1**	**13.87**	**< 0.001**
$R_a \times$ PVC	**1.24202**	**1**	**17.21**	**< 0.001**
Residuals	2.74309	38		

	PVC	Water contact angle	R_a	Peak density
PVC	1			
Water contact angle	0.72	1		
R_a	0.084	-0.11	1	
Peak density	0.038	-0.2	-0.0069	1

The first three principal components have eigenvalues greater than 1 and explain 94.6% of the variation. The first principal component (PC1) is mainly associated with PVC and water contact angle, whereas PC2 and PC3 are mainly linked with R_a and peak density (positive and negative associations) and hence mainly describe surface roughness. A linear model estimate for (arcsine-transformed) slipperiness based on the first three principal components is:

$$Slipperiness = 38.6 - 17.2\ PC1 + 6.7\ PC2 - 9.9\ PC3 \qquad (3.5)$$

Table A3.3: PCR loading matrix for the following factors: PVC, water contact angle, R_a and peak density. A linear model estimate for (arcsine-transformed) slipperiness using PC1, PC2 and PC3 is also presented.

Principal component analysis of explanatory variables				
Eigenvalue	1.741	1.041	1.001	0.216
Proportion	0.435	0.260	0.250	0.054
Cumulative	0.435	0.696	0.946	1.000

Loading matrix				
	PC1	PC2	PC3	PC4
PVC	-0.902	0.282	-0.102	-0.311
R_a	0.038	0.745	0.661	0.080
Water contact angle	-0.940	-0.103	-0.038	0.323
Peak density	0.205	0.630	-0.743	0.097

	Estimate	Standard error	t-value	P-value
Intercept	38.6	3.748	10.298	< 0.001
PC1	-17.198	2.873	-5.987	< 0.001
PC2	6.678	3.715	1.798	0.080
PC3	-9.937	3.788	-2.623	0.012

All three PCs were at least marginally significant, and PC1 had the strongest effect (Table A3.3).

A3.5 Long-term slipperiness

Table A3.4: Slipperiness and surface roughness average ($_R a$) comparison of 30 wt% TiO_2, PVC 70 paints with different $CaCO_3$ contents, before (t = 0) and after 5 months of continuous exposure to climbing ants. T-values and P-values are the results of paired t-tests on slipperiness ($\alpha = 0.05$). U-values and P-values are the results of Mann-Whitney tests on surface roughness ($\alpha = 0.05$). The values are expressed as mean $\pm$ standard deviation (SD).

Paint	$[TiO_2]$ (%)	$[CaCO_3]$ (%)	Slipperi-ness at t = 0 (%) (n = 20)	Slipperiness at t = 5 months (plateau) (%) (n $\approx$ 40)	T_2-value (P-value) (test for change in slipperi-ness)	R_a at t = 0 (μm) (n = 6)	R_a at t = 5 months (μm) (n = 10)	$U_{10,6}$-value (P-value) (test for change in R_a)
39	30	6.6	90 $\pm$ 5	33 $\pm$ 10	14.82 (0.004)	1.3 $\pm$ 0.4	9.5 $\pm$ 1.1	0 (0.001)
42	30	13	100 $\pm$ 5	60 $\pm$ 10	8.01 (0.015)	4.8 $\pm$ 0.1	5.7 $\pm$ 1.9	18 (0.211)
45	30	20	100 $\pm$ 5	70 $\pm$ 10	5.29 (0.034)	4.6 $\pm$ 0.1	7.6 $\pm$ 1.3	0 (0.001)

An estimate of the number of particles in the PVC 70 paint film (paint 45, 30 wt% TiO_2, 20 wt% $CaCO_3$) was calculated as follows:

$$N_{particles} = \sum \frac{m_{k,total}}{m_{k,single}} \tag{3.6}$$

Assuming spherical particles (300 nm TiO_2 and 1 μm $CaCO_3$ particles), the mass of the individual particles ($m_{k,single}$) are:

$$m_{TiO_2,single} = V_{TiO_2} \times \rho_{TiO_2} = 5.8 \times 10^{-17} \; kg$$

$$m_{CaCO_3,single} = V_{CaCO_3} \times \rho_{CaCO_3} = 1.4 \times 10^{-15} \; kg \tag{3.7}$$

Where $V_{TiO_2} \approx 1.4 \times 10^{-20}$ m^3 and $V_{CaCO_3} \approx 5.2 \times 10^{-19}$ m^3 is the volume (both calculated assuming spherical shape), and $\rho_{TiO_2} = 4.1$ g/cm^3 and $\rho_{CaCO_3} = 2.7$ g/cm^3 is the density of the particles. The total mass ($m_{k,total}$) of particles in the paint film is given by:

$$m_{TiO_2,total} = 0.30 \times A \times t \times d = 0.17 \; g$$

$$m_{CaCO_3,total} = 0.20 \times A \times t \times d = 0.11 \; g \tag{3.8}$$

With t, the dry film thickness (57 μm), A the film area (10.5 cm $\times$ 8.5 cm) and d the wet paint density (1.1 kg/L). Leading to:

$$N_{TiO_2} = 2.9 \times 10^{12} \; particles$$
$$N_{CaCO_3} = 7.9 \times 10^{10} \; particles$$

(3.9)

There were $N = 2.9 \times 10^{12}$ solid particles in the paint film, *i.e.* 14,000 ants climbing daily on the panel removed approximately 3.4% of particles.
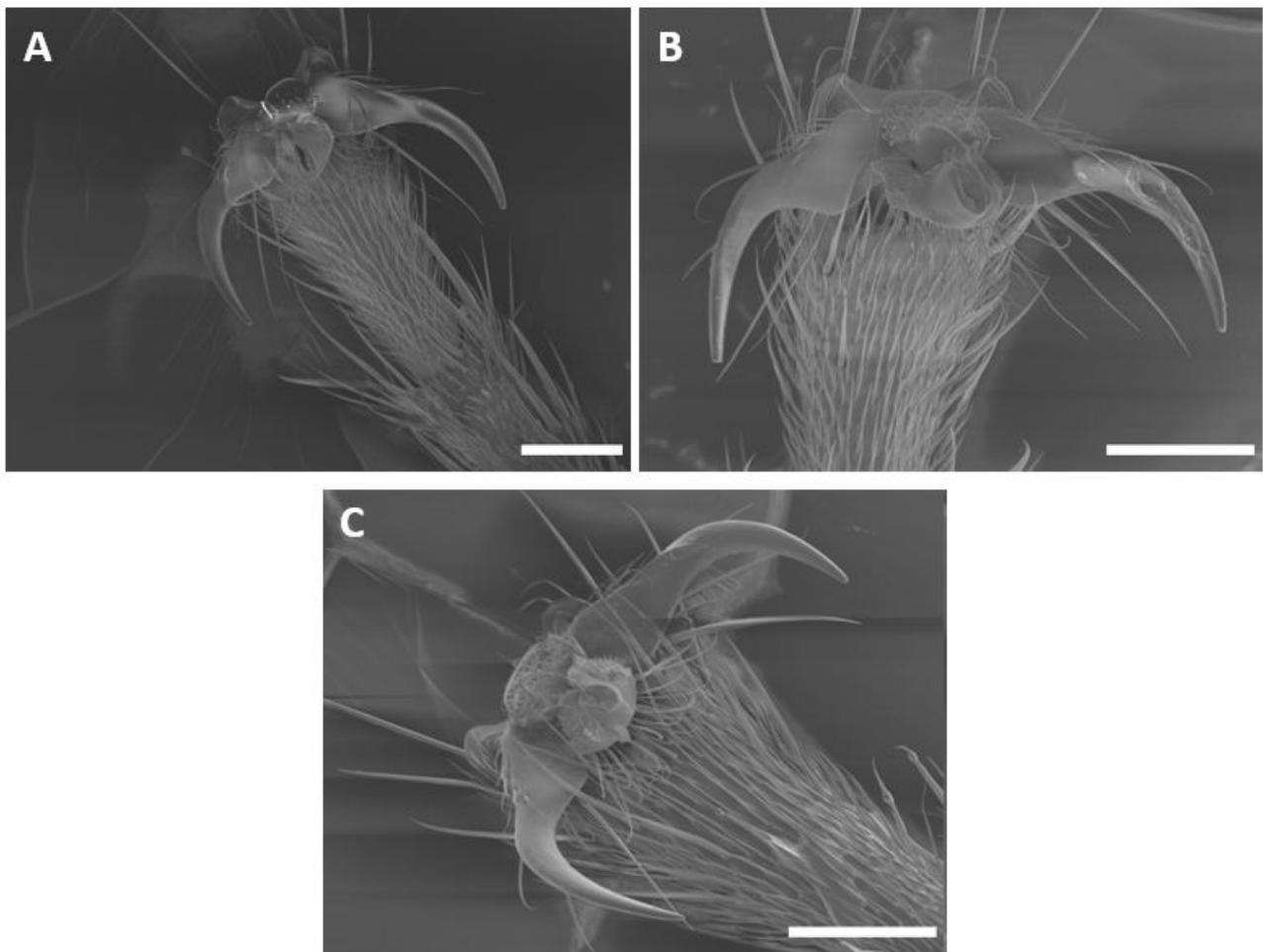

Figure A3.3: SEM of *A. cephalotes* ant tarsi after climbing on 70% PVC paints formulated with 30 wt% TiO$_2$ and (A) 6.6 wt% CaCO$_3$; (B) 13 wt% CaCO$_3$ and (C) 20 wt% CaCO$_3$. The paint panels had been left in the colony cage for five months and no particles could be observed on the tarsi. Scale bars: 100 μm.

4

Adhesion of PDMS lenses on ant-slippery paints

The feasibility of JKR-type experiments (Johnson–Kendall–Roberts) to investigate the adhesion properties of paint coatings slippery to ants was assessed with PDMS hemispheres mimicking insects' adhesive pads. In the presence of small pigment extender particles and low concentration of polymer binder, paints can be rendered slippery as insects' adhesive pads detach particles and fall from vertical painted surfaces. Using one hemisphere per paint sample, a decrease in adhesive stress (adhesion/contact area) was observed for all paints, even when they were non-slippery or when no pigment particles detached from the coatings, underlying that some uncured oligomers probably transferred from the PDMS to the coating, as shown by FTIR-ATR experiments. The experiments allowed us to access the number of pigment contaminants present at the surface of the PDMS hemispheres, which was found not to be related to the paint slipperiness, i.e. *the number of insects sliding from vertically oriented coatings. In its current form, the test needs to be improved in terms of reproducibility to be used as an alternative to insect climbing tests or to measure the adhesion of coatings in a reliable way.*

Aurélie Féat[a,b], Marleen Kamperman[b,c], Martin W. Murray[a] and Jasper van der Gucht[b]

[a]AkzoNobel Decorative Paints, Wexham Road, Slough, SL2 5DS, United Kingdom

[b]Physical Chemistry and Soft Matter, Wageningen University, Stippeneng 4, 6708 WE, Wageningen, The Netherlands

[c]Zernike Institute for Advanced Materials, University of Groningen, Nijenborgh 4, 9747 AG Groningen, The Netherlands

4.1 Introduction

Insects climb surfaces using two main, complementary mechanisms: interlocking with substrate protrusions and pad adhesion. Insect claws and spines cling with surface asperities, given that the claw tip diameter is smaller than the protrusions [1, 2]. Adhesive pads comply with surface asperities to maximise adhesion and are distinguished into two categories: hairy and smooth pads [3, 4]. Insects such as beetles and flies possess hairy pads, while smooth pads are found in e.g. ants and cockroaches. Both types of pads secrete an adhesive fluid which is thought to increase the pad/surface contact area through capillary adhesion by filling in surface asperities [2, 5–7]. The purpose and composition of the fluid is however still under debate [8–10].

Our previous studies (**Chapter 3**) showed that model coatings slippery to insects (*Atta cephalotes* ants) could be prepared when using a relatively large amount of pigment and extender, as the loose particles have been shown to detach and adhere to the adhesive pads of *A. cephalotes* ants. In particular, the paints become more slippery once the paints are formulated above their Critical Pigment Volume Concentration (CPVC), *i.e.* the pigment-to-binder ratio indicating at which Pigment Volume Concentration (PVC) there is not enough polymer binder to fully wet the particles [11], which can then easily detach upon contact with the sticky feet of insects. Such "insect-slippery" paint coatings can have applications for bio-friendlier alternatives to insecticides and insecticidal paints. Measuring the adhesion of the coatings, *i.e.* the force needed to detach PDMS from the coatings, is hence of interest to offer a better insight of their slippery properties as it is expected that adhesion decreases upon repeated measurements as particles detach from the paint.

Whereas adhesion tests are available in the coating industry, such as the "crude" cross-cut test consisting in cutting a cross-hatch lattice and removing it using tape [12], or the pull-off test which assesses the minimum tensile stress to detach a coating from its surface [13]; they cannot explain how pigment and extender particles detach from coatings at the scale of an insect pad. Atomic force microscopy (AFM) is a useful tool to measure the adhesive properties of surfaces at the nano- and micro-scale. It has for instance been used to measure the adhesion between contaminants and beetle pads [14] or to measure the adhesion of individual hairs (setae) of hairy pads [15, 16]. However, to the best of the authors' knowledge, AFM has not been used to directly measure the adhesion of pads to substrates, as one can imagine such tests would be

difficult to perform in practice.

Single insect pad adhesion (and friction) has been successfully measured with load cells in a various number of studies, see e.g. [5, 17, 18]. In short, insect pads are brought into contact with a surface, allowing both the adhesion and friction forces to be measured. Although possible [19], performing this test on ants remains challenging as they possess retractable adhesive pads [20, 21]. Purtov *et al.* recently reported that PDMS probes could be used in pull-off experiments to measure adhesion of epoxy substrates with varying roughness and presenting low adhesion [22]. Similarly, Gorb *et al.* recently compared the traction of Coccinellids and adhesion performances of PDMS probes on alkane wax coatings [23].

Using a similar procedure, we tested in the present work the feasibility of pull-off tests (Johnson–Kendall–Roberts (JKR)-type experiment) to investigate the adhesion properties of our slippery paint coatings (Figure 4.1). Repeated contacts were performed as the paints were connected to a load cell. The JKR test consists of approaching a rigid sphere onto a deformable sample with a known load and velocity, the pull-off force (adhesive force) being measured during the sphere retraction [24]. To this end, we prepared polydimethylsiloxane (PDMS) hemispheres (1 mm diameter) to mimic ants' adhesive pads ('deformable' sphere) and repeated some pull-off measurements using paint samples ('rigid' surface). PDMS, such as the commonly used Sylgard 184, is inexpensive, non-toxic, easy-to-use and chemically inert. The objectives of the present study were to assess if (1) pull-off experiments using PDMS insect pads can be used as models to understand why the paints are slippery to insects and (2) to quantify the contamination occurring after contact of PDMS on the paints and investigate if it is PVC-dependent as observed in tests with *Atta cephalotes* ants (**Chapter 3**). JKR-like experiments allowed us to measure the paint/PDMS contact area and pull-off force (adhesion force), while the hemispheres' contamination, if any, was assessed with optical microscopy.

4.2   Materials and methods

4.2.1   Materials

To formulate the paints, an acrylic binder prepared by emulsion polymerisation and presented in **Chapter 3** was used (68 nm $\pm$ 1 nm ($n = 10$, T_g 28.0 °C $\pm$ 0.8°C ($n = 3$)). The titanium dioxide pigment used was supplied by Cristal (Grimsby, UK) and is an aluminate- and zirconia-

coated rutile with a density of 4.1 g/cm^3 and a mean particle size of 300 nm. The extender was a ground calcium carbonate from Omya (Orgon, France), with a density of 2.7 g/cm^3 and a mean particle size of 1 μm. Sodium dodecyl sulphate (SDS, CMC = 7.9 mM) was used to disperse the pigment and extender in the paints and was supplied by VWR (Lutterworth, UK). Texanol (Eastman, Kingsport, TN, USA), a coalescent was used. The paints were neutralised using AMP 95 (Sigma-Aldrich, Gillingham, UK).

The surface energy of the coatings was measured using the following liquids: Milli-Q water, ethylene glycol (Fluka, Steinheim, Germany) and 1-bromonapthalene (Alfa Aesar, Heysham, UK).

For the fabrication of the PDMS spheres (procedure described below), we used OOMOO Clear Flex 50 (Smooth-On, Easton, PA, USA), perfluorodecyltrichlorosilane (Sigma-Aldrich, Zwijndrecht, The Netherlands) and Sylgard 184 (Dow Corning, Seneffe, Belgium).

4.2.2 Waterborne paint model systems and characterisation

Paint preparation

Twelve waterborne paints were prepared as follows: 70 wt% TiO$_2$ and 75 wt% CaCO$_3$ slurries were prepared by dispersing the solids in water at about 2000 rpm with 0.4 wt% and 0.3 wt% SDS, respectively. The optimum amount of surfactant was determined by the minimum viscosity dispersant demand method [25, 26]. Various TiO$_2$ and CaCO$_3$ quantities (10, 20, 30 wt% and 13, 20 wt%, respectively) were combined at three different PVCs (50, 60 and 70) by adding the corresponding amount of neutralised acrylic latex. 3 wt% Texanol, based on the total formulation, was added to each paint formulation to aid the latex coalescence process and limit the formation of cracks. The pH of the paints was brought to 8-8.5 by adding AMP 95. The paints displayed an average approximate CPVC of 59% $\pm$ 1%.

Coating characterisation

The paints were applied on metal panels (10.5 cm $\times$ 8.5 cm) using a film applicator (TQC Sheen, Rotterdam, The Netherlands) with a wet thickness of 100 μm and dried 24 hours at 21.5 $\pm$ 0.4°C and 49 $\pm$ 1.9%RH. The panels were 0.15 mm thick steel sheets from Ernst Sauter AG (Reinach, Switzerland) and possessed a surface roughness of 0.9 μm $\pm$ 0.2 μm.

Table 4.1: Surface tension and its components for model liquids used in the calculations.

Liquid	Surface tension (mN/m)	Dispersive contribution (mN/m)	Polar contribution (mN/m)
Water [27]	72.1	19.9	52.2
Ethylene glycol [28]	47.7	26.4	21.3
1-bromonapthalene [27]	44.4	44.4	0.0

The surface roughness of the coatings was measured using NanoFocus μScan Explorer (Oberhausen, Germany). Six measurements of 1 mm $\times$ 1 mm area (500 nm XY-resolution, 15 nm Z-resolution, 1001 pixels $\times$ 1001 pixels) were performed on the panels. The average roughness (R_a) profiles were analysed with μsoft analysis. A 'peak' was defined as any asperity larger than 5% of the highest asperity, enabling to access the peak density from the roughness profiles.

The surface energy of the coatings was calculated on an OCA 50, DataPhysics (Filderstadt, Germany) using the Owens-Wendt method [29]. Three model liquids were used to perform contact angle measurements: water (polar liquid), ethylene glycol and 1-bromonapthalene (nonpolar liquid) [27, 28] (Table 4.1). The total surface energy (SFE) is calculated as the sum of the dispersive (van der Waals interactions) and polar contribution (Coulomb interactions) towards the surface energy. Four measurements were performed per panel using 5 μL droplets. The tests were performed at 21.3°C $\pm$ 1.0°C and 40% $\pm$ 1%RH.

Insect climbing experiments

Leaf cutting ant workers (*Atta cephalotes* L.; Hymenoptera, Formicidae) were used as model insects in the climbing experiments. The ant workers first had their pads cleaned by allowing them to walk on soft tissue paper (Tork, Dunstable, UK) and were then placed on a paint-free starting platform (1 cm^2 of 201E masking tape, 3M, St. Paul, MN, USA) located in the middle of the vertically oriented paint panel (100 μm thickness). Once 4 (out of 6) legs had left the starting platform, the time needed to reach the edge of the paint panel was measured. The test was discarded if the insect slipped from the surface within less than three seconds after placing it on the starting platform. The insect was considered "unsuccessful" if it slipped or did not reach the edge of the panel within two minutes. Ants that reached the edge of the paint panel by walking were considered "successful". Ten ants were tested on each paint panel; each ant was not used more than three times per day to avoid any adaptive or learning effects [30]. The

paint slipperiness was calculated as follows:

$$Paint\ slipperiness\ (\%) = \frac{100 \times number\ of\ unsuccessful\ ants}{number\ of\ tested\ ants} \tag{4.1}$$

Indian stick insects (*Carausius morosus*, Sinéty; Phasmatodea, Phasmatidae) were used in contamination studies following the same climbing trial procedure. After the test, their front legs were isolated by fixing the rest of their body to a stiff wire using Blu-Tack (Bostik, Leicester, UK), allowing single-pad observation *via* light microscopy (Leica DRM (Heidelberg, Germany) connected to a Nikon D750 (Tokyo, Japan).

Scanning Electron Microscopy (SEM)

Scanning electron microscopy (SEM) images were obtained with JSM7001F from JEOL (Tokyo, Japan) by prior sample coating with a 30-nm carbon layer using Q150T ES (Quorum Technologies, Laughton, UK). The images were recorded at an acceleration voltage of 10.0 kV.

To observe ant legs under the SEM, the samples were prepared as follows: immediately after climbing paint surfaces, the legs were cut off and mounted on SEM stubs using conductive carbon double-sided adhesive tape. The samples were frozen for 48 hours to limit deflation of ants' adhesive pads (arolia) and facilitate the observation of particles [20]. Samples were then coated with a 30-nm carbon layer. Control ant samples which had not climbed the paints were observed under the SEM to verify that the contaminants present on pads only came from the coatings. The images were recorded at an acceleration voltage of either 5.0 or 10.0 kV.

4.2.3 JKR-like adhesion testing

We used PDMS hemispheres to model insect adhesive pads, which present the advantage that their flat side can be fixed to glass slides to observe the contact area from beneath. They were prepared as follows: a polyurethane mould was first prepared by mixing the two parts of OOMOO Clear Flex 50 (ratio 2:1) from Smooth-On and poured in a Petri dish. Steel spheres of 1 mm diameter with a surface roughness of 0.100 μm (Fabory Nederland, Tilburg, The Netherlands) were dropped into the polyurethane which had been previously degassed under vacuum. The OOMOO was left to cure for 15 hours, after which the steel spheres were removed using a pair of tweezers. Homogeneity of hollow depth created by the steel spheres was ensured
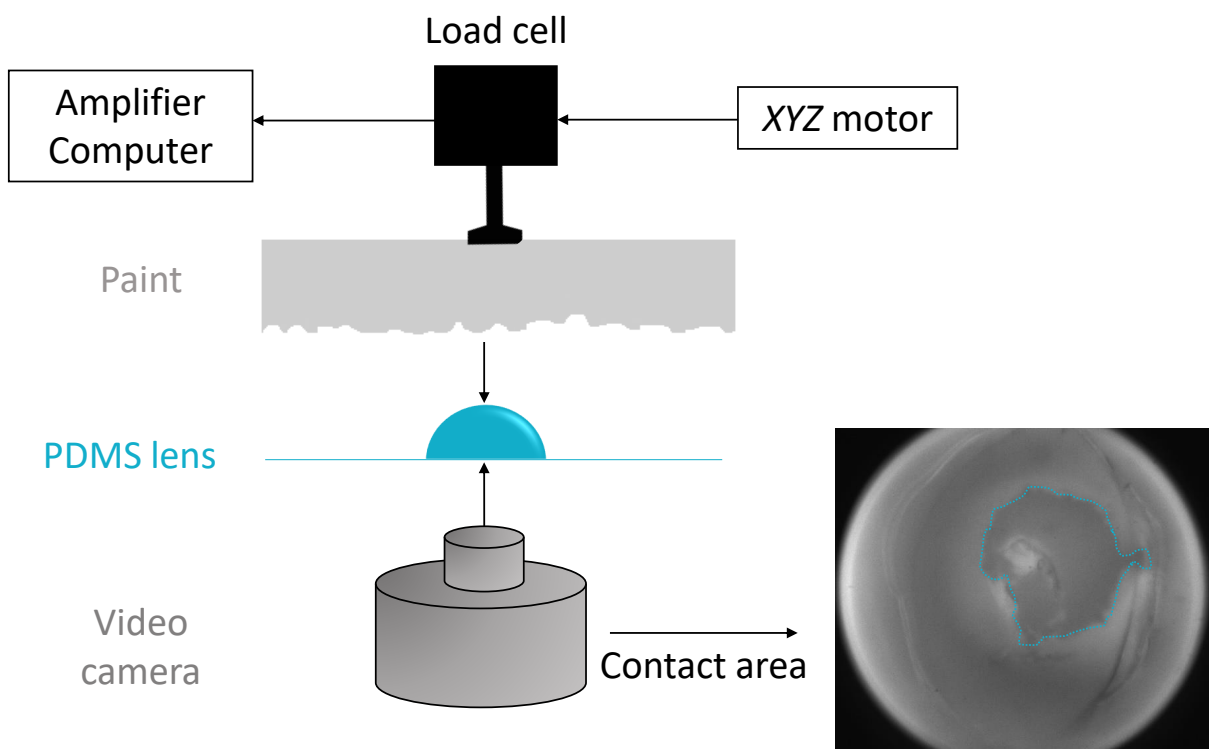
Figure 4.1: Schematic experimental set-up for measuring adhesion and contact area of PDMS/paint systems. The dashed line shows the contact area.

to form PDMS probes of same height in later stages [22]. The polyurethane rubber was coated by chemical vapor deposition of perfluorodecyltrichlorosilane by depositing a few drops on a glass slide in a desiccator where the rubber was placed. This treatment step allows to decrease the surface energy of OOMOO, hence decreasing its tackiness.

PDMS Sylgard 184, prepared at its 'standard' 10:1 ratio (pre-polymer (vinyl end-capped oligomeric dimethyl siloxane) to cross-linker (methyl hydrosiloxane)) was pre-mixed and poured onto the polyurethane. To cure the PDMS, the Petri dish was placed in a 65°C oven for 24 hours. This higher curing temperature than recommended by the supplier (48 hours, 25°C) was used to decrease the oligomer (non-crosslinked fraction) amount. In addition, PDMS was not used immediately after being prepared [31, 32]. Once cured, the PDMS was carefully peeled off from the polyurethane and the formed PDMS hemispheres could be readily used in the adhesion tests after fixing them to a glass cover slip. The probes were kept at room temperature before being used for measurements. The PDMS hemispheres could only be used in combination with one paint as washing them in ethanol and isopropanol led to a loss of their adhesive properties.

JKR-type adhesion experiments were performed to measure the adhesion forces of different paint samples on PDMS lenses (Figure 4.1) using a similar set-up to the one described in [33]. We used a 250 g capacity load cell from FUTEK (Irvine, CA, USA) and a signal amplifier (SG-3016, ICP DAS, Taipei, Taiwan). The load cell, to which the paint panel was glued (0.8 mm^2), was moved by a three-dimensional motor (C-663.12 Mercury Step Stepper Motor Controller, 1 Axis, Physik Instrumente, Karlsruhe, Germany) to be brought in contact with the PDMS (1 mm diameter) using a load of 10 mN (0.2 m/s speed). The resulting adhesion between the PDMS and the paint was recorded with a custom-made MatLab program. The contact area was recorded under reflected light using a Zyla 5.5 camera (Oxford Instruments, Abingdon, UK) and manually measured using ImageJ (Version 1.51r, National Institutes of Health, Bethesda, MD, USA). 10 mN load ensured the contact area to be visible within the camera's field of view. Three positions on the paint were randomly chosen in the experiments, where 21 pull-offs were performed on each.

A typical force-displacement curve obtained in pull-off experiments is given in Figure 4.2. The elastic modulus of the PDMS probes was evaluated using some of the force-displacement curves obtained on the paints according to the JKR-based 2-point method proposed by Ebenstein & Wahl [34]. The reduced E-modulus of the hemispheres was 1.3 ± 0.2 MPa, which is in line with PDMS prepared at its 'standard' ratio [32].
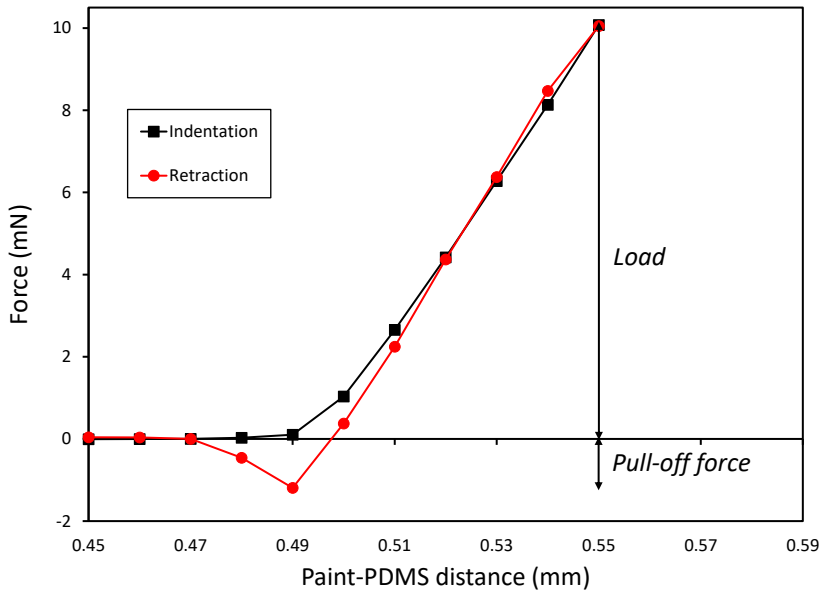

Figure 4.2: Typical force-displacement curve obtained during pull-off tests on different paint surfaces. The PDMS probe was approached until contact with the paint substrate was reached (indentation). After applying a 10 mN preload, the probe was retracted. The PDMS hemisphere adhered to the paint sample until a critical force, the pull-off force, was reached and the hemisphere detaches from the paint sample.

4.2.4 Post-test analysis of PDMS and paints

The contamination of the hemispheres after the 63 pull-offs was assessed by light microscopy (Olympus BX60, Tokyo, Japan). Note that this was only done after all pull-offs were performed so that the PDMS hemisphere's position remained unchanged with regards to the camera capturing the contact area. An estimate of the density of the contaminating pigment/extender particles was measured with ImageJ, where the size of the aggregates was not considered. In the studies where we investigated the effect of sample load on the density of contaminants, the PDMS hemispheres were observed by light microscopy after each pull-off, which were performed at increasing load.

The presence of oligomers of PDMS [31, 35–37] on the paints after being in contact with the PDMS lenses was assessed by FTIR-ATR using a Nicolet iS50 FTIR spectrometer (Thermo Scientific, Madison, WI, USA). The PDMS lenses were left in contact with the paints (11 g load, 24 to 120 hours contact) and the FTIR spectra of the paints were recorded regularly over time. These relatively high load and time were necessary due to the moderately low sensitivity of the method. The increase in the intensity of the PDMS-corresponding peaks was monitored on the coatings to see if PDMS oligomers transferred from the lenses to the paints. PDMS exhibits peaks at 789-796 cm^{-1} (-CH$_3$ rocking and Si-C stretching in Si-CH$_3$), 1020-1074 cm^{-1} (Si-O-Si stretching), 1260–1259 cm^{-1} (CH$_3$ deformation in Si-CH$_3$), and 2950–2960 cm^{-1} (asymmetric CH$_3$ stretching in Si-CH$_3$) [38].

4.2.5 Statistics

Unless otherwise stated, statistics were Pearson's correlations tests performed with Design-Expert 10. In other instances, unpaired t-tests and repeated measures ANOVA were carried out in Excel 2016 (Microsoft Office, Redmond, WA, USA). The data was assessed for normal distributions using Kolmogorov-Smirnov tests prior to statistical analysis using Social Science Statistics (`https://www.socscistatistics.com`).

4.3 Results and discussion

4.3.1 Pull-off experiments

Introduction

In this work, we assessed the feasibility of the method to mimic insect adhesive pads in climbing tests on paints by addressing the following questions: (1) Can different PDMS lens morphologies be used in a repeatable way? (2) Are the results relatable to the insect climbing tests? (3) Can we predict the number of pigment particles which adhere to ants' pads?

The paints contained different amounts of TiO_2 and $CaCO_3$ and different amounts of polymer binder (50%, 60% and 70% PVC). They presented slipperiness values ranging from 10% to 90% in ant climbing trials. The approximate CPVC of the paints, *i.e.* the PVC at which there is not enough binder to fully wet the pigment and extender particles, ranged between 58% to 61%. Examples of paint coatings with increasing PVC are shown in Figure 4.3, which highlight the effect of the PVC as the paints formulated above their CPVC (Figure 4.3B and C) lack polymer to bind efficiently all particles. This indicates that the particles detach more easily when PVC > CPVC.
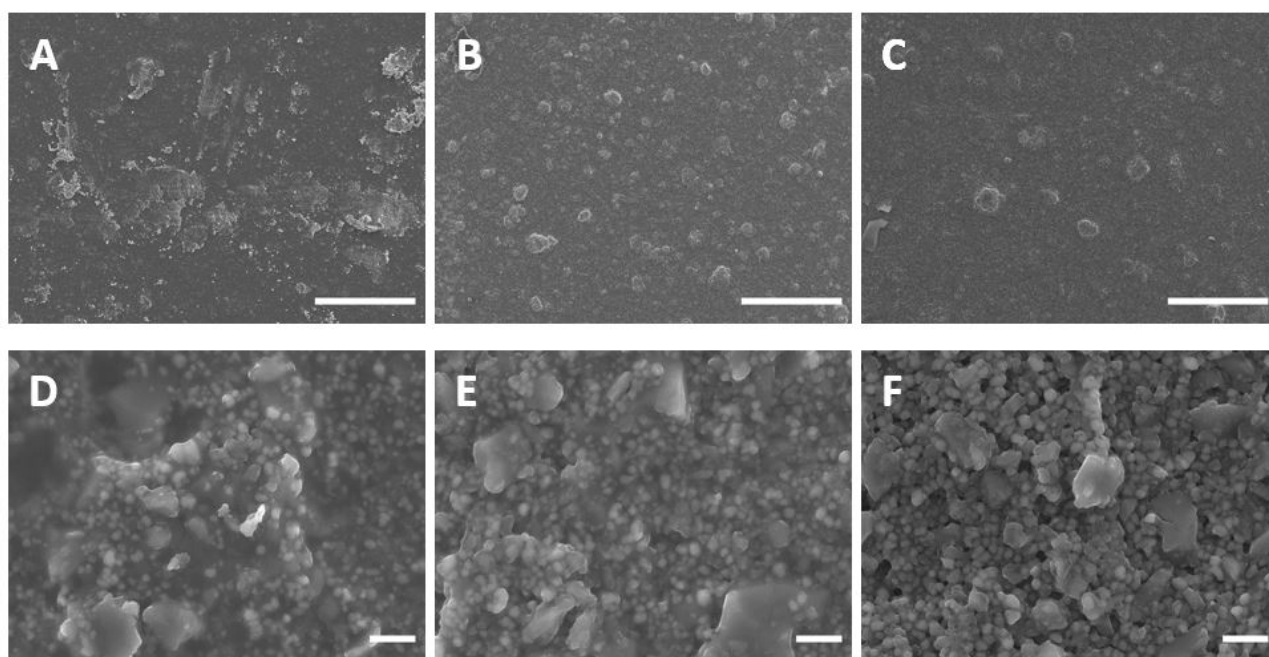

Figure 4.3: SEM images of 10 wt% TiO_2, 13wt % $CaCO_3$ paint surfaces with varying PVC: (A, D) PVC 50, (B, E) PVC 60 and (C, F) PVC 70. Paints showed in (B, E) and (C, F) are formulated above their CPVC. Scale bars: (A)-(C) 100 μm and (D)-(F) 1 μm. The images are from **Chapter 3**.

Data extracted from the pull-off force experiments

A typical force-displacement curve is given in Figure 4.2: the PDMS probe was approached until achieving contact with the paint substrate (indentation stage). After applying a 10 mN preload, the probe was retracted (retraction stage). The PDMS hemisphere adhered to the paint sample until a critical force, the pull-off force, was reached and the PDMS hemisphere detached from the paint sample. The PDMS/paint adhesion was likely due to van der Waals interactions, given that they are only significantly strong at very small distances (< 10 nm) and that the measured adhesion values were rather small (0.35 mN $\pm$ 0.17 mN for all paints) (Figure 4.2). PDMS was probably too deformable (viscous flow of the polymer near the surface [24, 39]) for interlocking between the paints' asperities and that of PDMS (surface roughness of 0.100 μm assuming a 1:1 replication of the steel spheres) to contribute to adhesion by mechanical interlocking [24]. The dependence of the adhesive stress (adhesive force/contact area) on the number of contacts showed four typical behaviours, which are shown in Figure 4.4A.
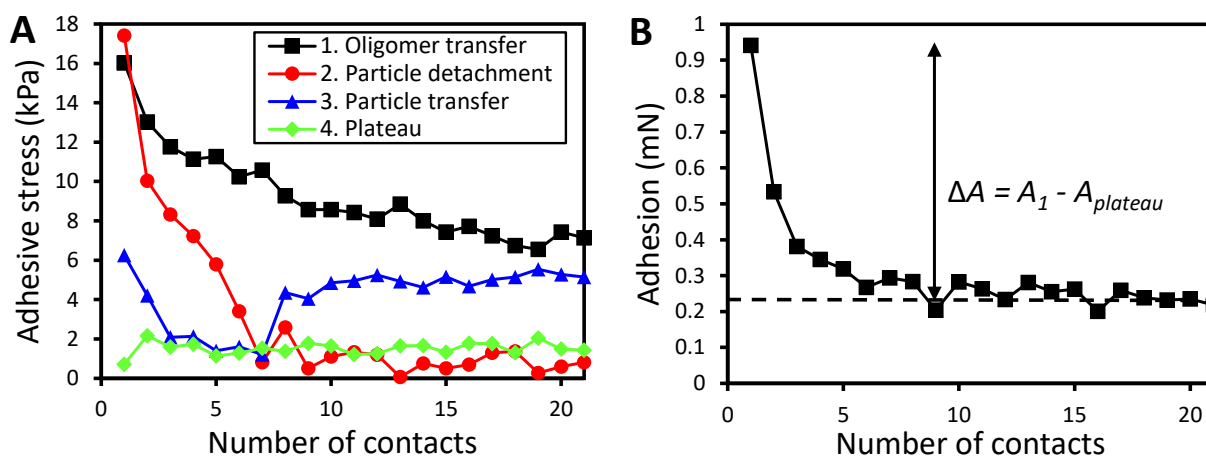

Figure 4.4: (A) Four behaviours of adhesive stress (adhesion force/contact area) were observed in the pull-off experiments which are hypothetically due to: (1) decrease of adhesive stress without observed particle detachment, suspected to be due to oligomer transfer, (2) sharp adhesive stress decrease due to particles adhering to PDMS, (3) hypothesised transfer of particles from PDMS back to the paint; and (4) plateau in case of "saturated" PDMS or non-detachable particles. These respective behaviours were observed following the pull-off experiments and microscopy observations for the 12 paints as follows: 1. 42%, 2. 83%, 3. 33% and 4. 33%. (B) Dependence of the pull-off force on number of contacts at the second position on paint 4 (10 wt% TiO$_2$, 20 wt% CaCO$_3$, PVC 70). The pull-off forces were extracted from the force-displacement curves (Figure 4.2). The A_1 adhesion value represents the first pull-off force value measured and should be the largest value in case of oligomer transfer or particle detachment. $A_{plateau}$ refers to the adhesion force once a plateau is reached and ΔA is proposed to be the adhesion necessary to either detach particles from a paint or to transfer uncured oligomers from the probe to the coating. In the occurrence of no particle detachment, the adhesion is expected to plateau from the first contact.

We hypothesised the following: if the particles detached from the paint, adhesion was expected to decrease until reaching a plateau as the contact area between PDMS and the paint was reduced. In this case, detachment of particles was probably owed to failure of the binder to retain pigment particles. Alternatively, a similar trend would be observed if some free, uncured oligomers transferred from PDMS to the coating, as observed on various substrates [31, 37]. We defined these behaviours as follows: (1) decrease of adhesive stress without observed particle detachment under microscopy, suspected to be due to oligomer transfer, (2) sharp adhesive stress decrease due to particles adhering to PDMS, (3) hypothesised transfer of particles from PDMS back to the paint (regain in adhesion); and (4) plateau in case of "saturated" PDMS with particles or alternatively, when no particles detached from the paint. In case of (3), we could not bring experimental evidence that some particles transferred back to coatings as microscopy was only done after all pull-offs were performed so that the PDMS hemisphere's position remained unchanged.

The dependence of the PDMS/paint adhesion force on the number of contacts for paint 4 (second position) is given in Figure 4.4B. We defined $A_{plateau}$ as the adhesion force at the plateau and $\Delta A = A_1 - A_{plateau}$. ΔA represented the force either needed to detach particles, or to remove uncured oligomers from PDMS, according to Figure 4.4A. The adhesive stress values were calculated as ratios of adhesion forces/contact area. The different parameters extracted from the experiments are displayed in Table 4.2.

Table 4.2: Parameters extracted from the pull-off experiments (see Figure 4.2).

Parameter	Contact area	Average adhesion	Plateau force	Detachment force	Adhesive stress	Plateau pressure	Detachment pressure
Definition	Average contact area over the 21 pull-offs at a given position	Average adhesion force over the 21 pull-offs at a given position	Adhesion at plateau	Force necessary to observe oligomer transfer or particle detachment $A = A_1 - A_{plateau}$ A_1 being the initial adhesion value	$\dfrac{<A>}{CA}$	$\dfrac{A_{plateau}}{CA}$	$\dfrac{\Delta A}{CA}$
Abbreviation	CA	$<A>$	$A_{plateau}$	ΔA	AS	$P_{plateau}$	ΔP

Reproducibility

After the 63 pull-offs, the adhesive properties of fouled PDMS lenses were found to be non-recoverable after cleaning them with ethanol, isopropanol, or even Scotch™ tape (Figure 4.5A). We instead used one PDMS hemisphere per paint. Despite being prepared using the same procedure (Materials and methods section), the PDMS lenses tended to present different 'morphologies', likely due to the peeling stage (Figure 4.6). Hence, the hemispheres yielded different contact areas (CA) at 10 mN load (73370 μm^2 ± 11112 μm^2). Although the average CA for each set of paints did not differ significantly from the overall average (single sample t-test: 73370 μm^2 ± 11112 μm^2, $t_{11} < 0.01$, $P = 0.99$), the pressure values, calculated with the contact areas, were used rather than the pull-off forces obtained directly in the tests (Table 4.2).

In addition to the standard procedure followed in (1), where 63 × 10 mN pull-offs were performed on paints 1-12 using one probe per paint, we investigated the adhesion properties of paints where: (2) the adhesion of paint 12 was measured using two PDMS different hemispheres; and (3) with increasing paint load on two PVC 50 and 70 paints (paints 3 and 4). The results of the pull-off experiments obtained in (1) and (2) are displayed in Table 4.3.
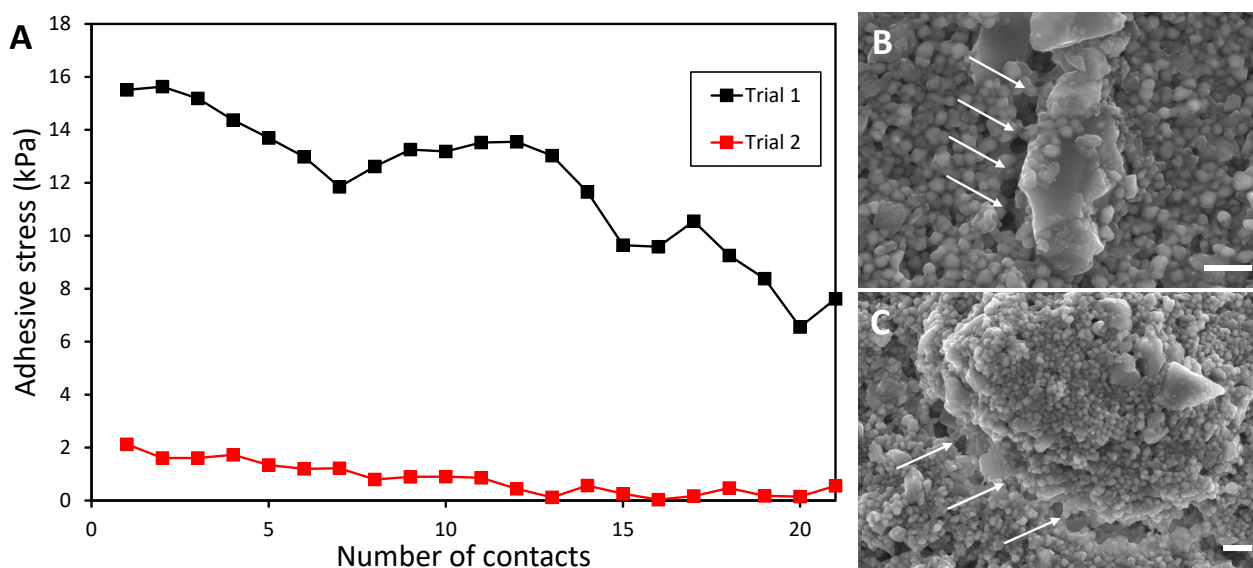

Figure 4.5: (A) Evolution of adhesive stress with number of contacts of paint 12 in contact with PDMS. Prior to Trial 2, the PDMS lens was washed with ethanol, isopropanol and Scotch^{TM} tape to remove the contaminating pigment particles. In Trial 1, the lens continuously detached particles from the paint, leading to a loss in adhesive stress; while in Trial 2, a plateau was quickly reached, indicating no-to-few particles were detached from the paint. This shows that the PDMS lenses change irreversibly after washing. (B) and (C) SEM pictures of paint 12 (30 wt% TiO$_2$, 20 wt% CaCO$_3$, PVC 70) showing polymer fibres surrounding pigment aggregates (shown by arrows). Scale bars: 1 μm.

Table 4.3: Composition, roughness (R_a), peak density and slipperiness of waterborne paints, and parameters obtained through the pull-off experiments with PDMS hemispheres: adhesive stress (AS), plateau pressure ($P_{plateau}$), detachment pressure (P_{detach}) and PDMS contamination density. The data is displayed for studies (1) and (2), *i.e.* separated for 'low' and 'medium' to 'high' PDMS contamination. The AS values were averaged from the 63 pull-offs, while $P_{plateau}$ and P_{detach} were averaged from the three sets of 21 contacts. The contamination density was estimated from a variable number of microscope images. The values are expressed as mean ± standard deviation (SD).

Study	Paint	[TiO$_2$] (%)	[CaCO$_3$] (%)	PVC (%)	R_a (μm) (n = 6)	Peak density (peaks.mm²) (n = 6)	Surface energy (mN/m) (n = 4)	Slipperiness (%) (n = 20)	AS (kPa) (n = 63)	$P_{plateau}$ (kPa) (n = 3)	P_{detach} (kPa) (n = 3)	Contamination density (particles/mm²)
1	1	10	13	50	1.5 ±0.1	1158 ± 17	39.9 ± 1.3	10 ± 10	3.5 ± 2.0	7.4 ± 0.5	2.2 ± 1.5	0 ± 0
	2	10	13	60	4.7 ± 0.1	1163 ± 39	34.3 ±0.4	20 ± 10	7.6 ± 2.1	10.0 ± 1.7	6.9 ± 1.5	1 ± 0
	3	10	20	50	4.6 ± 0.1	1167 ± 46	39.2 ± 0.8	10 ± 10	3.9 ± 2.0	7.1 ± 4.3	2.7 ± 1.6	13 ± 1
	4	10	20	70	1.9 ± 0.4	80 ± 14	36.4 ± 0.7	85 ± 5	3.1 ± 1.9	7.6 ± 2.8	2.4 ± 1.2	8 ± 1
	5	20	20	50	0.9 ± 0.2	547 ± 104	39.7 ± 1.1	0 ± 10	4.4 ± 3.8	9.6 ± 6.0	3.7 ± 2.6	0 ± 0
	6	30	20	60	4.9 ± 0.1	1110 ± 88	36.2 ± 0.6	10 ± 10	3.7 ± 0.8	4.9 ± 2.4	3.3 ±0.4	77 ± 33
	7	10	13	70	4.9 ± 0.1	1156 ± 15	36.6 ± 0.7	90 ± 5	3.2 ± 2.2	6.2 ± 3.9	3.4 ± 1.3	149 ± 109
	8	10	20	60	4.7 ± 0.1	1122 ± 42	34.0 ± 0.5	70 ± 10	2.4 ± 2.1	9.2 ± 0.9	1.5 ± 0.1	277 ± 155
	9	20	20	60	1.4 ± 0.1	438 ± 105	35.9 ± 0.6	10 ± 10	6.0 ± 3.2	11.1 ± 2.7	4.5 ± 1.8	282 ± 162
	10	20	20	70	1.9 ± 0.4	363 ± 77	36.6 ± 0.2	90 ± 5	3.8 ± 3.7	13.4 ± 6.5	1.8 ± 1.3	1944 ± 1883
	11	30	20	50	4.8 ± 0.1	1136 ± 33	41.5 ± 0.9	10 ± 10	4.9 ± 1.3	5.9 ± 2.0	4.6 ± 0.7	394 ± 137
	12	30	20	70	4.6 ± 0.1	1140 ± 46	37.2 ± 0.9	90 ± 10	9.5 ± 3.8	9.5 ± 2.8	8.6 ± 3.0	617 ± 333
2	12	30	20	70	4.6 ± 0.1	1140 ± 46	37.2 ± 0.9	90 ± 10	9.5 ± 3.8	9.5 ± 2.8	8.6 ± 3.0	617 ± 333
	12	30	20	70	4.6 ± 0.1	1140 ± 46	37.2 ± 0.9	90 ± 10	3.9 ± 2.8	1.9 ± 2.05	3.2 ± 2.8	75 ± 49

4.3.2 Adhesive properties of paints 1-12

Contamination of paints (by PDMS oligomers) and PDMS probes (by pigment particles)

Contamination of adhesive structures of insects leads to a loss of pad/substrate contact and therefore to reduced attachment [14, 40, 41]. We previously showed that our paints were slippery to insects due to pigment particles detaching and adhering to ant pads, and that this effect increased with increasing PVC as PVC > CPVC (**Chapter 3**). In the following, we tentatively assess if large drops in adhesive stress, followed by plateaus, were either due to contamination of paint by PDMS oligomers, or of PDMS by pigments (Figure A4.1).

The figures showing variations of adhesive stress with increasing contact number are given in Appendix A4.1 A4.1. 63×10 mN pull-offs were performed on the PDMS lenses (Table 4.3). In none of the pull-off tests performed on paints 1-12 were the variations in contact area significant (repeated measures ANOVA, $F_{2,4} = 1.19$, $P = 0.494$ on average), indicating that the observed changes in adhesive stress (adhesion/contact area) were mainly due to differences in adhesion force. One may expect that contamination, if occurring, would reduce both contact area and adhesion, leading to constant adhesive stress values over the course of experiments [40]. However, Figure 4.6 highlights that cracks were present in the centre of some hemispheres and were probably induced when removing the steel spheres from the polyurethane mould with tweezers during probe preparation (PDMS probes 5, 10, 11 and 12). These cracks may have further grown upon contact with the asperities of the paints. We did not observe any change in crack size under optical microscopy, but crack initiation occurring due to lack of cohesion in PDMS [22] may explain why differences in adhesion were observed.
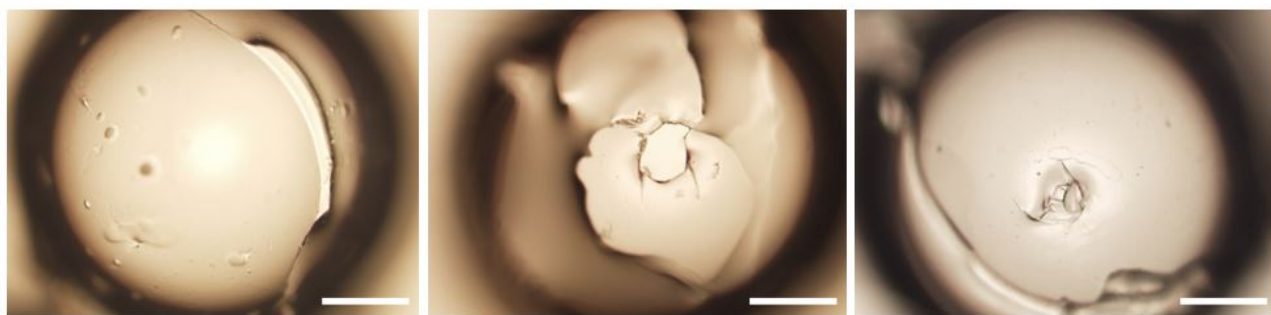

Figure 4.6: Examples of PDMS hemispheres observed by light microscopy used prior to adhesion testing with paints 1, 10 and 12. Scale bars: 200 μm.

Kroner *et al.* studied the transfer of PDMS oligomers to glass and found that the pull-off force continuously decreases as PDMS oligomers are transferred to glass until reaching a plateau as an equilibrium is reached, similarly to Figure 4.4B [31]. This initial drop in adhesion was found to be less pronounced when increasing the curing time, storage time and crosslinker concentration during PDMS preparation [31]. All paints showed a decrease of adhesive stress before plateauing (ΔP), similarly to Figure 4.4A1 and A2, even when no-to-little fouling could be observed under microscopy. Despite our precautions to cure PDMS for longer periods than recommended by the supplier to avoid the presence of oligomers, these results suggest that the decrease in AS observed for paints 1-6 was mainly due to oligomer transfer, as large polymer fractions do not undergo crosslinking (5-20% in PDMS) [31, 35] (Figure 4.4A1).

Large initial drops in adhesive stress (ΔP approximately larger than 4 kPa) were attributed to oligomer transfer rather than particle detaching between the first and second pull-offs, as no particles were observed on the PDMS hemispheres in these instances. AS plateaus were reached on average after 8 ± 4 contacts, which is way less than the 300 to 1,000 contacts needed in Kroner *et al.*'s study on glass [31]. From the adhesion stress data, microscopy was needed to formally distinguish oligomer from pigment particle transfer (Figure 4.4A1 and A2), which were respectively observed in 42% and 83% of paint coatings. More unlikely, individual TiO_2 particles may have detached from these paints and not be observable with light microscopy (mean diameter: 300 nm), or some particles/aggregates may have fallen off from PDMS during transport to the microscope.

FTIR-ATR allowed us to observe that PDMS oligomers were deposited on the paint coatings upon contact with PDMS hemispheres (11 g load). Paints exhibited PDMS-corresponding peaks typically after 24 hours of contact (Figure A4.15, Appendix A4.2, in particular in the 2820-3000 cm^{-1} (asymmetric CH_3 stretching in $Si-CH_3$) and 1220-1300 cm^{-1} regions (CH_3 deformation in $Si-CH_3$) [38]. Both the PDMS load and contact time between paints and PDMS were kept large in these experiments compared to pull-off measurements as FTIR-ATR is a relatively low sensitivity method to assess the presence of low amounts of oligomers. Interestingly, upon re-use of non-contaminated PDMS hemispheres on other paints, an initial drop in adhesion was still observed (data not shown).

Two other behaviours are presented in Figure 4.4A. We hypothesised that some PDMS lenses transferred some pigment particles back to paints (paints 3, 5, 7 and 12, Figure 4.4A3, 33% of paints). Some pigment aggregates were surrounded by polymer fibres (Figure 4.5B/C). Upon contact with PDMS or insect pads, it is likely they can detach easily as the binder fractures and fails to retain them. The polymer binder employed in this study had a glass transition temperature (T_g) of 28°C, and was lowered down when added to paints to maximum 9°C due to the addition of coalescent [42]. It is commonly acknowledged that low T_g polymer films are tacky [43]. Hence, one could imagine that the transfer of pigment particles back to the paint coatings may have occurred for loose particles and could stick again to broken polymer fibres if the PDMS probes were elastic enough [24] (Figure 4.4A3). When PDMS lenses were likely "saturated" with particles or when particles did not detach from paints if too tightly bound to polymer, the adhesive stress was plateauing at low values (Figure 4.4A4, 33% of paints).

If particles detach from the paint at position 1, the initial AS values at positions 2 and 3 should be lower than at position 1 due to fouling as impurities prevent full contact between the paint and PDMS [24, 39]. Similarly, the second and third adhesion plateaus should also be lower than the first one in case of additional contamination. However, these trends were not observed in many paints (see Figures in Appendix A4.1). If occurring, the transfer of particles from PDMS to paints may explain this effect. Overall, we propose that PDMS contamination by pigments was paint position-dependent, as it did not occur at every position (chosen randomly) on the paint. The effect of the paints' surface roughness on PDMS adhesion is reviewed in the next section.

Effect of surface roughness R_a of paints on pull-off experiments

The surface roughness has been found to greatly influence insect attachment forces and we assessed here if it was also the case for PDMS. Insects use their pads on 'smooth' surfaces (ca. 0 nm roughness), their claws on 'rough' substrates (asperity size > 3 μm), but both mechanisms are inefficient in the 'nano/micro-rough' intermediary range where attachment forces are minimised [2, 17, 44, 45]. Interestingly, the work of Purtov *et al.* [22] showed that very deformable PDMS (E-modulus of 70 kPa) probes did not reproduce these results: the adhesion of PDMS was the largest on microrough surfaces, while substrates with large asperities minimised contact and adhesion (Figure 4.7) [22].

The contamination was paint position-dependent with regards to the AS trends, suggesting an effect from the surface roughness, despite a non-significative impact of the roughness or the peak density on the contamination (Pearson's r = -0.15, P = 0.637 and r = -0.31, P = 0.327, respectively). Assuming R_a values are related to asperity size, then 'rough' coatings ($R_a > 3$ μm) presented similar contamination to the ones in the 'nano/micro-rough' ($R_a <$ 3 μm) range (t-test, T_4 = 0.59, P = 0.587). PDMS Sylgard 184, prepared at its 'standard' ratio (pre-polymer to cross-linker ratio 10:1), cannot comply with surface asperities as much as insects' soft, deformable pads as PDMS possesses a larger Young's modulus (ca. 1.3 MPa versus < 100 kPa, Dahlquist criterion for tackiness [6, 46]).

Furthermore, surface roughness (root-mean-square RMS) larger than 1 μm (min. 1.2 μm in our paints) can significantly reduce adhesion between rubber (E-modulus $\approx$ 1 MPa) and rigid substrates, explaining the low adhesion values (0.35 mN $\pm$ 0.17 mN) obtained in the pull-off experiments [24, 47]. However, all PDMS lenses yielded similar contact areas (73370 μm^2 $\pm$ 11112 μm^2), despite the presence of asperities on their surface (Figure 4.6). The surface roughness of the paints reduced the real contact area of the PDMS probes, as observed in [22], van der Waals forces being only active once surfaces are very close from each other. These results suggest that the particle detachment hypothesis does not explain alone why our paint coatings are slippery to ants. The likely additional mechanism is the surface roughness of the paints, even if not highlighted in these data (**Chapter 3**).
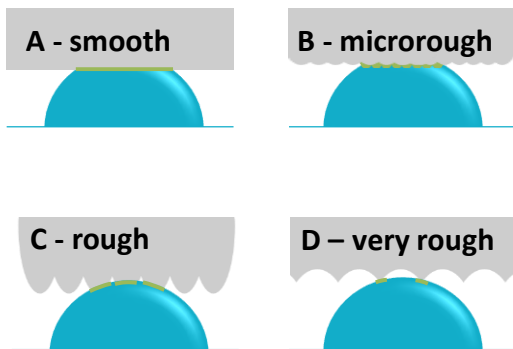

Figure 4.7: Schematic contact of PDMS probes on paints with increasing increasing roughness (asperity size) assuming PDMS is sufficiently elastic. (A) On smooth substrates, a full contact between the PDMS probe and the tested surface is achieved. The real contact area (green lines) is similar to the apparent contact area. (B) On microrough paint substrates, the soft PDMS probe adapts well to the surface profile and this results in a larger real contact area. (C) On rougher substrates, only partial contacts occurs. Purtov *et al.* hypothesised that the contact area is similar to the one obtained on smooth surfaces [22]. (D) On samples displaying large asperities, gaps between the PDMS probe and paint substrate are rather large and the real contact area decreases. The ranges of roughness using asperity sizes can approximately be defined as follows: (A) smooth: < 50 nm, (B) microrough: 50 nm-1.0 μm, (C) rough: 1-3 μm and (D) very rough: > 3 μm [2, 22]. Reproduced from [22].

Comparison with ants

The adhesion values needed to detach some particles from the paints were low at 10 mN load (0.35 mN $\pm$ 0.17 mN). PDMS lenses tested with paints 1 to 6 showed very little contamination (16 $\pm$ 27 particles/mm^2), while the ones tested with paints 7 to 12 showed medium to high fouling (611 $\pm$ 613 particles/mm^2 on average). Neither the paint PVC nor the insect slipperiness were correlated to the contamination density ($r = 0.45$, $P = 0.144$ and $r = 0.49$, $P = 0.105$, respectively). One PVC 50 paint (paint 11) surprisingly showed medium level contamination of PDMS while the pigment particles were embedded in the polymer matrix (PVC < CPVC), as shown by SEM (Figure 4.3A). Our work in **Chapter 3** suggested that ants do not detach many particles from paints when PVC < CPVC.

Estimating the number of pigment particles present on *A. cephalotes* pads from SEM micrographs is challenging due to the presence of polymer binder 'gluing' the particles together. For paint 12, we could approximate that 203 particles detached from the paint to adhere to one pad, *i.e.* about 348,000 particles/mm^2 (considering a contact area of 582 μm^2, from measurements on *Oecophylla smaragdina* (Fab.; Hymenoptera, Formicidae) [19]) (Figure 4.8A). This contamination density value is several orders of magnitude larger than the 617 particles/mm^2 we observed on PDMS for the same paint (Figure 4.8B).
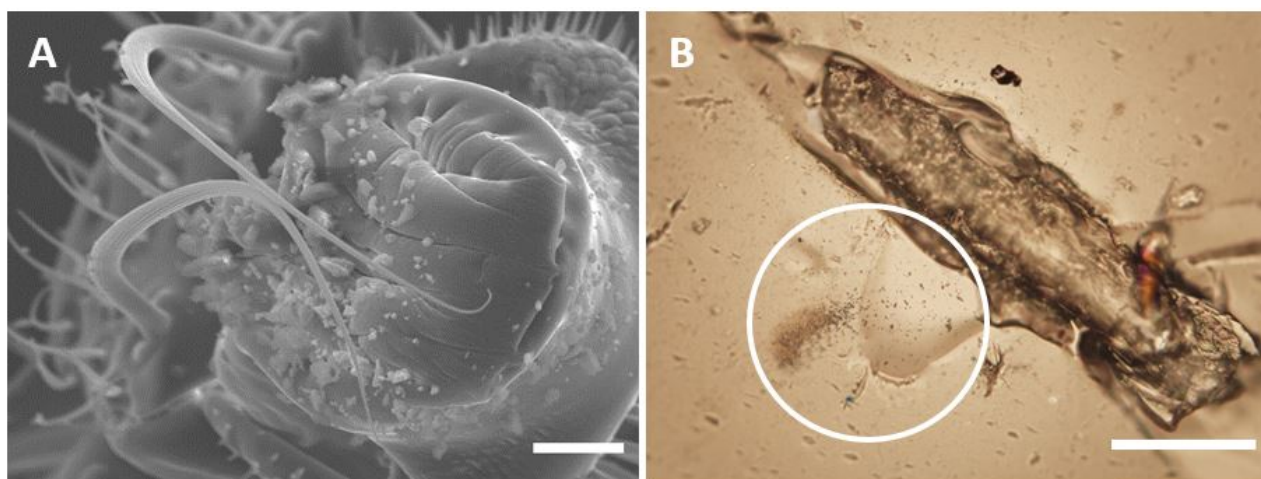

Figure 4.8: (A) SEM picture of an *Atta cephalotes* ant pad after climbing paint 12 (30 wt% TiO$_2$, 20 wt% CaCO$_3$, PVC 70), where pigment particles which detached from the paint coating (mainly CaCO$_3$) can be observed. (B) Light microscopy picture of a PDMS lens's apex after 63 pull-offs with paint 12, the white circle indicates where the pigment particles adhered to PDMS. The large feature is a defect from the casting. Scale bars: (A) 10 μm and (B) 200 μm.

First, ants do not climb surfaces by only means of normal forces, but also by generating friction forces [19]. Ants possess smooth pads secreting an adhesive fluid to compensate surface roughness by filling asperities (wet adhesion), which may help to wash away contaminants [5–7, 40]. Furthermore, smooth pads also present a stiffness gradient which help insects cope with surface roughness at smaller length scales [48]. Our results could possibly indicate the number of pigment contaminants ants could detach in dry adhesion conditions. However, Labonte & Federle proposed that adhesion of stick insects (smooth pads) in dry and wet conditions were similar [8].

Differences may also lie in the surface energy of insect pads and PDMS: contaminants cannot adhere well to low surface energy materials. Sylgard 184 is a low energy surface (24.7 ± 2.3 mN/m for our 24 hours cured PDMS at 65°C) and could even be lower in our case due to the presence of perfluorodecyltrichlorosilane, however necessary in the peeling stage to prepare the PDMS hemispheres. To the best of our knowledge, the surface energy of insect cuticle or adhesive pads has not been directly measured, likely due to the small size and unevenness of the pads. Preliminary data from Dirks & Federle suggested that smooth pads generate larger adhesion forces on substrates exhibiting higher dispersive than polar contribution [6]. Paints 1-12 displayed 28.4 ± 5.2 mN/m dispersive and 8.9 ± 6.4 mN/m polar contribution, hence enhancing attachment forces of climbing ants on the coatings ($r = $ -0.67, $P = 0.017$ for slipperiness-polar contribution). Low adhesion forces (nN-scale) have been recorded for particles adhering to insect cuticle [49], suggesting it is easier for fouling particles to adhere to fluid-wetted pads than to low surface energy PDMS.

In addition, the resulting adhesive stress values (force per unit contact area) were about eight times lower than the "load stress" (ground reaction normal force/contact area) measured in *O. smaragdina* ants (4.7 ± 2.0 kPa versus 39.6 ± 14.8 kPa) [19]. To the best of our knowledge, adhesive stresses generated by ants' arolia have not directly been measured, likely as they are retractable [20, 21]. Adhesive stress values smaller than 100 kPa have been reported for beetles and stick insects [40, 50]. Reducing the contact area would have allowed to obtain closer values to the loads yielded by insects. However, our experimental set-up did not allow this as 10 mN load was the minimum force necessary to observe the contact area. Alternatively, increasing the contact time should result in more intimate contact between the PDMS and the coating, leading

to greater AS [39, 51]. Interestingly, we did not observe such behaviour as both adhesion and contact area remained constant for contact times between 10 seconds to 150 min (data not shown).

4.3.3   Adhesive properties of paint 12 in reproducibility trials

Two PDMS lenses were tested on the same paint sample to assess the reproducibility of the pull-off method, the data is displayed in Table 4.3. As shown previously in Figure 4.5, PDMS lenses could only be used in combination with one paint as a loss of adhesive properties had been observed after cleaning.

Using two different hemispheres on the same paint led to different adhesive stress trends, despite displaying similar aspects (Figure A4.12 and Figure A4.14, Appendix A4.1). In addition, the PDMS probe used in the tests presented a crack which potentially grew and indicates a lack of PDMS cohesiveness (Figure 4.6). This shows that our hemisphere production method needs enhancement, as Purtov and colleagues prepared homogenous PDMS probes using a similar protocol [22]. In the first trial, particles were detached at the first and third position, while some particles were supposedly transferred back to the paint coating at position 2. With the second lens, particles only adhered to PDMS at the third position, with some of them being transferred back to the paint. Again, transfer of particles (Figure 4.4A3) could not be experimentally verified as microscopy was performed after the three sets of pull-offs so that the position of PDMS remained unchanged with regards to the camera capturing the contact area.

The two contamination densities were hence very different (617 particles/mm^2 versus 75 particles/mm^2). As previously discussed, the contamination seemed to be paint position-dependent and the lack of reproducibility probably indicates why some correlations could not be seen between the contamination density and the adhesion parameters in the previous section. These data may also indicate that the 63 pull-offs performed with the first PDMS hemisphere removed most of the particles detachable from the paint sample at 10 mN load. We hence investigated in the next section the effect of the paint load on the PDMS contamination, alongside with the effect of the paint PVC.

4.3.4 PDMS contamination studies with increasing load
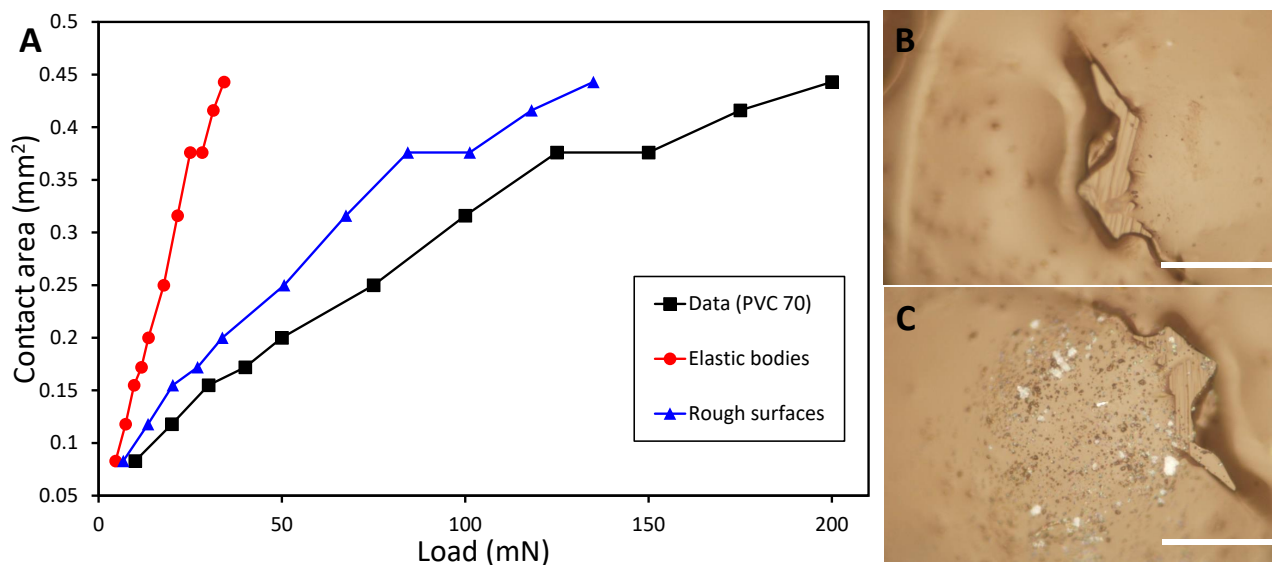

Figure 4.9: (A) Contact area increasing with paint load for paint 4. The experimental data is compared to contact between two elastic bodies (Hertz theory) and contact between rough substrates [52, 53]. The contact area standard deviations were below 4% and are hence not visible. (B, C) Micrographs of the apex of a PDMS lens (B) before and (C) after being in contact (175 mN load) with paint 4 (10 wt% TiO_2, 20 wt% $CaCO_3$, PVC 70). Scale bars: 50 μm.

An increasing load (10-200 mN) was applied onto the PDMS lenses using paints 3 and 4 (10 wt% TiO_2, 20 wt% $CaCO_3$, PVC 50 and 70, respectively). Only one pull-off was performed for each paint load and the tests were performed with different PDMS lenses. The aspect of the PDMS hemispheres was investigated with light microscopy after the pull-off experiments to visually assess if any particles had detached from the paints to adhere to PDMS (Figure 4.9B/C). The number of contaminating particles was approximated from the micrographs. The data resulting from the experiments is shown in Table 4.4.

For both paints 3 and 4, the contact area significantly increased with load for both paints ($r = 0.98$ and $P < 0.001$ for both paints), as predicted by the JKR theory and the theory developed by Bush *et al.* for contact on rough surfaces at low normal loads [24, 52]. Figure 4.9A shows the increase of the contact area with load for paint 4, compared to values obtained for contact between two elastic bodies (Hertz model, eq. 4.2) and between a rough elastic substrate and a flat rigid surface (eq. 4.3) [52, 53]:

$$CA \propto F^{2/3} \tag{4.2}$$

$$CA \;=\; \frac{\kappa F}{E \times \nabla RMS} \tag{4.3}$$

Where CA is the contact area, F the normal load, ∇RMS the root mean square gradient of the surface profile, E the effective modulus and κ a dimensionless constant ≈ 2 [53]. ∇RMS is difficult to measure for "real" surfaces and for the sake of convenience, the RMS value for paint 4 (2.8 μm) was directly used [53]. It can be seen from Figure 4.9A that our experimental data did not follow Hertz's prediction for contact between two elastic bodies as we had $CA \propto F$ (Eq. 4.2). Our data was more in line with the model developed for contact between a rough elastic substrate and a flat rigid surface, assuming that $\nabla RMS \approx RMS$ [53].

Accordingly, the density of contaminating particles increased with the load ($r = 0.85$, $P = 0.013$ and $r = 0.87$, $P = 0.001$ for paints 3 and 4, respectively, Figure 4.10). For the PVC 50 paint, the AS values gradually decreased as the load force increased ($r = -0.72$, $P = 0.012$), until plateauing from 50 mN onwards. However, for the PVC 70 paint, there was no such trend regarding AS as large variations in adhesion were observed ($r = -0.49$, $P = 0.129$). The PDMS probe employed in the latter tests showed indeed a heterogeneous appearance (Figure A4.4B).

Table 4.4: Parameters obtained through the pull-off experiments with PDMS hemispheres and paints 3 and 4: contact area (CA), adhesive stress (AS), and PDMS contamination density with increasing load (10-200 mN). These data correspond to the study (3), where the paint load gradually increased to study PDMS contamination. The standard deviations on CA were below 4% and are not given for the adhesive stress as the tests could only be performed once for a given PDMS lens. The values are expressed as mean $\pm$ standard deviation (SD).

| Load (mN)	10	20	30	40	50	75	100	125	150	175	200
Paint 3 – PVC 50 – 10% slipperiness											
CA (mm^2)	0.072	0.115	0.146	0.163	0.179	0.241	0.299	0.333	0.360	0.389	0.392
AS (kPa)	13.1	10.0	4.9	4.2	2.0	2.9	1.6	1.5	1.5	1.3	1.3
Contamination density (particles/mm^2)	79 $\pm$ 26	66 $\pm$ 23	158 $\pm$ 38	221 $\pm$ 34	206 $\pm$ 90	445 $\pm$ 397	324 $\pm$ 96	287 $\pm$ 112	520 $\pm$ 162	544 $\pm$ 95	897 $\pm$ 151
Paint 4 – PVC 70 – 85% slipperiness											
CA (mm^2)	0.083	0.118	0.155	0.172	0.200	0.250	0.316	0.376	0.376	0.416	0.443
AS (kPa)	11.8	5.1	23.2	10.5	4.7	3.0	2.9	13.3	2.1	2.2	3.7
Contamination density (particles/mm^2)	0	78 $\pm$ 33	145 $\pm$ 117	148 $\pm$ 49	290 $\pm$ 208	410 $\pm$ 70	447 $\pm$ 238	1540 $\pm$ 310	1175 $\pm$ 537	1644 $\pm$ 130	3090 $\pm$ 1530
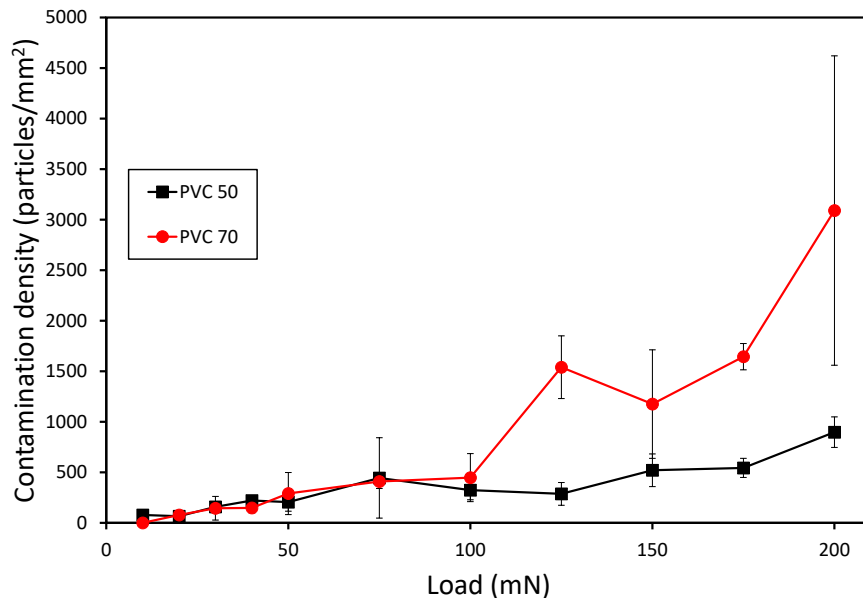
Figure 4.10: Contamination density increasing with load for paints 3 and 4 (10 wt% TiO_2, 20 wt% $CaCO_3$, PVC 50 and 70, respectively).

Both paints led to similar contamination densities for 0-100 mN loads (unpaired t-test, T_{12} = 0.03, $P = 0.97$), from which the PVC 70 paint led to a sharp increase in the density of fouling particles, evidencing the effect of the PVC (Figure 4.10). These data show that is it possible to achieve 'high' contamination from low PVC, non-slippery paints (10% slipperiness to ants for paint 3) at 'high' load (> 200 particles/mm^2 above 40 mN), which could possibly be achieved by large insects. PDMS contamination might have been easier to study at higher loads, but the decreasing AS data in Table 4.4 shows that this would have increased the gap between AS generated produced by PDMS and ant pads [19].

Assuming scaling between contamination density and load would be obtained at higher loads, then the same contamination density of 348,000 particles/mm^2 we observed on ant pads for paint 12 would be theoretically possible at 26 N load (Figure 4.10), which is one order of magnitude larger than our set-up's load threshold. Indian stick insects (*C. morosus*) were found to yield similar adhesive stresses on glass compared to PDMS on paints 3 and 4 at 10 mN load (ca. 15 kPa versus 12.5 kPa) [40]. When used in the climbing trials on paints 3, 8 and 4, pigment particles were indeed observed on their pads (Figure A4.16, Appendix A4.3). While the PVC 60 paint (paint 8) exhibited the largest PDMS contamination, the PVC 70 paint (paint 4) was however the most slippery to *A. cephalotes* ants, underlining differences between the PDMS hemispheres and ant pads.

What would happen if such paints, with insect-slippery properties, were to be applied on walls? Fingers pressing at 'low' load (< 2 N) on flat surfaces exhibit pressures ranging between

0 and 60 kPa [54, 55]. Given the relative high roughness of the coatings, which would decrease the paint/finger contact area, it is quite unlikely that particles would detach from painted walls.

4.4   Conclusions

We have studied the feasibility of JKR-like experiments using PDMS hemispheres to replicate climbing tests performed on paint coatings with *Atta cephalotes* ants. In its current form, the test cannot be used to do so as several issues arose:

1. The test lacks reproducibility as the PDMS lenses presented discrepancies in both their aspect and smoothness.

2. Some paints present decreasing adhesive stress trends even in the absence of contamination, indicating some PDMS oligomers might have transferred to the paint, despite our precautions to cure and store the PDMS for longer periods than recommended by the supplier. Large uncured fractions have indeed been previously observed in PDMS [35]. The presence of oligomers on the paint coatings after being in contact with PDMS has been suggested by FTIR-ATR. Removing the oligomers upon numerous contacts with glass slides could have been done prior to the adhesion tests with the paints [31], however AS plateaus were reached within only 8 ± 4 contacts.

3. The contamination results do not follow the PVC and slipperiness trends as it was expected that the higher the PVC, the larger the contamination (as this leads to higher slipperiness). This underlies the existence of an additional mechanism providing slipperiness, which seems to be neither the surface roughness nor the peak density. Even if not shown in our set of data, this is however likely as (1) the effect of surface roughness is known to greatly influence insect adhesion [2, 17, 44, 45] and (2) the contamination was found to be paint position-dependent. The surfaces of PDMS and ants' smooth pads also present different affinities to TiO_2 and $CaCO_3$: PDMS is a low energy surface while insect pads generate higher adhesion forces on surfaces with greater dispersive contribution [6].

4. Furthermore, PDMS hemispheres do not model well enough insect pads in dry adhesion conditions, likely due to the absence of claws, and the lack of compliance with surface roughness compared to ants' soft pads [22]. Smooth pads present a stiffness gradient which help insects cope with surface roughness at smaller length scales [48]. Interestingly,

a recent study from Gorb *et al.* [23] using the same PDMS probes with low *E*-modulus (70 kPa, as described in [22]) obtained different results when comparing adhesion pull-offs and traction experiments of *Coccinella septempunctata* beetles on wax coatings. Similarly to us, even if the PDMS hemispheres and insect pads exhibit similar elastic properties, the material properties are different.

This means that at present, climbing tests still must be performed to measure slipperiness of coatings to insects. Ways to improve the experiment may include:

1. The preparation of smoother PDMS lenses in a reproducible manner. Very small hemispheres could for example be prepared using lithography or 3D printing. Purtov and coworkers seemed to have prepared smooth hemispheres in a reproducible manner starting from sapphire spheres as a starting patterned master [22].

2. The removal of all PDMS oligomers by increasing curing time and/or temperature [31, 32]. Higher molecular weight PDMS would lead in an increase in *AS* when in contact with surfaces [51].

3. The use of stickier and/or more compliant materials. Different types of PDMS can be prepared by changing the cross-linker to pre-polymer ratio, thus changing the modulus, compliance and adhesive properties of PDMS. However, the latter did not allow Gorb and colleagues to match the adhesive properties of beetles even with similar elastic properties [23].

Acknowledgements

References

[1] Dai, Z., Gorb, S. N., and Schwarz, U. (2002) Roughness-dependent friction force of the tarsal claw system in the beetle *Pachnoda marginata* (Coleoptera, Scarabaeidae). *J. Exp. Biol.,* **205**, 2479–2488.

[2] Bullock, J. M. R. and Federle, W. (2011) The effect of surface roughness on claw and adhesive hair performance in the dock beetle *Gastrophysa viridula*. *Insect Sci.,* **18**(3), 298–304.

[3] Gorb, S. N. (2002) Attachment Devices of Insect Cuticle, Kluwer Academic Publishers, Dordrecht.

[4] Federle, W. (2006) Why are so many adhesive pads hairy?. *J. Exp. Biol.,* **209**(14), 2611–2621.

[5] Drechsler, P. and Federle, W. (2006) Biomechanics of smooth adhesive pads in insects: Influence of tarsal secretion on attachment performance. *J. Comp. Physiol. A,* **192**(11), 1213–1222.

[6] Dirks, J.-H. and Federle, W. (2011) Fluid-based adhesion in insects - principles and challenges. *Soft Matter,* **7**(23), 11047.

[7] Dirks, J. H. (2014) Physical principles of fluid-mediated insect attachment - Shouldn't insects slip?. *Beilstein J. Nanotechnol.,* **5**(1), 1160–1166.

[8] Labonte, D. and Federle, W. (2015) Rate-dependence of 'wet' biological adhesives and the function of the pad secretion in insects. *Soft Matter,* **11**(44), 8661–8673.

[9] Dirks, J.-H., Clemente, C. J., and Federle, W. (2010) Insect tricks: two-phasic foot pad secretion prevents slipping.. *J. R. Soc. Interface,* **7**, 587–593.

[10] Reitz, M., Gerhardt, H., Schmitt, C., Betz, O., Albert, K., and Lammerhofer, M. (2015) Analysis of chemical profiles of insect adhesion secretions by gas chromatography-mass spectrometry. *Anal. Chim. Acta,* **854**, 47–60.

[11] Asbeck, W. K. and Loo, M. V. (1949) Critical Pigment Volume Relationships.. *Ind. Eng. Chem.,* **41**(7), 1470–1475.

[12] Lambourne, R. and Strivens, T. A. (1999) Paint and Surface Coatings, Woodhead Publishing, Cambridge 2nd edition.

[13] Sonmez, A., Budakci, M., and Bayram, M. (2009) Effect of wood moisture content on adhesion of varnish coatings. *Sci. Res. Essay,* **4**(12), 1432–1437.

[14] Amador, G. J., Endlein, T., and Sitti, M. (2017) Soiled adhesive pads shear clean by slipping: a robust self-cleaning mechanism in climbing beetles. *J. R. Soc. Interface,* **14**(131), 20170134.

[15] Langer, M. G., Ruppersberg, J. P., and Gorb, S. (2004) Adhesion forces measured at the level of a terminal plate of the fly's seta. *Proc. R. Soc. B Biol. Sci.,* **271**(1554), 2209–2215.

[16] Kesel, A. B., Martin, A., and Seidl, T. (2004) Getting a grip on spider attachment: an AFM approach to microstructure adhesion in arthropods. *Smart Mater. Struct.,* **13**(3), 512–518.

[17] Gorb, E. V., Hosoda, N., Miksch, C., and Gorb, S. N. (2010) Slippery pores: anti-adhesive effect of nanoporous substrates on the beetle attachment system. *J. R. Soc. Interface,* **7**(52), 1571–1579.

[18] England, M. W., Sato, T., Yagihashi, M., Hozumi, A., Gorb, S. N., and Gorb, E. V. (2016) Surface roughness rather than surface chemistry essentially affects insect adhesion. *Beilstein J. Nanotechnol.,* **7**(1),

1471–1479.

[19] Endlein, T. and Federle, W. (2015) On heels and toes: How ants climb with adhesive pads and tarsal friction hair arrays. *PLoS One,* **10**(11), e0141269.

[20] Federle, W., Brainerd, E. L., McMahon, T. A., and Hölldobler, B. (2001) Biomechanics of the movable pretarsal adhesive organ in ants and bees. *Proc. Natl. Acad. Sci.,* **98**(11), 6215–6220.

[21] Endlein, T. and Federle, W. (2008) Walking on smooth or rough ground: Passive control of pretarsal attachment in ants. *J. Comp. Physiol. A,* **194**(1), 49–60.

[22] Purtov, J., Gorb, E. V., Steinhart, M., and Gorb, S. N. (2013) Measuring of the hardly measurable: adhesion properties of anti-adhesive surfaces. *Appl. Phys. A,* **111**(1), 183–189.

[23] Gorb, E., Böhm, S., Jacky, N., Maier, L. P., Dening, K., Pechook, S., Pokroy, B., and Gorb, S. (2014) Insect attachment on crystalline bioinspired wax surfaces formed by alkanes of varying chain lengths. *Beilstein J. Nanotechnol.,* **5**(1), 1031–1041.

[24] Johnson, K. L., Kendall, K., and Roberts, A. D. (1971) Surface energy and the contact of elastic solids. *Proc. R. Soc. London A,* **324**(1558), 301–313.

[25] Davies, J. and Binner, J. G. P. (2000) The role of ammonium polyacrylate in dispersing concentrated alumina suspensions. *J. Eur. Ceram. Soc.,* **20**(10), 1539–1553.

[26] Baklouti, S., Romdhane, M. R. B., Boufi, S., Pagnoux, C., Chartier, T., and Baumard, J. F. (2003) Effect of copolymer dispersant structure on the properties of alumina suspensions. *J. Eur. Ceram. Soc.,* **23**(6), 905–911.

[27] Busscher, H. J., van Pelt, A. W. J., de Boer, P., de Jong, H. P., and Arends, J. (1984) The effect of surface roughening of polymers on measured contact angles of liquids. *Colloids and Surfaces,* **9**(4), 319–331.

[28] Annamalai, M., Gopinadhan, K., Han, S. A., Saha, S., Park, H. J., Cho, E. B., Kumar, B., Patra, A., Kim, S.-W., and Venkatesan, T. (2016) Surface energy and wettability of van der Waals structures. *Nanoscale,* **8**(10), 5764–5770.

[29] Owens, D. K. and Wendt, R. C. (1969) Estimation of the surface free energy of polymers. *J. Appl. Polym. Sci.,* **13**(8), 1741–1747.

[30] Dukas, R. (2008) Evolutionary Biology of Insect Learning. *Annu. Rev. Entomol.,* **53**(1), 145–160.

[31] Kroner, E., Maboudian, R., and Arzt, E. (2010) Adhesion Characteristics of PDMS Surfaces During Repeated Pull-Off Force Measurements. *Adv. Eng. Mater.,* **12**(5), 398–404.

[32] Johnston, I. D., McCluskey, D. K., Tan, C. K. L., and Tracey, M. C. (2014) Mechanical characterization of bulk Sylgard 184 for microfluidics and microengineering. *J. Micromechanics Microengineering,* **24**(3), 35017.

[33] Boots, J. N. M., Fokkink, R., van der Gucht, J., and Kodger, T. E. (2019) Development of a multi-position indentation setup: Mapping soft and patternable heterogeneously crosslinked polymer networks. *Rev. Sci. Instrum.,* **90**(1), 15108.

[34] Ebenstein, D. M. and Wahl, K. J. (2006) A comparison of JKR-based methods to analyze quasi-static and dynamic indentation force curves. *J. Colloid Interface Sci.,* **298**(2), 652–662.

[35] Andersson, L. H. U. and Hjertberg, T. (2003) Silicone elastomers for electronic applications. I. Analyses of the noncrosslinked fractions. *J. Appl. Polym. Sci.,* **88**(8), 2073–2081.

[36] Kim, J., Park, M., Chae, G. S., and Chung, I.-J. (2008) Influence of un-cured PDMS chains in stamp using PDMS-based lithography. *Appl. Surf. Sci.,* **254**(16), 5266–5270.

[37] Yunus, S., de Crombrugghe de Looringhe, C., Poleunis, C., and Delcorte, A. (2007) Diffusion of oligomers from polydimethylsiloxane stamps in microcontact printing: Surface analysis and possible application. *Surf. Interface Anal.,* **39**(12-13), 922–925.

[38] Johnson, L. M., Gao, L., Shields IV, C., Smith, M., Efimenko, K., Cushing, K., Genzer, J., and López, G. P. (2013) Elastomeric microparticles for acoustic mediated bioseparations. *J. Nanobiotechnology,* **11**(1), 22.

[39] Hamed, G. R. and Shieh, C.-H. (1985) Relationship between the Cohesive Strength and the Tack of Elastomers: Part II, Contact Time Effects. *Rubber Chem. Technol.,* **58**(5), 1038–1044.

[40] Clemente, C. J., Bullock, J. M. R., Beale, A., and Federle, W. (2010) Evidence for self-cleaning in fluid-based smooth and hairy adhesive systems of insects. *J. Exp. Biol.,* **213**(4), 635–642.

[41] Gorb, E., Haas, K., Henrich, A., Enders, S., Barbakadze, N., and Gorb, S. (2005) Composite structure of the crystalline epicuticular wax layer of the slippery zone in the pitchers of the carnivorous plant *Nepenthes alata* and its effect on insect attachment. *J. Exp. Biol.,* **208**(24), 4651–4662.

[42] Toussaint, A., De Wilde, M., Molenaar, F., and Mulvihill, J. *Prog. Org. Coatings,.*

[43] DeFusco, A. J., Sehgal, K. C., and Bassett, D. R. (1997) Overview of Uses of Polymer Latexes, Springer Netherlands, Dordrecht.

[44] Voigt, D., Schuppert, J. M., Dattinger, S., and Gorb, S. N. (2008) Sexual dimorphism in the attachment ability of the Colorado potato beetle *Leptinotarsa decemlineata* (Coleoptera: Chrysomelidae) to rough substrates. *J. Insect Physiol.,* **54**(5), 765–776.

[45] Scholz, I., Buckins, M., Dolge, L., Erlinghagen, T., Weth, A., Hischen, F., Mayer, J., Hoffmann, S., Riederer, M., Riedel, M., and Baumgartner, W. (2010) Slippery surfaces of pitcher plants: *Nepenthes* wax crystals minimize insect attachment *via* microscopic surface roughness. *J. Exp. Biol.,* **213**(7), 1115–1125.

[46] Dahlquist, C. (1969) Pressure-sensitive adhesives, Dekker, M., New York.

[47] Persson, B. N. J. (2007) Biological Adhesion for Locomotion on Rough Surfaces: Basic Principles and A Theorist's View. *MRS Bull.,* **32**(6), 486–490.

[48] Scholz, I., Baumgartner, W., and Federle, W. (2008) Micromechanics of smooth adhesive organs in stick insects: pads are mechanically anisotropic and softer towards the adhesive surface. *J. Comp. Physiol. A,* **194**(4), 373–384.

[49] (2011) Fouling of nanostructured insect cuticle: adhesion of natural and artificial contaminants. *Biofouling,* **27**, 1125–1137.

[50] Bullock, J. M. R., Drechsler, P., and Federle, W. (2008) Comparison of smooth and hairy attachment pads in insects: friction, adhesion and mechanisms for direction-dependence. *J. Exp. Biol.,* **211**(20), 3333–3343.

[51] Galliano, A., Bistac, S., and Schultz, J. (2003) Adhesion and friction of PDMS networks: molecular weight

effects. *J. Colloid Interface Sci.,* **265**(2), 372–379.

[52] Bush, A. W., Gibson, R. D., and Thomas, T. R. (1975) The elastic contact of a rough surface. *Wear,* **35**(1), 87–111.

[53] Hyun, S. and Robbins, M. O. (2007) Elastic contact between rough surfaces: Effect of roughness at large and small wavelengths. *Tribol. Int.,* **40**, 1413–1422.

[54] Derler, S., Gerhardt, L.-C., Lenz, A., Bertaux, E., and Hadad, M. (2009) Friction of human skin against smooth and rough glass as a function of the contact pressure. *Tribol. Int.,* **42**(11-12), 1565–1574.

[55] Liu, X., Carré, M. J., Zhang, Q., Lu, Z., Matcher, S. J., and Lewis, R. (2018) Measuring contact area in a sliding human finger-pad contact. *Ski. Res. Technol.,* **24**(1), 31–44.

Appendix

A4.1 Evolution of adhesive stress with number of contacts between paints 1-12 and PDMS hemispheres
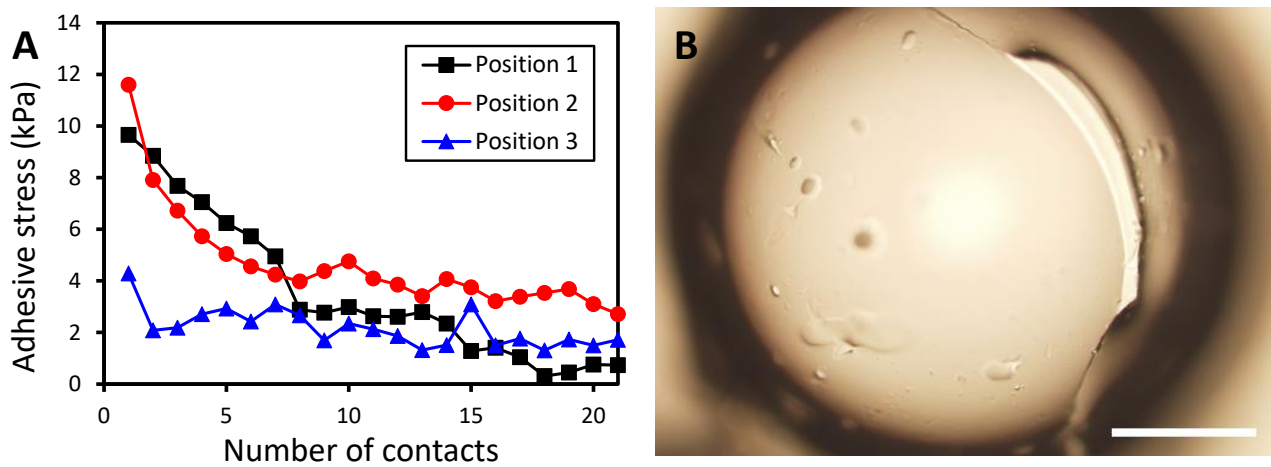

Figure A4.1: (A) Adhesive stress with increasing number of contacts of paint 1 on PDMS. Trends at positions 1 and 2 indicate particle detachment, although no particles were observed *via* microscopy, suggesting oligomer transfer. (B) PDMS lens used in the tests. Scale bar: 200 μm.
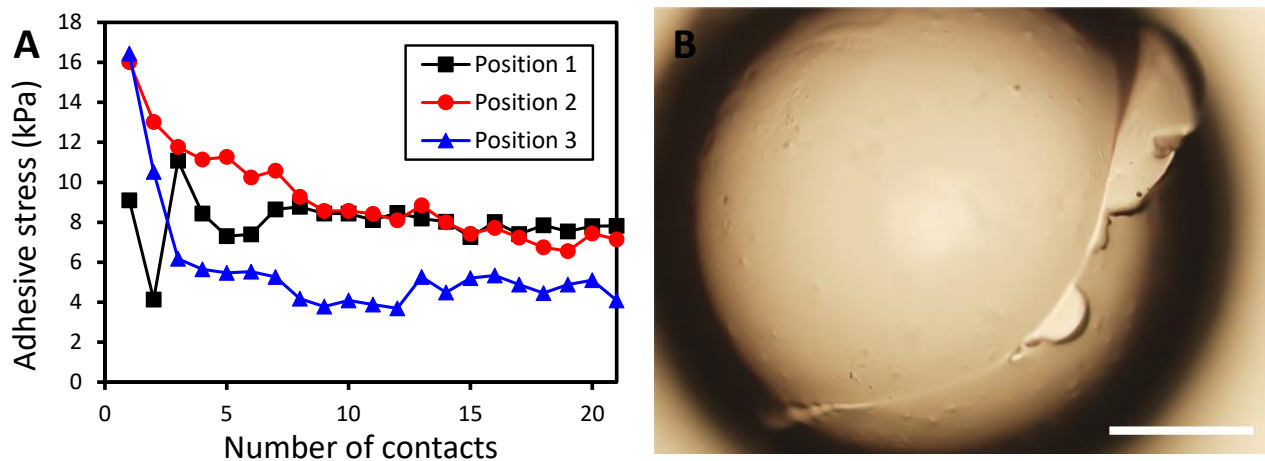

Figure A4.2: (A) Adhesive stress with increasing number of contacts of paint 2 on PDMS. Trends at all positions indicate particle detachment, although no particles were observed *via* microscopy, suggesting oligomer transfer. (B) PDMS lens used in the tests. Scale bar: 200 μm.
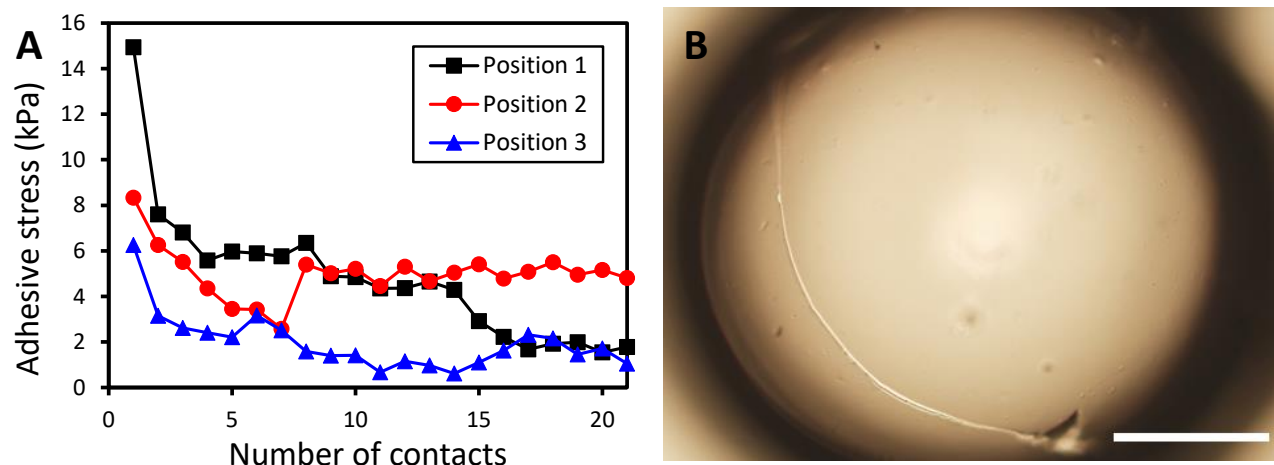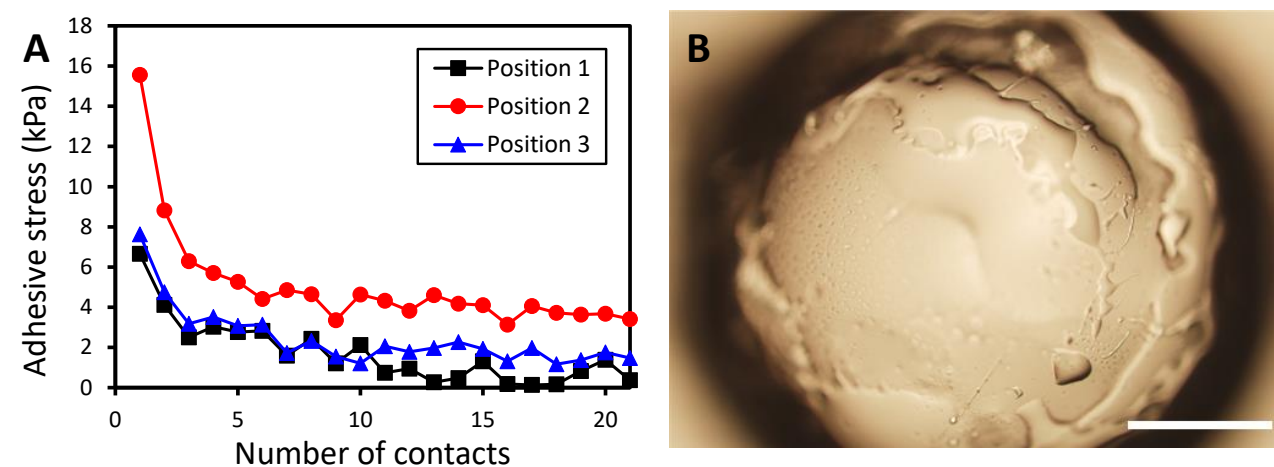
Figure A4.3: (A) Adhesive stress with increasing number of contacts of paint 3 on PDMS. Trends at positions 1 indicate particle detachment, while some particles were likely transferred back to the paint at positions 2 and 3. (B) PDMS lens used in the tests. Scale bar: 200 μm.

Figure A4.4: (A) adhesive stress with increasing number of contacts of paint 4 on PDMS. Trends at all positions indicate particle detachment, although only a few particles were observed *via* microscopy, suggesting oligomer transfer. (B) PDMS lens used in the tests. Scale bar: 200 μm.
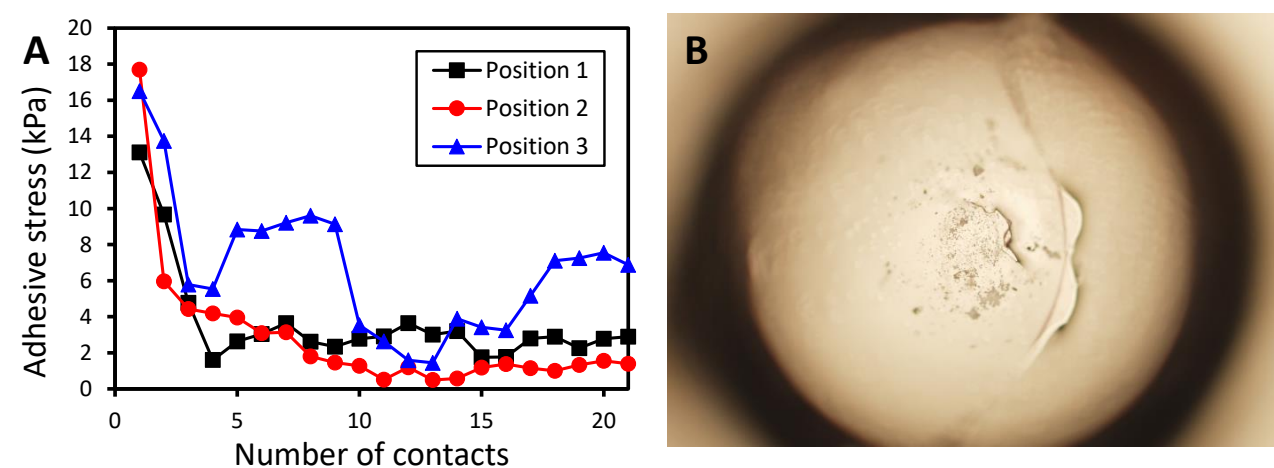

Figure A4.5: (A) Adhesive stress with increasing number of contacts of paint 5 on PDMS. Trends at positions 1 and 2 indicate particle detachment, while pigment particles were likely transferred back to the paint. No particles could be observed *via* microscopy. (B) PDMS lens used in the tests. Scale bar: 200 μm.
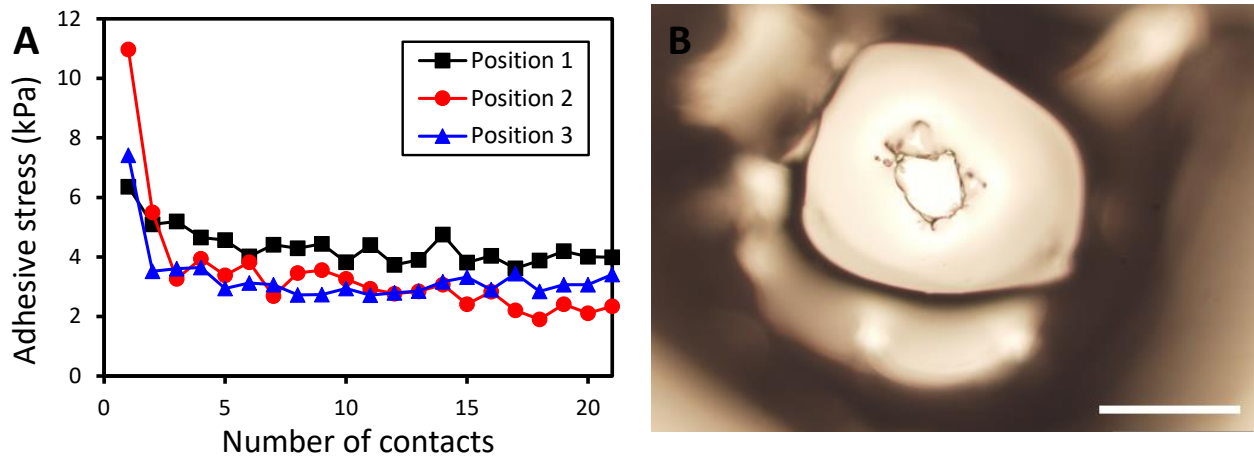
Figure A4.6: (A) Adhesive stress with increasing number of contacts of paint 6 on PDMS. Trends at positions 2 and 3 indicate particle detachment, although only a few particles were observed *via* microscopy, suggesting the initial decreases in adhesive stress were due to oligomer transfer. (B) PDMS lens used in the tests. Scale bar: 200 μm.
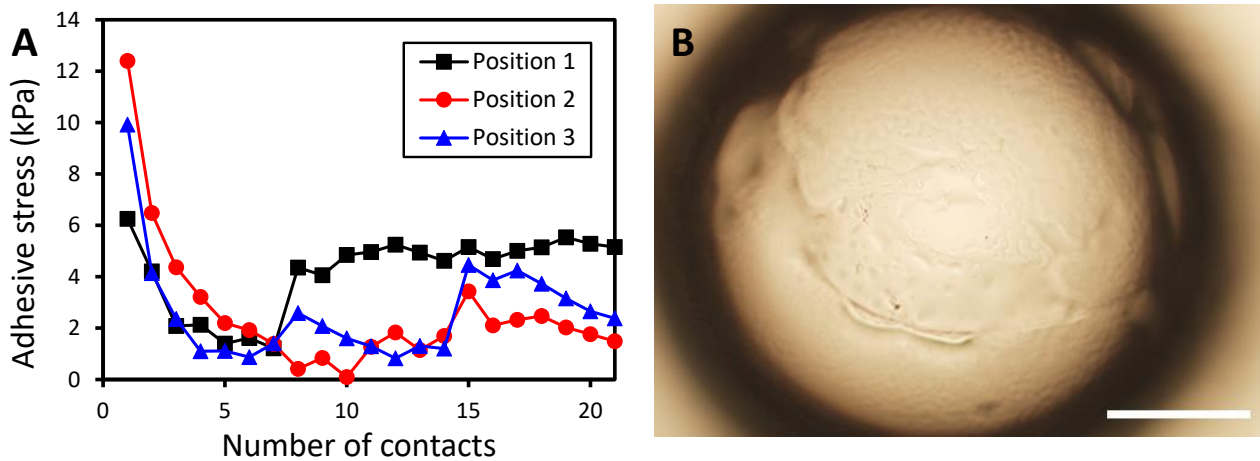

Figure A4.7: (A) Adhesive stress with increasing number of contacts of paint 7 on PDMS. Trends at all positions suggest the PDMS lens detached pigment particles before some of them were transferred back to the coating. (B) PDMS lens used in the tests. Scale bar: 200 μm.
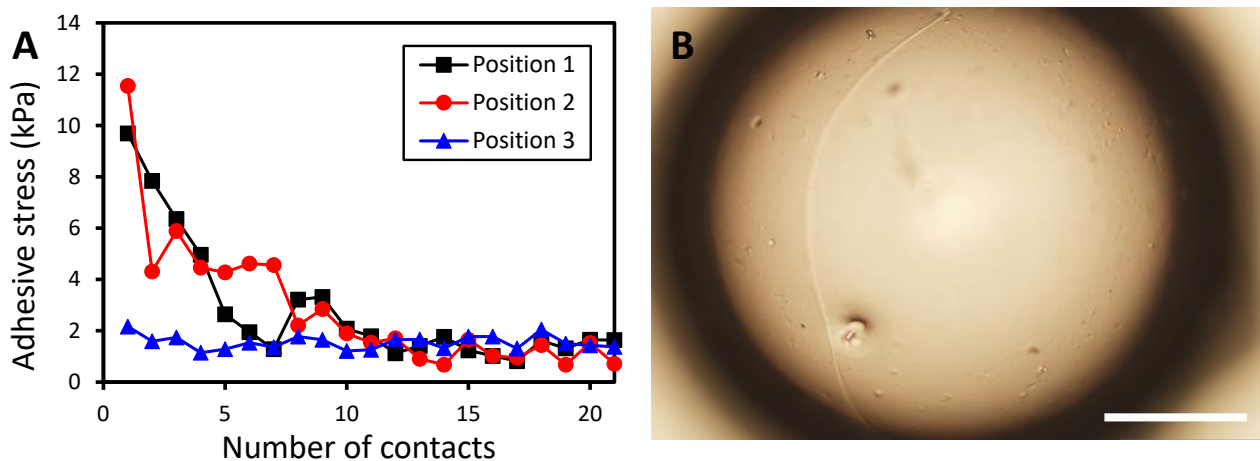

Figure A4.8: (A) Adhesive stress with increasing number of contacts of paint 8 on PDMS. Trends at positions 1 and 2 suggest particle detachment, with "saturation" at position 3. (B) PDMS lens used in the tests. Scale bar: 200 μm.
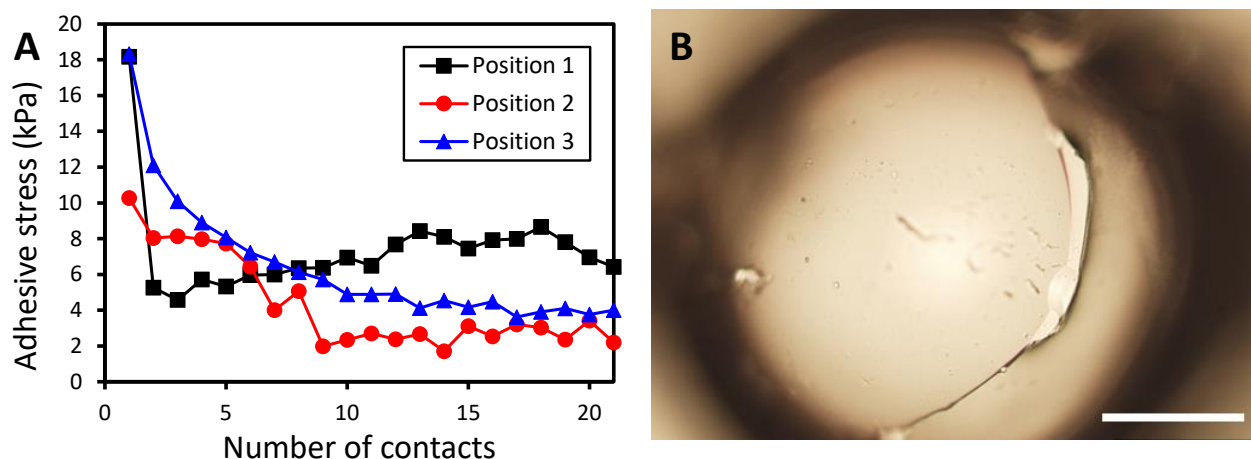
Figure A4.9: (A) Adhesive stress with increasing number of contacts of paint 9 on PDMS. Trends at positions 2 and 3 suggest particle detachment. The large initial decrease in adhesive stress at position 1 is likely due to oligomer transfer. (B) PDMS lens used in the tests. Scale bar: 200 μm.

Figure A4.10: (A) Adhesive stress with increasing number of contacts of paint 10 on PDMS. Trends at positions 2 and 3 suggest particle detachment. (B) PDMS lens used in the tests. Scale bar: 200 μm.

Figure A4.11: (A) Adhesive stress with increasing number of contacts of paint 11 on PDMS. Trends at all positions suggest particle detachment. (B) PDMS lens used in the tests. Scale bar: 200 μm.
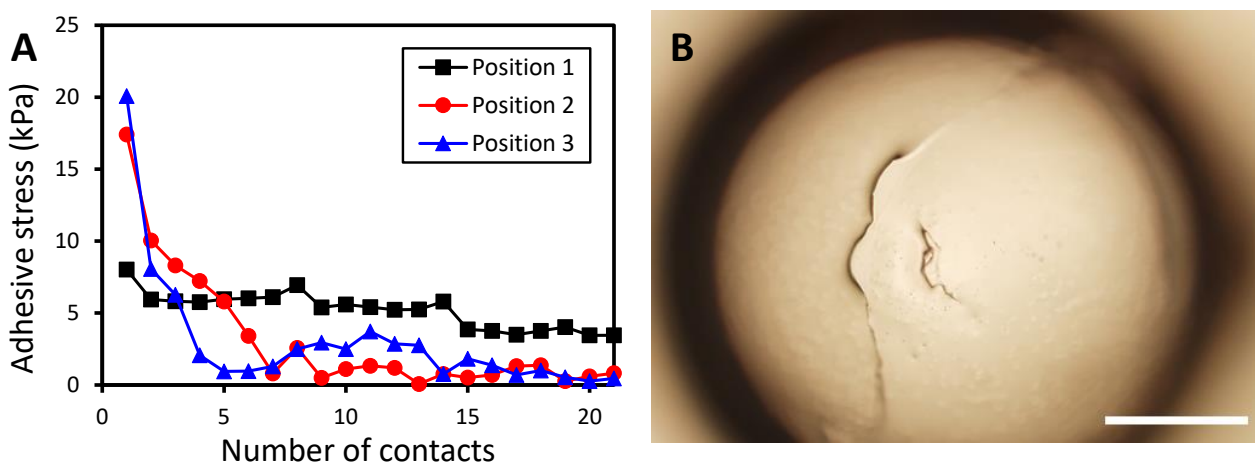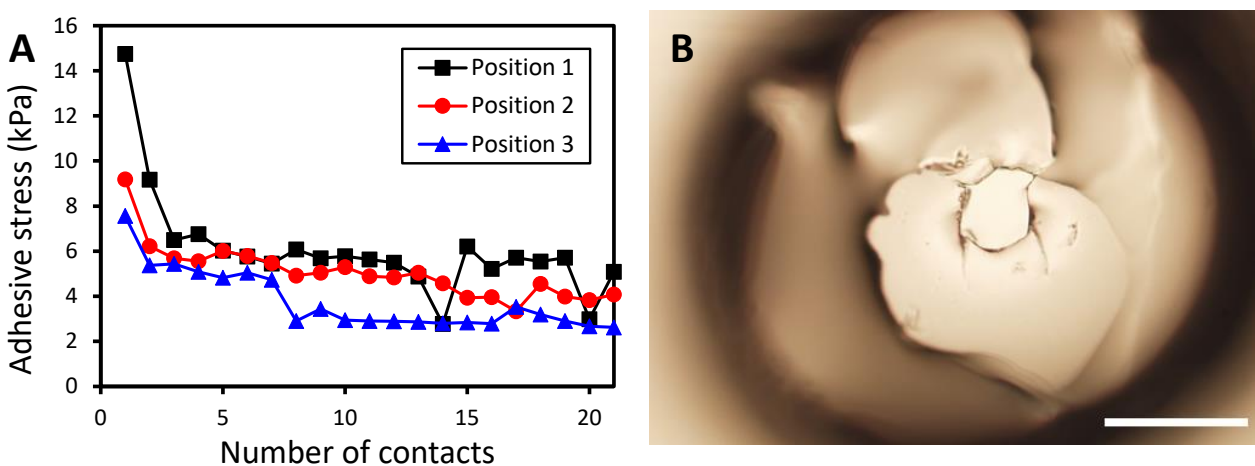
Figure A4.12: (A) Adhesive stress with increasing number of contacts of paint 12 on PDMS. Trends at positions 1 and 3 suggest particle detachment. Some pigment particles were likely transferred back to the paint at position 2. (B) PDMS lens used in the tests. Scale bar: 200 μm.
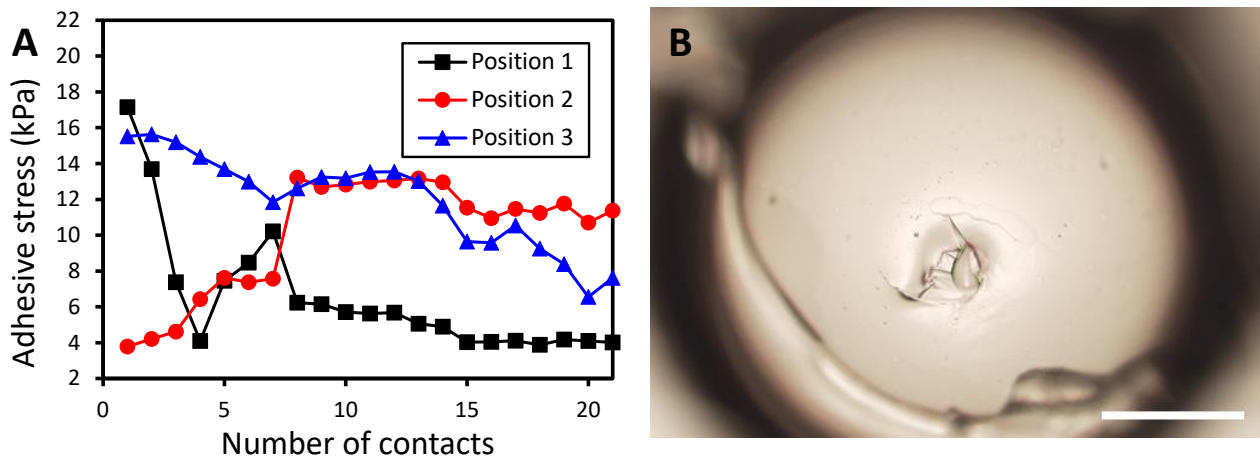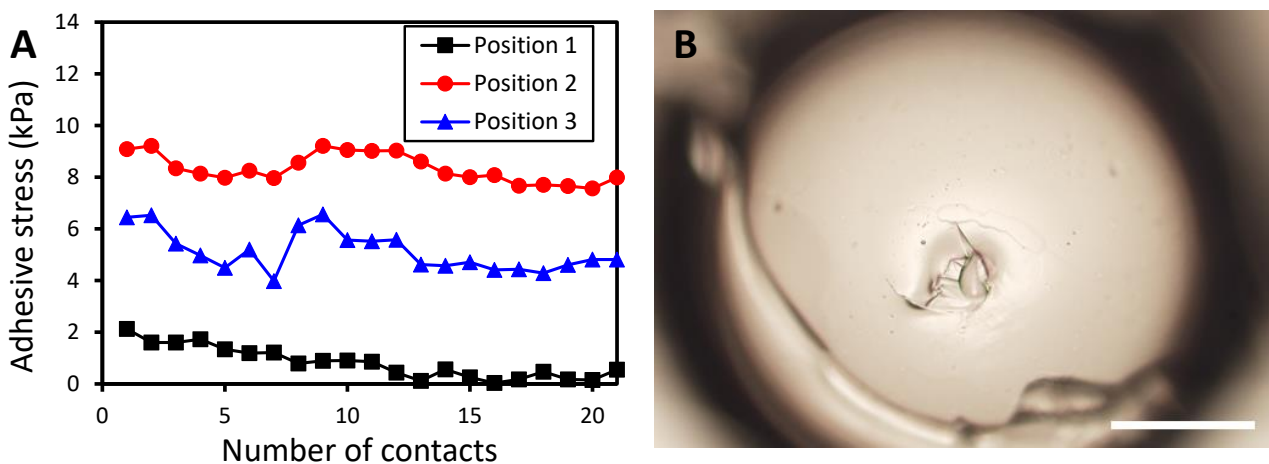

Figure A4.13: (A) Adhesive stress with increasing number of contacts of paint 12 on PDMS. Trends at positions 1 and 3 suggest particle detachment. Some pigment particles were likely transferred back to the paint at position 2. (B) PDMS lens used in the tests. Scale bar: 200 μm.
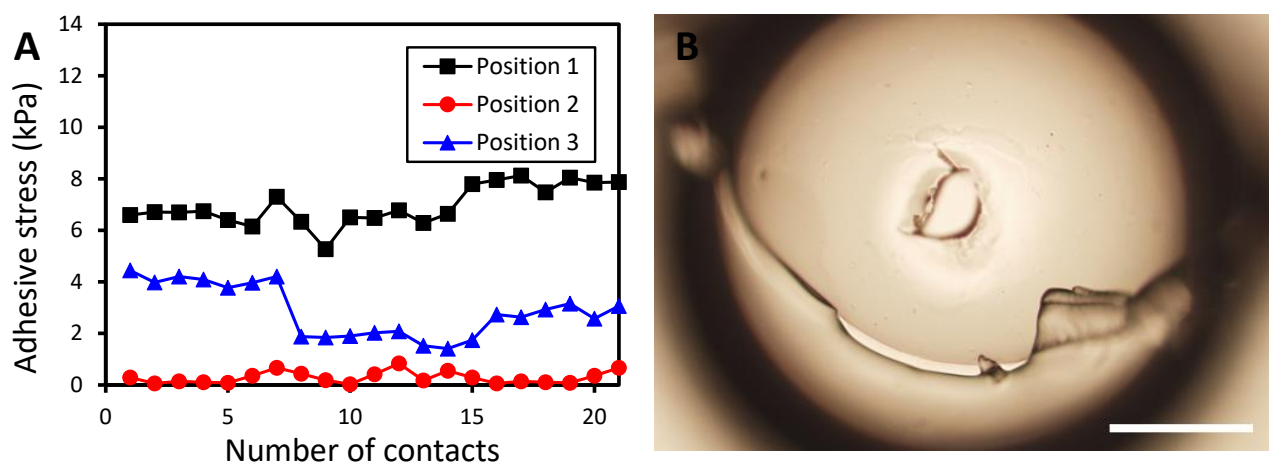
Figure A4.14: (A) Adhesive stress with increasing number of contacts of paint 12 on PDMS (reproducibility measurement). Trends at positions 1 and 2 approximately indicate there was no PDMS contamination, while some particles detached at position 3 with some of them being transferred back to the coating. (B) PDMS lens used in the tests. Scale bar: 200 μm.

A4.2   FTIR-ATR spectra of paint 3
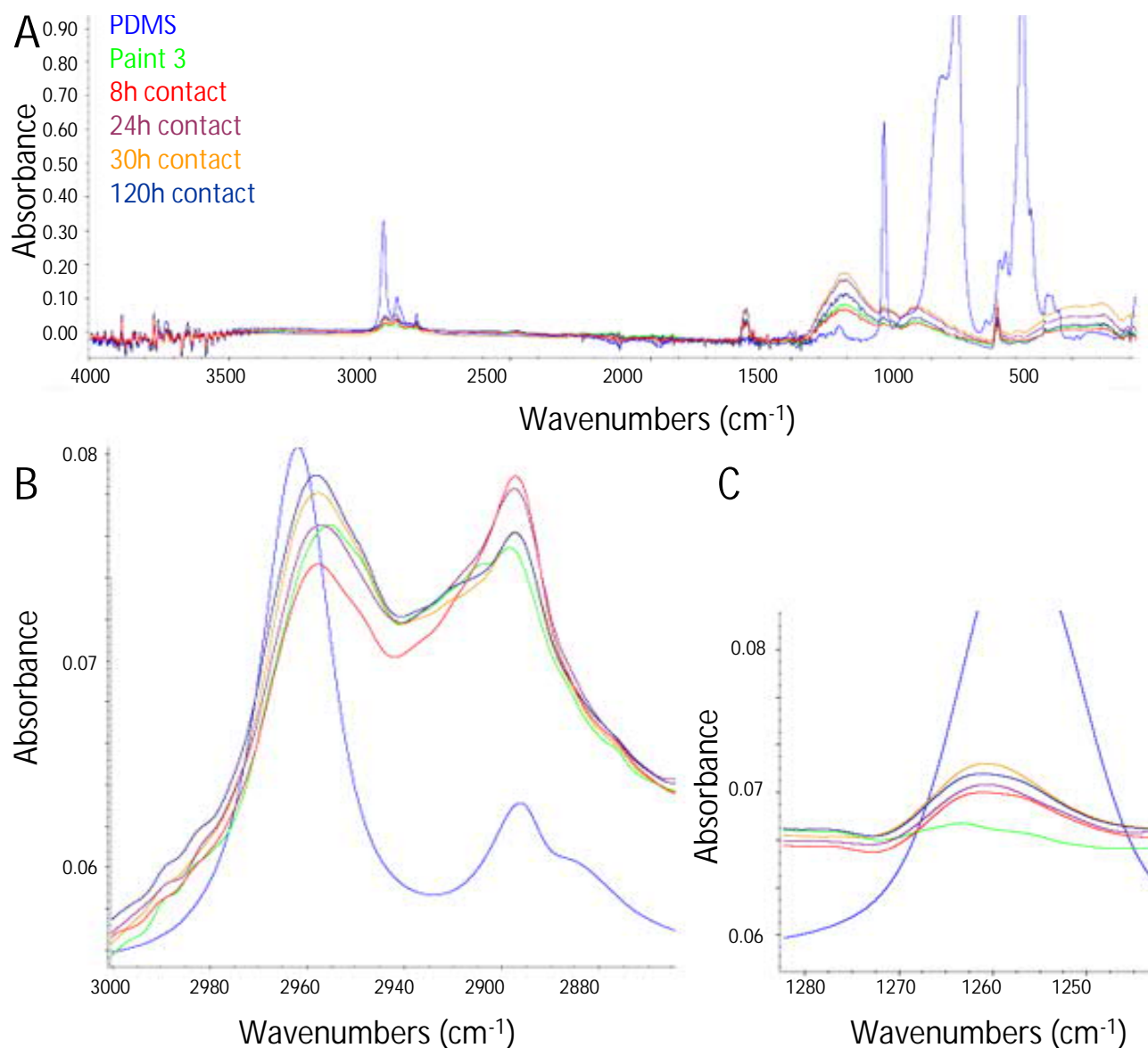
Figure A4.15: (A) ATR-FTIR spectra of PDMS, paint 3 (10 wt% TiO_2, 20 wt% $CaCO_3$, PVC 50) and of the paint after 24 hours, 30 hours and 120 hours contact with PDMS. (B) 2820-3000 cm^{-1} region, where the peak intensity increased after the paint was in contact with PDMS (asymmetric CH_3 stretching in Si-CH_3). (C) 1220-1300 cm^{-1} region, where the peak intensity increased after the paint was in contact with PDMS (CH_3 deformation in Si-CH_3) [32].

A4.3 Stick insect (*Carausius morosus*) adhesive pads after climbing paints containing 10 wt% TiO$_2$ and 20 wt% CaCO$_3$
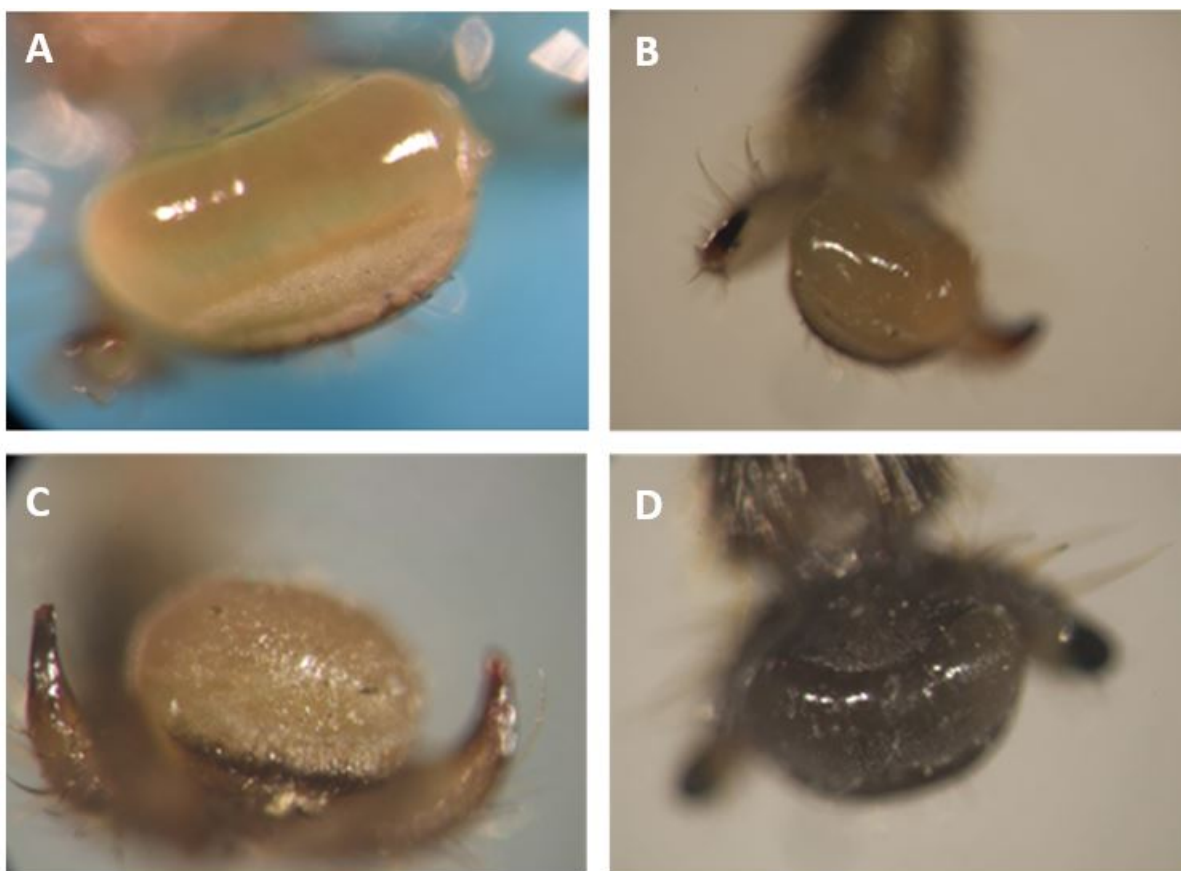
Figure A4.16: Light microscopy images of stick insect (*C. morosus*) pads: (A) control and after climbing paints (B) 3, (C) 8 and (D) 4 (10 wt% TiO$_2$, 20 wt% CaCO$_3$, PVC 50, 60 and 70, respectively). The variations in colour are due to ageing.

5

Slippery paints: how tuning polymer and pigment size can prevent ants from walking on walls

*As an environmentally friendlier alternative to insecticides, paints inspired by the inner wall surface of pitcher plants were formulated to provide a slippery mechanical barrier for crawling insects (*Atta cephalotes *ant workers). Model waterborne paint systems containing only acrylic binder and $CaCO_3$ extender pigment have been prepared. Controlling the particle size of the binder (> 250 nm) and the diameter of the $CaCO_3$ particles ($\leq$ 10 µm) can strongly decrease insect attachment to paint surfaces. The coatings were characterised in terms of contact angle, surface roughness, porosity and scrub resistance, and their slipperiness to insects was measured in climbing tests. Our data suggests that insects slip due to a combination of (1) transfer of particles from the paint surface to the sticky pads of insects, (2) adhesive fluid absorption by pores in the paint; and (3) surface roughness. In optimised formulations, 100% of* Atta cephalotes *ants slipped and fell from vertical paint panels.*

Aurélie Féat[a,b], Martin W. Murray[a], Jasper van der Gucht[b] and Marleen Kamperman[b,c]

[a]AkzoNobel Decorative Paints, Wexham Road, Slough, SL2 5DS, United Kingdom

[b]Physical Chemistry and Soft Matter, Wageningen University, Stippeneng 4, 6708 WE, Wageningen, The Netherlands

[c]Zernike Institute for Advanced Materials, University of Groningen, Nijenborgh 4, 9747 AG Groningen, The Netherlands

5.1   Introduction

Coatings are mostly used for decorative, protective, or functional purposes, for example self-cleaning, antifouling, anti-corrosive or water-repellency and find applications in many areas such as vehicles, buildings and furniture [1–3]. In the past decades, global demand for insect-repellent coatings has risen: many insects are indeed considered pests as they are highly detrimental to agriculture, forestry, buildings and human health, despite many insects such as pollinators and seed dispersers being indispensable for ecosystems [4–7]. A major application of such coatings is found in buildings: for instance, wood-feeding termite damage alone has been estimated to cost between \$2 and \$40 billion per annum [5, 8, 9]. Approximately 0.5% of ant species are considered pests as they search for food or establish their nests in walls, some of which have been acknowledged to be the most difficult pests to eliminate [10–12]. Insecticides are efficient at preventing insects from entering buildings, but are harmful to the environment and human health as well as lacking selectivity [13–16]. Hence, eco-friendlier strategies such as insect-repellent and low insect adhesion coatings are being developed [17–20].

In the latter case, it is important to understand how insects adhere to surfaces. Briefly, insects climb surfaces by means of (1) interlocking with substrate asperities, (2) adhering to surfaces using their sticky, compliant pads and (3) by secreting an adhesive fluid which compensates surface roughness to increase the contact area and hence, adhesion through van der Waals, capillary and viscous forces [21–24]. Depending on the type of insect, adhesive pads present different morphologies and are either referred to as 'smooth' or 'hairy', as respectively observed in e.g. ants and cockroaches, or beetles and flies (Figure 5.1).

Due to their sticky pads, insects tend to accumulate particles on their bodies and adhesive pads. Insects remove these particles through self-cleaning to keep their adhesive properties and locomotion intact [25–27]. The size of contaminating particles is of particular importance for the effectiveness of self-cleaning of the pads of ants (smooth pads), Coccinellids and dock beetles (hairy pads) [25, 28–30]. 1 μm particles and particles larger than 45 μm can be easily removed through self-cleaning, while insects need more steps to remove 10-20 μm sized contaminants [25, 28, 29]. For hairy pads, large particles cannot fit in between fibrillar setae, leading to rapid particle removal [25, 29, 31].
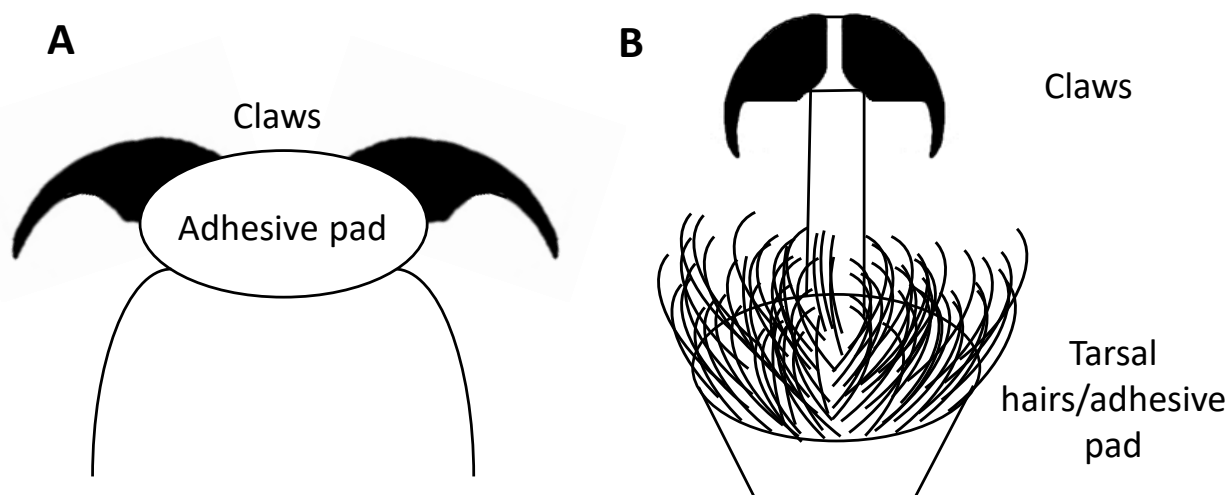
Figure 5.1: Schematic morphologies (ventral views) of (A) smooth pad composed of claws and adhesive pad, from which the adhesive fluid is secreted and (B) hairy pad showing the claws and fibrillar adhesives of distal pad (furthest away from the body). The adhesive fluid is secreted through the hairs or setae [21].

The effect of surface roughness on the ability to climb surfaces has been widely investigated in e.g. [32–36]. Insects can cope with roughness by using either their claws or their adhesive pads in combination with adhesive fluid secretion: on 'smooth' substrates (asperity size ca. < 50 nm), insects mainly use their pads, while on 'rough' substrates (asperity size > 3 μm), they mostly use their claws and spines which cling to asperities [22, 32, 33, 35–38]. Their adhesive fluid enhances attachment on rough substrates [23, 36, 39]. In intermediary 'nano/micro-rough' surfaces, insects' attachment forces are considerably reduced as the substrate protrusions are too small for the claw tip to interlock with, and too rough to develop sufficient contact area by the adhesive pads [33, 36]. Additionally, some insects, e.g. some species of ants and beetles, do not possess adhesive structures that would allow them to climb up smooth surfaces [40, 41].

Substrate roughness has been found to dominate insect attachment forces over surface chemistry [34, 42, 43]. Indeed, the effect of surface chemistry or surface hydrophobicity on fluid-mediated insect attachment has been studied on both natural and synthetic surfaces, and only weak or no effects were observed [42–44].

In nature, many plants are known to be slippery to insects, in particular some species of the genus *Nepenthes*. These are pitcher plants which possess surfaces covered in micro-rough lipid epicuticular wax crystals [45–49]. The rough epicuticular wax crystals detach from the surface of the inner surface of the pitcher and adhere to the sticky pads of insects (generally ants [50]). Their claws and fouled adhesive pads cannot generate large enough forces to exit this deadly, nectar-lubricated trap (Figure 5.2A). Two additional mechanisms have been proposed
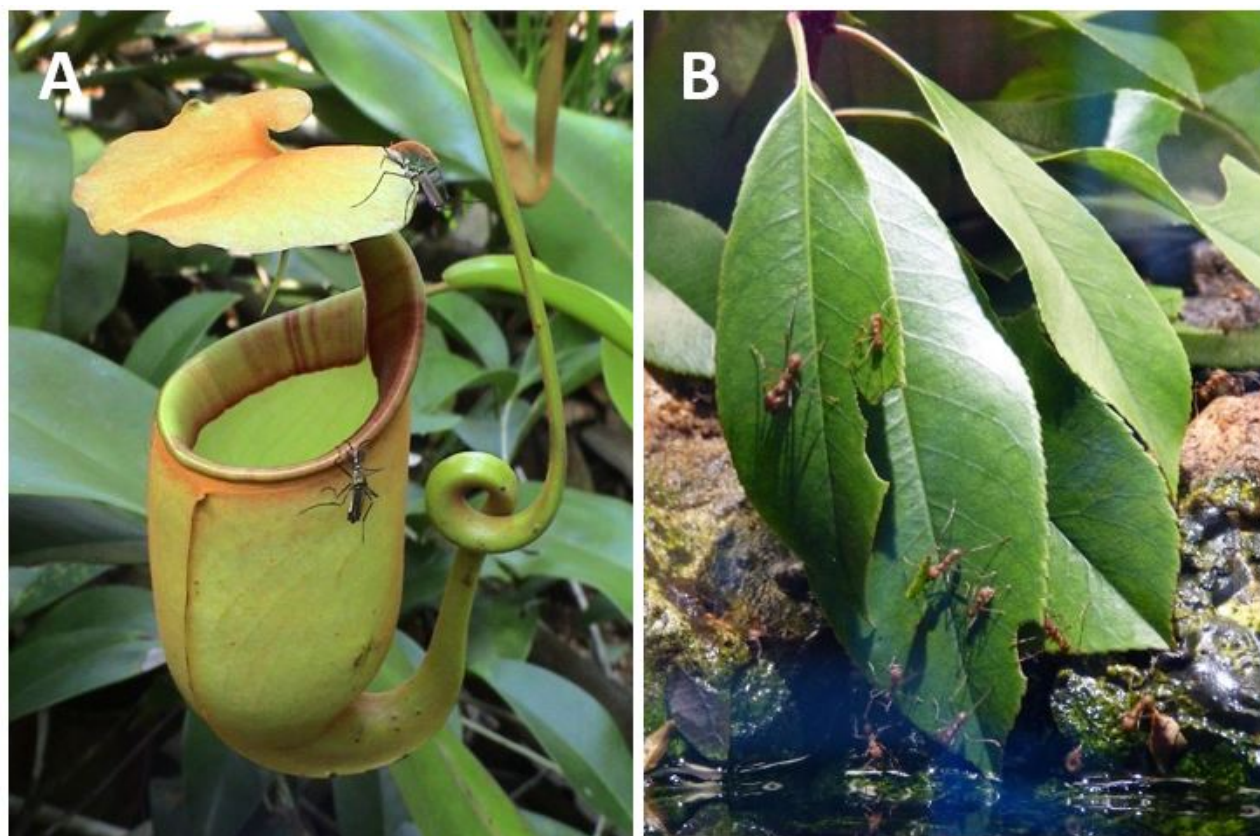
Figure 5.2: (A) Ants climbing up a pitcher plant of the *Nepenthes* genus (courtesy of W. Federle). (B) *Atta cephalotes* ants walking on leaves (courtesy of C. Jadoul).

by Gorb and Gorb [51]: (1) the wax-dissolution hypothesis: the insect adhesive fluid may dissolve the epicuticular wax crystals, resulting in a slippery thick layer of fluid; and (2) the fluid absorption hypothesis: the wax coverage may absorb the insect adhesive secretion. Such surface properties, featuring particle detachment, surface roughness and surface lubrication are of particular interest for bio-inspired insect-repellent coatings, as for instance observed in the SLIPS technology [18]. It has even been suggested that spray coatings made of epicuticular wax crystals could be used for this purpose [49].

The studies discussed above suggest that coatings with low adhesive properties for insects could be prepared using 'nano/micro-rough' surfaces (asperity size 50 nm – 3 μm) [33, 36], detachable particles in the 10-20 μm size range [25, 28, 29], epicuticular wax crystals and highly porous surfaces [38, 46, 49]. As an eco-friendlier alternative to insecticides and insecticidal coatings, we have formulated model waterborne paints which provide a slippery physical barrier through pigment transfer to *Atta cephalotes* L. ant workers (Hymenoptera, Formicidae, Figure 5.2B) on vertical surfaces, as discussed in **Chapter 3**. Paints are made of four major ingredients: (1) the solvent, most paints are now waterborne for improved health and environ-

mental impact [52, 53]; (2) the pigment, which brings opacity to the coating, e.g. TiO_2; (3) the polymer binder, or latex, which wets the solid particles and forms a film *via* coalescence once applied to a substrate [54, 55]; and (4), the additives, such as dispersing and biocide agents [56]. Extender pigments are additional pigments to enhance the opacity and other properties in combination with traditional pigments [57, 58].

The Pigment Volume Concentration (PVC) is a major formulation parameter and is commonly described in the paint industry as the volumetric amount of pigment present in a paint [59]:

$$PVC = \frac{Volume\ of\ pigments}{Volume\ of\ pigments + volume\ of\ binder} \tag{5.1}$$

The PVC of a paint gives information on how much polymer binder is needed to wet the pigment particles. At the Critical Pigment Volume Concentration (CPVC), a concept introduced by Asbeck and van Loo [59], the coating lacks binder to fully wet the pigment particles. In latex coatings, voids are formed during coalescence for drying temperatures close to the glass transition temperature (T_g, see e.g. [60]), while pore formation in paint coatings occurs when PVC > CPVC as the polymer cannot fill all the gaps between the pigment particles [59, 61]. Above the CPVC, the coating properties dramatically change, so that the CPVC value can be determined using paints formulated with increasing PVC values *via* (1) mechanical properties, e.g. tensile strength or hardness; (2) transport properties such as permeability or corrosion resistance; or (3) optical properties like gloss, contrast ratio or colour difference [62, 63]. The CPVC was found to depend on the type of binder, functionalities and size of the polymer binder [62, 64].

Our previous results (**Chapter 3**) on model paints composed of acrylic binder, TiO_2 and $CaCO_3$ showed that the slipperiness was mostly due to an increase in the PVC; when the paints were formulated above their CPVC, some pigment and extender particles were sufficiently loose to be detached by the adhesive pads of *A. cephalotes*. The surface roughness impacted the slipperiness to a lesser extent. In this chapter, we investigate the effect of (1) the latex particle size and (2) the extender pigment diameter on the slipperiness mechanism. The former is expected to impact the CPVC, while the latter should influence the self-cleaning abilities of insects. The latex particle size and the extender pigment were systematically varied to

investigate the effect on wettability, porosity, surface roughness and scrub resistance, as well as their slipperiness to insects (*A. cephalotes* ant workers).

5.2 Materials and methods

5.2.1 Materials

Methyl methacrylate (MMA), butyl acrylate (BA), acrylic acid (AA), sodium bicarbonate, tert-Butyl hydroperoxide (*t*-BHP), sodium persulfate (NaPS), sodium dodecylbenzenesulfonate and AMP 95 were obtained from Sigma-Aldrich (Gillingham, UK). Sodium dodecyl sulphate (SDS) was supplied by VWR and was used as both latex stabiliser and pigment dispersant in the paints (Lutterworth, UK). Disponil FES surfactants (Figure 5.3) were kindly provided by BASF (Ludwigshafen, Germany) and were used as additional stabilisers in the latexes. Bruggolite FF6 was purchased from Brueggemann (Heilbronn, Germany). Texanol was added as a coalescent in the paints and was obtained from Eastman (Kingsport, TN, USA). The ground calcium carbonate extender pigments were kindly supplied by Omya (from different sites across Europe), with densities of 2.7-2.85 g/cm^3 and mean particle sizes of 1-45 μm. All chemicals were used as received.
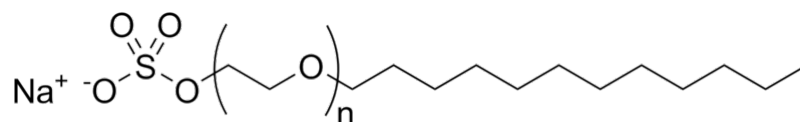
Figure 5.3: Structure of the surfactants used in this study, with $n = 0, 2, 12, 30$, where $n = 0$ is SDS and $n > 0$ is a surfactant from the Disponil FES range.

Model paint formulations were prepared, which didn't contain typical additives found in paints, such as anti-foaming agents, thickeners or biocides to limit the number of ingredients and interactions thereof.

5.2.2 Latex synthesis and characterisation

We prepared acrylic latexes displaying varying particle size and constant glass transition temperature (T_g), by tuning the surfactant amount. Surfactants were chosen among the sodium lauryl ether sulphate (SLES) series with varying ethylene oxide-chain length (n), with sodium dodecyl sulphate (SDS) considered as $n = 0$ (Table 5.1). The Critical Micelle Concentration (CMC) values of the surfactants were measured by tensiometry (K12 tensiometer, Krüss. Ham-

burg, Germany) and were close to the values available in literature and given by the supplier [65] (Table 5.1). The amount of surfactant in the latexes was expressed with regards to its CMC (factor x). Large particle sizes ($>$ 350 nm) could be easily prepared by using longer ethylene oxide chain surfactants.

45 wt% solids content poly(methyl methacrylate-*co*-butyl acrylate-*co*-acrylic acid) (52/45/3) latexes were prepared by seeded semi-batch emulsion polymerisation following a conventional procedure, see e.g. [53, 64, 66]. SDS, sodium bicarbonate and demineralised water were first pre-heated at 70°C and stirred at 200 rpm. The seed was composed of 10 wt% of total monomers and 20 wt% of total initiator (sodium persulfate (NaPS)) and was prepared by batch emulsion polymerisation. The remaining monomers and initiator were then added over the course of three hours at 75°C. After cooling to 70°C and 60°C, 0.05 wt% *t*-BHP and 0.05 wt% Bruggolite FF6 were respectively injected to react any remaining monomers and reduce the Volatile Organic Components (VOC) [67].

The particle sizes of the latexes were determined by Dynamic Light Scattering (DLS, Zetasizer Nano ZS, Malvern, Worcestershire, UK) and ranged between ca. 65 and 840 nm. After drying the latexes for 24 hours at room temperature, their glass transition temperatures (T_g) were measured by DSC (Differential Scanning Calorimetry, Q2000, TA Instruments, Elstree, UK). The T_g values decreased slightly with increasing particle size (Pearson's r = -0.75, P = 0.020); however, the variations in T_g being low (single sample t-test, t_8 = -0.10, P = 0.922), we considered it to be a constant parameter (22.7 $\pm$ 1.5°C). Statistical analyses are later described in the section.

5.2.3 Waterborne paint model systems and characterisation

Paint preparation

Two different paint series were prepared following the procedure described below: (1) to investigate the effect of the latex particle size on the paint slipperiness, acrylic latexes of varying particle sizes (64-838 nm) and approximately constant T_g (22.7 $\pm$ 1.5°C) were used in combination with 1 μm extender pigment; (2) to assess the effect of the pigment size on the slipperiness, different CaCO$_3$ particle diameters (1-45 μm) were used with a 64 nm sized latex (latex 6, T_g = 23.9°C).

Table 5.1: Latexes used in the present work, sorted by particle size, where x: concentration factor with regards to the CMC of the respective surfactants. CMC and particle size values are expressed as mean $\pm$ standard deviation (SD). [a]: literature value [65].

Latex	Surfactant	EO-chain length (n)	CMC stated by supplier (mM)	Measured CMC (mM) ($n = 2$)	[Surfactant] (x.CMC)	Particle size (nm) ($n = 10$)
6	SDS	0	8.3[a]	7.9 $\pm$ 0.3	5	64 $\pm$ 2
11	SDS	0	8.3[a]	7.9 $\pm$ 0.3	2	85 $\pm$ 2
23	SDS	0	8.3[a]	7.9 $\pm$ 0.3	0.5	122 $\pm$ 1
25	SDS	0	8.3[a]	7.9 $\pm$ 0.3	0.1	259 $\pm$ 2
1-F27	FES 27	2	1.0	1.2 $\pm$ 0.1	1	359 $\pm$ 3
1-F77	FES 77	30	0.17	0.24 $\pm$ 0.02	1	462 $\pm$ 28
2-F993	FES 993	12	0.27	0.28 $\pm$ 0.02	0.25	728 $\pm$ 5
2-F27	FES 27	2	1.0	1.2 $\pm$ 0.1	0.25	805 $\pm$ 26
2-F77	FES 77	30	0.17	0.24 $\pm$ 0.02	0.25	838 $\pm$ 23

The paints were prepared as follows: 50-75 wt% extender pigment slurries were prepared by dispersing the solids and SDS in water at about 2000 rpm with a Dispermat high speed disperser blade (VMA–Getzmann, Reichshof, Germany). The optimum amount of surfactant was determined by the minimum viscosity dispersant demand method [68, 69]. 60% and 70% PVC paints were formulated by adding the corresponding amount of latex to the slurries. 5 wt% Texanol (expressed on the total amount of paint) was added to the paints to aid the latex coalescence process and limit the formation of cracks. The pH of the paints was increased to 8-8.5 by adding a few drops of AMP 95. Alkaline pH values are typically used in the coating industry, as it optimises the effect of Texanol and ensures that the anionic surfactants that stabilise the latexes and pigments are fully ionised [70].

Paint characterisation

The paints were applied on metal panels (10.5 cm $\times$ 8.5 cm) using a film applicator (TQC Sheen, Rotterdam, The Netherlands) at a wet film thickness of 100 μm and dried for a minimum of 24 hours at 20 $\pm$ 2°C and 50 $\pm$ 2%RH. The panels were 0.15 mm thick steel sheets from Ernst Sauter AG (Reinach, Switzerland) and possessed a surface roughness of 0.9 μm $\pm$ 0.2 μm.
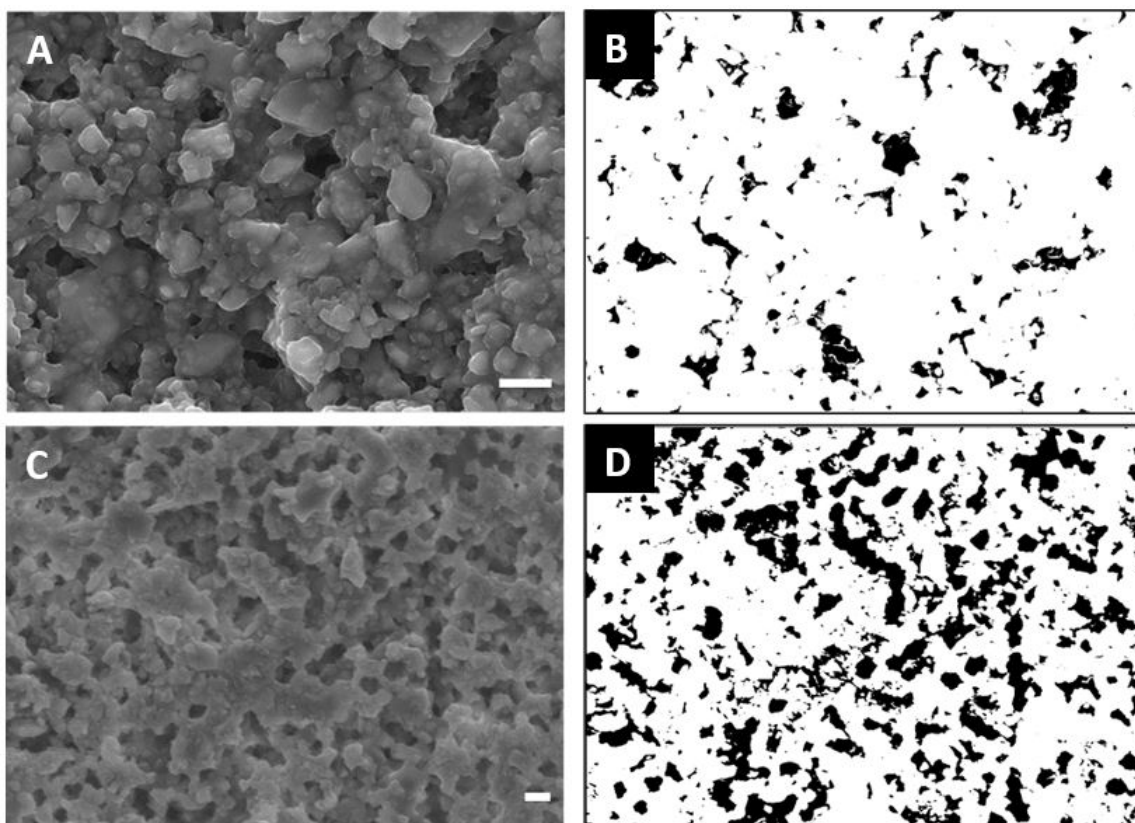
Figure 5.4: Porosity measurements performed on SEM images of 70% PVC paint surfaces containing 1 μm CaCO$_3$ particles with varying latex particle size: (A) 85 nm and (C) 805 nm before applying a threshold. (B) and (D) thresholded images from (A) and (C) in ImageJ according to [71, 72]. Scale bars: 1 μm.

Eight water contact angle measurements were performed on each paint panel with an optical contact angle device, using 5 μL droplets of Milli-Q water at 20.5 $\pm$ 0.5°C and 38 $\pm$ 2.0%RH (OCA 50, DataPhysics, Filderstadt, Germany).

The surface roughness of paint coatings was measured using NanoFocus μScan Explorer (Oberhausen, Germany). Six measurements of 1 mm $\times$ 1 mm area (500 nm XY-resolution, 15 nm Z-resolution, 1001 pixels$\times$1001 pixels) were performed on the panels. The roughness profiles were analysed with μsoft analysis to calculate the average surface roughness (R_a).

Scanning electron microscopy (SEM) images of the PVC 70 paints were obtained with JSM7001F from JEOL (Tokyo, Japan) by coating the samples with a 30-nm carbon layer using Q150T ES, Quorum (Quorum Technologies, Laughton, UK). The images were recorded at an acceleration voltage of 10.0 kV. The apparent surface porosity was manually measured from the SEM micrographs with ImageJ (Version 1.51r, National Institutes of Health, Bethesda, MD, USA) following the segmentation method [71, 72]. A threshold was applied before using the "analyse particles" function, the calculated "%area" corresponding to the apparent porosity. The level of threshold was manually tuned to fit the pores as accurately as possible and hence

varied between the various paints (Figure 5.4). This quick procedure was preferred to the specific surface area determination by the BET method [73] as the porosity at the surface is more likely to be of importance with regards to insect pads.

To measure the water uptake of the PVC 70 paint films, the paint panels were soaked in Milli-Q water for 7 days at 19.1°C ± 1.9°C and their weight was measured after carefully removing excess water from the panels at room temperature. The weight difference between t = 0 and t = 7 days gives the water uptake.

The scrub resistance of PVC 70 coatings was determined by abrasion weight loss tests according to the ASTM D4213-96 standard method. The paints (wet thickness = 400 μm) were applied to PVC scrub panels and dried for 7 days at 40°C ± 1°C. The coated panels were then scrubbed to either 200 or 2000 cycles at a speed of 36 cycles/min with a nylon-silicon carbide abrasive pad (40 mm × 94 mm, R_a = 30.0 ± 16.9 μm, Scotch-Brite, 3M, St. Paul, MN, USA). A force of 2.4 N was applied onto the pads in a surfactant-based scrub medium (2.5 g/L sodium dodecylbenzenesulfonate). The scrub resistance is measured as follows:

$$Scrub\ resistance\ (mg/cm^2) = \frac{weight\ loss}{scrubbed\ area} \tag{5.2}$$

The CPVC of the paints was estimated by using the absorption values of linseed oil provided by suppliers [59]:

$$CPVC(\%) = \frac{100}{1 + \frac{pigment\ density \times oil\ absorption}{linseed\ oil\ density}} \tag{5.3}$$

where the linseed oil density is 0.93 kg/L and the oil absorption value is the required amount of linseed oil to saturate 100 grams of pigment or extender, which indicates how much binder will be needed to wet the solid particles. The approximate CPVC values of the paint systems were 63% and 66 ± 3% for the paints with varying latex particle size and extender pigment size, respectively.

Insect climbing experiments

The adhesive performance of both types of pad is very similar [22], and substrates known to be slippery for one type are also slippery for the other [74, 75]. Therefore, leaf-cutting ant workers (*Atta cephalotes*) were used as model insects in the climbing experiments as they are

"motivated" climbers. The ants first had their pads cleaned by walking on cleaning tissue and were then placed on a starting surface (1 cm^2 201E masking tape from 3M) located at the middle of the vertically oriented panel, to which a 100 μm paint layer was applied. Once 4 (out of 6) legs left the starting platform, the time needed to reach any edge of the painted surface was measured. The test was discarded if the insect slipped from the surface under three seconds after placing it on the tape. The insect was considered unsuccessful if it slipped or could not reach any edge of the panel within two minutes. Otherwise, the ant was considered to have successfully climbed the paint. Adult ant workers were taken from a laboratory colony kept at 24°C, about 120 ants were tested per day. Ten ants were tested on each paint panel; each ant was not used more than three times per day to avoid any adaptive or learning effects [76]. The paint slipperiness was calculated as follows:

$$Paint\ slipperiness\ (\%) = \frac{100 \times number\ of\ unsuccessful\ ants}{number\ of\ tested\ ants} \tag{5.4}$$

To observe ant legs under the SEM, the samples were prepared as follows: immediately after climbing paint surfaces, legs were removed and frozen for 48 hours. Samples were then coated with a 30-nm carbon layer. Control ant samples which had not climbed the paints were observed under SEM to verify that the contaminants present on pads only came from the coatings.

5.2.4 Statistics

When values with distributions are given in the text, they are expressed as mean $\pm$ standard deviation (SD). All data were tested for normal distribution. Pearson's correlations and single t-tests were carried out in Excel 2016 for normally distributed data. Mann–Whitney tests (U-tests) were used for non-parametric data distributions using the online tool Social Science Statistics (available at: `https://www.socscistatistics.com`). All the performed tests were two-tailed; P-values below $\alpha = 0.05$ were interpreted as significant differences.

5.3 Results and discussion

5.3.1 Varying latex particle size

To study the effect of the paint composition on insect attachment, we systematically varied the latex particle size in PVC 60 and PVC 70 paints by modifying either the surfactant amount or the surfactant type in the binder formulation. The calcium carbonate used had a mean diameter of about 1 μm (941 nm $\pm$ 156 nm, $n = 20$, measured *via* SEM) and the paints had an approximate CPVC value of 63% (Eq. 5.3).

Examples of coatings formulated with increasing latex particle size are displayed in Figure 5.5. One can see that increasing the binder particle size also increased the paint porosity in PVC 70 paints (Pearson's $r = 0.83$, $P = 0.006$) (Table 5.2), as also described in literature [62].

We showed in **Chapter 3** that the slipperiness increased with the PVC, but here we did not observe a significant increase, likely because only two PVC values were tested in this study (Table 5.2, $r = 0.32$, $P = 0.196$). At higher PVCs, pigment particles easily detach from the coatings to adhere to the sticky arolia of *A. cephalotes* (Figure 5.6), similarly to what has been observed in the inner wall of pitcher plants [46, 77]. The effect of the PVC on the slipperiness is shown in Figure 5.7.
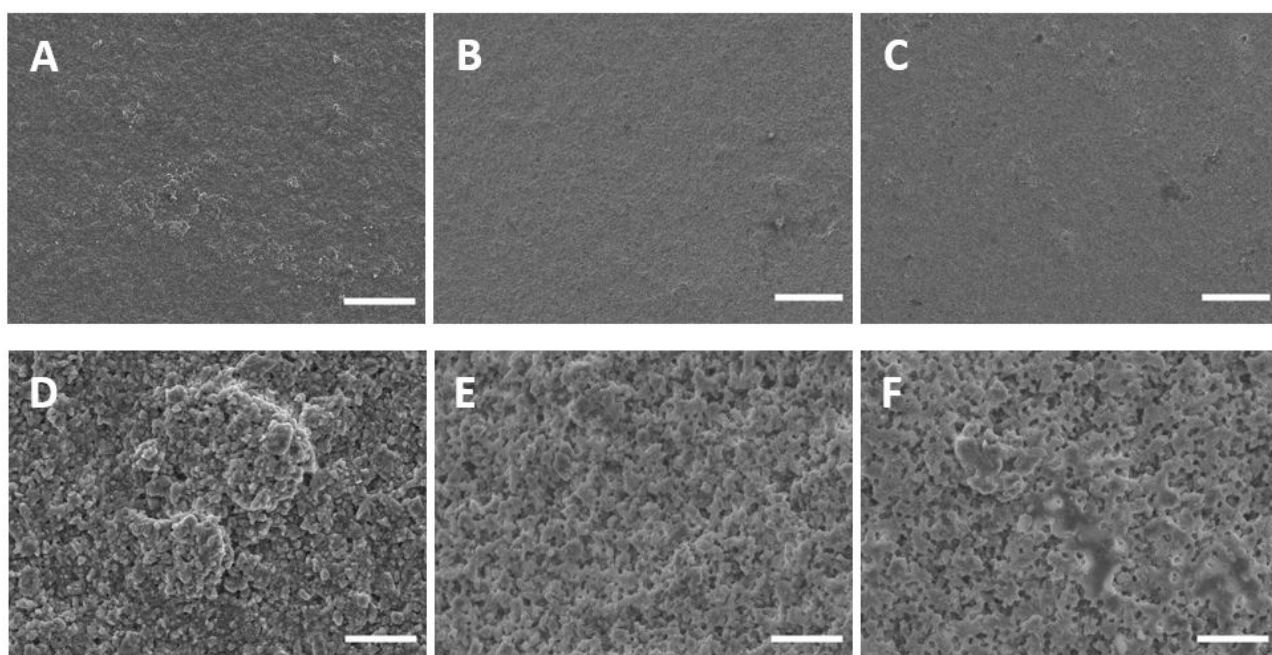

Figure 5.5: SEM images of 70% PVC paint surfaces containing 1 μm CaCO$_3$ particles with varying latex particle size: (A, D) 85 nm, (B, E) 462 nm and (C, F) 805 nm. Scale bars: (A)-(C) 100 μm and (D)-(F) 10 μm.

Table 5.2: Composition, surface roughness, wettability, slipperiness, porosity and scrub resistance values of waterborne paints formulated with increasing latex particle size. The porosity, water uptake and scrub resistance were only measured in PVC 70 paints. Values are expressed as mean ± standard deviation (SD).

Paint	PVC (%)	Latex particle size (nm) ($n = 10$)	R_a (µm) ($n = 6$)	Water contact angle (°) ($n = 4$)	Porosity (%) ($n = 6$)	Water uptake after 7 days (%) ($n = 2$)	Scrub resistance (mg/cm^2) ($n = 2$)	Slipperi-ness (%) ($n = 10$)
1	60	64 ± 2	30.0 ± 15.1	71 ± 1				20 ± 20
2	60	85 ± 2	0.4 ± 0.1	98 ± 1				65 ± 5
3	60	122 ± 1	3.2 ± 0.3	103 ± 1				75 ± 5
4	60	259 ± 2	0.7 ± 0.1	105 ± 3				90 ± 5
5	60	359 ± 3	17.0 ± 1.9	93 ± 6				100 ± 10
6	60	462 ± 28	3.1 ± 0.6	89 ± 5				90 ± 10
7	60	728 ± 5	13.1 ± 0.8	89 ± 3				100 ± 10
8	60	805 ± 26	31.1 ± 10.6	89 ± 2				100 ± 10
9	60	838 ± 23	37.4 ± 2.3	90 ± 2				100 ± 10
10	70	64 ± 2	3.6 ± 1.8	84 ± 2	5.8 ± 0.6	0.13 ± 0.04	5.8 ± 0.6	75 ± 5
11	70	85 ± 2	0.4 ± 0.7	108 ± 1	6.2 ± 0.5	0.25 ± 0.05	7.2 ± 0.7	90 ± 10
12	70	122 ± 1	2.0 ± 1.4	106 ± 2	9.9 ± 3.3	0.23 ± 0.04	7.9 ± 0.8	90 ± 5
13	70	259 ± 2	0.4 ± 0.6	103 ± 1	11.6 ± 2.4	0.26 ± 0.02	6.6 ± 0.7	97.5 ± 4
14	70	359 ± 3	7.3 ± 0.4	93 ± 3	8.3 ± 1.5	0.69 ± 0.09	8.2 ± 1.2	100 ± 10
15	70	462 ± 28	1.6 ± 1.7	90 ± 3	13.7 ± 1.1	0.64 ± 0.10	7.1 ± 1.1	100 ± 10
16	70	728 ± 5	2.2 ± 1.5	90 ± 4	11.6 ± 1.4	0.47 ± 0.10	8.7 ± 0.9	100 ± 10
17	70	805 ± 26	2.2 ± 1.8	89 ± 1	27.9 ± 7.4	0.71 ± 0.10	13.9 ± 0.7	100 ± 10
18	70	838 ± 23	1.4 ± 0.7	93 ± 3	21.6 ± 3.3	0.97 ± 0.09	10.0 ± 0.5	100 ± 10

On the other hand, the slipperiness, the scrub resistance and the surface porosity were found to increase with the latex particle size ($r = 0.61$, $P = 0.007$; $r = 0.76$, $P = 0.017$ and $r = 0.83$, $P = 0.006$, respectively, Figure 5.7 and Table 5.3). The slipperiness reached 100% for latex particles larger than 350 nm, showing that coatings with large binder particles are very effective in preventing ant attachment (Figure 5.7). It has been demonstrated that increasing the latex particle size decreases the Critical Pigment Volume Concentration (CPVC) [62, 64, 66, 78], and hence, increases the surface porosity [62]. Figure 5.5 and Figure 5.7 show indeed that the porosity varied with latex particle size in this paint series. While measuring the experimental CPVC of our paints was beyond the scope of the study, this increased porosity suggests that the CPVC also increased with particle size. Hence, for paints formulated at PVC 60 and 70 in

the presence of 'large' latexes (> 250 nm), the $CaCO_3$ particles are likely not tightly bound so that they transfer easily to the ants' tarsi. This supposition is supported by the higher weight loss values in scrubs tests for larger latexes in PVC 70 paints ($r = 0.76$, $P = 0.017$) (Table 5.2).

It has been hypothesised that the wax in the inner wall of some *Nepenthes* pitcher plants may absorb the insect adhesive secretion (fluid absorption hypothesis) [45]. In addition to the particle detachment mechanism, one can speculate that porous paints ($> 10\%$ porosity) also have the potential to absorb the adhesive fluid. We used a simple indicative test to assess this hypothesis by measuring the water uptake of the PVC 70 paint films. Given the complex nature of the adhesive fluid (whose composition and rheological behaviour are dependent on the insect), water was used as a model fluid for the sake of simplicity, the water uptake being a common test in the coating industry [24, 79–81].
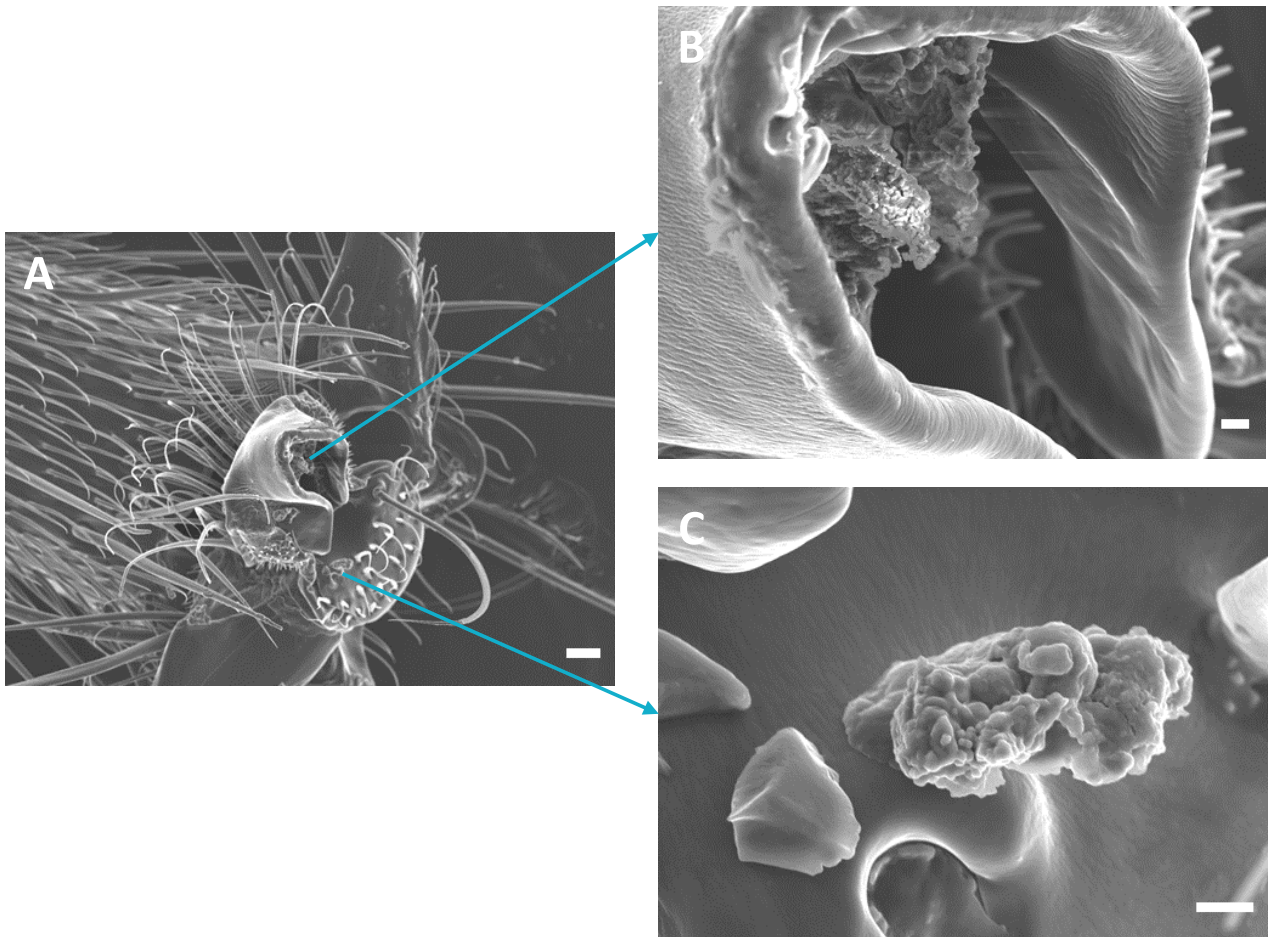

Figure 5.6: SEM images of contaminated *Atta cephalotes* tarsus after climbing paint 12 (122 nm latex). (B) shows bound $CaCO_3$ particles inside the (deflated) arolium and (C) on the manubrium. Scale bars: (A) 10 μm and (B), (C) 1 μm.

Table 5.3: Covariations between variables 1 and 2, correlation coefficient r and P-values obtained by Pearson's correlation tests for the following parameters: the paint PVC, surface roughness (R_a), wettability, slipperiness, surface porosity, water uptake and scrub resistance. Only P-values indicating significant correlations (below $\alpha = 0.05$) have been indicated for more clarity. [a]: the scrub resistance, water uptake and porosity were only measured for PVC 70 paints.

Variable 1	Variable 2	Correlation coefficient r	P-value
Latex particle size	Slipperiness	0.61	0.007
Total surfactant amount	Slipperiness	-0.89	< 0.001
Total surfactant amount	Water contact angle	-0.49	0.037
Total surfactant amount	Latex particle size	-0.60	0.009
Latex particle size	Surface porosity[a]	0.83[a]	0.006[a]
Surface porosity[a]	Scrub resistance[a]	0.89[a]	0.001[a]
Surface porosity[a]	Water uptake[a]	0.72[a]	0.029[a]
Latex particle size	Scrub resistance[a]	0.76[a]	0.017[a]
Latex particle size	Water uptake[a]	0.84[a]	0.005[a]
Water uptake[a]	Slipperiness	-0.60[a]	0.025[a]
PVC	R_a	-0.55	0.019
R_a	Water contact angle	-0.53	0.022

The adhesive secretion was found to be a water-in-oil emulsion for e.g. weaver ants and stick insects, allowing them to adhere to a wide variety of hydrophilic and hydrophobic substrates [24, 82]. The paint coatings were soaked in distilled water for 7 days at 19.1°C $\pm$ 1.9°C and their weight was regularly measured after carefully removing excess water from the panels. The paints absorbed a relatively small amount of water (0.48% $\pm$ 0.27% on average) and the uptake increased with the porosity ($r = 0.72$, $P = 0.029$) (Table 5.2).

Additionally, the paints formulated with larger latexes had less surfactant, hence impacting the surface wettability ($r = $ -0.49, $P = 0.037$) (Table 5.2) as the excess surfactant migrates to the paint/air interface to decrease the surface tension. The slipperiness was found to decrease as larger amounts of surfactant were present in the paints ($r = $ -0.89, P < 0.001), indicating that the adhesive fluid might have spread on the paints.

These results suggest that 'large' (> 250 nm) latex paints are very slippery to insects as their adhesive fluid (1) spreads and (2) gets trapped in the pores more easily (larger and more numerous pores with increasing size). This would lead to a reduction of pad/paint contact as the secretion (1) has been shown to compensate surface roughness by filling in substrate asperities [22–24, 39], (2) has been suggested to ensure rapid pad detachment from surfaces [39, 83] and (3) provides capillary adhesion [49]. Similarly, beetles (hairy pads) have been
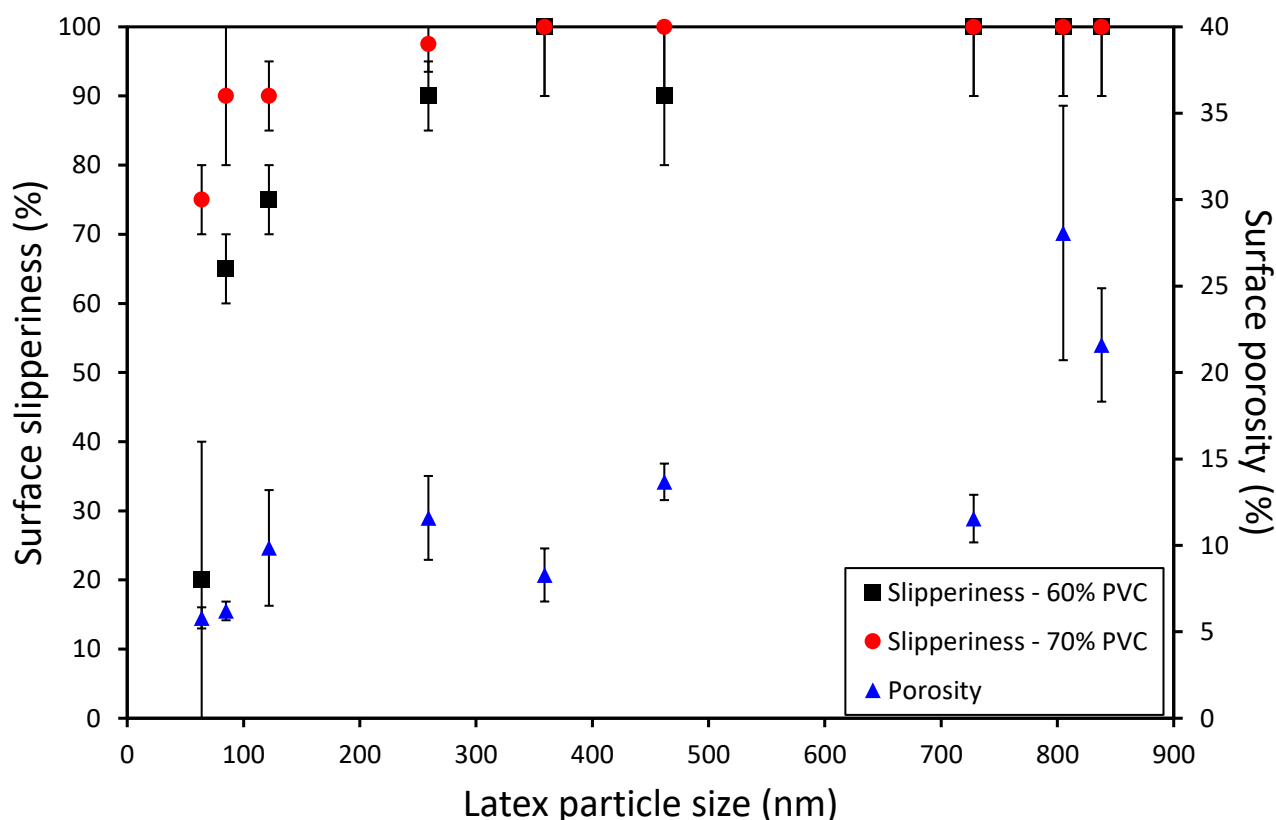
Figure 5.7: Surface slipperiness 60% PVC (black squares), 70% PVC (red circles) and surface porosity (blue triangles) with increasing latex particle size in paints containing 1 μm CaCO$_3$ particles. 100% slipperiness is reached from approximately 700 nm and 350 nm onwards for PVC 60 and 70 paints, respectively. Standard errors for latex particle size are not shown for more clarity and are below 6%.

found to generate lower attachment forces on surfaces with increasing porosity [38]. Gorb *et al.* suggested that the pores could absorb both hydrophilic and hydrophobic liquids [38]. Interestingly, the porosity of clay/latex paper coatings was the lowest at pH 8 in [84], which is also the optimum working pH for Texanol [70], suggesting that porous paints made at slightly lower pH values could become even more slippery.

The slipperiness was neither directly affected by the surface wettability ($r = 0.41$, $P = 0.088$), but rather by the surfactant concentration, nor the surface roughness ($r = -0.20$, $P = 0.418$). The roughness decreased as the PVC increased ($r = -0.55$, $P = 0.019$) as at PVC 60, the paints were close to their CPVC and hence tended to be rougher [61]. While it is commonly accepted that the higher the PVC, the rougher the surface, some coatings exhibited large discrepancies in surface roughness R_a [62, 64, 85]. Macro-roughness defects in paint coatings are likely due to (1) rheological issues, e.g. low flow and levelling, although our paints flowed well enough to be applied to metal panels [62] and (2) due to the formation of pigment/extender aggregates at the surface, despite the dispersant amount was added following the dispersant

demand procedure [68, 69]. This suggests that the slipperiness of surfaces is not only based on roughness average R_a, but also on the lateral dimensions of surface roughness (e.g. asperity spacing and slope) and that optical profilometry could not entirely capture the lateral length scale of the surface roughness (500 nm XY-resolution).

Nano- to micro-rough substrates (asperity size < 3 μm) were shown to minimise insects' attachment forces to surfaces as both claws (and spines) and pads are inefficient at interlocking and developing sufficient contact area with the substrate, respectively [33, 35, 36]. Zhou observed that micro-rough paints were slippery to various insects [75]. This suggests that some other mechanism is at play such as particle detachment or insect adhesive fluid absorption by the pores. Both mechanisms will become more likely as the porosity of the paints increases.

5.3.2   Varying extender pigment size

To study the effect of the extender on insect attachment, we systematically varied the calcium carbonate extender size in PVC 60 and PVC 70 paints formulated with a 64 nm acrylic latex (latex 6, Table 5.1). Using the oil absorption values provided by the supplier, the 14 paints of this study had a mean CPVC of 66% $\pm$ 3% according to Eq. 5.3 (Table 5.4). The PVC 70 coatings showed little porosity (4.3% $\pm$ 2.8% on average, Table 5.5). This indicates that most of the paints at 70% PVC were formulated close to their CPVC [59, 61]. Examples of coatings formulated with increasing extender diameter are displayed in Figure 5.8. Importantly, we did not observe any insect dying after climbing up our paint coatings, as sharp particles have been reported to abrade their cuticle by abrasion [86]. However, several leg samples exposed haemolymph (blood) or damaged arolia under SEM, which probably further impeded the locomotory behaviour of the ants (Figure 5.9).

In this series, the slipperiness was found to be significantly impacted by (1) the extender particle $d_{50\%}$ diameter ($r = $ -0.75, $P = 0.002$, Table 5.6), (2) the surface porosity ($r = 0.95$, $P = 0.001$) and, more surprisingly with regards to our previous studies, by (3) the surface roughness ($r = $ -0.58, $P = 0.029$) (see Table 5.4). The surface wettability did not impact the slipperiness ($r = 0.35$, $P = 0.223$).

In the case of the extender diameter, one can see from Figure 5.10 that the slipperiness increased with the extender size for particles possessing a diameter between 1-10 μm and from then onwards, dramatically decreased to approximately 0%. When considering the $d_{98\%}$ size
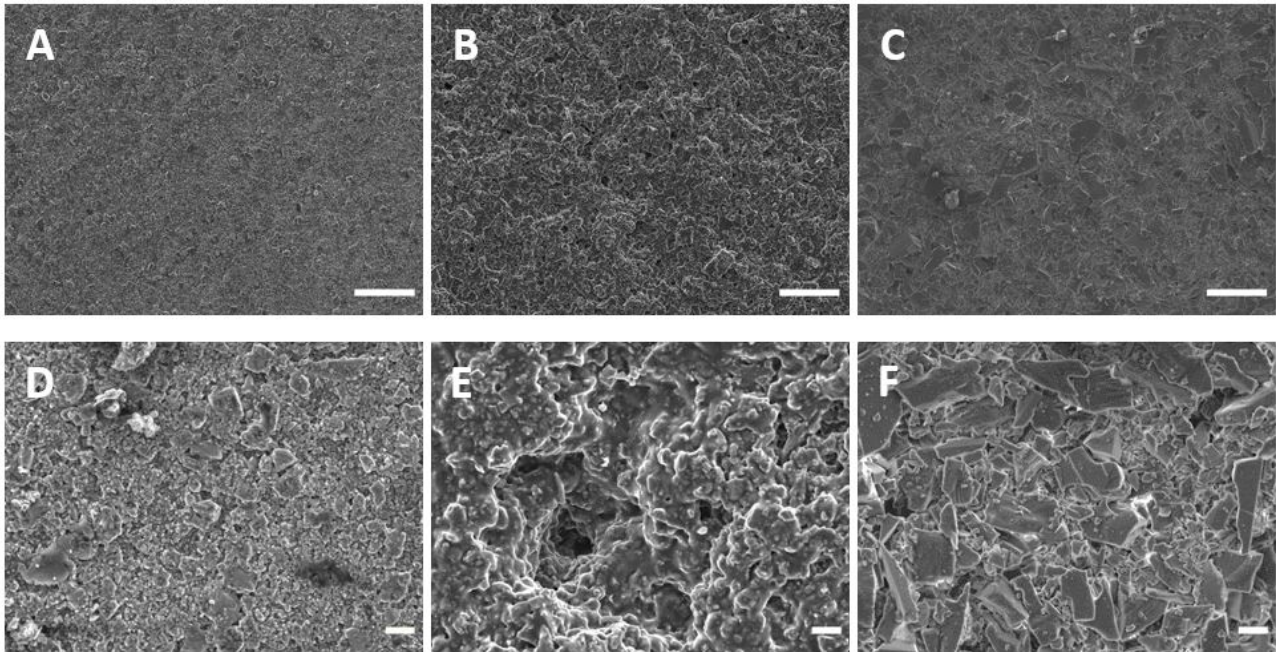
Figure 5.8: SEM images of 70% PVC paint surfaces containing 64 nm latex and varying extender pigment diameter: (A, D) 5 μm, (B, E) 23 μm and (C, F) 40 μm. Scale bars: (A)-(C) 100 μm and (D)-(F) 10 μm.

values rather than the $d_{50\%}$ diameters (98% of particles smaller than the threshold), the slipperiness dramatically decreased from 60 μm onwards (Figure 5.10). We tentatively explain this behaviour by arguing that before reaching the threshold value of 10 μm ($d_{50\%}$), the slipperiness increase is due to larger contaminating particles impeding more efficiently insect locomotion. This is quite an unexpected result as between 0-10 μm, the CPVC increases as the particles get larger (smaller oil absorption values, Eq. 5.3), meaning larger particles should not detach easily at a given PVC.

From 10 μm onwards, our results suggest that most of the particles are too large to adhere to insect arolia, although all the particles we tested are smaller than the basal claw spacing (69 $\pm$ 11 μm, $n = 25$) [30]. This is likely due to ants using their claws to interlock with surface asperities and to increasing pad contact area on larger particles [21, 36]. When considering the $d_{98\%}$ size values, only the smaller particles could adhere to insects' pads, the slipperiness dramatically decreased from 60 μm onwards, which is closer to the basal claw distance.

Our data are in good agreement with the literature with regards to the $d_{50\%}$ pigment diameters: both smooth and hairy pads can remove 1 μm and larger than 45 μm contaminants *via* self-cleaning ('low' slipperiness), while 10-20 μm particles were not removed as easily by hairy pads ('high' slipperiness) [25, 28, 29].

Table 5.4: Composition, surface roughness, wettability and slipperiness values of waterborne paints formulated with increasing extender size. Values are expressed as mean ± standard deviation (SD). [a]: values provided by supplier.

| Paint	PVC (%)	Approx. CPVC (%) (Eq. 5.2)	$d_{50\%}$ size $(\mu m)^a$	$d_{98\%}$ size $(\mu m)^a$	OA $(mL/100g)^a$	R_a (μm) ($n = 6$)	Water contact angle (°) ($n = 4$)	Slipperiness (%) ($n = 10$)
1	60	63	1	5	20.5	30.0 ± 15.1	71 ± 1	20 ± 20
19	60	64	2	12	19	13.0 ± 6.8	52 ± 16	40 ± 10
20	60	68	5	25	16	1.6 ± 0.1	62 ± 10	50 ± 10
21	60	71	10	50	14	2.3 ± 1.3	67 ± 5	75 ± 5
22	60	65	23	60	18	4.9 ± 0.2	84 ± 3	0 ± 10
23	60	69	40	125	15	19.4 ± 9.8	34 ± 9	10 ± 10
24	60	66	45	200	17.6	11.1 ± 1.4	42 ± 15	0 ± 10
10	70	63	1	5	20.5	3.6 ± 1.8	84 ± 2	75 ± 5
25	70	64	2	12	19	9.9 ± 0.7	97 ± 5	73 ± 13
26	70	68	5	25	16	1.8 ± 1.4	67 ± 13	100 ± 5
27	70	71	10	50	14	2.1 ± 0.6	81 ± 14	90 ± 5
28	70	65	23	60	18	6.2 ± 0.4	82 ± 5	20 ± 10
29	70	69	40	125	15	19.5 ± 1.7	68 ± 6	0 ± 10
30	70	66	45	200	17.6	12.2 ± 1.5	72 ± 9	0 ± 10
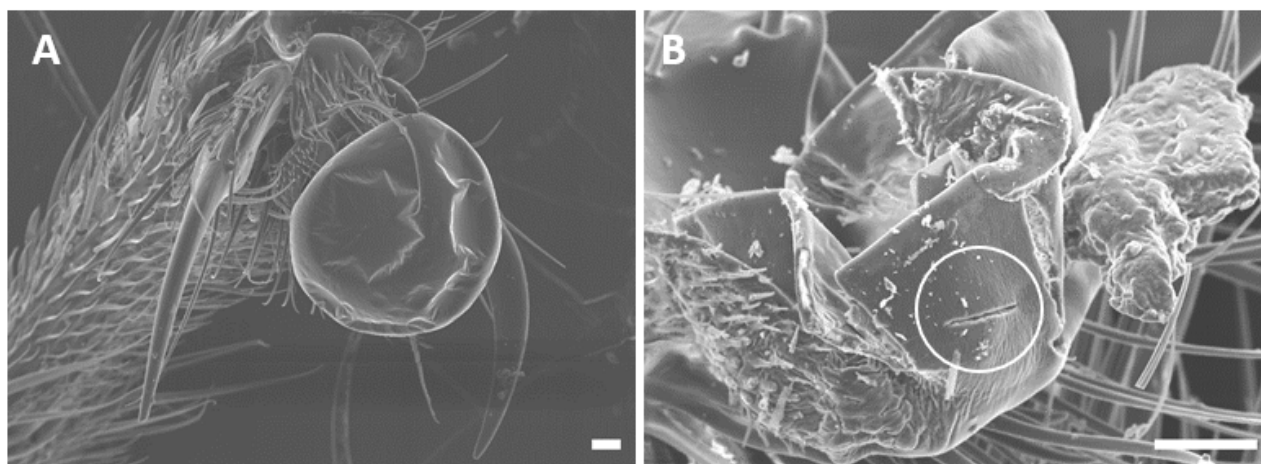
Figure 5.9: SEM images of damaged *A. cephalotes* tarsi after climbing slippery paints. (A) shows that haemolymph (blood) formed on top of the arolium. (B) The contaminated arolium is damaged and a "cut" is highlighted in the circle. Scale bars: 10 μm.

Table 5.5: Composition, surface roughness, wettability and slipperiness values of waterborne paints formulated with increasing extender size. Values are expressed as mean $\pm$ standard deviation (SD).
[a]: values provided by supplier.

Paint	$d_{50\%}$ size $(\mu m)^a$	R_a before scrubs (μm) $(n = 6)$	R_a after scrubs (μm) $(n = 6)$	Porosity (%) $(n = 6)$	Water uptake after 7 days (%) $(n = 2)$	Scrub resistance (mg/cm^2) $(n = 2)$	Slipperiness before scrubs (%) $(n = 10)$	Slipperiness after scrubs (%) $(n = 10)$
10	1	3.6 ± 1.8	13.6 ± 2.4	5.8 ± 0.6	0.13 ± 0.04	5.8 ± 0.6	75 ± 5	100 ± 10
25	2	9.9 ± 0.7	7.4 ± 6.1	7.4 ± 2.4	0.21 ± 0.01	1.7 ± 0.1	73 ± 13	100 ± 10
26	5	1.8 ± 1.4	2.2 ± 0.4	7.8 ± 1.7	0.11 ± 0.09	2.2 ± 0.4	100 ± 5	100 ± 10
27	10	2.1 ± 0.6	5.4 ± 1.5	5.2 ± 1.0	0.15 ± 0.04	1.7 ± 0.2	90 ± 5	100 ± 10
28	23	6.2 ± 0.4	19.0 ± 3.9	2.0 ± 0.4	0.44 ± 0.17	1.4 ± 0.04	20 ± 10	30 ± 5
29	40	19.5 ± 1.7	4.8 ± 1.6	1.1 ± 0.4	1.32 ± 0.76	1.0 ± 0.2	0 ± 10	90 ± 5
30	45	12.2 ± 1.5	116.7 ± 39.1	0.5 ± 0.2	0.52 ± 0.21	1.9 ± 0.2	0 ± 10	80 ± 10
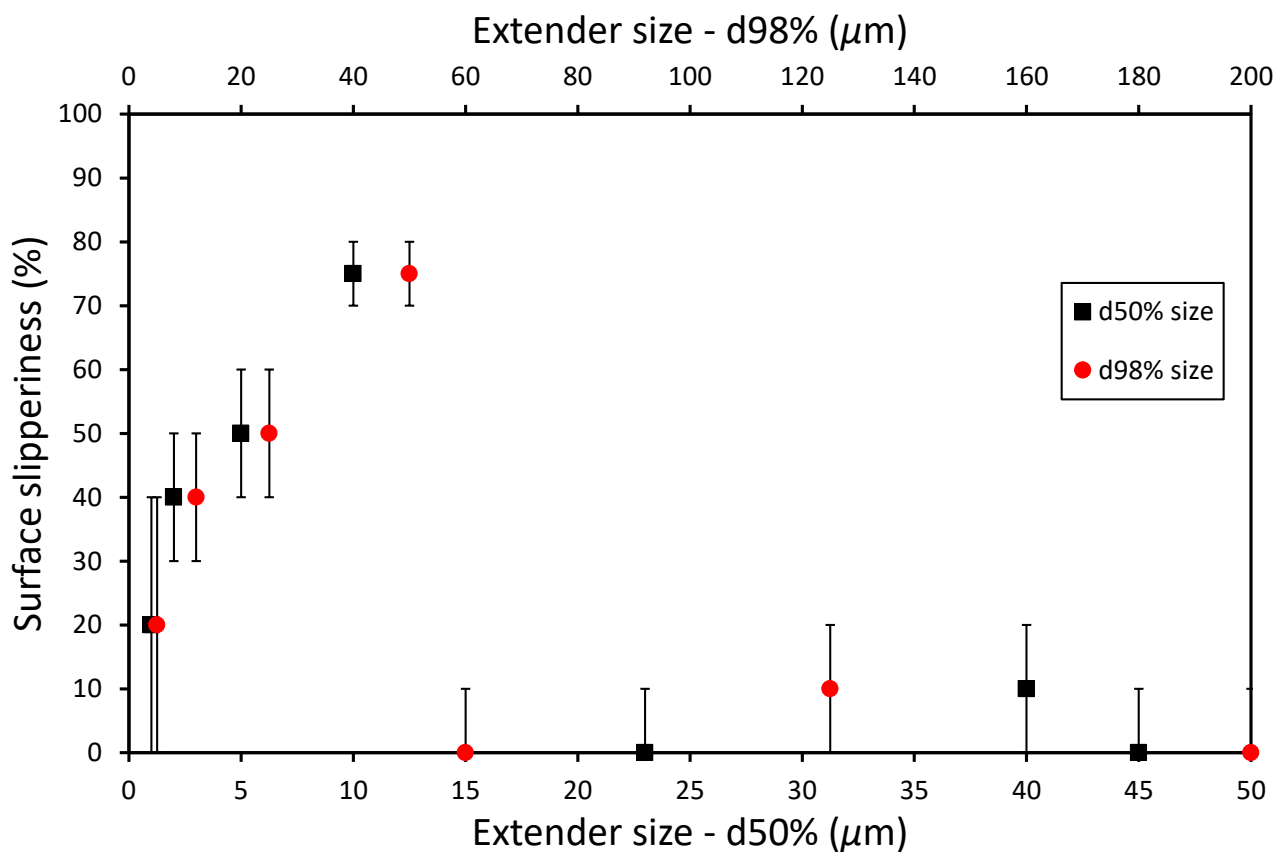
Figure 5.10: Surface slipperiness as a function of the extender pigment diameter $d_{50\%}$ (black squares) and $d_{98\%}$ (red circles) for PVC 60 paints. From 10 μm onwards, the slipperiness decreased dramatically as the particles become too large to adhere to insect pads.

As observed in the study with varying latex size, the slipperiness was found to increase with the surface porosity ($r = 0.95$, $P = 0.001$) (Table 5.4). The variations in both porosity and slipperiness with the extender size were indeed similar ($P = 0.002$ for both, 5.6), as the porosity increased for sizes between 1 and 5 μm and decreased from 10 μm onwards. Again, the presence of pores may have increased the slipperiness as the insects' adhesive secretion is absorbed by the voids. The paints absorbed a relatively small amount of water (0.41% ± 0.40% on average); however, the uptake was negatively correlated to the slipperiness ($r = $ -0.80, $P = 0.032$), suggesting that the pores might not absorb enough fluid to provide slipperiness and that liquid absorption was not the cause for slipperiness in these paints.

The other parameter to significantly impact the paint slipperiness was the surface roughness ($r = $ -0.58, $P = 0.029$, Table 5.6). Apart from the paints formulated with 1 μm and 19 μm CaCO$_3$ particles, Mann-Whitney tests showed that roughness did not significantly change with the PVC for a given extender particle size (Mann–Whitney, $U_{6,6} > 5$, P> 0.05) and was not impacted by the $d_{50\%}$ extender sizes ($r = 0.27$, $P = 0.353$). The slipperiness was found to decrease for increasing roughness values (Figure 5.11), with highest slipperiness values obtained for roughness values, R_a, smaller than 5 μm for both PVCs. Although non-significant for $\alpha = 0.05$, R_a and the extender diameter exhibited a strong linear correlation for the PVC 70 paints ($r = 0.75$, $P = 0.054$).

Table 5.6: Covariations between variables 1 and 2, correlation coefficient r and P-values obtained by Pearson's correlation tests for the following parameters: the paint PVC, surface roughness (R_a), wettability, slipperiness, surface porosity, water uptake. Only P-values indicating significant correlations (below $\alpha = 0.05$) have been indicated for more clarity. [a]: the porosity and water uptake were only measured for PVC 70 paints.

Variable 1	Variable 2	Correlation coefficient r	P-value
PVC	Water contact angle	0.59	0.025
Extender size	Slipperiness	-0.75	0.002
Extender size	Water uptake[a]	0.78[a]	0.039[a]
Extender size	Surface porosity[a]	-0.94[a]	0.002[a]
R_a	Slipperiness	-0.58	0.029
R_a	Water uptake[a]	0.91[a]	0.005[a]
Surface porosity[a]	Slipperiness	0.95[a]	0.001[a]
Water uptake[a]	Slipperiness	-0.80[a]	0.032[a]
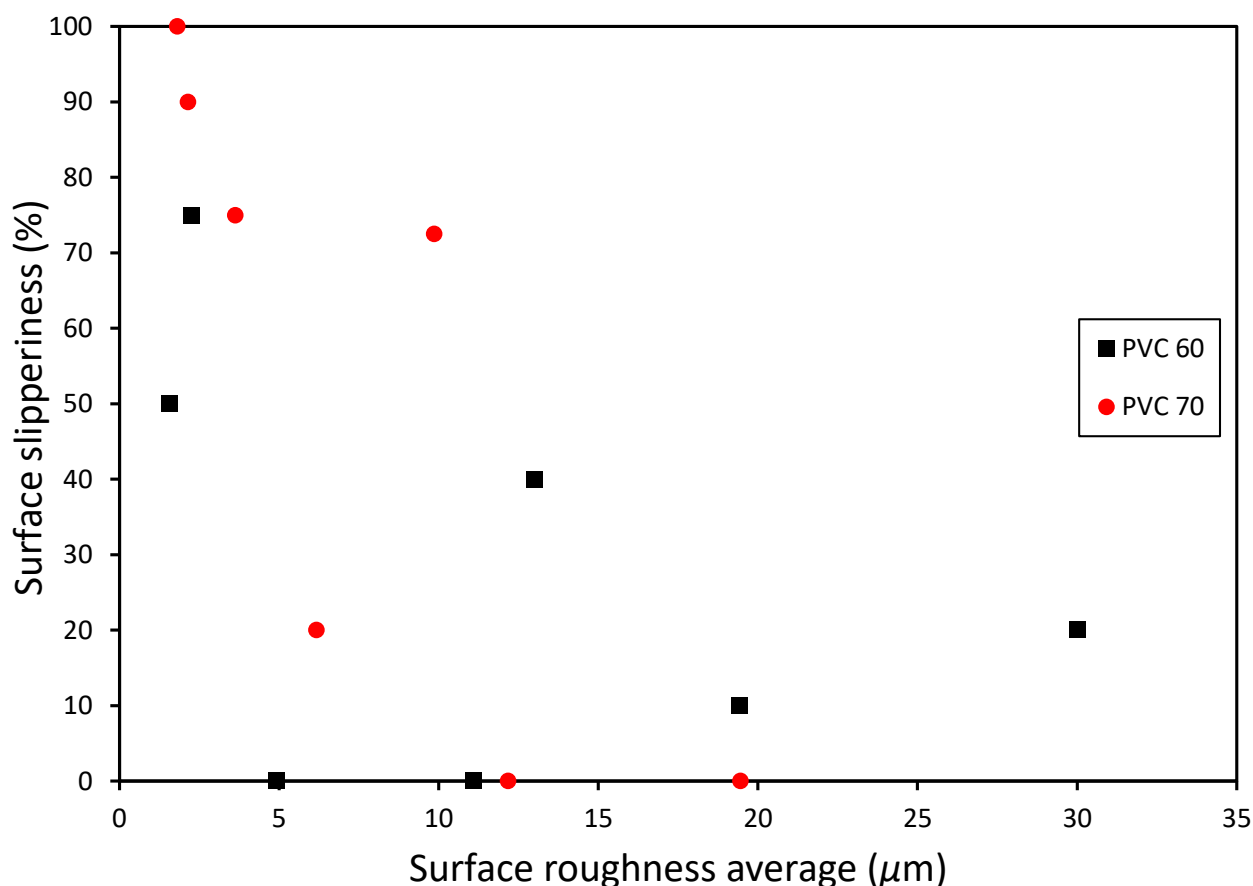
Figure 5.11: Surface slipperiness as a function of the surface roughness. For both PVC values (60% (black squares) and 70% (red circles)), the paint slipperiness was found to decrease with the roughness. The dashed line shows the *Atta cephalotes* claw tip diameter, 5.0 ± 1.7 μm ($n = 31$). Error bars were not included for more clarity.

We can hence approximate that the extender and asperity sizes were similar. Such a correlation was not observed in 60% PVC paints as paints containing 1 μm and 2 μm exhibited large R_a values (> 10 μm). The slipperiness data follow the literature well as (1) 'microrough' surfaces (asperity size < 3 μm) minimise the attachment of insects [33, 36], and (2) claws can cling to protrusions larger than the claw tip diameter, which we measured as 5.0 ± 1.7 μm ($n = 31$) for *A. cephalotes* [36, 37]. Since we did not find similar results in our previous studies from **Chapter 3** or when varying the latex particle size in section 1, this suggests that slipperiness is not only due to particle detachment when using extenders of different diameters. In fact, we surprisingly found *via* SEM that some $CaCO_3$ particles adhered to ant pads after they walked on low slipperiness paints (> 23 μm particles, data not shown).

One can see from Table 5.5 that for the PVC 70 paints, the scrub resistance did not affect the slipperiness ($r = 0.33$, $P = 0.411$). Except for paint 10 (1 μm particles), all scrub resistance values were similar and relatively low (1.6 ± 0.4 mg/cm^2), suggesting that the particles were

well bound to the paint coatings, which supports the impact of the surface roughness on the slipperiness of the unscrubbed paints. After being scrubbed to 2000 cycles, all 70% PVC paints showed an increase in slipperiness, in particular for the paints formulated with 40 and 45 μm CaCO$_3$ particles (Table 5.5). This indicates that once the layer of well bound particles was rubbed off, the particles present in the remaining film were looser and could transfer to insect pads. A dramatic increase in the surface roughness was observed for most of the paints, which did not impact the slipperiness for the scrubbed paints (r = -0.20, P = 0.188). The slipperiness of the scrubbed paint with 23 μm particles was only 30% as SEM revealed that they were still well bound by the polymer.

5.4   Conclusions

By formulating paints with acrylic binders and CaCO$_3$ pigments of varying size, we have shown that paints can prevent *Atta cephalotes* ants from climbing up vertical paint panels:

1. For paints containing latexes of varying size prepared by tailoring the amount of surfactant, the slipperiness increased with the latex particle size, which also increased the surface porosity. This is consistent with both detaching particles and adhesive fluid-absorbing pores impeding insect locomotion, hence rendering the surfaces slippery. In the presence of 1 μm CaCO$_3$ particles, the use of 'large' latexes ($>$ 250 nm) was necessary to obtain extremely slippery coatings. However, a balance between porosity, water permeability, opacity and scrub resistance is needed for optimal paint performance.

2. Paints formulated with different diameters of CaCO$_3$ particles presented an increase of slipperiness with extenders sized between 1-10 μm ($d_{50\%}$ values), and then a decrease from 10 μm onwards. Here, the slipperiness was found to be mainly due to a combination between particle detachment and surface roughness. For paints formulated with larger extenders, the slipperiness is mainly attributed to surface roughness, as the scrub resistance experiments supported that the particles were well bound to the coatings. SEM also showed that ants climbing low slipperiness paints exhibited some extender pigment on their arolia.

Such paints open the field for novel, low insect-adhesion coatings. By increasing the latex particle size, and hence decreasing the CPVC, we showed that it is possible to obtain very

slippery coatings. This is of particular interest for outdoor applications, where it is common practice in the coating industry to use PVC values ranging between 40% and 50%. For large enough latexes, PVC 60 paints can be used to obtain slippery enough coatings. Although weathering-resistant, large PVC paints exposing many calcium carbonate particles at their surface could be problematic as the extender could potentially react with the acid rains, found in the geographic areas of interest for our insect-slippery paints (e.g. Southeast Asia) [58, 87], or be inefficient due to humidity as observed in slippery PTFE-coatings [88]. The coatings were however surprisingly resistant to water absorbance. Further research could include on one hand the use of more additives to get closer to "real" paint systems, using e.g. thickeners, which would be expected to reduce pigment aggregation and hence, the surface roughness of the coatings; or fungicide and/or algicide to prevent organic growth on the film [3].

Acknowledgements

References

[1] Ghosh, S. K. (2006) Functional Coatings and Microencapsulation: A General Perspective, Wiley-VCH Verlag GmbH & Co. KGaA, Weinheim, FRG.

[2] Streitberger, H. and Dossel, K. (2008) Automotive Paints and Coatings, Wiley-VCH Verlag GmbH & Co. KGaA, Weinheim, Germany.

[3] Lambourne, R. and Strivens, T. A. (1999) Paint and Surface Coatings, Woodhead Publishing, Cambridge 2nd edition.

[4] Oerke, E.-C. (2006) Crop losses to pests. *J. Agric. Sci.,* **144**, 31–43.

[5] Ghaly, A. and Edwards, S. (2011) Termite Damage to Buildings: Nature of Attacks and Preventive Construction Methods. *Am. J. Eng. Appl. Sci.,* **4**(2), 187–200.

[6] Greenwood, B. M., Fidock, D. A., Kyle, D. E., Kappe, S. H. I., Alonso, P. L., Collins, F. H., and Duffy, P. E. (2008) Malaria: progress, perils, and prospects for eradication. *J. Clin. Invest.,* **118**(4), 1266–1276.

[7] Bonnefoy, X., Kampen, H., and Sweene, K. (2008) Public health significance of urban pests, World Health Organization, Copenhagen.

[8] Su, N.-Y. and Scheffrahn, R. H. (2000) Termites as Pests of Buildings, Springer Netherlands, Dordrecht.

[9] Mahapatro, G. K. and Chatterjee, D. (2018) Termites as Structural Pest: Status in Indian Scenario. *Proc. Natl. Acad. Sci. India Sect. B Biol. Sci.,* **88**(3), 977–994.

[10] Birkemoe, T. (2002) Structural infestations of ants (Hymenoptera, Formicidae) in southern Norway. **49**(2), 139–142.

[11] Oi, D. H., Vail, K. M., Williams, D. F., and Bieman, D. N. (1994) Indoor and Outdoor Foraging Locations of Pharaoh Ants (Hymenoptera: Formicidae) and Control Strategies Using Bait Stations. *Florida Entomol.,* **77**(1), 85.

[12] Lee, C. Y. (2002) Tropical household ants: pest status, species diversity, foraging behavior and baiting studies. *Proc. Fourth Int. Conf. Urban Pests,* pp. 3–18.

[13] Maloney, K. M., Ancca-Juarez, J., Salazar, R., Borrini-Mayori, K., Niemierko, M., Yukich, J. O., Naquira, C., Keating, J. A., and Levy, M. Z. (2013) Comparison of insecticidal paint and deltamethrin against *Triatoma infestans* (Hemiptera: Reduviidae) feeding and mortality in simulated natural conditions. *J. Vector Ecol.,* **38**(1), 6–11.

[14] Mosqueira, B., Chabi, J., Chandre, F., Akogbeto, M., Hougard, J.-M., Carnevale, P., and Mas-Coma, S. (2010) Efficacy of an insecticide paint against malaria vectors and nuisance in West Africa - Part 2: Field evaluation. *Malar. J.,* **9**(1), 341.

[15] Pimentel, D. (2005) Environmental and economic costs of the application of pesticides primarily in the United States. *Environ. Dev. Sustain.,* **7**(2), 229–252.

[16] Devine, G. J. and Furlong, M. J. (2007) Insecticide use: Contexts and ecological consequences. *Agric. Human Values,* **24**(3), 281–306.

[17] Overman, G. R. Method for admixing plant essential oils to coatings for the purpose of repelling insects. (2009) US Patent 20090155394.

[18] Wong, T.-S., Kang, S. H., Tang, S. K. Y., Smythe, E. J., Hatton, B. D., Grinthal, A., and Aizenberg, J. (2011) Bioinspired self-repairing slippery surfaces with pressure-stable omniphobicity. *Nature,* **477**(7365), 443–447.

[19] Boiteau, G., Pelletier, Y., Misener, G. C., and Bernard, G. (1994) Development and Evaluation of a Plastic Trench Barrier for Protection of Potato from Walking Adult Colorado Potato Beetles (Coleoptera: Chrysomelidae). *J. Econ. Entomol.,* **87**(5), 1325–1331.

[20] Féat, A., Federle, W., Kamperman, M., and van der Gucht, J. (2019) Coatings preventing insect adhesion: An overview. *Prog. Org. Coatings,* **134**, 349–359.

[21] Gorb, S. N. (2002) Attachment Devices of Insect Cuticle, Kluwer Academic Publishers, Dordrecht.

[22] Bullock, J. M. R., Drechsler, P., and Federle, W. (2008) Comparison of smooth and hairy attachment pads in insects: friction, adhesion and mechanisms for direction-dependence. *J. Exp. Biol.,* **211**(20), 3333–3343.

[23] Drechsler, P. and Federle, W. (2006) Biomechanics of smooth adhesive pads in insects: Influence of tarsal

secretion on attachment performance. *J. Comp. Physiol. A,* **192**(11), 1213–1222.

[24] Dirks, J.-H. and Federle, W. (2011) Fluid-based adhesion in insects - principles and challenges. *Soft Matter,* **7**(23), 11047.

[25] Clemente, C. J., Bullock, J. M. R., Beale, A., and Federle, W. (2010) Evidence for self-cleaning in fluid-based smooth and hairy adhesive systems of insects. *J. Exp. Biol.,* **213**(4), 635–642.

[26] Clemente, C. J. and Federle, W. (2012) Mechanisms of self-cleaning in fluid-based smooth adhesive pads of insects. *Bioinspir. Biomim.,* **7**(4), 46001.

[27] Amador, G. J. and Hu, D. L. (2015) Cleanliness is next to godliness: mechanisms for staying clean. *J. Exp. Biol.,* **218**(20), 3164–3174.

[28] Orchard, M. J., Kohonen, M., and Humphries, S. (2012) The influence of surface energy on the self-cleaning of insect adhesive devices. *J. Exp. Biol.,* **215**(2), 279–286.

[29] Amador, G. J., Endlein, T., and Sitti, M. (2017) Soiled adhesive pads shear clean by slipping: a robust self-cleaning mechanism in climbing beetles. *J. R. Soc. Interface,* **14**(131), 20170134.

[30] Anyon, M. J., Orchard, M. J., Buzza, D. M. A., Humphries, S., and Kohonen, M. M. (2012) Effect of particulate contamination on adhesive ability and repellence in two species of ant (Hymenoptera; Formicidae). *J. Exp. Biol.,* **215**(4), 605–616.

[31] Mengüç, Y., Röhrig, M., Abusomwan, U., Hölscher, H., and Sitti, M. (2014) Staying sticky: contact self-cleaning of gecko-inspired adhesives. *J. R. Soc. Interface,* **11**(94), 20131205–20131205.

[32] Ditsche-Kuru, P., Barthlott, W., and Koop, J. H. E. (2012) At which surface roughness do claws cling? Investigations with larvae of the running water mayfly *Epeorus assimilis* (Heptageniidae, Ephemeroptera). *Zoology,* **115**(6), 379–388.

[33] Voigt, D., Schuppert, J. M., Dattinger, S., and Gorb, S. N. (2008) Sexual dimorphism in the attachment ability of the Colorado potato beetle *Leptinotarsa decemlineata* (Coleoptera: Chrysomelidae) to rough substrates. *J. Insect Physiol.,* **54**(5), 765–776.

[34] Gorb, E. and Gorb, S. (2009) Effects of surface topography and chemistry of *Rumex obtusifolius* leaves on the attachment of the beetle *Gastrophysa viridula. Entomol. Exp. Appl.,* **130**(3), 222–228.

[35] Scholz, I., Buckins, M., Dolge, L., Erlinghagen, T., Weth, A., Hischen, F., Mayer, J., Hoffmann, S., Riederer, M., Riedel, M., and Baumgartner, W. (2010) Slippery surfaces of pitcher plants: *Nepenthes* wax crystals minimize insect attachment *via* microscopic surface roughness. *J. Exp. Biol.,* **213**(7), 1115–1125.

[36] Bullock, J. M. R. and Federle, W. (2011) The effect of surface roughness on claw and adhesive hair performance in the dock beetle *Gastrophysa viridula. Insect Sci.,* **18**(3), 298–304.

[37] Dai, Z., Gorb, S. N., and Schwarz, U. (2002) Roughness-dependent friction force of the tarsal claw system in the beetle *Pachnoda marginata* (Coleoptera, Scarabaeidae). *J. Exp. Biol.,* **205**, 2479–2488.

[38] Gorb, E. V., Hosoda, N., Miksch, C., and Gorb, S. N. (2010) Slippery pores: anti-adhesive effect of nanoporous substrates on the beetle attachment system. *J. R. Soc. Interface,* **7**(52), 1571–1579.

[39] Betz, O., Frenzel, M., Steiner, M., Vogt, M., Kleemeier, M., Hartwig, A., Sampalla, B., Rupp, F., Boley, M., and Schmitt, C. (2017) Adhesion and friction of the smooth attachment system of the cockroach

Gromphadorhina portentosa and the influence of the application of fluid adhesives. *Biol. Open,* **6**(5), 589–601.

[40] Orivel, J., Malherbe, M. C., and Dejean, A. (2001) Relationships between pretarsus morphology and arboreal life in ponerine ants of the genus *Pachycondyla* (Formicidae: Ponerinae). *Ann. Entomol. Soc. Am.,* **94**(1), 449–456.

[41] Bußhardt, P., Kunze, D., and Gorb, S. N. (2014) Interlocking-based attachment during locomotion in the beetle *Pachnoda marginata* (Coleoptera, Scarabaeidae). *Sci. Rep.,* **4**(6998).

[42] England, M. W., Sato, T., Yagihashi, M., Hozumi, A., Gorb, S. N., and Gorb, E. V. (2016) Surface roughness rather than surface chemistry essentially affects insect adhesion. *Beilstein J. Nanotechnol.,* **7**(1), 1471–1479.

[43] Prüm, B., Florian Bohn, H., Seidel, R., Rubach, S., and Speck, T. (2013) Plant surfaces with cuticular folds and their replicas: Influence of microstructuring and surface chemistry on the attachment of a leaf beetle. *Acta Biomater.,* **9**(5), 6360–6368.

[44] Grohmann, C., Blankenstein, A., Koops, S., and Gorb, S. N. (2014) Attachment of *Galerucella nymphaeae* (Coleoptera, Chrysomelidae) to surfaces with different surface energy. *J. Exp. Biol.,* **217**(23), 4213–4220.

[45] Gorb, S. N. (2010) Biological and biologically inspired attachment systems, Springer Berlin Heidelberg, Berlin, Heidelberg.

[46] Gorb, E., Haas, K., Henrich, A., Enders, S., Barbakadze, N., and Gorb, S. (2005) Composite structure of the crystalline epicuticular wax layer of the slippery zone in the pitchers of the carnivorous plant *Nepenthes alata* and its effect on insect attachment. *J. Exp. Biol.,* **208**(24), 4651–4662.

[47] Koch, K., Bhushan, B., and Barthlott, W. (2010) Multifunctional plant surfaces and smart materials, Springer, Würzburg.

[48] Gorb, E. V., Baum, M. J., and Gorb, S. N. (2013) Development and regeneration ability of the wax coverage in *Nepenthes alata* pitchers: a cryo-SEM approach. *Sci. Rep.,* **3**.

[49] Gorb, E. V. and Gorb, S. N. (2017) Anti-adhesive effects of plant wax coverage on insect attachment. *J. Exp. Bot.,* **68**(19), 5323–5337.

[50] Bohn, H. F. and Federle, W. (2004) Insect aquaplaning: *Nepenthes* pitcher plants capture prey with the peristome, a fully wettable water-lubricated anisotropic surface. *Proc. Natl. Acad. Sci.,* **101**(39), 14138–14143.

[51] Gorb, E. and Gorb, S. (2002) Attachment ability of the beetle *Chrysolina fastuosa* on various plant surfaces. *Entomol. Exp. Appl.,* **105**(1), 13–28.

[52] Hansen, M. K., Larsen, M., and Cohr, K.-H. (1987) Waterborne paints: A review of their chemistry and toxicology and the results of determinations made during their use. *Scand. J. Work. Environ. Health,* **13**(6), 473–485.

[53] Mariz, I. d. F. A., Millichamp, I. S., de la Cal, J. C., and Leiza, J. R. (2010) High performance water-borne paints with high volume solids based on bimodal latexes. *Prog. Org. Coatings,* **68**(3), 225–233.

[54] Sperry, P. R., Snyder, B. S., O'Dowd, M. L., and Lesko, P. M. (1994) Role of water in particle deformation

and compaction in latex film formation. *Langmuir,* **10**(8), 2619–2628.

[55] Steward, P. A., Hearn, J., and Wilkinson, M. C. (2000) An overview of polymer latex film formation and properties. *Adv. Colloid Interface Sci.,* **86**(3), 195–267.

[56] Scholz, W. (1993) Paint Additives, Springer Science+Business Media, Dordrecht.

[57] Adams, J. M. (1993) Particle size and shape effects in materials science: examples from polymer and paper systems. *Clay Miner.,* **28**(4), 509–530.

[58] Broad, R., Power, G., and Sonego, A. (1993) Extender Pigments, Springer Netherlands, Dordrecht.

[59] Asbeck, W. K. and Loo, M. V. (1949) Critical Pigment Volume Relationships.. *Ind. Eng. Chem.,* **41**(7), 1470–1475.

[60] Keddie, J. L. (1997) Film formation of latex. *Mater. Sci. Eng. R Reports,* **21**(3), 101–170.

[61] Wang, J., Xu, H., Battocchi, D., and Bierwagen, G. (2014) The determination of critical pigment volume concentration (CPVC) in organic coatings with fluorescence microscopy. *Prog. Org. Coatings,* **77**(12), 2147–2154.

[62] del Rio, G. and Rudin, A. (1996) Latex particle size and CPVC. *Prog. Org. Coatings,* **28**(4), 259–270.

[63] Rodríguez, M. T., Gracenea, J. J., Kudama, A. H., and Suay, J. J. (2004) The influence of pigment volume concentration (PVC) on the properties of an epoxy coating: Part I. Thermal and mechanical properties. *Prog. Org. Coatings,* **50**(1), 62–67.

[64] Alvarez, V. and Paulis, M. (2017) Effect of acrylic binder type and calcium carbonate filler amount on the properties of paint-like blends. *Prog. Org. Coatings,* **112**, 210–218.

[65] Miura, M. and Kodama, M. (1972) The Second CMC of the Aqueous Solution of Sodium Dodecyl Sulfate. I. Conductivity. *Bull. Chem. Soc. Jpn.,* **45**(2), 428–431.

[66] Ding, T., Daniels, E. S., El-Aasser, M. S., and Klein, A. (2005) Film Formation from Pigmented Latex Systems: Mechanical and Surface Properties of Ground Calcium Carbonate/Functionalized Poly (*n*-butyl methacrylate-*co-n*-butyl acrylate) Latex Blend Films. *J. Appl. Polym. Sci.,* **100**(6), 4550–4560.

[67] Daniels, Christian Leonard Gruber, B. High solids pigmented latex compositions. US Patent 20120234490.

[68] Davies, J. and Binner, J. G. P. (2000) The role of ammonium polyacrylate in dispersing concentrated alumina suspensions. *J. Eur. Ceram. Soc.,* **20**(10), 1539–1553.

[69] Baklouti, S., Romdhane, M. R. B., Boufi, S., Pagnoux, C., Chartier, T., and Baumard, J. F. (2003) Effect of copolymer dispersant structure on the properties of alumina suspensions. *J. Eur. Ceram. Soc.,* **23**(6), 905–911.

[70] Lohmeijer, B., Balk, R., and Baumstark, R. (2012) Preferred partitioning: the influence of coalescents on the build-up of mechanical properties in acrylic core-shell particles (I). *J. Coatings Technol. Res.,* **9**(4), 399–409.

[71] Segmentation - ImageJ. `https://imagej.net/Segmentation` (accessed 18.11.2018).

[72] Haeri, M. and Haeri, M. (2015) ImageJ Plugin for Analysis of Porous Scaffolds used in Tissue Engineering. *J. Open Res. Softw.,* **3**, 500–512.

[73] Brunauer, S., Emmett, P. H., and Teller, E. (1938) Adsorption of Gases in Multimolecular Layers. *J. Am.*

Chem. Soc., **60**(2), 309–319.

[74] Bauer, U. and Federle, W. (2009) The insect-trapping rim of *Nepenthes* pitchers. *Plant Signal. Behav.,* **4**(11), 1019–1023.

[75] Zhou, Y. (2015) Insect adhesion on rough surfaces and properties of insect repellent surfaces (PhD thesis), University of Cambridge, Cambridge.

[76] Dukas, R. (2008) Evolutionary Biology of Insect Learning. *Annu. Rev. Entomol.,* **53**(1), 145–160.

[77] Koch, K., Dommisse, A., Barthlott, W., and Gorb, S. N. (2007) The use of plant waxes as templates for micro- and nanopatterning of surfaces. *Acta Biomater.,* **3**(6), 905–909.

[78] Ding, T., Daniels, E. S., El-Aasser, M. S., and Klein, A. (2006) Film Formation from Pigmented Latex Systems: Drying Kinetics and Bulk Morphologies of Ground Calcium Carbonate/Functionalized Poly (*n*-butyl methacrylate-*co-n*-butyl acrylate) Blend Films. *J. Appl. Polym. Sci.,* **100**(3), 2267–2277.

[79] Dirks, J.-H., Clemente, C. J., and Federle, W. (2010) Insect tricks: two-phasic foot pad secretion prevents slipping.. *J. R. Soc. Interface,* **7**, 587–593.

[80] Peisker, H., Heepe, L., Kovalev, A. E., and Gorb, S. N. (2014) Comparative study of the fluid viscosity in tarsal hairy attachment systems of flies and beetles. *J. R. Soc. Interface,* **11**(99), 20140752.

[81] Reitz, M., Gerhardt, H., Schmitt, C., Betz, O., Albert, K., and Lammerhofer, M. (2015) Analysis of chemical profiles of insect adhesion secretions by gas chromatography-mass spectrometry. *Anal. Chim. Acta,* **854**, 47–60.

[82] Gorb, S. N. (2007) Smooth Attachment Devices in Insects: Functional Morphology and Biomechanics, Vol. 34, , .

[83] Labonte, D. and Federle, W. (2015) Rate-dependence of 'wet' biological adhesives and the function of the pad secretion in insects. *Soft Matter,* **11**(44), 8661–8673.

[84] Alince, B. and Lepoutre, P. (1980) Porosity and optical properties of clay coatings. *J. Colloid Interface Sci.,* **76**(2), 439–444.

[85] Tang, J., Daniels, E. S., Dimonie, V. L., Klein, A., and El-Aasser, M. S. (2002) Influence of particle surface properties on film formation from precipitated calcium carbonate/latex blends. *J. Appl. Polym. Sci.,* **86**(4), 891–900.

[86] Hackmann, A. (2015) Contamination and biomechanics of cleaning structures in insects (PhD thesis), University of Cambridge, Cambridge.

[87] Balik, C. M. and Xu, J. R. (1994) Simultaneous measurement of water diffusion, swelling, and calcium carbonate removal in a latex paint using FTIR-ATR. *J. Appl. Polym. Sci.,* **52**(7), 975–983.

[88] Hölldobler, B. and Wilson, E. (1990) The Ants, Harvard University Press, Cambridge.

6

Linseed oil-based emulsions to protect plants against thrips

Many species of thrips (order: Thysanoptera) damage crops by feeding on them but mainly through the transmission of viral diseases. Inspired from the sticky trichomes which provide certain plants a defence against insects, we have formulated emulsified sticky crosslinked linseed oil beads, which can be sprayed on plants. Performances of the adhesive beads were visually assessed by spraying the emulsions on glass slides and covering them with sand, as sand particles possess a similar size range as thrips' attachment pads. The beads provide protection against Frankliniella occidentalis *thrips as they remain trapped at the surface of the plant and reduced damage to* Chrysanthemum baltica *in leaf disc dual choice bioassays. Additionally, the choice of emulsifier was found to be of major importance to reduce leaf damage. Crosslinking is necessary to obtain beads rather than coalesced film on plants, which was improved as follows: (i) by using zinc naphthenate, a metal catalyst, (ii) by increasing the amount of atmospheric oxygen in contact at room temperature with linseed oil and (iii) with larger oil droplets.*

Aurélie Féat[a,b], Marleen Kamperman[b,c], Thomas E. Kodger[b] and Martin W. Murray[a]

[a]AkzoNobel Decorative Paints, Wexham Road, Slough, SL2 5DS, United Kingdom
[b]Physical Chemistry and Soft Matter, Wageningen University, Stippeneng 4, 6708 WE, Wageningen, The Netherlands
[c]Zernike Institute for Advanced Materials, University of Groningen, Nijenborgh 4, 9747 AG Groningen, The Netherlands

6.1 Introduction

Many species of thrips (order Thysanoptera) are invasive pests detrimental to agriculture. They are small insects (less than a few millimetres) and about 40% of the known species feed on plants or grasses [1]. They lay their eggs either outside of host material or inside plant tissues and are hence difficult to detect and eliminate with insecticides [1]. Damage to plants by thrips do not only cause loss of aesthetic value, but may also be the result of disease transfer (e.g. leaf gall, fungi), which affects crop yields [1–4]. Introduction of thrips in new areas is generally accidental, for instance, 55 suborders of Thysanoptera, of which 35% were economically significant, were introduced to the Netherlands between 1980-1993 after trading with foreign countries [3]. A study from 1993 showed that 20% of flower cuts and 12% of plants imported into Switzerland were infested by western flower thrips *Frankliniella occidentalis* [5]. In addition to negatively impacting trade, thrips cause severe crop loss [1, 3, 4].

Tackling thrips through biological control has proved difficult as first, upon their introduction in a new area, they lack natural enemies (e.g. mites and predatory thrips) [1, 6]. Second, parasitoids that attack thrips eggs and larvae only induce low levels of mortality and hence show little potential to control thrips population [1, 7].

Therefore, control methods mainly rely on chemical strategies, in particular insecticides, whose harmful effect on health and environment as well as their side-economic costs has been widely described in the literature (see e.g. [8–10]). The serious worldwide decline of insects may also be partly based on the widespread use of insecticides [11]. Eco-friendlier alternatives to conventional pesticides are therefore needed. For example, safer pesticides based on jasmonic acid and its derivatives have been successfully developed [12]. Jasmonic acid is a phytohormone synthesised by plants upon attack by herbivores or pests and affect their survival and reproduction rate [13–15]. The efficacy of jasmonic acid has been linked to an increase in parasitism of herbivores [16] and trichome density [17].

Trichomes are hairy leaf structures developed from epidermal cells that can be classified as non-glandular or glandular (Figure 6.1) [18]. Trichomes defend plants against herbivores by impeding their locomotion and/or by direct toxicity through chemicals they produce and/or release, which range from toxic ones released after an insect herbivore touches the trichome to deterrent volatile terpenes [18]. In addition, glandular trichomes can produce sticky threads

that can immobilise small insects, as seen in e.g. sundews (*Drosera*) [19].

Inspired by the role of trichomes in the plant's defence system, we studied the feasibility to mimic trichomes in crop protection. To this end, we produced sprayable emulsions of 'sticky' crosslinked oil droplets which may immobilise *F. occidentalis* thrips through adhesion (Figure 6.2). For the sake of durability, these droplets should not dissolve in rainwater to limit the number of spray applications. The emulsion stabiliser employed will enter the soil upon water rinsing and therefore should be both biodegradable and non-toxic. Such technology should avoid contributing to the development of chemical resistance by insect pests. We favoured this option to (1) spraying emulsified, non-crosslinked oil directly on the plant as this only affects insects present during the application and fatty acids may cause plant phytotoxicity [20, 21] and to (2) crop coatings due to the ease of application of sprays and, if glossy, coatings could potentially inhibit the plant's photosynthesis [22]. To prevent killing essential insects such as pollinators or seed dispersers, or causing imbalances between primary and secondary pests [23], the technology should be selective to certain insects by tuning the droplet size, as observed for insect-plant selectivity occurring through trichome density, shape, size and physiology [18, 24, 25].
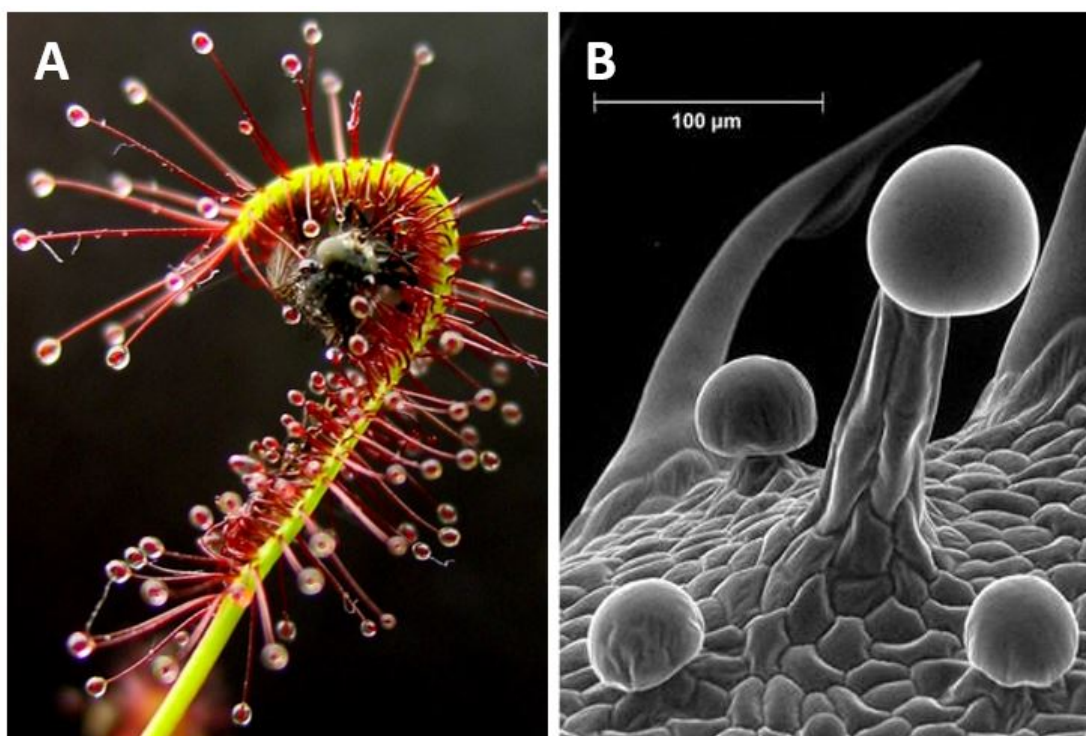

Figure 6.1: Glandular trichomes of (A) *Drosera capensis* and (B) *Cannabis sativa*. (A) 'The leaf of a *Drosera capensis* "bending" in response to the trapping of an insect' by N. Elhardt is licensed under CC-BY-SA 3.0. (B) Adapted with kind permission from [26].
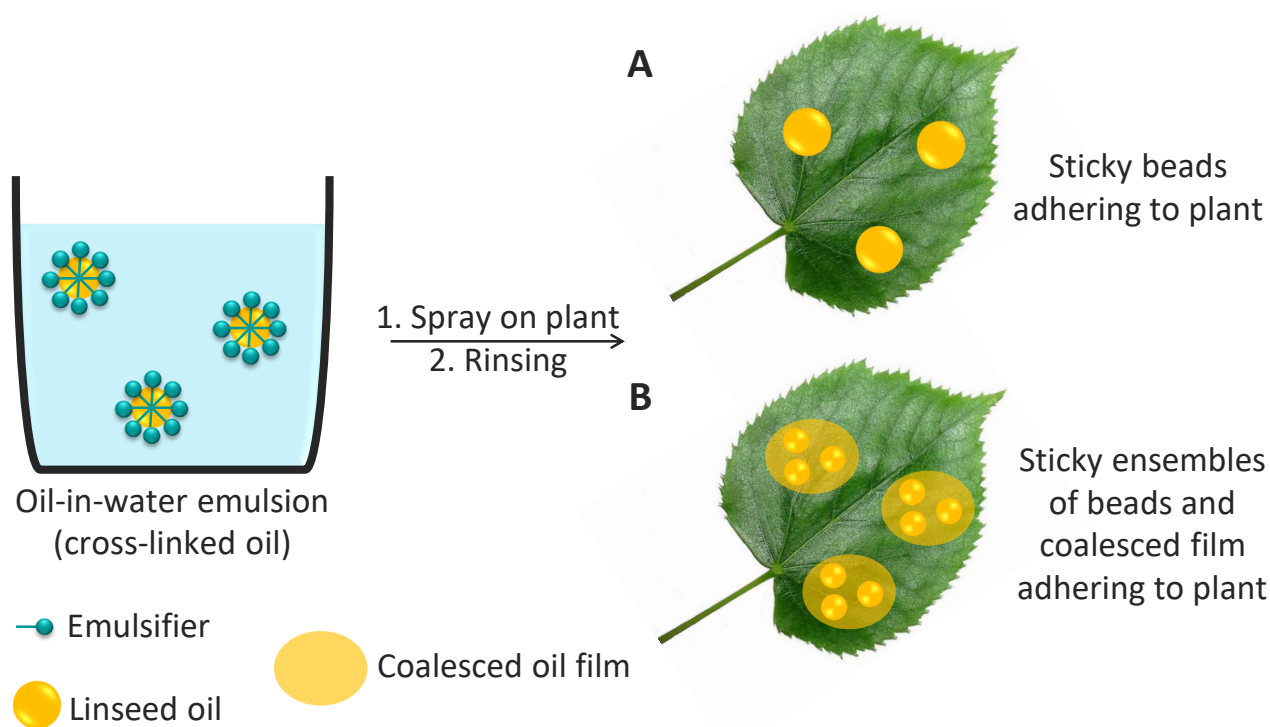
Figure 6.2: Schematic concept to protect plants using oil-in-water emulsions made of linseed oil and biodegradable emulsifier. (A) shows "perfect" crosslinked beads formed on the leaf, while (B) underlines what we mainly obtained in this project, *i.e.* heterogeneous ensembles of beads and coalesced oil forming a film. The leaf picture, 'Leaf of *Tilia tomentosa* (Silver lime tree)' by K. P. Jasiutowicz is licensed under CC-BY-SA 3.0.

Owing to its crosslinking properties, linseed (flaxseed) oil (LO), a well-known compound in the coating industry [27], was used as a model oil. Its market revenue in the food industry was estimated to be $165 million in 2016 [28]. LO hardens (or dries) as a result of the autoxidation of linoleic (14 to 19%) and linolenic (48 to 60%) acids (Figure 6.3): oxygen reacts with the double-bonds of the triglycerides, forming unstable peroxides, which give rise to crosslinking by formation and reaction of radicals [29, 30]. LO hardens faster than other conventional vegetable oils due to its high content of linolenic acid, each triglyceride having about 7 double-bonds, allowing for crosslinking [29, 31]. The process is accelerated upon exposure to temperature or UV [29]. While crosslinked fractions are highly water-insoluble [29], the dispersed oil should remain fluid and elastic enough to form spherical droplets [32]. The remaining unreacted LO droplets with low molecular weight should provide tackiness through capillary adhesion, as they have low viscosity, with insect legs landing on the sticky spheres so that they remain trapped [29].

Although we cannot exclude that the LO sticky droplets could impede plant photosynthesis after several insects would adhere to the plant, plants sprayed with petroleum and soybean oil emulsions presented the same photosynthesis rates as the water-sprayed ones a few days after

treatment [33, 34]. If the oil was to enter the soil, oxidised LO films were found to be ca. 90% biodegradable after 70 days in soil at 30°C [31].

In the present work, we studied the following parameters to produce sprayable, eco-friendly pest controlling crosslinked LO-based emulsions to protect plants against *F. occidentalis* thrips: (1) the emulsifier type, (2) reaction conditions to improve crosslinking, and (3) the optimisation of LO droplet size. Western flower thrips (*F. occidentalis*) was chosen as a model insect owing to its major pest status [1, 4] and small size (less than 1.5 mm length) [35].

6.2 Materials and methods

6.2.1 Materials

Linseed oil (LO), sodium dodecyl sulphate (SDS) and sodium docusate (DOSS) were obtained from Sigma-Aldrich (Gillingham, UK). Emulsogen LCN 158 and LCN 287 were kindly supplied by Clariant (Frankfurt, Germany). AG 6206 was donated by AkzoNobel (Stenungsund, Sweden). The polydimethylsiloxane (PDMS) was Sylgard 184 (Dow Corning, Seneffe, Belgium). Alfa Aesar (Heysham, UK) provided zinc naphthenate (10 wt% zinc in 67% mineral spirits). Tetrahydrofuran (THF) was from VWR (Lutterworth, UK). All chemicals were used without any further purification. The emulsions were sprayed with spray bottles coming from a local store (Windsor, UK). The main component of the dispersing phase was either ultrapure water (Milli-Q) or tap water (Slough, UK) with a conductivity of 598 μS.m^{-1} and pH 6.95.
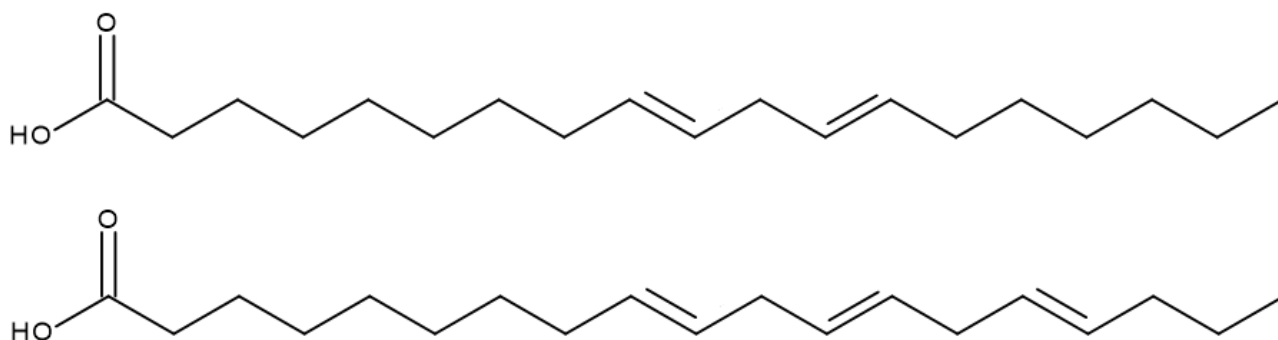

Figure 6.3: Structures of linoleic and linolenic acids.

6.2.2 Emulsion preparation

The LO-in-water emulsions were prepared as follows: 2 g LO, 6 g of emulsifier stock (appropriate amount of emulsifier dissolved in 6 g of Milli-Q water) and 14 g water were added to 30 mL glass vials. When present, zinc naphthenate was added to LO before the addition of the aqueous phase. The amount of LO was kept low ($\phi \approx 0.099$) to ensure the emulsions would be sprayable. 2% oil-in-water petroleum-based emulsions were found to provide sufficient coverage on plants [21].

Several emulsion preparation methods were employed: (1) Shear using a T18 basic Ultra-Turrax from IKA (Staufen, Germany). The emulsions were sheared for 5 minutes at 11,000 rpm, to ensure all LO was dispersed. After shearing, the vials were either placed on a tube rotator (Glas-Col, Terre Haute, IN, USA) or on magnetic stirrers (Stuart SB 162, Cole-Parmer, Stone, UK) at constant speed (450 rpm) and different temperatures (room temperature: 21.3°C ± 1.0°C, 50°C or 70°C). (2) To prepare larger LO droplets, magnetic stirring, at different speeds (150 or 450 rpm) and room temperature (21.3°C ± 1.0°C; RH = 40% ± 1%) was directly used to emulsify the systems. (3) Alternatively, emulsions were prepared by vibrations using a circular multi-slot shaker at 450 rpm (Multi-reax shaker, Heidolph Instruments, Schwabach, Germany). Up to twelve samples can be placed simultaneously on the device, which ensures more reproducibility than magnetic stirring due to homogeneous shear across samples. In (2) and (3), the vials were either closed or left open to promote oxidation of LO's double-bonds by reacting with atmospheric oxygen [29, 30]. In the latter case, water evaporated in some instances, whose amount was monitored every 24 hours.

6.2.3 Blown linseed oil

We studied the potential of blown linseed oil (BLO) to accelerate the rate of crosslinking of LO once incorporated in emulsions. Unsaturated ketones responsible for yellowing of the oil are formed during the process [27]. To prepare BLO, 100 g of LO was introduced in a 1L three-necked flask fitted with a mechanical stirrer, a cooling condenser and an inlet for compressed air. The air was blown through the oil, which was heated to 100°C and stirred at 120 rpm. After 72h heating, the stirring speed was increased to 150 rpm as the viscosity had increased. Oil samples were taken after 11, 43, 63 and 77 hours of preparation. The ultimate viscosity of

the oil was very high, but not measured due to the low volume of LO employed.

6.2.4   Leaf disc dual choice bioassay

Thysanoptera insects rely on vision and olfaction to orient towards host plants [36]. *Frankliniella occidentalis* (Pergande; Thysanoptera: Thripidae) thrips are attracted by some species of *Chrysanthemum* and are invasive pests to *Chrysanthemum baltica* (Asterales: Asteraceae) [36]. The latter were hence chosen as model plants in the test described below. *F. occidentalis* females were chosen as they induce more damage to leaves than males [37].

Dual choice assays were used to test the thrips (*F. occidentalis*) preference for pairs of leaf discs treated with either emulsions, emulsifier or water standards as described by Leiss *et al.* [38]. In short, discs of 10 mm in diameter were punched from *C. baltica* and were sprayed with emulsions, emulsifier or water (both standards) and were left to dry for 24 hours (Figure 6.4).

The leaves were rinsed with tap water to remove the emulsifier from their surfaces. It is assumed that the LO droplets were sufficiently crosslinked not to get removed from the leaves. After another 24 hours drying, two discs with different treatments were placed on a thin layer of 1% water agar in a 9-cm diameter Petri dish. A piece of filter paper (5 × 5 mm) was positioned between the discs. Ten female thrips (*F. occidentalis*), which had been starved for one night, were placed on the filter paper. Damage to the leaves was estimated by counting the silver damage.

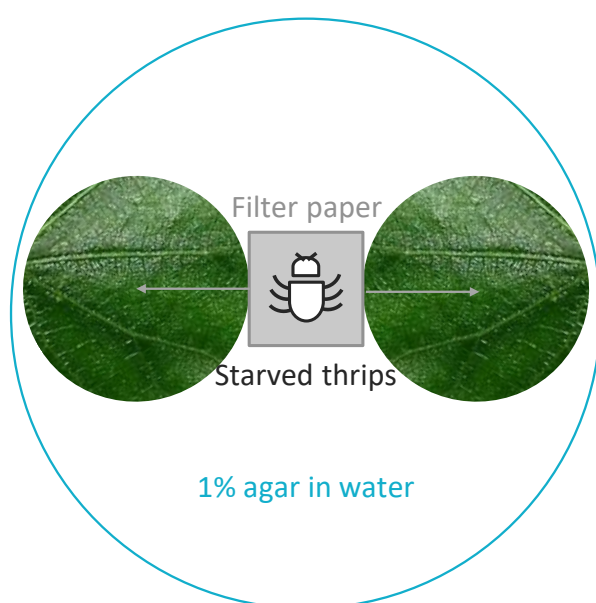Figure 6.4: Schematic leaf disc dual choice bioassay performed on punched *C. baltica* leaves (10 mm diameter) and *F. occidentalis* thrips (not drawn to scale). In short, after being starved for one night, the insect selects which leaf to feed on. The leaves are either subject to the same treatment (water standard) or compare emulsion vs. water or emulsion vs. emulsifier stock spray treatment.

6.2.5 Coarse adhesion testing

In order to assess if the sprayed emulsions were sufficiently sticky to immobilise thrips, emulsions were sprayed on glass slides and were left to dry for 24 hours. Glass was selected for the sake of convenience to mimic smooth leaves, although plant surfaces display a wide range of textures and microstructures [39]. Halves of the slides were rinsed with tap water to remove the emulsifier from their surfaces. After another 24 hours drying, some sand was coarsely applied to the slides. The sand originated from a construction site in Wageningen, The Netherlands.

Species of the *Frankliniella* genus have tarsi terminated with a single bladder-shaped adhesive structure, the arolium, of approximately 27 μm in diameter (measured from SEM micrographs in [40]). The sand particles were found to be 27 ± 19 μm ($n = 27$) in width, measured with an Olympus BX60 microscope (Tokyo, Japan). Therefore, if treated glass was found to retain the sand, we hypothesised the emulsions could be sufficiently sticky for thrips.

6.2.6 Rough locomotion test with *Atta cephalotes* ants

Emulsions were sprayed on glass slides and treated similarly to leaves as described in the previous section. 'Small' and 'large' *Atta cephalotes* L. ant workers (Hymenoptera, Formicidae) ant workers (ca. 2 mm and 6 mm in length, respectively) were placed on horizontally and vertically-oriented treated glass substrates. We visually assessed if their locomotion was impeded after walking/climbing on treated glass.

A. cephalotes possess inflatable adhesive structures on their pads (arolium). Similarly, the width of *Oecophylla smaragdina* (Fab., Hymenoptera, Formicidae) ants' arolia varies between 160 and 280 μm [41]. Using ants resulted in testing the size selectivity of the emulsions as their arolia is several times larger than the ones of *F. occidentalis*.

6.2.7 Crosslinking testing of linseed oil droplets

The size of LO droplets in emulsions was measured by Dynamic Light Scattering using a Zetasizer Nano ZS from Malvern Instruments (Worcestershire, England).

While ongoing crosslinking of LO droplets was performed through different treatments, a visual assessment of the beading was performed by depositing drops of emulsion with pipettes on glass slides (every 24 hours). The appearance of the drop was checked upon after overnight
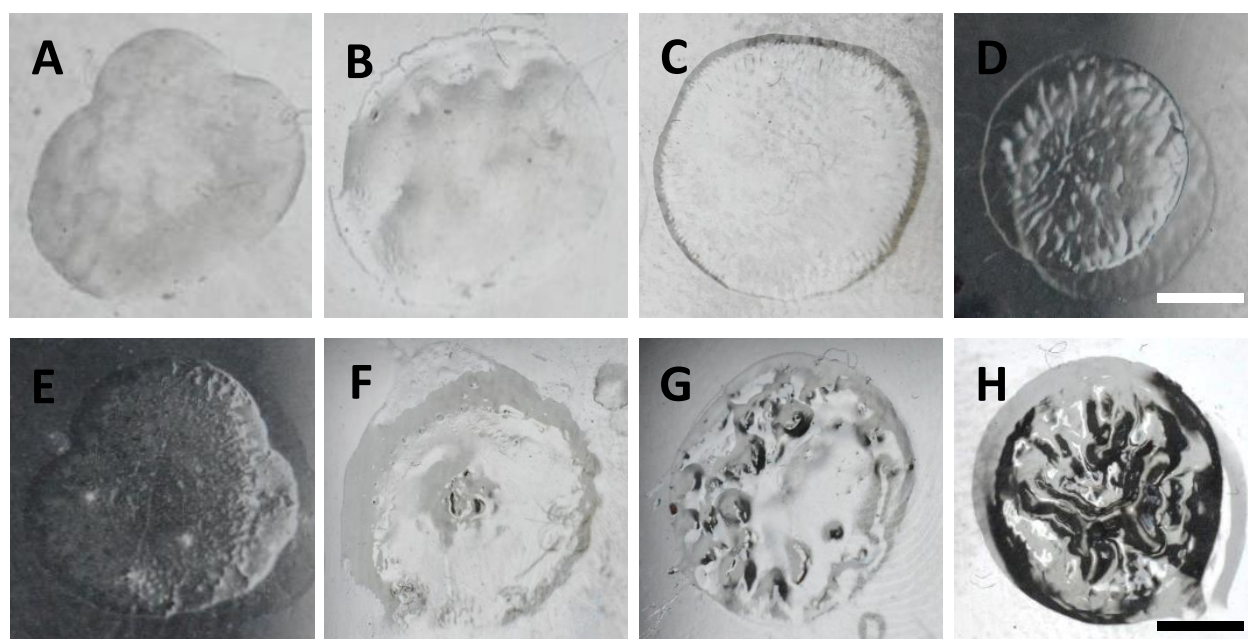
Further crosslinking

Figure 6.5: Top view photographs of the different observations of drying LO-based emulsions drops on glass upon evaporation of water after the emulsions were crosslinked using either temperature or air oxidation treatments. (A), (B) LO forms a film as the droplets coalesce. (C), (D) A "skin" of LO was sometimes observed at the edges of the drop, which would act as a oxygen diffusion barrier to slow down crosslinking [42]. (E)-(G) Beads are progressively formed in the drop (appearance of hollows). (H) "Wrinkles" typically appear for emulsions which crosslinked for too long periods, leading to LO beads forming on the walls of vials. Scale bars: 0.5 cm.

drying at room temperature (21.3°C $\pm$ 1.0°C; RH = 40% $\pm$ 1%). Figure 6.5 shows the three main types of behaviour observed upon drying: (A)-(B) film formation of the drop due to coalescence of LO droplets, (E)-(F) sticky oil "puddles" with beads of LO formed at the edges of the drop, and (G) drop displaying several LO beads. The time to obtain beads (Figure 6.5G) was recorded as t_{bead}. Photographs of the different drying stages were taken with a Nikon D3200 digital camera (Nikon, Tokyo, Japan) (Figure 6.5). If formed, micrographs of the LO bead agglomerates were taken with a VH-Z100UR microscopy (Keyence, Osaka, Japan).

In addition, the crosslinking of LO was assessed by a modified swelling test, where THF was directly added to a small amount of emulsion (Figure 6.6). If LO was sufficiently crosslinked, then the mixture became cloudy when enough THF was added, and bead precipitation was observed for emulsions presenter greater crosslinking (poor solvent condition, $\chi > 0.5$) [43].

The emulsion-THF mixtures were filtered and the weight of LO left on filter papers was recorded ($\%_{LO, filter}$). Some emulsions presented a lot of solid crosslinked LO on the cells of the glass vial (Figure 6.5H), which was weighed after drying the residues at 40°C for 24 hours
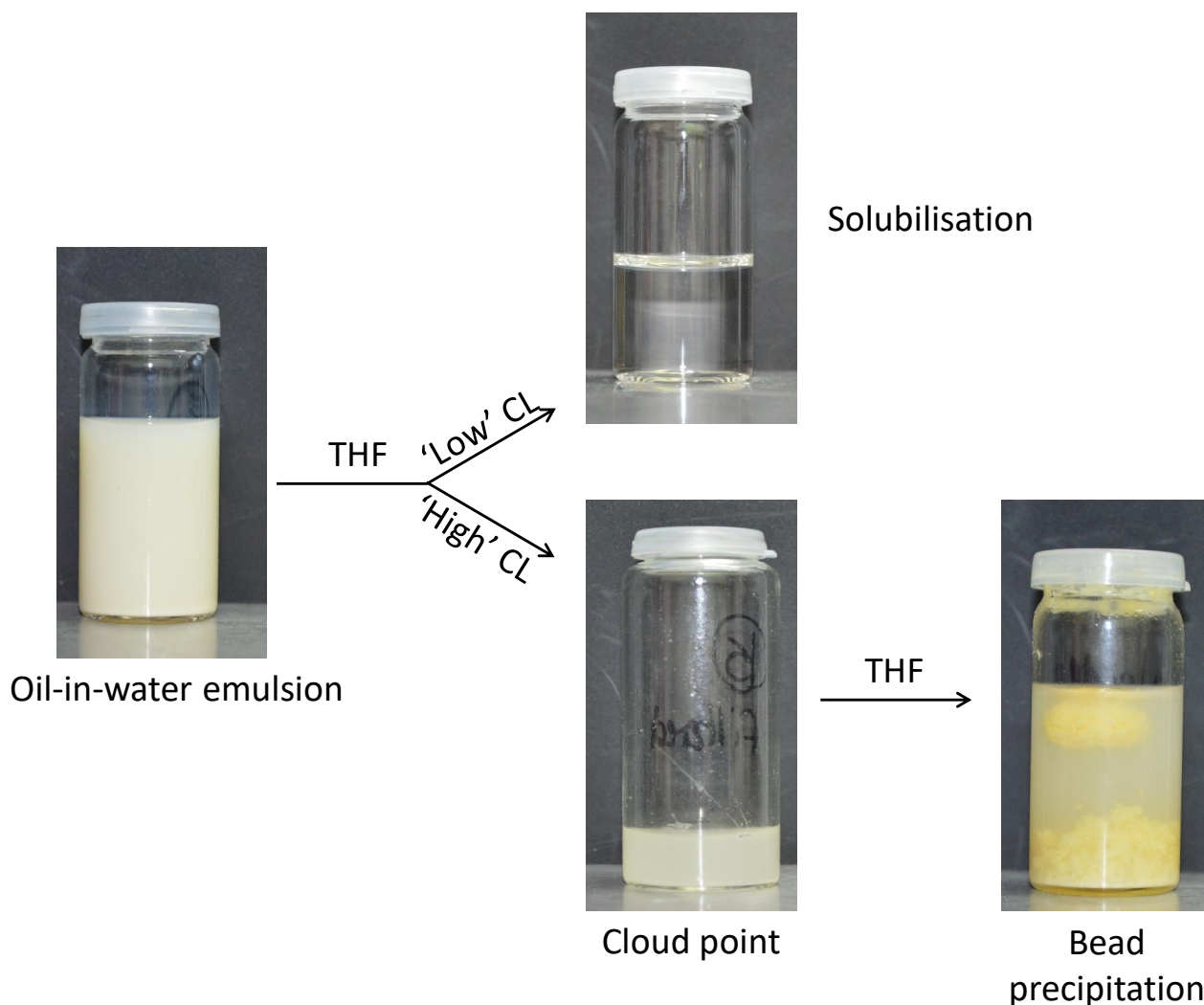
Figure 6.6: Modified swelling test employing THF: a few drops of THF were added to emulsions. 'Low' crosslinking densities (CL) resulted in solubilisation of the droplets by the THF/water mixture as the crosslinks are dissolved upon addition of solvent, leading to high soluble fraction (SF) values. Otherwise, 'high' CL are observed as the crosslinks collapse. Precipitation of the beads was sometimes observed for the highest CL. 'High' CL lead to smaller SF values.

($\%_{LO, \ glass}$). The final soluble fraction of LO (SF) was calculated as:

$$SF \ (\%) = 100 - \ \%_{LO, \ filter} - \%_{LO, \ glass} \tag{6.1}$$

6.2.8   Statistics

All data were tested for normal distribution. Two-tailed Mann–Whitney tests (U-tests) were used for non-normally distributed unpaired tests. P-values below $\alpha = 0.05$ indicated significant differences between the results and were performed using Social Science Statistics (`https://www.socscistatistics.com`). Repeated measures and one-way ANOVA and Pearson's correlations tests were carried out in Excel 2016.

6.3   Results and discussion

6.3.1   Model PDMS-in-water emulsions

In order to establish a proof of concept, model PDMS/SDS/water emulsions were prepared and tested in leaf choice experiments with thrips. Sylgard 184 PDMS was chosen as it cures relatively fast (48 hours) at room temperature [44].

Two PDMS pre-polymer (vinyl end-capped oligomeric dimethyl siloxane) to cross-linker (methyl hydrosiloxane) ratios, 50:1 and 80:1, were used to favour tackiness/adhesiveness compared to the standard ratio (10:1) [45]. 2 g of the two PDMS components were added to 1.0 wt% SDS in 20 mL Milli-Q water (Table 6.1). The mixtures were vortexed for 30 seconds at 1000 rpm. The vials were placed on a tube rotator (40% speed) and were mixed for 48 hours at room temperature to achieve PDMS curing [44]. Unlike emulsion S80:1, non-fully cured filaments of PDMS were surprisingly formed in S50:1.
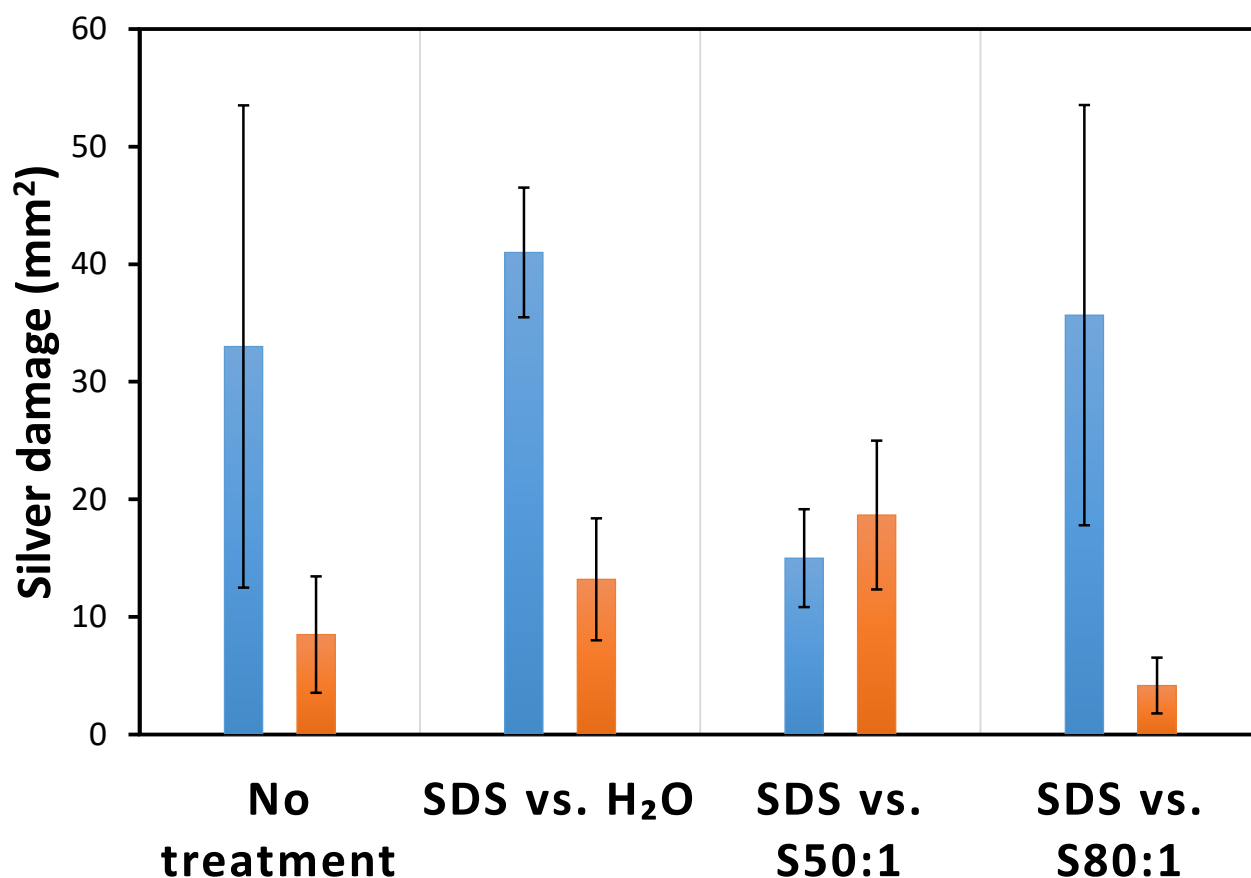

Figure 6.7: Silver damage to *C. baltica* leaves by *F. occidentalis* using SDS standard and PDMS-in-water emulsions stabilised by SDS in leaf disc dual choice bioassays. Blue and orange bars indicate the first and second mentioned treatments, respectively.

Table 6.1: Model PDMS-in-water emulsion droplet size and performances in leaf choice assay. The values are expressed as mean $\pm$ standard error on the mean (s.e.m.).

Emulsion	Pre-polymer to cross-linker ratio	[Emulsifier] (wt%)	Droplet size (μm)	Leaf damage: emulsifier vs. water (%)	Leaf damage: emulsifier vs. emulsion (%)
S50:1	50:1	1.0	7 ± 2	41 ± 21 vs. 13 ± 5	15 ± 4 vs. 19 ± 6
S80:1	80:1	1.0	14 ± 4	41 ± 21 vs. 13 ± 5	36 ± 18 vs. 4 ± 2

The leaf preparation procedure (discussed in the Materials and methods section) was performed on *C. baltica* leaves, which were tested in leaf disc dual choice bioassays by thrips against leaves treated with water or a SDS standard (1.0 wt% solution, Figure 6.7). This test tends to present large standard errors, although non-significant for $\alpha = 0.05$, as highlighted with the non-treated leaves, where we observed 33% vs. 9% damage (Mann–Whitney, $U_{6,6} = 6, P = 0.066$). The large standard errors are due to thrips eating from the edges of the leaves, which can be difficult to distinguish from the damage caused by punching the disks.

Using the coarse adhesion test, all glass slides, except the non-treated one, with and without emulsifier, were found to retain the sand, indicating they could be sufficiently sticky for thrips due to the similar size of the grains and the arolia of thrips. Interestingly, *A. cephalotes* ants' locomotion was not impeded after walking on the treated slides, indicating potential selectivity to insects.

The SDS treatment led to more leaf damage than in the absence of treatment or water treatment. This either indicates the thrips fed more on the former leaves, or that the aggressive SDS solution damaged them. With the S80:1 emulsion treatment, the presence of the PDMS particles reduced the damage to leaves. These preliminary results indicate that sticky emulsions droplets could be used to reduce insect damage to plants. In the next section, we describe the use of biocompatible systems based on linseed oil and biodegradable emulsifiers.

6.3.2   Emulsifier screening in LO-in-water emulsions

PDMS-based model emulsions showed reduced silver damage by thrips and we investigate in this section if emulsions based on LO also have such properties. To this end, we prepared LO-based emulsions (A-D) with thermo-resistant biodegradable emulsifiers similarly to the PDMS-in-water procedure. At this stage, we did not investigate the crosslinking rate of LO as we performed this test to select an emulsifier for further experiments: hence, all emulsions
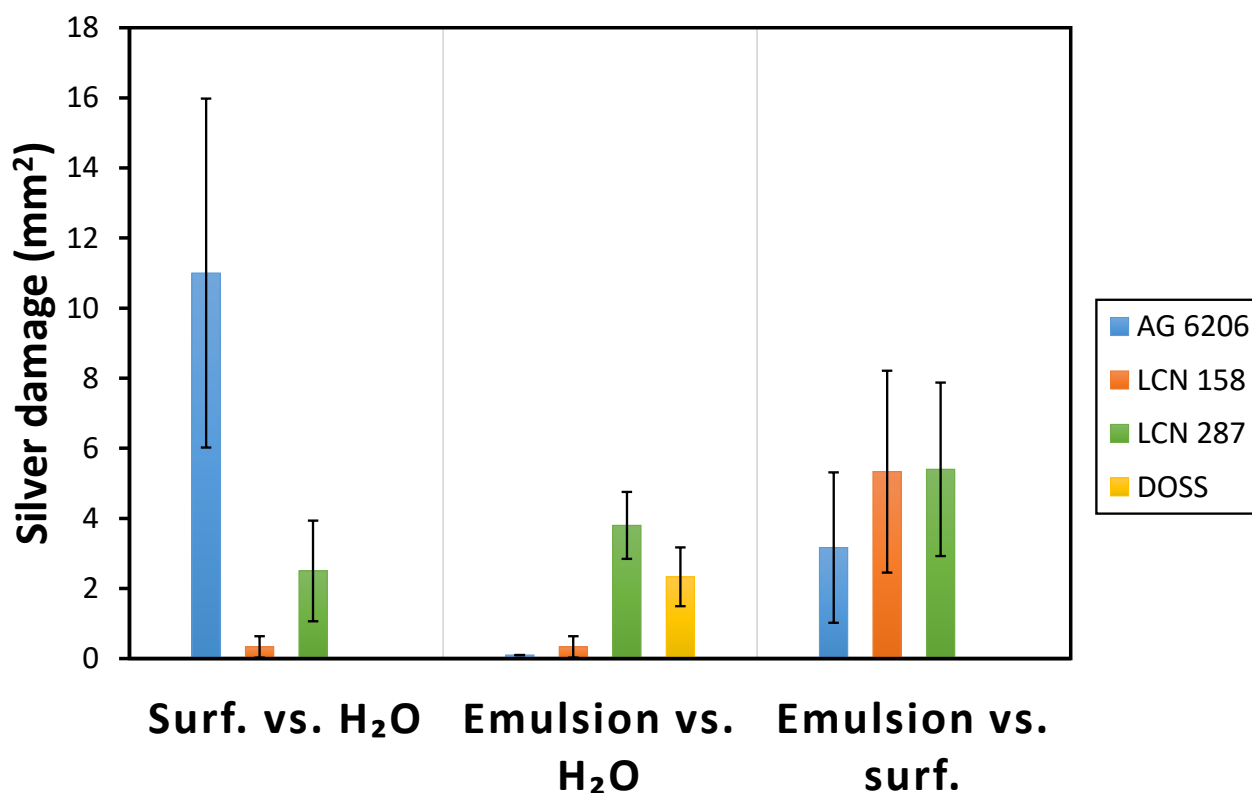
Figure 6.8: Silver damage to *C. baltica* leaves by *F. occidentalis* in leaf disc dual choice bioassays using LO-in-water emulsions stabilised by different biodegradable emulsifiers. Silver damage could not be estimated for the DOSS stock solution as immediate damage was observed due to the heating necessary to dissolve the emulsifier. For the sake of clarity, only the damages obtained on leaves treated with emulsifier and emulsions are shown here.

showed large soluble fractions of LO ($SF > 90\%$) (Figure 6.5A, B).

Some pre-crosslinked LO was prepared by heating the oil under mechanical stirring in a closed vial for 48 hours to 65°C. This temperature ensures only a low fraction of double bonds converts to crosslinks [46]. The LO, emulsifier and ultrapure water were sheared for 5 minutes. Here, shearing was favoured to vortexing to prevent the rapid creaming of the oil, *i.e.* when the oil phase moves to the top of the vial. DOSS needs to be heated to ca. 40°C to be water-soluble and the amounts of emulsifiers were tuned until no macroscopic creaming could be observed and were hence above their critical micelle concentration (CMC) (Table 6.2). The vials were placed on a tube rotator (40% speed) and were mixed for 48 hours at room temperature to further crosslink linseed oil.

The sprayed emulsions formed sticky coatings rather than beads once sprayed on glass and *C. baltica* leaves as the oil droplets coalesced. Sand showed improved adhesion on sprayed glass slides compared to the PDMS-based emulsions. Interestingly, the coalesced oil films did not affect *A. cephalotes* ants' locomotion.

Table 6.2: LO-in-water emulsion droplet size and performances in leaf choice assay of emulsions A-D. The emulsifier amount is based on the oil phase. Leaf damage could not be estimated for the DOSS solution as immediate damage was observed due to the heating necessary to dissolve the emulsifier in the stock solution). ^{a}: the biodegradability was measured as the decomposition of the emulsifier in a water buffer after 28 days, values supplied by the manufacturers. Different OECD test guidelines were used. The values are expressed as mean ± standard error on the mean (s.e.m.).

Emulsion	Emulsifier, type	Biodegrad-ability (%)^a	[Emulsifier] (wt%)	Droplet size (nm)	Leaf damage: emulsion vs. water (%)	Leaf damage: emulsifier vs. emulsion (%)	Comments
A	AG 6206, non-ionic	71%	50	215 ± 1	0 vs. 23 ± 4	10 ± 4 vs. 3 ± 2	A lot of emulsifier needed at RT
B	LCN 158, non-ionic	75%	18	283 ± 4	1 ± 0 vs. 24 ± 8	4 ± 2 vs. 5 ± 3	Emulsion and emulsifier give similar results
C	LCN 287, non-ionic	75%	22	313 ± 3	4 ± 1 vs. 40 ± 10	2 ± 2 vs. 5 ± 2	Emulsion and emulsifier give similar results
D	DOSS, anionic	91%	2	330 ± 10	2 ± 1 vs. 38 ± 13	N/A	Emulsifier needs heat to be dissolved

Besides the bead size effect potentially observed with PDMS-based emulsions, this also shows that ants are not affected when walking on tacky surfaces, possibly due to the adhesive fluid their pads secrete to remove contaminants [47].

The silver damage to treated *C. baltica* leaves by thrips is shown in Figure 6.8. Although the formulae were not optimised with regards to the droplet size or the crosslinking, one can see the emulsions greatly reduced damage produced by the insect pests compared to the water standards (*U*-test, $U_{6,6} < 5$, $P < 0.05$ for the 4 emulsions). Some *F. occidentalis* remained trapped for a few seconds, or eventually died at the surface of the treated leaves, especially with emulsion A (formulated with AG 6206). When tested against water, leaves treated with this emulsion exhibited no damage. However, the emulsifier does not stabilise LO well, which would be problematic for long-term storage. Although DOSS is a readily biodegradable emulsifier (91% after 28 days, supplier data) and the DOSS-based treatment led to only $2\% \pm 1\%$ damage against water-treated leaves, the need to heat the standard emulsifier stock solution prior to the test makes its use impractical in leaf choice assays. Therefore, LCN 158 was selected in the further experiments to develop crop protection formulae.

After showing the efficacy on silver damage reduction using LO-based emulsions, we now need to consider the optimisation of LO crosslinking and droplet size to maximise adhesion of thrips to treated leaves.

6.3.3   Linseed oil crosslinking optimisation

In this section, we describe how to accelerate the crosslinking of LO using (1) a metal dryer, zinc naphthenate; (2) blown LO, prepared by bubbling air into LO under heating; and (3) by increasing the amount of oxygen by blowing air through the emulsions and opening the vials. Since the LO-based emulsions forming tacky coatings and "puddles" described above were sticky to thrips, the following emulsions (Table 6.3) were not tested on *F. occidentalis* and *C. baltica* leaves.

All emulsions were prepared using an Ultra-Turrax (11,000 rpm for 5 minutes), followed by mechanical agitation at 450 rpm (Table 6.3). Here, we used tap water (conductivity = 598 μS.m-1 and pH = 6.95) rather than ultrapure water in an attempt to accelerate crosslinking as it contains dissolved oxygen [29]. Using tap water would not be possible with ionic emulsifiers as stabilisation would be reduced due to water's ions charge screening [48].

Table 6.3: Preparation conditions, t_{bead}, size of LO droplets after t_{bead} was reached and SF of emulsions prepared in different conditions. All emulsions were formulated with 6 g LCN 158 (18% expressed on the oil phase), 2 g LO and approximately 14 g water. All emulsions were prepared using an Ultra-Turrax (11,000 rpm for 5 minutes), followed by mechanical stirring at 450 rpm. Emulsions LO-70-1ZN, LO-70-10ZN and the ones made from BLO, as well as the standard, were heated to 70°C while stirring. The amounts of zinc are based on the oil phase using zinc naphthenate containing 10% zinc. The number of BLO hours refers to the number of hours used to produce blown linseed oil. Bubbling indicates that compressed air bubbles were blown into the emulsions, RT conditions were 21.3°C $\pm$ 1.0°C and 40% $\pm$ 1%RH. [a]: (c) indicates a cloud transition was observed upon addition of THF (Figure 6.6). The values are expressed as mean $\pm$ standard error on the mean (s.e.m.).

Emulsion	Conditions	Time (t_{bead}) to observe beading on glass (hours)	Droplet size after t_{bead} (nm)	SF^a (%)
Standard	Standard	601	321 $\pm$ 9	92 (c)
LO-70-1ZN	0.1% zinc	477	374 $\pm$ 24	92 (c)
LO-70-10ZN	1% zinc	68	800 $\pm$ 41	92 (c)
BLO-11	BLO, 11 hours	504	744 $\pm$ 44	93 (c)
BLO-43	BLO, 43 hours	624	796 $\pm$ 79	73
BLO-63	BLO, 63 hours	355	755 $\pm$ 47	45
BLO-77	BLO, 77 hours	92	929 $\pm$ 74	45
LO-B-RT	Bubbling, RT, 1% zinc	44	374 $\pm$ 11	88 (c)
LO-B-RT-10ZN	Bubbling, RT, 1% zinc	44	108 $\pm$ 1	94 (c)
LO-B-50-10ZN	Bubbling, 50°C, 1% zinc	44	564 $\pm$ 28	87
LO-O-RT	Open vial, RT	111	705 $\pm$ 32	89 (c)
LO-O-RT-10ZN	Open vial, RT, 1% zinc	111	682 $\pm$ 50	94 (c)

Use of zinc naphthenate

Metallic catalysts (siccatives or driers) are mainly derivatives of heavy metals to accelerate the drying properties of oils in paint coatings. Metallic naphthenates are typically used as siccatives, lead has been almost entirely eliminated because of its toxicity, and has been replaced with e.g. aluminium and zirconium naphthenate [49]. The catalysis mechanism of cobalt driers inducing crosslinking in alkyd resins has been described in [50]. Drier partitioning in the aqueous phase has been observed in alkyd emulsions when using strongly hydrophilic anionic emulsifiers [51], which was likely reduced here since we used a non-ionic emulsifier.

As a proof of concept, we used in this study zinc naphthenate (ZN) owing to its lower toxicity. Zinc is a plant nutrient but at higher concentrations, it is toxic [52]. Zinc can be phytoremediated by some hyperaccumulator plants [53]. Interestingly, ZN has been found to

be toxic to termites, and one could think it may be efficient against thrips [54]. Small amounts of ZN (0.1 wt% and 1 wt% ZN) were used in emulsions LO-70-1ZN and LO-70-10ZN, these amounts of naphthenate salts are typically used to accelerate the drying of LO [55]. The emulsions were heated to 70°C.

It can be seen from Table 6.3 that the time to observe beading, t_{bead}, of LO was decreased compared to the standard when using ZN, in particular when using 1 wt% zinc, where an approximate 9-fold decrease was observed. Although not measured here, this suggests that most of the ZN was present in the oil phase [51]. All sprayed emulsions were tacky to sand particles. The longer the crosslinking time, the smaller the droplets ($r^2 = 0.98$). The soluble fraction (SF) of the three emulsions was large, 92%, although a cloud transition was observed upon addition of solvent for all of them. The filtrates were clear, indicating that the precipitated LO particles were large enough not to pass the filter pore size. Emulsions displaying large SF could actually be beneficial as tackiness to insects would be provided by the low crosslinked LO fractions through capillary forces upon contact with their legs [29]. If the use of ZN may be detrimental to plants, these tests nonetheless nicely showed that t_{bead} can be considerably reduced. Using enzymes as alternatives to metal catalysts seems to be a promising, bio-friendly method to crosslink linseed oil, but the enzymes are not yet readily available [56].

Blown linseed oil

Hardening of LO occurs through reaction between atmospheric oxygen and the double-bonds present in triglycerides, which further react with one another to form crosslinks [29]. Therefore, one way to catalyse the reaction is to increase the liquid/air interface. Samples of BLO were taken every few hours and were added to LCN 158 and water to be further heated to 70°C under mechanical agitation at 450 rpm.

The use of BLO reduced t_{bead} compared to the standard emulsion, especially in emulsion BLO-77 where it was reduced by approximately 6 times. All emulsions displayed similar particle sizes after beading was observed (one-way ANOVA, $F_{3,71} = 1.47, P = 0.231$). Although efficient, the use of BLO was impractical owing to its large viscosity which rapidly increased over time, especially after 63 hours preparation. Hence, the BLO which was prepared for 63 and 77 hours (emulsions BLO-63 and BLO-77) was not easily dispersible in the water/emulsifier mixture. In
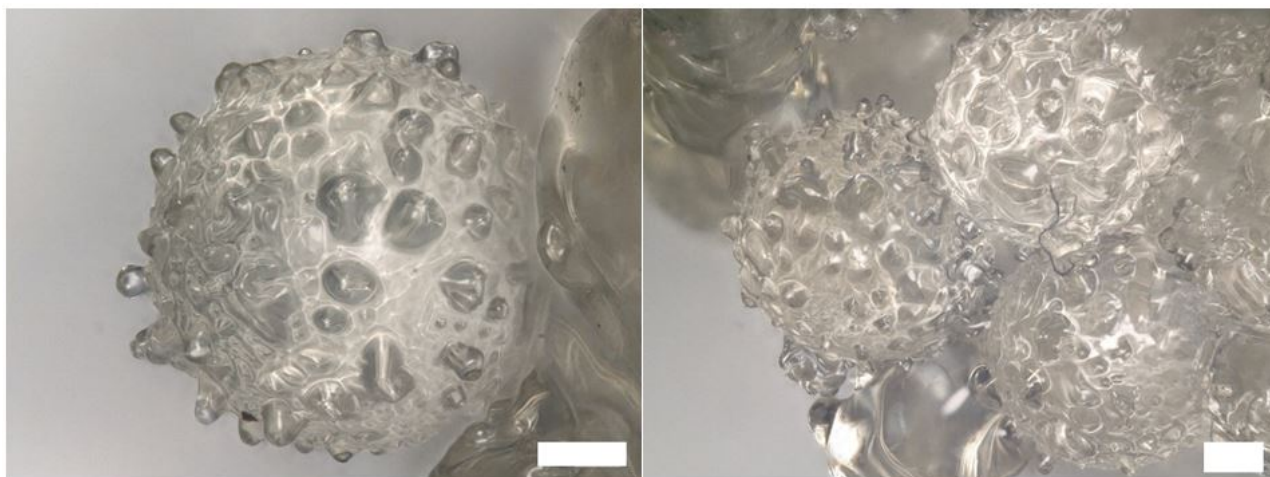
Figure 6.9: BLO irregular beads which formed on the walls of glass vials in emulsions BLO-63 and BLO-77 (594 ± 83 μm, $n = 22$). Scale bars: 100 μm.

all samples, once t_{bead} was reached, 4% to 57% of BLO had polymerised on the walls of the glass vials of emulsions BLO-11 to BLO-77, likely because of the low dispersibility of BLO when using an emulsifier amount of 18 wt% on LO. This explains the low SF values (45%) obtained for emulsions BLO-63 and BLO-77 and the fact that no cloud transitions were observed (Table 6.3). The LO polymers formed agglomerates of irregular spheres in both emulsions (594 ± 83 μm, $n = 22$, Figure 6.9). After formation of the agglomerates, LO formed "wrinkled" films upon deposition of drops of emulsions on glass slides (Figure 6.5H). Hence, such emulsions cannot be used for crop protection purposes.

Increased oxidation with atmospheric air

In this section, we compare the crosslinking performances between emulsions prepared with open vials and by bubbling air through the emulsions to increase the amount of oxygen present at the liquid/air interface (Table 6.3) .

Bubbling air and opening the vials was efficient at reducing t_{bead}: 44 hours (emulsion LO-B-RT) and 111 (LO-O-RT) hours were respectively needed to observe beading on glass, vs. 601 hours for the standard emulsion (Table 6.3). However, the addition of ZN or heating treatment (emulsions LO-B-RT-10ZN, LO-B-50-10ZN and LO-O-RT-10ZN) led to the same results in both cases.

All emulsions presented in Table 6.3 had submicron-sized LO droplets. Although all sprayed emulsions were sticky to sand particles on glass slides, they proved to be too small to efficiently stick to 'small' and 'large' *A. cephalotes* ant pads, as the ants could walk on and climb up

the treated glass slides as easily as on non-treated surfaces, indicating potential selectivity to insects. In these samples, the emulsifier level of 18 wt% on LO (3 times the CMC, with CMC $\approx$ 5.1 g/L based on 80% active material, supplier data) is above the surface coverage necessary to provide stabilisation, leading to many, small oil droplets. In fact, one could think that an excess of surfactant, in addition to the droplet stabiliser, could increase the coverage of the sprays on plants, but a surplus could cause them to runoff [57]. Hence, the following section explores the increase of droplet size at room temperature. Since opening the vials is an easier procedure to perform on many samples at a time, it was favoured to blowing air through the liquid.

6.3.4   Optimisation of LO droplet size

Now that the crosslinking has been successfully optimised, we attempt in this section to increase the size of LO droplets. It is important to note that to the best of our knowledge, no integrative studies investigating attachment systems or adhesion performances of *F. occidentalis* have been performed, unlike many other types of insects (e.g. [39, 58]). This means it is difficult to target a precise bead size which can immobilise thrips on leaves. Species of the *Frankliniella* genus have tarsi terminated with a single bladder-shaped adhesive structure, the arolium, of approximately 27 μm in diameter (measured from SEM micrographs in [40]). Upon landing on treated leaves, droplets larger than this size would ensure large contact areas between their arolia and the beads as well as increased adhesive forces [59]. Therefore, formulating large oil beads is a presumably more efficient strategy to retain insects on sprayed leaves.

Leaf choice bioassays with model PDMS-in-water emulsions showed that ca. 14 μm PDMS particles efficiently reduced silver damage as they were sticky to thrips. Unlike the sticky puddles and coatings tested in section 2 (where the bead size did not matter due to film formation), LO droplets sized below 1 μm might be too small to efficiently adhere to their pads and immobilise them efficiently, despite that all sprayed emulsions were sticky to sand particles. Experiments to test emulsions prepared in this section in leaf disc dual choice bioassays are underway.

In this section, we tentatively produced emulsions with LO droplets larger than 1 μm using open vials. Lowering the amount of emulsifier (3 wt% and 0.6 wt% on LO) led to unstable emulsions as about 75% of water evaporated within a few days. Using a water condenser

Table 6.4: Preparation conditions, t_{bead}, size of LO droplets after t_{bead} was reached and SF of emulsions prepared in different conditions. All emulsions were formulated with 6 g LCN 158 (18% expressed on the oil phase), 2 g LO and approximately 14 g water. They were prepared at 21.3°C $\pm$ 1.0°C and 40% $\pm$ 1%RH. [a]: (c) indicates a cloud transition was observed upon addition of THF (Figure 6.6). The values are expressed as mean $\pm$ standard error on the mean (s.e.m.).

Emulsion	Emulsion preparation method	Conditions	Time (t_{bead}) to observe beading on glass (hours)	Droplet size after t_{bead} (nm)	SF^a (%)
Standard	Ultra-Turrax, followed by magnetic stirring	Standard, 450 rpm	601	321 $\pm$ 9	92 (c)
LO-150-MS	Magnetic stirring	150 rpm	175	3209 $\pm$ 476	93
LO-450-MS	Magnetic stirring	450 rpm	175	2216 $\pm$ 301	93
LO-450-S	Multi-slot shaker	450 rpm	222	339 $\pm$ 82	84

would have prevented evaporation but may have slowed the autoxidation of LO. We therefore increased the size of oil droplets keeping the amount of 18 wt% LCN 158 (based on LO).

Consequently, the emulsions were either prepared directly by mechanical agitation with stir bars (150 or 450 rpm) or placed on a multi-slot shaker in the presence of 18 wt% LCN 158 (based on the oil phase). Stir bars had the same size to ensure identical shear across samples (Table 6.4). The multi-slot shaker, despite allowing homogeneous mixing across a large number of samples, led to poor dispersion of oil (emulsion LO-450-S). Mixing speeds as high as 1,750 rpm were needed to obtain similar dispersion and particle size distribution than emulsions prepared under shearing, followed by mechanical agitation at 450 rpm (data not shown).

Increasing the amount of oxygen in contact with emulsions decreased t_{bead} by approximately 3 times (Table 6.4). The emulsion prepared with the multi-slot shaker at 450 rpm (LO-450-S) displayed submicron-sized LO droplets. Emulsion LO-450-MS, with the same composition, but prepared using magnetic stirring at the same speed, presented relatively large droplets (2216 nm $\pm$ 301 nm). The droplet size distribution significantly varied over time for both emulsions (repeated measures ANOVA, $F_{4,24} = 7.46$, $P < 0.001$ and $F_{6,54} = 14.44$, $P < 0.001$ for emulsions LO-450-MS and LO-450-S, respectively) and was much wider for emulsion LO-450-MS (Figure 6.10). Both emulsions presented narrow bimodal droplet size distributions, likely growing due to limited (heterogeneous) coalescence [48, 60]. The oil solubility is likely too low in water to allow the droplets to grow in size through Ostwald ripening [48].
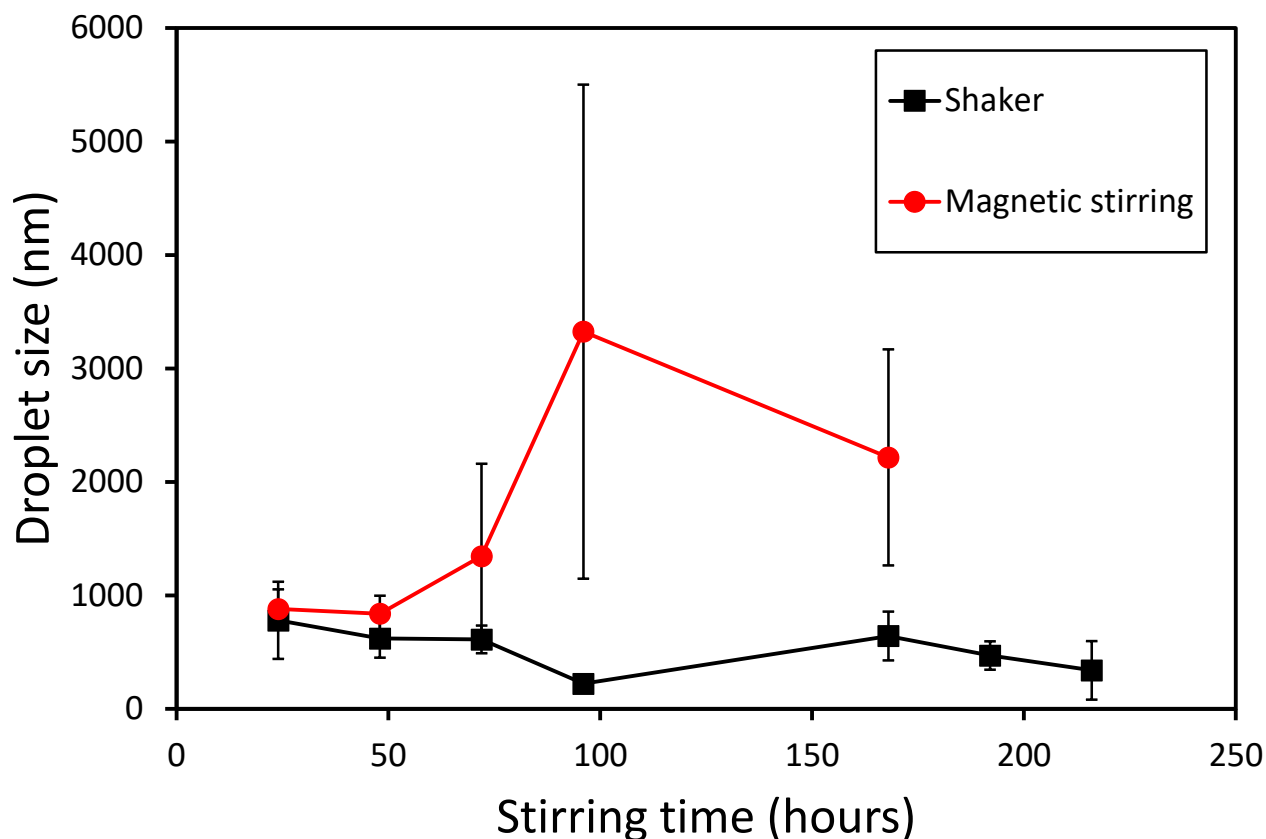
Figure 6.10: Evolution of LO droplet size over time for LO-in-water emulsions prepared with 18% LCN 158 (based on the oil phase) at 450 rpm using: multi-slot shaker (black squares, LO-450-S) and magnetic stirring (red circles, LO-450-MS). DLS measurements were performed until t_{bead} was reached. Lines are guides to the eye.

The emulsion prepared at 150 rpm (LO-150-MS), was prepared at too low shear to emulsify the full content of LO and therefore showed the largest droplet size and large polydispersity (the polydispersity index by cumulant analysis was 0.98 after t_{bead} [61]). Emulsions LO-150-MS and LO-450-MS formed large beads after deposition on glass slides (Figure 6.5G).

Although a relative short beading time was reached owing to the increased air/liquid interface with regards to the standard emulsion, large soluble oil fractions (SF) were obtained (Table 6.4). Unlike the previous section and in the standard emulsion, there was no cloud transition observed upon addition of THF to emulsions (Figure 6.6). This indicates that many of the droplets were not highly crosslinked and hence provided stickiness [29]. Even if non-significant at $\alpha = 0.05$, the fraction of SF was found to increase for smaller LO droplets in the emulsion series described in section 6.3.3 (Pearson's $r = 0.54, P = 0.067$).

Emulsions described in Table 6.4 were sticky enough to retain sand. Once sprayed on glass slides, they formed heterogeneous ensembles of tacky beads and puddles (Figure 6.5G), which could be detrimental to plant photosynthesis. Although we succeeded in preparing emulsions

177

with LO droplets larger than 1 μm, the aspect of such emulsions is difficult to control once sprayed on surfaces as some LO coalesces (Figure 6.2B, Figure 6.5).

Larger droplets can be prepared by reducing the amount of emulsifier in closed vials to prevent water evaporation. The addition of a dryer, e.g. zinc naphthenate, would reduce the time to observe crosslinking of LO. However, emulsions prepared at lower emulsifier concentration or using "unsophisticated" alternative mixing devices (whisk, milkshake maker or food mixer) showed irreversible coalescence and/or most of the oil crosslinked on the walls of vials (data not reported). Emulsogen LCN 158 is a non-ionic PEG-based emulsifier and provides stabilisation through steric effects. Anionic emulsifiers, like the SDS and DOSS emulsifiers tested in this work, would likely provide enhanced stabilisation *via* ionic repulsions. However, SDS is an aggressive emulsifier and SDS-based emulsions were found to damage *C. baltica* leaves. Cationic emulsifiers should not be selected as they may be toxic to soils [62].

6.4 Conclusions

This preliminary work successfully showed that by bio-mimicking glandular trichomes, sticky spheres present at the surface of plants to retain insects, the damage to *C. baltica* leaves by *F. occidentalis* thrips could be reduced. Our proof of concept produced bio-degradable emulsion sprays based on linseed oil, which, once dried on a substrate, form tacky beads and films of coalesced oil droplets (Figure 6.2B).

In addition to leaf choice dual disc bioassays with thrips, we used "crude" adhesion and locomotion testing with sand particles and *A. cephalotes* ants. Sand particles served as models of attachment pads of *Frankliniella* thrips, which are in the same size range. All treated glass slides were tacky and retained sand, but did not hamper ants' free-roaming, which possess larger pads, which indicates potential selectivity to insects. While thrips were mainly tested with coalesced LO films, 14 μm PDMS beads were sticky to their pads, but not to ants'. Large beads may be beneficial to impede insect adhesion as insects' pads generate greater contact areas [59]. The natural enemies of certain thrips are either larger in size, e.g. the 10-20 millimetres *Chysoperla carnea* [6, 63], or share the same length range (*Neoseiulus cucumeris* < 1 millimetre [64], *Franklinothrips vespiformis* 2.5-3 millimetres [65] [1]. This suggests the technology, as it is, might not be selective enough to only target thrips pests. Integrative studies to understand how thrips adhere to surfaces (e.g. use of claws, adhesive pads or secretion) may aid to further

tune our strategy.

After selecting Emulsogen LCN 158 as an emulsifier, the challenging formulation steps were to obtain (1) sufficiently crosslinked linseed oil beads and (2) sufficiently large beads, which have been overcome by (1) increasing the amount of oxygen at the air/liquid interface by opening the preparation vials. This solution was favoured to heating emulsions to 70°C, as this lacked efficiency in terms of reducing t_{bead}, and to adding 1 wt% zinc as this may be detrimental to plants. Using enzymes as replacers of metal catalysts appears to be an efficient, bio-friendly way to crosslink linseed oil [56]. For (2), we simply reduced the shear rate by decreasing the stirring rate during preparation. Decreasing the amount of non-ionic emulsifier led to destabilisation (coalescence, creaming). The use of anionic emulsifiers may overcome this problem owing to improved repulsive interactions.

Since ageing LO films form crosslinks over long periods, the stickiness of the beads may be decreased over time, but is slowed down as unreacted glycerides act as plasticisers in the network [29]. Some coalesced LO films became tack-free after the glass slides were left at RT (were 21.3°C ± 1.0°C and 40% ± 1%RH) for several months. We used in this work "crude" tests to assess adhesiveness to different insects (*F. occidentalis* thrips and *A. cephalotes* ants) and sand, hence more "sophisticated" testing should be employed to this end. Field experiments should be performed to assess how long the sprayed emulsions would remain tacky enough to retain thrips. Investigating if such treatment may be detrimental to the plant's photosynthesis would be of interest, as once sprayed onto glass panels, sufficiently crosslinked emulsions formed heterogeneous ensembles of sticky beads and puddles. The control of the appearance of the beads appears essential for further testing. Further crosslinking could be achieved by using e.g. UV-treatment, reactive emulsifiers which anchor at the droplet's surface [51] or by reducing the LO fraction to increase the amount of oxygen per droplet.

Slow release of e.g. deterrent compounds to *F. occidentalis*, such as jasmonic acid derivatives, attractants to their enemies, or pesticides [13, 36, 66], if incorporated in the oil beads, may be very efficient at repelling or killing thrips in the field. Our strategy, although only a proof of concept at present, could become a sustainable alternative to pesticides and petroleum-based sprays in agriculture with further research. Their use in the control of thrips could be exploited in combined pest management strategies [36].

Acknowledgements

References

[1] Morse, J. G. and Hoddle, M. S. (2006) Invasion Biology of Thrips. *Annu. Rev. Entomol.,* **51**(1), 67–89.

[2] Mound, L. A. (2009) Thysanoptera, Elsevier, .

[3] Vierbergen, G. (1995) International Movement, Detection and Quarantine of Thysanoptera Pests, Springer US, Boston, MA.

[4] Jones, D. R. (2005) Plant viruses transmitted by thrips. *Eur. J. Plant Pathol.,* **113**(2), 119–157.

[5] Frey, J. (1993) The analysis of arthropod pest movement through trade in ornamental plants, British Crop Protection Council Monograph, Farnham.

[6] Hoddle, M. S. and Robinson, L. (2004) Evaluation of factors influencing augmentative releases of *Chrysoperla carnea* for control of Scirtothrips perseae in California avocado orchards. *Biol. Control,* **31**(3), 268–275.

[7] Loomans, A. J. M. (2003) Parasitoids as biological control agents of thrips pests (PhD thesis), Wageningen University, Wageningen.

[8] Pimentel, D. (2005) Environmental and economic costs of the application of pesticides primarily in the United States. *Environ. Dev. Sustain.,* **7**(2), 229–252.

[9] Tilman, D., Fargione, J., Wolff, B., D'Antonio, C., Dobson, A., Howarth, R., Schindler, D., Schlesinger, W. H., Simberloff, D., and Swackhamer, D. (2001) Forecasting agriculturally driven global environmental change. *Science,* **292**(5515), 281–284.

[10] Devine, G. J. and Furlong, M. J. (2007) Insecticide use: Contexts and ecological consequences. *Agric. Human Values,* **24**(3), 281–306.

[11] Sánchez-Bayo, F. and Wyckhuys, K. A. (2019) Worldwide decline of the entomofauna: A review of its drivers. *Biol. Conserv.,* **232**, 8–27.

[12] Wei, Z. and Xiaojuan, L. Pesticide composition containing jasmonic acid or methyl jasmonate. (2017) CN Patent 106259338.

[13] Egger, B. and Koschier, E. H. (2014) Behavioural responses of *Frankliniella occidentalis* Pergande larvae to methyl jasmonate and *cis*-jasmone. *J. Pest Sci. (2004).,* **87**(1), 53–59.

[14] Omer, A. D., Granett, J., Karban, R., and Villa, E. M. (2001) Chemically-induced resistance against multiple pests in cotton. *Int. J. Pest Manag.*, **47**(1), 49–54.

[15] Zhang, N. X., Messelink, G. J., Alba, J. M., Schuurink, R. C., Kant, M. R., and Janssen, A. (2018) Phytophagy of omnivorous predator *Macrolophus pygmaeus* affects performance of herbivores through induced plant defences. *Oecologia*, **186**(1), 101–113.

[16] Thaler, J. S. (1999) Jasmonate-inducible plant defences cause increased parasitism of herbivores. *Nature*, **399**(6737), 686–688.

[17] Boughton, A. J., Hoover, K., and Felton, G. W. (2005) Methyl jasmonate application induces increased densities of glandular trichomes on tomato, *Lycopersicon esculentum*. *J. Chem. Ecol.*, **31**(9), 2211–2216.

[18] Glas, J. J., Schimmel, B. C., Alba, J. M., Escobar-Bravo, R., Schuurink, R. C., and Kant, M. R. (2012) Plant glandular trichomes as targets for breeding or engineering of resistance to herbivores. *Int. J. Mol. Sci.*, **13**(12), 17077–17103.

[19] Huang, Y., Wang, Y., Sun, L., Agrawal, R., and Zhang, M. (2015) Sundew adhesive: A naturally occurring hydrogel. *J. R. Soc. Interface*, **12**(107).

[20] Johnson, W. T. (1980) Spray oils as insecticides. *J. Arboric.*, **6**(7), 169–174.

[21] DeOng, E. R., Knight, H., and Chamberlin, J. C. (1927) A preliminary study of petroleum oil as an insecticide for citrus trees. *Hilgardia*, **2**(9), 351–386.

[22] Decoteau, D., Kasperbauer, M., Daniels, D., and Hunt, P. (1988) Plastic mulch color effects on reflected light and tomato plant growth. *Sci. Hortic. (Amsterdam).*, **34**(3-4), 169–175.

[23] Pascual, S., Cobos, G., Seris, E., and González-Núñez, M. (2010) Effects of processed kaolin on pests and non-target arthropods in a Spanish olive grove. *J. Pest Sci. (2004).*, **83**(2), 121–133.

[24] Tian, D., Tooker, J., Peiffer, M., Chung, S. H., and Felton, G. W. (2012) Role of trichomes in defense against herbivores: comparison of herbivore response to *woolly* and *hairless* trichome mutants in tomato (*Solanum lycopersicum*). *Planta*, **236**(4), 1053–1066.

[25] Dalin, P., Ågren, J., Björkman, C., Huttunen, P., and Kärkkäinen, K. (2008) Leaf Trichome Formation and Plant Resistance to Herbivory, Springer Netherlands, Dordrecht.

[26] Small, E. and Naraine, S. G. U. (2016) Size matters: evolution of large drug-secreting resin glands in elite pharmaceutical strains of *Cannabis sativa* (marijuana). *Genet. Resour. Crop Evol.*, **63**(2), 349–359.

[27] Masschelein-Kleiner, L. (1995) Ancient binding media, varnishes and adhesives, ICCROM, Rome.

[28] Grand View Research Linseed Oil Market Analysis By Application (Paints & Varnishes, Flooring, Processed Food, Cosmetics, Pharmaceuticals), By Region (North America, Europe, Asia Pacific, CSA, MEA), And Segment Forecasts, 2018 - 2025. (2017).

[29] Lazzari, M. and Chiantore, O. (1999) Drying and oxidative degradation of linseed oil. *Polym. Degrad. Stab.*, **65**(2), 303–313.

[30] Oyman, Z., Ming, W., and van der Linde, R. (2005) Oxidation of drying oils containing non-conjugated and conjugated double bonds catalyzed by a cobalt catalyst. *Prog. Org. Coatings*, **54**(3), 198–204.

[31] Shogren, R. L., Petrovic, Z., Liu, Z., and Erhan, S. Z. (2004) Biodegradation behavior of some vegetable

oil-based polymers. *J. Polym. Environ.,* **12**(3), 173–178.

[32] Mason, T. G., Bibette, J., and Weitz, D. A. (1995) Elasticity of Compressed Emulsions. *Phys. Rev. Lett.,* **75**(10), 2051–2054.

[33] Wedding, R. T., Riehl, L. A., and Rhoads, W. A. (1952) Effect of Petroleum Oil Spray on Photosynthesis and Respiration in Citrus Leaves. *Plant Physiol.,* **27**(2), 269–278.

[34] Cannon, A. L. Evaluation of botanical oil Formulations for management of powdery mildew and mites PhD thesis Knoxville (2004).

[35] Steenbergen, M., Abd-el Haliem, A., Bleeker, P., Dicke, M., Escobar-Bravo, R., Cheng, G., Haring, M. A., Kant, M. R., Kappers, I., Klinkhamer, P. G. L., Leiss, K. A., Legarrea, S., Macel, M., Mouden, S., Pieterse, C. M. J., Sarde, S. J., Schuurink, R. C., De Vos, M., Van Wees, S. C. M., and Broekgaarden, C. (2018) Thrips advisor: exploiting thrips-induced defences to combat pests on crops. *J. Exp. Bot.,* **69**(8), 1837–1848.

[36] Koschier, E. H. (2008) Essential oil compounds for thrips control - A review. *Nat. Prod. Commun.,* **3**(7), 1171–1182.

[37] van de Wetering, F., Hulshof, J., Posthuma, K., Harrewijn, P., Goldbach, R., and Peters, D. (1998) Distinct feeding behavior between sexes of *Frankliniella occidentalis* results in higher scar production and lower tospovirus transmission by females. *Entomol. Exp. Appl.,* **88**(1), 9–15.

[38] Leiss, K. A., Choi, Y. H., Abdel-Farid, I. B., Verpoorte, R., and Klinkhamer, P. G. L. (2009) NMR Metabolomics of Thrips *Frankliniella occidentalis*) Resistance in *Senecio* Hybrids. *J. Chem. Ecol.,* **35**(2), 219–229.

[39] Gorb, E. and Gorb, S. (2002) Attachment ability of the beetle *Chrysolina fastuosa* on various plant surfaces. *Entomol. Exp. Appl.,* **105**(1), 13–28.

[40] Friedemann, K., Spangenberg, R., Yoshizawa, K., and Beutel, R. G. (2014) Evolution of attachment structures in the highly diverse Acercaria (Hexapoda). *Cladistics,* **30**(2), 170–201.

[41] Federle, W., Brainerd, E. L., McMahon, T. A., and Hölldobler, B. (2001) Biomechanics of the movable pretarsal adhesive organ in ants and bees. *Proc. Natl. Acad. Sci.,* **98**(11), 6215–6220.

[42] Stenberg, C., Svensson, M., and Johansson, M. (2005) A study of the drying of linseed oils with different fatty acid patterns using RTIR-spectroscopy and chemiluminescence (CL). *Ind. Crops Prod.,* **21**(2), 263–272.

[43] Flory, P. (1953) Principles of polymer chemistry, Cornell University Press, Ithaca, NY.

[44] Johnston, I. D., McCluskey, D. K., Tan, C. K. L., and Tracey, M. C. (2014) Mechanical characterization of bulk Sylgard 184 for microfluidics and microengineering. *J. Micromechanics Microengineering,* **24**(3), 35017.

[45] Efimenko, K., Wallace, W. E., and Genzer, J. (2002) Surface Modification of Sylgard-184 Poly(dimethyl siloxane) Networks by Ultraviolet and Ultraviolet/Ozone Treatment. *J. Colloid Interface Sci.,* **254**(2), 306–315.

[46] Zovi, O., Lecamp, L., Loutelier-Bourhis, C., Lange, C. M., and Bunel, C. (2011) Stand reaction of linseed

oil. *Eur. J. Lipid Sci. Technol.,* **113**(5), 616–626.

[47] Clemente, C. J., Bullock, J. M. R., Beale, A., and Federle, W. (2010) Evidence for self-cleaning in fluid-based smooth and hairy adhesive systems of insects. *J. Exp. Biol.,* **213**(4), 635–642.

[48] McClements, D. J. (2015) Food Emulsions, CRC Press, Boca Raton.

[49] Lambourne, R. and Strivens, T. A. (1999) Paint and Surface Coatings, Woodhead Publishing, Cambridge 2nd edition.

[50] Oyman, Z. O., Ming, W., and van der Linde, R. (2003) Oxidation of model compound emulsions for alkyd paints under the influence of cobalt drier. *Prog. Org. Coatings,* **48**(1), 80–91.

[51] Hulden, M., Bergenstahl, B., Holmberg, K., and Ostberg, G. (1994) Alkyd emulsions. *Prog. Org. Coatings,* **24**, 281–297.

[52] Welch, R. M. and Shuman, L. (1995) Micronutrient Nutrition of Plants. *CRC. Crit. Rev. Plant Sci.,* **14**(1), 49–82.

[53] Brown, S. L., Angle, J. S., Chaney, R. L., and Baker, A. J. M. (1995) Zinc and Cadmium Uptake by Hyperaccumulator *Thlaspi caerulescens* Grown in Nutrient Solution. *Soil Sci. Soc. Am. J.,* **59**(1), 125.

[54] Programme, U. N. E. Finding alternatives to persistent organic pollutants (POPS) for termite management. (2000).

[55] Suryanarayana, C., Rao, K. C., and Kumar, D. (2008) Preparation and characterization of microcapsules containing linseed oil and its use in self-healing coatings. *Prog. Org. Coatings,* **63**(1), 72–78.

[56] Greimel, K. J., Perz, V., Koren, K., Feola, R., Temel, A., Sohar, C., Herrero Acero, E., Klimant, I., and Guebitz, G. M. (2013) Banning toxic heavy-metal catalysts from paints: Enzymatic cross-linking of alkyd resins. *Green Chem.,* **15**(2), 381–388.

[57] Hock, W. K. Spray Adjuvants. (2015).

[58] Federle, W., Riehle, M., Curtis, A. S., and Full, R. J. (2002) An integrative study of insect adhesion: mechanics and wet adhesion of pretarsal pads in ants. *Integr. Comp. Biol.,* **42**(6), 1100–1106.

[59] Song, Y., Dai, Z., Wang, Z., Ji, A., and Gorb, S. N. (2016) The synergy between the insect-inspired claws and adhesive pads increases the attachment ability on various rough surfaces. *Sci. Rep.,* **6**, 26219.

[60] Arditty, S., Whitby, C. P., Binks, B. P., Schmitt, V., and Leal-Calderon, F. (2003) Some general features of limited coalescence in solid-stabilized emulsions. *Eur. Phys. J. E,* **11**(3), 273–281.

[61] Stetefeld, J., McKenna, S. A., and Patel, T. R. (2016) Dynamic light scattering: a practical guide and applications in biomedical sciences. *Biophys. Rev.,* **8**(4), 409–427.

[62] Scott, M. J. and Jones, M. N. (2000) The biodegradation of surfactants in the environment. *Biochim. Biophys. Acta - Biomembr.,* **1508**(1-2), 235–251.

[63] Hupman, K. *Chrysoperla carnea.* `https://wiki.bugwood.org/Chrysoperla_carnea` (2015) (accessed 08.03.2019).

[64] Kakkar, G., Kumar, V., McKenzie, C., and Osborne, L. S. cucumeris mite - *Neoseiulus cucumeris.* `http://entnemdept.ufl.edu/creatures/BENEFICIAL/Neoseiulus_cucumeris.htm#top` (2016) (accessed 08.03.2019).

[65] Mao, R., Xiao, Y., and Arthurs, S. P. vespiform thrips - *Franklinothrips vespiformis.* `http://entnemdept.ufl.edu/creatures/BENEFICIAL/vespiform_thrips.htm` (2015) (accessed 08.03.2019).

[66] Khot, L. R., Sankaran, S., Maja, J. M., Ehsani, R., and Schuster, E. W. (2012) Applications of nanomaterials in agricultural production and crop protection: A review. *Crop Prot.,* **35**, 64–70.

7

General discussion

7.1 Introduction

This thesis aimed to investigate novel, eco-friendlier alternatives to insecticides for use in buildings and agriculture. As reviewed in **Chapter 2**, insect pests are detrimental to human activity, in particular to buildings, agriculture, forestry and health. While pesticides are an efficient way to tackle them, they often pose health and environmental issues [1, 2].

Alternatives to insecticides include, but are not limited to: biological pest control, plant-based repellents, slippery surfaces or particle-transferring films [3–7] (**Chapter 2**). In many cases these strategies are inspired by natural insect-repelling mechanisms, as many plants deter herbivores by chemical or physical means. We studied eco-friendlier paint coatings and crop protection sprays which "repel" insects *via* mechanical means inspired by the carnivorous plant *Nepenthes alata* and by plant surfaces covered in trichomes, respectively. The former possesses inner walls covered in epicuticular wax crystals, which are very slippery to many ant species due to their detachability and fluid-absorbing properties [8]. The latter plant presents sticky adhesive droplets to capture and digest insects on the surface of their leaves [9].

We provide answers to the questions addressed at the beginning of the thesis: what formulating parameters are important to produce (1) wall paints slippery to *Atta cephalotes* ants?

and (2) spray emulsions sticky to *Frankliniella occidentalis* thrips on plants? This chapter aims to provide guidelines to formulators and we therefore address the following underlying questions: (i) the importance of the choice of the pigment (diameter, type) and (ii) of the polymer binder (size, glass transition temperature (T_g) and type) to provide slipperiness to paints; and (iii) the importance of formulation parameters for the formation of adhesive beads with regards to emulsion sprays for crop protection will then be summarised. Some of these aspects have not been mentioned in the chapters related to coatings, preliminary results will hence be discussed. Questions relating to further research will then be examined.

7.2   Coatings slippery to insects (*Atta cephalotes* ants)

Existing solutions preventing insects from adhering and climbing surfaces include SLIPS (Slippery liquid infused porous surfaces) and Fluon (PTFE) coatings [5, 6]. The former is based on the combination a porous solid infused by a lubricant inspired from the peristome surface of *Nepenthes* plants [10]. The latter are slippery coatings employed in insect nest containers to prevent them from escaping as they possess detachable particles which adhere to insects' legs (**Chapter 3**). Fluon coatings are however expensive solutions [11, 12]. Cheaper alternatives may include paints: Zhou produced paint prototypes which were found to be slippery to several insect species, likely due to substrate roughness [13]. The work presented in this section is the continuation of this project, our results showed that the slipperiness in our paints is partly due to particles detaching from the coatings and contamination insects' pads.

Pad contamination can impede insect locomotion [14–16] and is overcome by self-cleaning, *i.e.* by means of grooming, brushing or by using special structures [16–19]. Bringing their pads into contact with a surface with greater attraction forces to these contaminating particles has also been suggested to impact self-cleaning [20].

In **Chapters 3-5**, we studied ant-slippery paints which were inspired by the inner wall surface found in some species of pitcher plants: in both cases, their anti-adhesive properties to insects are mainly due to particles detaching from the surfaces and adhering to insect pads [8]. We found in **Chapter 3** that the efficacy of the paint slipperiness primarily lies in the balance between the amount of polymer binder and pigment, the PVC (Pigment Volume Concentration). In other words, when there is not enough polymer binder to wet all pigment particles, they detach from the paint coatings, adhering to the sticky feet of *Atta cephalotes* L. (Hymenoptera,

Formicidae). This leads to a loss of contact between the pad/substrate and the insect is hence likely to slide from the surface before the pad can self-clean. Optimising particle detachment to reduce self-cleaning and improve surface slipperiness is therefore of importance and can be easily tailored through the choice of pigment and binder properties. In the next sections, we compare the findings obtained in **Chapters 3-5** to understand what mechanisms provide slipperiness to insects in paint coatings. Preliminary results on the type of pigment and binder as well as binder T_g which have not been presented in previous chapter are discussed here.

7.2.1 Importance of pigment

Pigment diameter

The fouling particle size has been demonstrated to impact self-cleaning of ant pads [20], but not those of stick insects [18]. It has also been suggested that small particles contaminate ant pads when smaller than the claw basal distance [20, 21]. We review in this section how the size of the pigments employed in paints affected slipperiness.

In **Chapter 3**, we showed that 1 μm CaCO$_3$ particles adhered better to the sticky feet of *A. cephalotes* than 300 nm TiO$_2$ particles. Our results also demonstrated that the self-cleaning time increases with the PVC.

Paints containing different grades of CaCO$_3$ particles (1-45 μm, $d_{50\%}$ values) in the presence of a 64 nm acrylic latex showed an optimum slipperiness for 10 μm particles (**Chapter 4**). However, the calcium carbonate particles have a very broad distribution and small particles (ca. 1 μm) were found to have adhered to insect tarsi for every grade (Figure 7.1). We therefore attribute the observed dependence on the slipperiness to a change in roughness: the extender pigment diameter influences the roughness of the coating, and the slipperiness decreased for paints displaying asperity sizes larger than the claw tip diameter (5.0 $\pm$ 1.7 μm), as observed for other insects [22, 23].
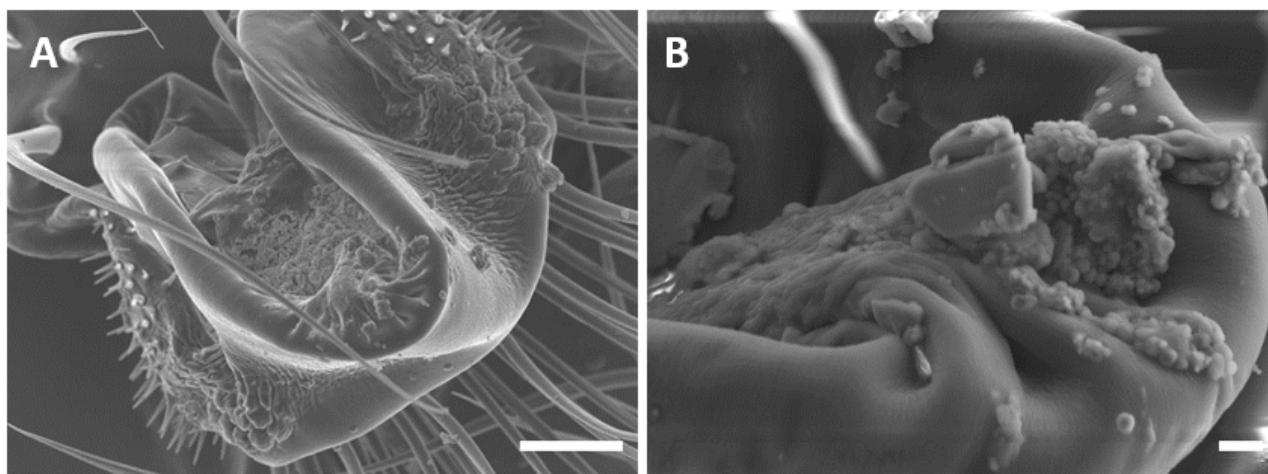
Figure 7.1: CaCO₃ particles observed under SEM on arolia of *Atta cephalotes* ants after climbing a paint formulated with 45 μm ($d_{50\%}$) extender particles. Only the smaller particles were observed (ca. 1 μm). Scale bars: (A) 10 μm and (B) 1 μm.

Importantly, several ant leg samples exhibited either haemolymph (blood) or damaged arolia under SEM after the ants climbed the paints containing extender pigments larger than 5 μm, which probably further impeded their locomotory behaviour (**Chapter 5**). However, we did not observe insects dying after climbing due to pad abrasion [24].

These results highlight the complexity of the slipperiness mechanism induced by our paints. In addition to the pigment diameter, statistical analysis in **Chapter 3** showed that the slipperiness was due to a combination between PVC, surface roughness, wettability and peak density. The effect of pigment type is reviewed in the next section.

Pigment type

In addition to particle size, the self-cleaning time has been found to be impacted by the surface energy of fouling particles [21]. It has been observed in **Chapter 3** that ant pads detached platelet-shaped CaCO₃ particles more easily than the spherical TiO₂ particles. Is this only due to particle size, or also because of shape or chemistry effects? To test this, we investigate here three different silicate extenders: kaolin, mica, and talc. The grades of kaolin, mica and talc chosen here are thin, platy particles with diameters ranging between 1.6-5.0 μm and present large oil absorption (OA) values (Table 7.1).

Paints formulated with 20 wt% extender pigment in the presence of SDS and a 64 nm acrylic latex at PVC 60 and 70 were characterised in terms of surface roughness, wettability, porosity

Table 7.1: Pigment and extender pigments used in this study. OA is oil absorption, *i.e.* the required amount of linseed oil to saturate 100 grams of pigment or extender, which indicates how much binder will be needed to wet the solid particles. The Critical Pigment Volume Concentration (CPVC) is calculated from OA values [25]. [a]: values stated by the suppliers. Examples of platelet and thin platy morphologies are given in Figure 7.2.

Extender	Supplier	Type	Morphology	Size $(d_{50\%}, \mu m)^a$	OA $(mL/100g)^a$	CPVC (%)
Tiona 595	Cristal (Grimsby, UK)	Titania	Spherical	0.3	19	54
Omyacoat 850 OG	Omya (Orgon, France)	Chalk	Platelet	0.9	21	63
ASP 170	BASF (Florham Park, NJ, USA)	Kaolin	Thin platy	1.6	45	44
Mica Mu M2/1	Imerys (Toulouse, France)	Mica	Thin platy	5.0	65	35
Jetfine 1	Imerys (Toulouse, France)	Talc	Thin platy	3.5	70	32

(PVC 70 paints only) and slipperiness to *A. cephalotes* ants.

We showed in **Chapter 3** that the PVC increase is the main driving factor to enhance coating slipperiness to ants when using $CaCO_3$ particles. It does not seem to be the case for all particle types, as the slipperiness was found to be greater for PVC 60 paints containing TiO_2 (due to larger cracks providing grip to insect claws at PVC 70), talc and mica (Figure 7.2A).

One would expect pigments exhibiting large OA values to be easily detached from the coatings at a given PVC as these lead to low CPVC values [25]. However, the paints in this study were not very slippery (max. 85% for the talc, 60% PVC paint), and paints formulated with mica showed little slipperiness (OA 65, Figure 7.2A), while calcium carbonate and kaolin performed similarly at PVC 70 (OA 21 vs. 45, Figure 7.2A) (slipperiness × OA, Pearson's r = 0.19, $P = 0.590$). Only the pigment type, regardless of their shape and size, significantly impacted the slipperiness at both PVCs (one-way ANOVA, $F = 14.97, P < 0.001$).

One could think that the thin, platy shape of particles favour large pad attachment forces due to their large surface-area-to-volume ratio, making them less slippery to insects. When comparing the slipperiness obtained for platelet ($CaCO_3$) and thin platy (silicates) extenders (Figure 7.2B, C), the shape of the particles was found not to have a significant impact on the slipperiness (*t*-test, $t = 0.085, P = 0.93$). Spherical (TiO_2) particles were not considered in the test as the low slipperiness ($\leq 10\%$) in these paints is driven by the cracks (**Chapter 3**).

In comparison with the paints formulated with chalk, SEM highlighted that there more loose particles on top of the silicate coatings than with mica and talc (3.5 μm and 5.0 μm,

respectively) (Figure 7.2C). For the paint containing mica (5.0 μm, $d_{50\%}$), the particles coming out of the paint film's surface were large (31.2 μm $\pm$ 12.1 μm, $n = 43$). For the silicate paints, only a few individual particles were observed on insect tarsi under SEM. Therefore, rather than due to their shape, particles with sizes larger than 3.5 μm ($d_{50\%}$) are likely too large to contaminate the sticky pads of *A. cephalotes* ants, as observed in **Chapter 5** (Figure 7.2A) [21].

Rather than their shape and OA, the diameter of the extender pigments impacts the slipperiness: increasing $d_{50\%}$ diameters between 0.3 and 3.5 μm optimised the slipperiness for insects (**Chapter 5**). This suggests that in addition to the pigment diameter, the relative pad/particle and binder/particle interactions are also important factors impacting insect attachment.

We showed that the choice of pigment can significantly impact the slipperiness to insects. From a practical perspective, we provide the following guidelines on its choice: if one wants to use this type of paints to provide slipperiness on outdoor walls, the PVC of the paints should be reduced, so they resist weathering and rain. A PVC decrease could be performed using a 3.5 μm talc extender to provide similar levels of slipperiness to ants to the ones obtained with the 0.9 μm CaCO$_3$ grade used in **Chapter 3**. If used indoors, PVC 70 paints are very efficient when formulated with 10 μm CaCO$_3$ particles in combination with a 65 nm acrylic latex at PVC 70.
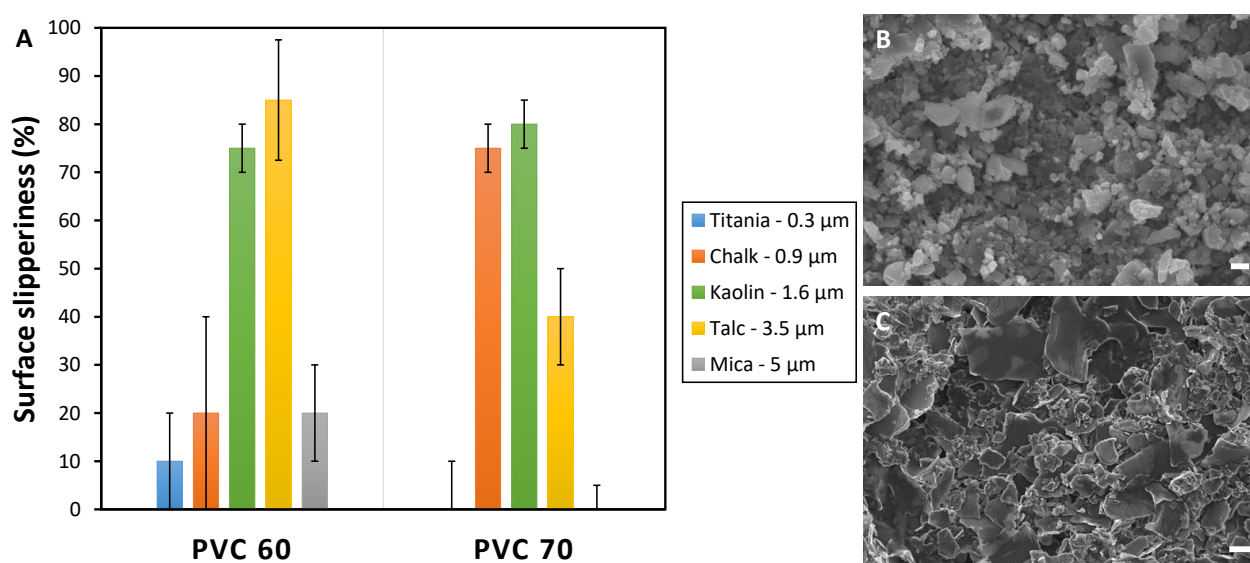

Figure 7.2: (A) Slipperiness to *A. cephalotes* (ratio of fallen off ants) comparison of 20 wt% pigment PVC 60 and 70 paints for TiO$_2$, CaCO$_3$ and silicate paints. (B) SEM of 20 wt% CaCO$_3$ PVC 70 paint. CaCO$_3$ particles are platelet-shaped. (C) SEM of 20 wt% mica PVC 70 paint. Coatings made of silicate particles (platy particles) showed little porosity. Scale bars: 1 μm.

7.2.2 Importance of polymer binder

Binder size

On the inner wall of some *Nepenthes* pitcher plants, the epicuticular wax crystals have been suggested to absorb the adhesive fluid secreted by insects, leading to a loss of contact between their pads and the surface (fluid absorption hypothesis) [26, 27]. In addition, the hairy pads of *Coccinella septempunctata* (L.) (Coleoptera, Coccinellidae) beetles have been found to generate lower attachment forces on surfaces with increasing porosity as their fluid is absorbed by pores [28]. Therefore, can porous paint coatings perform similarly?

We have, in **Chapter 5**, prepared porous paint coatings by increasing the size of the latex binders (sized between 65 and 850 nm), which also reduces the Critical Pigment Volume Concentration (CPVC) as well as the wettability as less surfactant is used [29, 30]. The slipperiness to *A. cephalotes* increased with both larger binders and lower surfactant amounts. Lower CPVC values should also favour particle detachment when PVC > CPVC for large PVC values (**Chapter 3**). We hypothesised in **Chapter 5** that paints made of 'large' (> 250 nm) latexes were very slippery to ants as the pores absorbed their adhesive fluid, resulting in a loss of contact between the pad and the paint. The secretion has several uses to insects: (1) it provides attachment through capillary forces (wet adhesion) [27, 31], (2) fills in substrate protrusions to compensate surface roughness [14, 32–34], and (3) ensures rapid pad detachment from surfaces [32, 35] (**Chapter 2**).

Tailoring the binder particle size offers a simple solution to formulate slippery coatings to ants. We found that the use of 'large' acrylic latexes (> 250 nm) in the presence of 0.9 μm CaCO$_3$ particles produced very slippery paints. However, increasing the binder size negatively affects the water permeability and scrub resistance, two essential parameters for outdoor paints. One therefore needs to take into consideration this delicate balance to optimise paint properties and slipperiness. We review in the two following sections if in addition to particle size, the binder T_g and chemistry may be tuned to maximise slipperiness.

Binder T_g

In addition to the work carried out in **Chapter 5**, we did preliminary work to study the effect of glass transition temperature (T_g) of the binder on slipperiness to ants. High T_g polymer films are acknowledged to be less tacky than low T_g ones [36]. To assess whether T_g can impact ant attachment, paints were formulated with 20 wt% extender pigment (0.9 μm $CaCO_3$) in the presence of SDS and acrylic latexes of increasing T_g (from -10.7 to 47.8°C) and a constant particle size (88 ± 3 nm, single factor ANOVA, $F_{4,5} = 0.39$, $P = 0.806$) at PVC 60 and 70. The T_g was varied by changing the ratio between monomers, methyl methacrylate (MMA) and butyl methacrylate (BA) (Table 7.2).

In this work, the slipperiness was impacted significantly by PVC ($r = 0.60$, $P = 0.042$) and water contact angles measured on paints ($r = 0.75$, $P = 0.013$). These results are in line with the PVC > CPVC condition, as there was not enough polymer to fully wet all extender pigment particles. Toikka *et al.* noted that pull-off forces between micron-sized solid particles and polymer films were largest when $T \approx T_g$ ($T_g = 43$°C, with T ranging between 20-70°C) and this is what we observe here at PVC 60 as the slipperiness was the lowest for the paint formulated with latex 11 (T_g 24.7°C ± 0.4°C) [37]. However, the T_g of the coatings did not significantly influence insect attachment as similar slipperiness values were obtained for all latexes for both PVCs (82% ± 11%, $r = -0.34$, $P = 0.342$) (Figure 7.3B, PVC 70 paints).
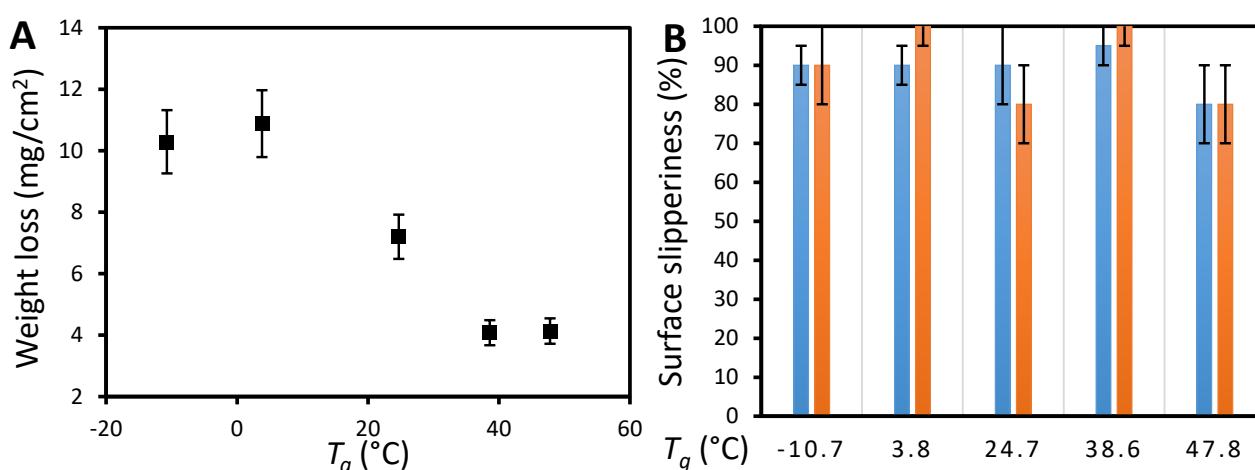

Figure 7.3: (A) Weight loss of paints scrubbed to 2000 cycles vs. glass transition temperature (T_g) of the latexes used in the paints. S.D. values of T_g are below 0.5°C and are hence not visible. (B) Surface slipperiness of PVC 70 paints before (blue bars) and after (orange bars) the paints were cycles for 2000 cycles.

Table 7.2: Latexes employed in this study, with varying T_g and constant particle size (84 $\pm$ 8 nm). The values are expressed as mean $\pm$ standard deviation (SD).

Latex	Composition (MMA/BA/AA)	Particle size (nm)	T_g (°C)
13	30/67/3	87 $\pm$ 1	-10.7 $\pm$ 0.2
14	40/57/3	90 $\pm$ 1	3.8 $\pm$ 0.1
11	45/52/3	92 $\pm$ 2	24.7 $\pm$ 0.4
15	60/37/3	84 $\pm$ 1	38.6 $\pm$ 0.1
16	65/32/3	89 $\pm$ 1	47.8 $\pm$ 0.1

Interestingly, the T_g of the coatings negatively correlated to the weight loss occurring after performing scrub resistance tests (r = -0.95, P = 0.014) (Figure 7.3A). The PVC 70 paints showed excellent slipperiness values once scrubbed (min. 80%), as $CaCO_3$ particles were easily detached by ant pads (Figure 7.3B). This is of interest for further applications: high T_g latexes can maximise the scrub resistance at equal slipperiness performances.

Binder type

During the research it became clear that the binder type is also of key importance to provide slipperiness and is a topic that needs further investigation in the future, as underlined by the promising preliminary data described in this section. Minimising the adsorption of polymer onto pigment or extender particles could indeed improve slipperiness to *A. cephalotes* ant workers as their sticky pads detach particles from the coating (**Chapters 3-5**). Several studies showed that selecting the right binder can decrease pigment agglomeration [30, 38–40]. In particular, Farrokhpay and colleagues investigated the adsorption isotherms of various polymers on titania [41–43]. They found that polymers adsorb onto TiO_2 particles *via* anionic and hydrogen bonding between TiO_2's hydroxide groups and polymers' carboxylate groups. Therefore, stronger interactions are favoured when the pH is lower than the isoelectric point of the pigment [41].

We carried out preliminary investigations to study the effect of the polymer type on slipperiness. Common acrylic monomers used in waterborne latexes were used in the following study: methyl methacrylate (MMA), 2-ethylhexyl acrylate (EHA), butyl acrylate (BA), vinyl acetate (VA) and acrylic acid (AA). The use of 3% AA ensured that the latexes were negatively charged at the working pH (ca. pH 8). The latexes obtained are separated into two groups of same particle size and T_g: (1) 143 $\pm$ 7 nm, T_g 30.8°C $\pm$ 2.2°C and (2) 197 $\pm$ 8 nm, T_g 29.6°C

Table 7.3: Latexes employed in this study, with different monomer compositions and constant T_g and varying particle size across groups (group 1: T_g 30.8 ± 2.2°C, 143 ± 7 nm; group 2: T_g 29.6 ± 2.3°C, 197 ± 8 nm). The values are expressed as mean ± standard deviation (SD).

Latex	Group	Composition	Particle size (nm)	T_g (°C)
MB-1	1	52/45/3 (MMA/BA/AA)	134 ± 1	28.3 ± 0.5
ME-1	1	59/38/3 (MMA/EHA/AA)	144 ± 1	33.7 ± 2.1
VB-1	1	79/18/3 (VA/BA/AA)	150 ± 1	30.3 ± 0.8
MB-2	2	52/45/3 (MMA/BA/AA)	187 ± 1	26.7 ± 0.4
ME-2	2	59/38/3 (MMA/EHA/AA)	207 ± 1	32.4 ± 5.1
VB-2	2	79/18/3 (VA/BA/AA)	197 ± 1	29.6 ± 0.8

± 2.3°C (Table 7.3). The polymers of group 2 were formulated with less surfactant (SDS) and were hence larger. These binders were incorporated in PVC 60 and 70 paints containing 20 wt% $CaCO_3$ (Omyacoat 850 OG) stabilised by SDS.

In this work, the paints made from ME and VB latexes were very slippery for *A. cephalotes* ant workers (min. 70% ants fell off from the panels). The slipperiness increased with PVC ($r = 0.64$, $P = 0.026$), as shown in Figure 7.4A for the paints formulated with latexes from group 2. One can see that ME and VB latexes increased the slipperiness compared to MB polymers (30% vs. 70% slipperiness at PVC 60).

The data suggest that the binders employed in this study presented different binding abilities (adsorption) with $CaCO_3$ particles. All polymers were formulated with 3% AA, *i.e.* the latex particles had similar negative charge coverages. At the working pH (ca. pH 8), $CaCO_3$ particles are negatively charged, so that repulsive interactions are expected to lower the adsorption of polymer onto particles [41]. Hydrogen bonding was found to be the main interaction between TiO_2 particles and polymers with carboxylic groups [39, 44]. In our dry paints, polar interactions are likely responsible for binding between acrylic polymers and $CaCO_3$.

Once coated on metal sheets, the VB latex paints showed low aggregation at the macroscopic level whereas the MB and ME binders led to the formation of some agglomerates at the surface of the coatings [38]. This may suggest that VB polymers adsorb to chalk particles more strongly to prevent its self-aggregation and that both $CaCO_3$ and VB latex particles remain stable during the drying process [40, 47]. However, all latex particles approximately possessed similar monomer functionalities and similar AA coverage.
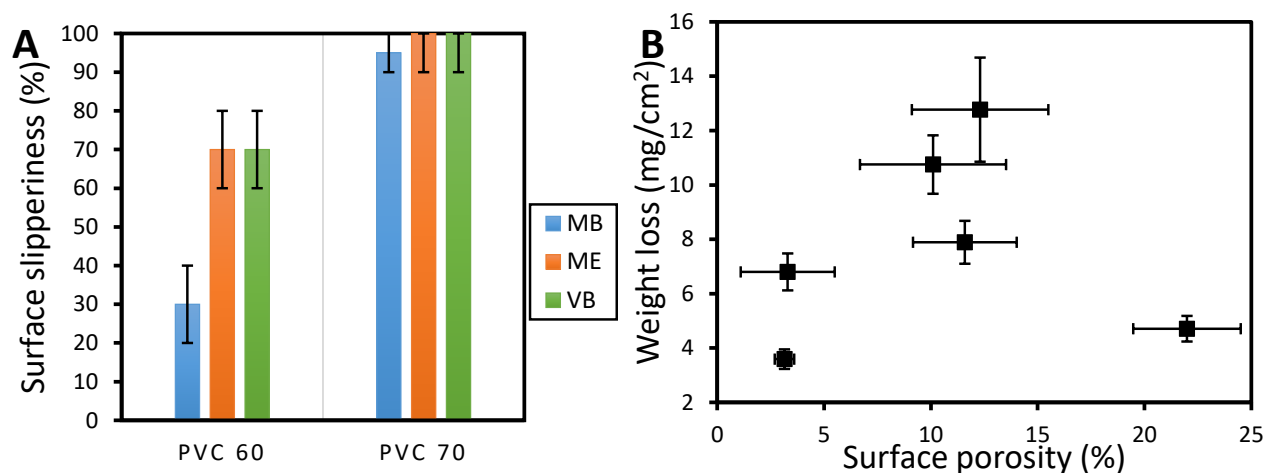
Figure 7.4: (A) Surface slipperiness to *A. cephalotes* (ratio of fallen off ants) of paints formulated with latexes from group 2 (197 ± 8 nm, T_g 29.6°C ± 2.3°C) at PVC 60 and 70. (B) Weight loss of paints (from both groups) scrubbed to 2000 cycles vs. their surface porosity before being scrubbed. The surface porosity was measured from SEM micrographs according to [45, 46].

As an alternative to adsorption isotherms, one could think that scrub resistance testing could relate to a polymer's binding ability. 70% PVC paints showed various levels of scrub resistance (3.6 to 12.8 mg/cm^2 weight loss), as well as porosity (3.3% to 22.0%), which may influence the weight loss results (Figure 7.4B). Neither data showed any correlation with the slipperiness as the paints at PVC 70 were at least 90% slippery to ants. Paints with VB latexes actually showed the lowest scrub resistance (highest weight loss), which does not support our reduced agglomerate formation observation as this suggests that these polymers have the lowest binding ability. Scrub resistance is mainly impacted by both binding ability and hydrophilicity of the latex as tested in a surfactant medium [48]. The VB latexes were indeed the most hydrophilic among the tested polymer binders. After climbing on all paint surfaces, regardless of their scrub resistance, ants' pads were found to be heavily contaminated with CaCO$_3$ particles (Figure 7.5).

The slipperiness cannot only be explained by the binding ability of the polymer, as the change of binder chemistry also likely affected coating hardness and yield strength (not tested here) [39, 49]. It is known that insect claws or spines can dig into soft substrates to get a grip [50]. The yield strength and Young's modulus of a coating were found to increase for strongly bound pigment-polymer systems or for latexes having large acid surface coverage [39].

This section provided a useful insight into the tuning of the size, T_g and chemistry of the polymer binder to efficiently maximise slipperiness. We showed in **Chapter 5** that porosity increases with the particle size of the polymer. For commercial purposes, paints combining low porosity, high scrub resistance and high slipperiness would be of interest. Low porosity would
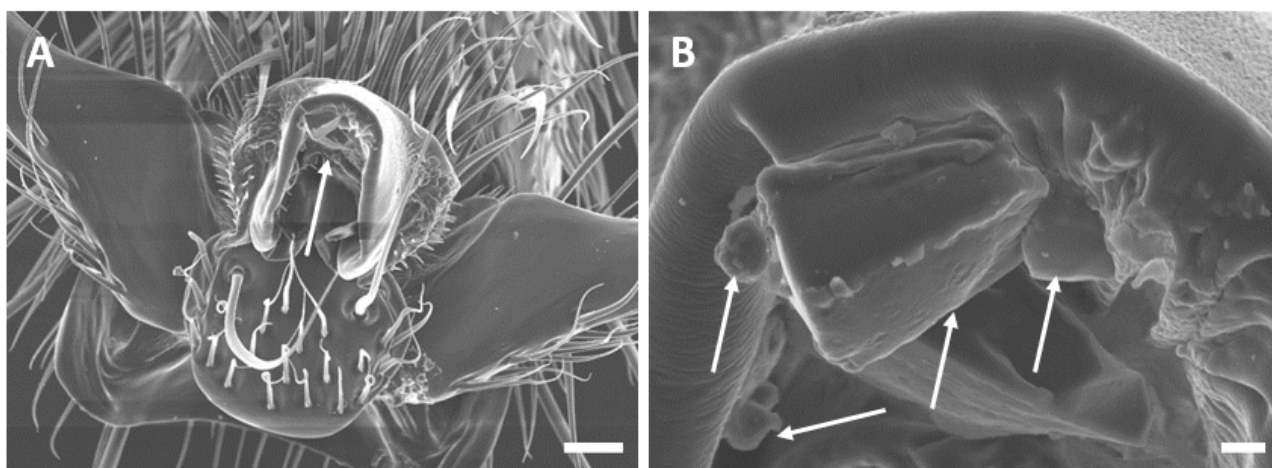
Figure 7.5: SEM micrographs of an *A. cephalotes* tarsi after climbing tests on the 70% PVC paint formulated with latex VB-1. Arrows show CaCO₃ particles which detached from the coating. Scale bars: (A) 10 μm and (B) 1 μm.

ensure reduced water permeability. Paints incorporating ME-1 binders (MMA/EHA/AA) fulfil these conditions. Alternatively, if used for outdoor applications, they could be used at PVC 60 as they led to acceptable slipperiness performances (70%-80%).

7.2.3 Importance of surface parameters

In addition to PVC, other surface parameters, namely the surface roughness (R_a), wettability and porosity were found to affect attachment of ants to paint coatings in **Chapters 3** and **5**. We also discuss the limitations related to surface roughness measurements and to the downsides of an increase in porosity in paints.

Surface roughness (asperity size)

The effect of roughness (asperity size) on insect attachment have been widely studied in literature and summarised in **Chapter 2** (Figure 7.6). In short, fluid-mediated adhesion in insects occurs by means of a two-fold mechanism. Insects use their adhesive pads (either smooth or hairy) which secrete an adhesive fluid to reduce friction to attach to 'smooth' surfaces (asperity size < 50 nm) [23, 27, 32]. Their claws cling to surface protrusions on 'rough' substrates with asperities larger than their claw tip diameter (ca. 3 μm), while their adhesive pads secrete an adhesive fluid to compensate surface roughness [22, 32, 34]. In the intermediary roughness range, the attachment forces generated are smallest [23, 51].

In paints, the impact of surface roughness (R_a) has proven to be difficult to understand. The exact nature of the roughness profiles of the paints could not be precisely defined as the presence
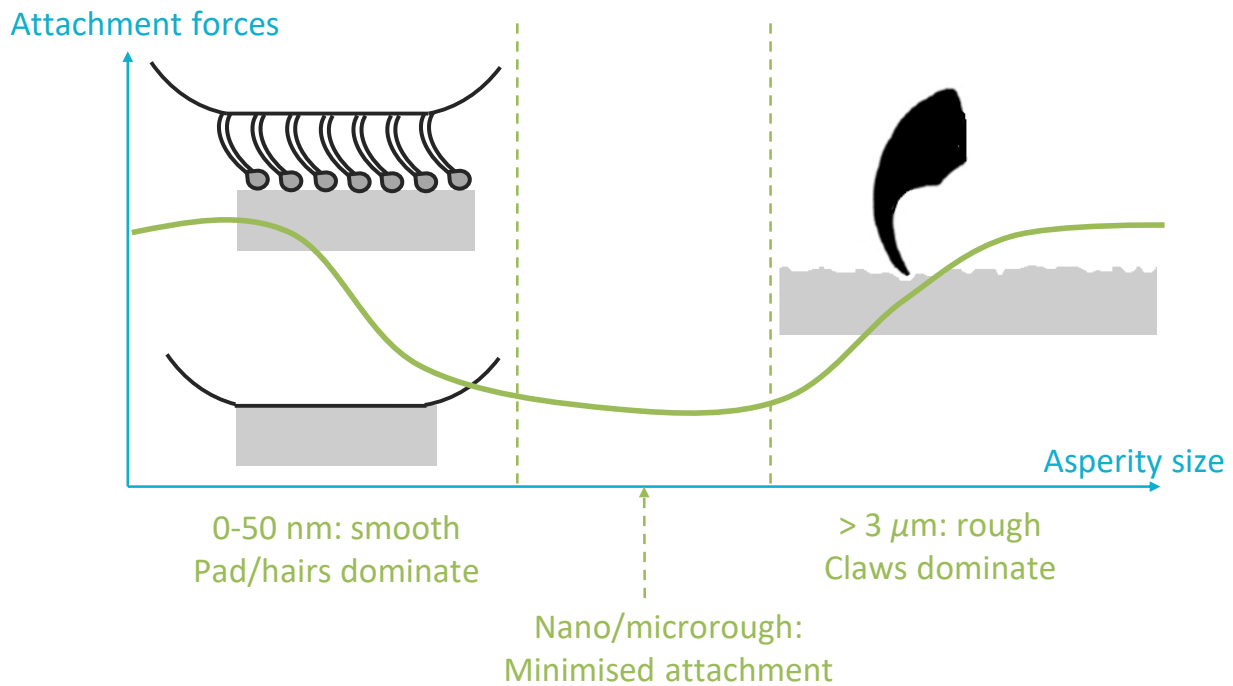
Figure 7.6: Schematic attachment forces generated by insects (both hairy and smooth pads) on surfaces possessing different asperity sizes. It can be divided into three categories: (1) smooth surfaces (0-50 nm asperity size) where adhesion is dominated by smooth pads and hairs, whose adhesive secretion reduces friction forces [32]; (2) nano/microrough substrates where attachment forces are minimised as they are too rough to allow for pad compliance, and the asperities are too small for claw interlocking; (3) claws and spines clinging to asperities dominate attachment on rough surfaces (asperity size > 3 μm), the adhesive secretion compensates surface roughness by filling asperities. The approximate attachment force trend (green curve) is taken from the centrifugal force data obtained with *Gastrophysa viridula* De Geer (Coleoptera, Chrysomelidae) in [23].

of large pigment agglomerates (Z-scale) at the surface of the coatings complicated roughness measurements (by both profilometry and atomic force microscopy), rendering the lateral length scale of asperities negligible. Further investigation of paints with surface roughness well defined at every length scale would help to address this problem, as studied in e.g. [52]. In **Chapter 5** however, when varying the pigment extender diameter, we could estimate the $d_{50\%}$ diameter to be similar to the asperity size. In this case, the slipperiness to ants decreased on rougher substrates, especially for asperity sizes larger than 5 μm, which corresponds to the claw tip diameter of *A. cephalotes* workers.

Surface wettability

Investigating the influence of surface energy (or wettability) on insect attachment is complex as insect pads may be specialised to natural surfaces, e.g. plants [53], which may lead to inconsistencies when studying different types of substrates. For example, beetles were found not to be affected by surface wettability on leaves [54], but generated larger attachment forces

on high energy surfaces [26, 55, 56]. A comprehensive review of insect adhesion on substrates with different surface energies is given in [53]. Overall, insects' attachment abilities seem to be mostly dominated by the substrate roughness rather than surface chemistry [55, 56].

As a rule of thumb, ants slipped more on paints with high water contact angles (**Chapter 3**). We hypothesise that this is mainly due to the fact that both the slipperiness and contact angle increase with the PVC. Preliminary results from Dirks & Federle suggested that smooth pads generate larger adhesive stresses on substrates exhibiting higher dispersive than polar contribution [14]. Our data in **Chapter 4** showed that paints with a greater dispersive contribution presented reduced slipperiness values. In **Chapter 5**, the surface wettability did not significantly affect insect attachment, while surface roughness and porosity were the predominant effects.

Surface porosity

Gorb *et al.* showed that porous Al_2O_3 membranes can absorb the adhesive secretion of C. septempunctata beetles [28]. Beetles generated lower attachment forces on membranes with greater porosity [28].

As mentioned above when we discussed the effect of binder size, increasing the latex particle size led to more porous paint films [29]. The higher the porosity, the more slippery the surface (**Chapter 5**). We therefore hypothesise that our paints also absorb the adhesive fluid secreted by *A. cephalotes* ants. Reduction of the fluid layer would decrease contact between insect pads and the surface, thus favouring sliding from the substrate, as suggested by the fluid absorption hypothesis [26, 28].

To conclude, coating formulators can play on surface parameters to reduce insect attachment forces to substrates. Tuning the surface roughness and porosity seem to be more favourable than the surface wettability as its impact on attachment is still unclear [54–56]. While measuring the surface roughness is not a trivial [23], is it generally acknowledged to increase with the paint PVC [29, 30, 57]. Micro-rough substrates (asperity size between 50 nm and 3 um) would need to be produced. Alternatively, increasing the surface porosity suggested that the pores absorb the ants' adhesive fluid which helps them climb surfaces. However, doing so would lead to potentially undesirable properties, such as enhanced water permeability.

7.2.4 Future perspectives

We prepared model paints containing polymer binder (MMA/BA/AA), pigment ($CaCO_3$ and/or TiO_2) stabilised by SDS and coalescing agent. We studied the impact of formulation and surface parameters on ant slipperiness (**Chapters 3** and **5**) and particle detachment from the coatings (**Chapter 4**). These paints present eco-friendly alternatives to insecticidal paints.

Chapters 3 and **5** showed that the following parameters could maximise the slipperiness to *Atta cephalotes* ant workers:

- Having PVC > CPVC, ideally, PVC 70, which can be tuned with the following:

- Using 'large' acrylic binders (> 250 nm) in combination with 0.9 μm $CaCO_3$ particles.

- Using 10 μm $CaCO_3$ particles in the presence of a 'small' 64 nm sized acrylic binder.

This work highlighted that slipperiness is a complex phenomenon, as the formulation and surface parameters tend to interact with each other (Figure 7.7). Moreover, **Chapter 4** underlined that insect attachment is difficult to reproduce using synthetic adhesive pads made of PDMS. One also needs to take into consideration that there is a delicate balance between optimising slipperiness to ants and paint properties (e.g. scrub resistance, visual appearance, water permeability, etc.) [49].

In this chapter, by using additional data not shown in **Chapters 3-5**, we offered useful insight into optimisation of slipperiness to ants and we can provide the following formulation guidelines:

- Using different extenders than $CaCO_3$: especially, using 3.5 μm talc at PVC 60 to obtain similar slipperiness performances.

- Higher T_g: no effect on slipperiness but leads to better scrub resistance.

- If cost-effective, employing polymer binders with other chemistries than MMA/BA/AA, in particular latexes based on MMA/EHA/AA. Their use is possible at PVC 60.

This research evoked some interesting questions which remain open for further research. At present, the model paints cannot be used in outdoor conditions as they do not contain additives to make them resistant to weathering and rain. In particular, paints exposing many
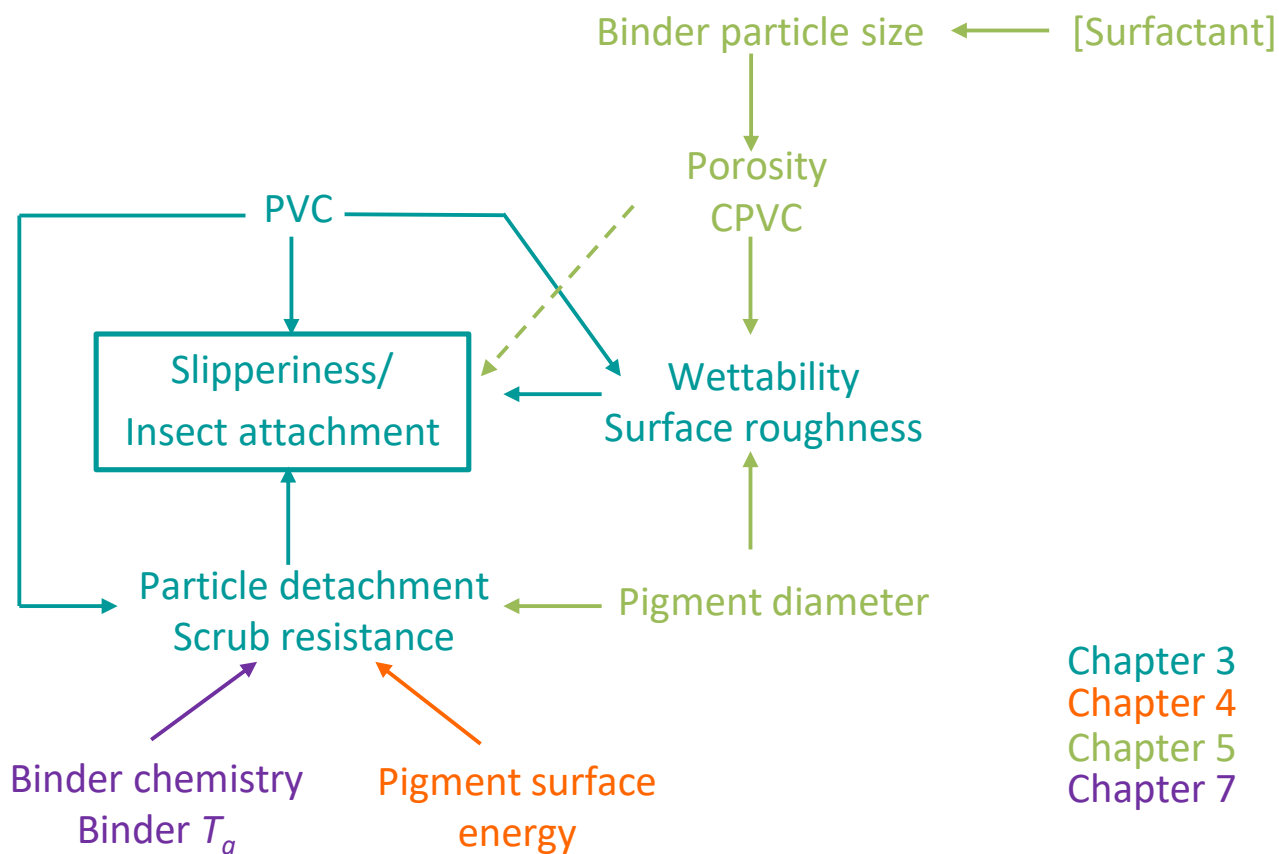
Figure 7.7: Schematic showing the interactions between studied parameters, underlying the complexity of ant slipperiness in our model paints. The different colours indicate in which chapters the parameters influencing ant attachment to paint surfaces were mainly investigated.

calcium carbonate particles at their surface could be problematic as the particles could react with acid rains, which are present in regions where insect-slippery paints would present interest (e.g. Southeast Asia) [58, 59]. However, one could use them as cheaper alternatives to slippery Fluon aqueous dispersions, which are based on PTFE, in insect colonies to coat the walls of nest containers [6]. Therefore, testing the paints in different humidity conditions should be investigated, as Fluon (PTFE) is ineffective in moist conditions [60]. Interestingly, ants' ability to collect loose glass and PTFE particles on their arolia is not affected by humidity [21]. Alternatively, they could be used indoors (e.g. hospitals or restaurants) to trap insects inside buildings, removing the need to use insecticides.

The paints tested in this thesis are simple models prepared with the least number of ingredients. These systems were nonetheless complex to study (Figure 7.7). Essential ingredients needed for commercial paints are: thickeners, which lead to increased stability and less pigment agglomeration; wetting agents to increase the wetting and coverage of a paint on a surface; defoamers to decrease foam formation during application; and paint tinters to add colour. An

optimal dispersant would also reduce pigment aggregation [38, 61]. Eco-friendlier paints could be made from bio-based polymers. They would need to display little adsorption to pigments to ensure they detach to provide slipperiness to insects.

Testing these paints with other insect types is of major importance. **Chapter 4** showed that it is difficult to replicate smooth insect pads to perform JKR adhesion tests instead of climbing experiments. *A. cephalotes ants* were chosen as model insects with relatively good climbing abilities and it is assumed that most insects, regardless of their pad type, would perform similarly to them [13, 34, 62].

To conclude, many questions remain unanswered around the formulation of insect-slippery commercial paints. Further work would benefit from close collaboration between coating and insect scientists.

7.3 Linseed oil-in-water emulsions sticky to insects (*Frankliniella occidentalis* thrips)

Existing sprayable alternatives to insecticides and pesticides employed in agriculture are conventionally based on petroleum-based emulsions [63]. Vegetable and botanical oil sprays are being developed as they are based on a renewable feedstock and do not damage plants as much as petroleum sprays [63–66]. However, volatile sprays require frequent applications [66]. We therefore employed in **Chapter 6** an alternative to pesticides based on adhesion by mimicking glandular trichomes, which release toxic chemicals to insects and/or produce sticky threads to immobilise insects at their surface [9, 67].

To this end, we produced emulsions of sprayable 'sticky' crosslinked linseed oil (LO) droplets stabilised in water to immobilise thrips through permanent adhesion [68], similarly to flytraps. Crosslinking is the result of the autoxidation of linoleic and linolenic acids present in LO by means of oxidation in contact with oxygen, upon exposure to UV, upon heating or by adding drying agents [69, 70]. Crosslinking is needed to ensure bead formation when emulsions are sprayed on leaves, as non-crosslinked oil would lead to coalescence of oil droplets, resulting in an oil film covering the surface [71]. Such strategy may for example reduce the rate of photosynthesis, and LO's unreacted acids may damage plants [63, 72].

We found in **Chapter 6** that both the crosslinking and size of LO beads was crucial to provide adhesiveness to insects once sprayed onto surfaces. Tailoring the size of the beads

may provide selectivity towards immobilisation of insects. The major parameters affecting crosslinking were the reaction time, the size of the primary oil droplets and the amount of oxygen and catalyst. The next sections review how the efficiency of emulsion sprays was optimised to produce tacky LO beads to *Frankliniella occidentalis* (Pergande; Thysanoptera: Thripidae) thrips and how the emulsions can be further improved.

7.3.1   Importance of emulsifier

The choice of emulsifier (ionic or non-ionic) is of major importance as it determines the stability of the emulsion, by causing either steric or electrostatic repulsion [71]. In this work, the emulsifier should be biodegradable as it enters soil upon water rinsing after the emulsion is sprayed on the plant. Cationic emulsifiers cannot be selected as they may be toxic to soils [73].

Four thermo-resistant biodegradable emulsifiers (three non-ionic, one anionic) were used to prepare linseed oil-in-water emulsions. The concentrations of emulsifiers were carefully selected to avoid macroscopic creaming of oil (oiling off) and were hence above their respective critical micelle concentrations (CMC). This led to the production of small LO droplets (< 350 nm).

Small emulsified LO droplets may be subject to slower crosslinking as high emulsifier coverage may reduce the diffusion of oxygen molecules in oil droplets and as larger droplets may encounter oxygen more often [71]. LO droplets consequently crosslink at a slower rate than films of LO as water reduces oxygen diffusion [74], films have been typically studied in the literature to investigate the drying properties of LO [69, 75]. On the other hand, droplet coalescence is faster in small droplets if they are not well stabilised by emulsifier [71].

Although the oil had been subjected to crosslinking treatments for 96 hours (48 hours at 65°C and 48 hours at room temperature), it was not sufficiently crosslinked to form spheres once sprayed onto *Chrysanthemum baltica* (Asterales, Asteraceae) leaves. Once the emulsions are sprayed onto leaves and emulsifier molecules are removed by rinsing, further coalescence occurs if the oils are not sufficiently crosslinked as the viscosity of droplets remains low. We thus observed a homogeneous, glossy film at the surface of the leaves after they were sprayed. The films were however sufficient to reduce silver damage caused by *F. occidentalis* thrips compared to leaves sprayed with water in leaf disc choice bioassays, as they were trapped at the surface of the leaves.

Further crosslinking would prevent the beads from coalescing on substrates. Using other types of emulsifiers, such as reactive surfactants which crosslink with LO's double-bonds and anchors to the surface of oil droplets, may provide faster crosslinking and additional stabilisation towards coalescence. In conclusion, the emulsifier should provide enough droplet stability to prevent coalescence of the dispersed phase and should not be in excess to allow oxygen diffusion into the particles to initiate the reactions in the droplets.

7.3.2   Importance of oil droplet size

As previously discussed, the rate of coalescence is reduced in large oil droplets with reduced emulsifier coverage [71]. Consequently, this may allow for faster crosslinking. In addition, tuning the droplet size, and hence the bead size once applied onto leaves, is important to target one type of insect.

After choosing a single emulsifier to formulate emulsions (Emulsogen LCN 158), we generally observed a decrease in beading time (t_{bead}) for larger LO droplets. t_{bead} is the time after which sufficiently crosslinked droplets form spheres when applied on glass slides. The droplet size, and hence t_{bead}, could be modified by:

- Increasing the amount of oxygen at the air/liquid interface (by bubbling air through emulsions, or by opening vials),

- Adding a drying agent (zinc naphthenate),

- By "pre-crosslinking" LO *via* the preparation of blown oil [76],

- Or by using mechanical agitation rather than shear provided by rotor-stator instruments (Ultra-Turrax).

It is important to note, however, that the emulsions applied on glass produced both beads and coalesced film (**Chapter 6**). This is due to the crosslinking of LO being incomplete, as the low molecular weight crosslinked fractions provide stickiness.

Although we lack data on emulsions producing beads in leaf disc dual choice bioassays, we interestingly found that our model PDMS-in-water emulsions (droplet size 14 μm) could reduce leaf damage and were sticky to *F. occidentalis* thrips. Conversely, they did not impede the locomotion of *A. cephalotes* ants on vertical sprayed glass substrates. Their adhesive pads

(arolia) have evolved differently. *F. occidentalis* possess retractable bladder-shaped arolia of ca. 27 μm in diameter [77], while *A. cephalotes* have an almost circular and smooth, inflatable arolia. The width of the arolia of *Oecophylla smaragdina* (Fab., Hymenoptera, Formicidae) ants varies between 160 and 280 μm, depending on the applied pressure [78].

These "crude" tests provide evidence that selectivity towards insects may be possible with sprayable emulsions of tailored droplet size, as observed in sticky trichomes [67]. This is important to allow e.g. pollinators to access plants, but not pests as they remain trapped at the surface of plants. A simple strategy to maximise the oil droplet size is reducing the fraction of LO in the presence of a minimum amount of emulsifier: with increasing inter-droplet distance, coalescence between droplets would be reduced, and more oxygen would be available to droplets.

7.3.3   Future perspectives

Our proof of concept in **Chapter 6** successfully showed that sticky coatings and spheres made of crosslinked LO, formed after spraying an LO-in-water emulsion, can reduce damage to *C. baltica* leaves by *F. occidentalis* thrips.

After selecting Emulsogen LCN 158 as an emulsifier, the challenging steps in formulation were to obtain (1) sufficiently crosslinked linseed oil beads and (2) sufficiently large beads, summarised in Figure 7.8. These were overcome by:

- Increasing the amount of oxygen,

- Increasing the reaction rate by adding a drying agent,

- By "pre-crosslinking" LO before incorporating it into emulsions,

- Or by using magnetic stirring to obtain coarser emulsions.

At present, once the emulsions are applied to substrates and the water evaporates, the drying oil forms heterogeneous ensembles of tacky beads and coalesced film. The latter is due to incomplete formation of crosslinks, but these fractions do however provide stickiness [69]. Their tackiness may actually decrease over time as they react with air and crosslink over long periods of time [69]. We offer some simple potential solutions to improve the aspect of the sprayed emulsions:

- Further crosslinking which would prevent the beads from having enough flow to coalesce on substrates. Long reaction times were sometimes needed to observe bead formation (e.g. > 600 hours), which should be reduced. Alternatively, UV-treatment has not been tested here and could be used to crosslink LO.

- Reducing the fraction of LO (we used $\phi \approx 0.099$): less oil would increase the distance between droplets, thereby limiting coalescence and increase the amount of oxygen for each droplet.

- Using reactive emulsifiers which form crosslinks with LO's double-bonds and hence anchors to the surface of beads, providing further droplet stabilisation. These emulsifiers would hence not be rinsible by water and should be biocompatible.

- Greimel *et al.* described a novel method to crosslink LO based on laccase-mediator systems. Both the laccase and mediator can be bio-sourced and are thus good alternatives to toxic common metal drying agents [79].

One should be certain that beads applied onto the plants' surface, in addition to dead insects, do not impede the plant's photosynthesis, which would in turn affect its growth and crop yield.
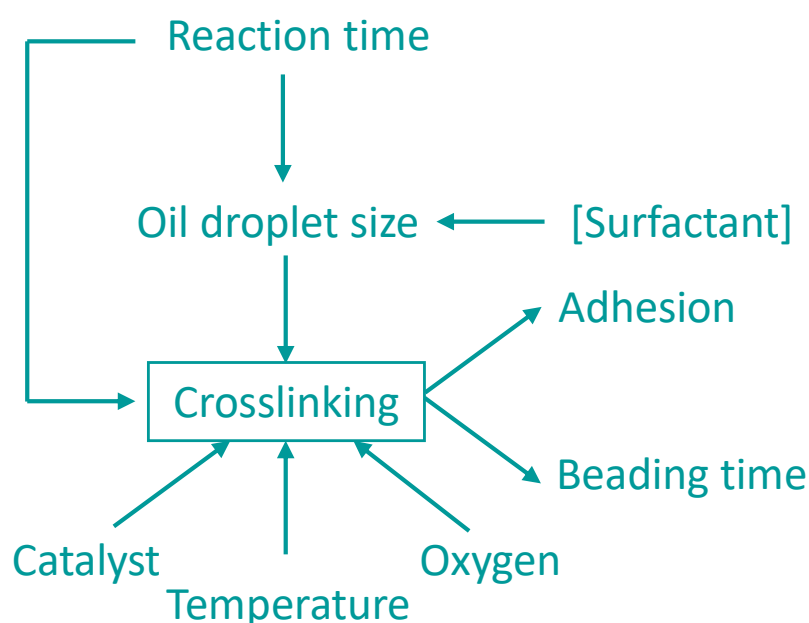

Figure 7.8: Schematic showing the interactions between studied parameters in linseed oil-in-water emulsions to produce sticky oil beads to *F. occidentalis* thrips.

In addition to bead size, the slow release of attractants or deterrents to thrips by incorporating them in the oil phase could improve the insect selectivity. *F. occidentalis* are attracted to many volatiles, e.g. geraniol or linalool, and are repelled by e.g. jasmonic acid derivatives [80, 81]. Our strategy, although only a proof of concept at present, could become a sustainable alternative to pesticides and petroleum-based sprays in agriculture with further research. Their use in the control of thrips could be exploited in combined pest management strategies [80].

References

[1] Pimentel, D. (2005) Environmental and economic costs of the application of pesticides primarily in the United States. *Environ. Dev. Sustain.,* **7**(2), 229–252.

[2] Devine, G. J. and Furlong, M. J. (2007) Insecticide use: Contexts and ecological consequences. *Agric. Human Values,* **24**(3), 281–306.

[3] Meissle, M., Mouron, P., Musa, T., Bigler, F., Pons, X., Vasileiadis, V. P., Otto, S., Antichi, D., Kiss, J., J.; Pálinkás, Z., Dorner, Z., van der Weide, R., Groten, J., Czembor, E., Adamczyk, J., Thibord, J.-B., Melander, B., Cordsen Nielsen, G., Poulsen, R. T., Zimmermann, O., Verschwele, A., and Oldenburg, E. (2010) Pests, pesticide use and alternative options in European maize production: current status and future prospects. *J. Appl. Entomol.,* **134**, 357–375.

[4] Overman, G. R. Method for admixing plant essential oils to coatings for the purpose of repelling insects. (2009) US Patent 20090155394.

[5] Wong, T.-S., Kang, S. H., Tang, S. K. Y., Smythe, E. J., Hatton, B. D., Grinthal, A., and Aizenberg, J. (2011) Bioinspired self-repairing slippery surfaces with pressure-stable omniphobicity. *Nature,* **477**(7365), 443–447.

[6] Chen, J. (2007) Advancement on techniques for the separation and maintenance of the red imported fire ant colonies. *Insect Sci.,* **14**(1), 1–4.

[7] Glenn, D. M. and Puterka, G. J. (2010) Particle films: a new technology for agriculture, Vol. 31, John Wiley & Sons, Inc., .

[8] Scholz, I., Buckins, M., Dolge, L., Erlinghagen, T., Weth, A., Hischen, F., Mayer, J., Hoffmann, S., Riederer, M., Riedel, M., and Baumgartner, W. (2010) Slippery surfaces of pitcher plants: *Nepenthes* wax crystals minimize insect attachment *via* microscopic surface roughness. *J. Exp. Biol.,* **213**(7), 1115–1125.

[9] Huang, Y., Wang, Y., Sun, L., Agrawal, R., and Zhang, M. (2015) Sundew adhesive: A naturally occurring hydrogel. *J. R. Soc. Interface,* **12**(107).

[10] Bohn, H. F. and Federle, W. (2004) Insect aquaplaning: *Nepenthes* pitcher plants capture prey with the peristome, a fully wettable water-lubricated anisotropic surface. *Proc. Natl. Acad. Sci.,* **101**(39), 14138–14143.

[11] Chen, J. and Wei, X. (2007) Coated containers with reduced concentrations of Fluon to prevent ant escape. *J. Entomol. Sci.,* **42**(1), 119–121.

[12] Allison, J. D., Graham, E. E., Poland, T. M., and Strom, B. L. (2016) Dilution of fluon before trap surface treatment has no effect on Longhorned Beetle (Coleoptera: Cerambycidae) captures. *J. Econ. Entomol.,* **109**(3), 1215–1219.

[13] Zhou, Y. (2015) Insect adhesion on rough surfaces and properties of insect repellent surfaces (PhD thesis), University of Cambridge, Cambridge.

[14] Dirks, J.-H. and Federle, W. (2011) Fluid-based adhesion in insects - principles and challenges. *Soft Matter,* **7**(23), 11047.

[15] Amador, G. J. and Hu, D. L. (2015) Cleanliness is next to godliness: mechanisms for staying clean. *J. Exp. Biol.,* **218**(20), 3164–3174.

[16] Hackmann, A., Delacave, H., Robinson, A., Labonte, D., and Federle, W. (2015) Functional morphology and efficiency of the antenna cleaner in *Camponotus rufifemur ants*. *R. Soc. Open Sci.,* **2**(7), 150129.

[17] Persson, B. N. J. (2007) Biological Adhesion for Locomotion on Rough Surfaces: Basic Principles and A Theorist's View. *MRS Bull.,* **32**(6), 486–490.

[18] Clemente, C. J., Bullock, J. M. R., Beale, A., and Federle, W. (2010) Evidence for self-cleaning in fluid-based smooth and hairy adhesive systems of insects. *J. Exp. Biol.,* **213**(4), 635–642.

[19] Mengüç, Y., Röhrig, M., Abusomwan, U., Hölscher, H., and Sitti, M. (2014) Staying sticky: contact self-cleaning of gecko-inspired adhesives. *J. R. Soc. Interface,* **11**(94), 20131205–20131205.

[20] Orchard, M. J., Kohonen, M., and Humphries, S. (2012) The influence of surface energy on the self-cleaning of insect adhesive devices. *J. Exp. Biol.,* **215**(2), 279–286.

[21] Anyon, M. J., Orchard, M. J., Buzza, D. M. A., Humphries, S., and Kohonen, M. M. (2012) Effect of particulate contamination on adhesive ability and repellence in two species of ant (Hymenoptera; Formicidae). *J. Exp. Biol.,* **215**(4), 605–616.

[22] Dai, Z., Gorb, S. N., and Schwarz, U. (2002) Roughness-dependent friction force of the tarsal claw system in the beetle *Pachnoda marginata* (Coleoptera, Scarabaeidae). *J. Exp. Biol.,* **205**, 2479–2488.

[23] Bullock, J. M. R. and Federle, W. (2011) The effect of surface roughness on claw and adhesive hair performance in the dock beetle *Gastrophysa viridula*. *Insect Sci.,* **18**(3), 298–304.

[24] Hackmann, A. (2015) Contamination and biomechanics of cleaning structures in insects (PhD thesis), University of Cambridge, Cambridge.

[25] Asbeck, W. K. and Loo, M. V. (1949) Critical Pigment Volume Relationships.. *Ind. Eng. Chem.,* **41**(7), 1470–1475.

[26] Gorb, E. and Gorb, S. (2002) Attachment ability of the beetle *Chrysolina fastuosa* on various plant surfaces. *Entomol. Exp. Appl.,* **105**(1), 13–28.

[27] Gorb, S. N. (2010) Biological and biologically inspired attachment systems, Springer Berlin Heidelberg, Berlin, Heidelberg.

[28] Gorb, E. V., Hosoda, N., Miksch, C., and Gorb, S. N. (2010) Slippery pores: anti-adhesive effect of

nanoporous substrates on the beetle attachment system. *J. R. Soc. Interface,* **7**(52), 1571–1579.

[29] del Rio, G. and Rudin, A. (1996) Latex particle size and CPVC. *Prog. Org. Coatings,* **28**(4), 259–270.

[30] Alvarez, V. and Paulis, M. (2017) Effect of acrylic binder type and calcium carbonate filler amount on the properties of paint-like blends. *Prog. Org. Coatings,* **112**, 210–218.

[31] Dixon, A. F. G., Croghan, P. C., and Gowing, R. P. (1990) The mechanism by which aphids adhere to smooth surfaces. *J. Exp. Biol.,* **152**(1), 243–253.

[32] Betz, O., Frenzel, M., Steiner, M., Vogt, M., Kleemeier, M., Hartwig, A., Sampalla, B., Rupp, F., Boley, M., and Schmitt, C. (2017) Adhesion and friction of the smooth attachment system of the cockroach *Gromphadorhina portentosa* and the influence of the application of fluid adhesives. *Biol. Open,* **6**(5), 589–601.

[33] Bullock, J. M. R., Drechsler, P., and Federle, W. (2008) Comparison of smooth and hairy attachment pads in insects: friction, adhesion and mechanisms for direction-dependence. *J. Exp. Biol.,* **211**(20), 3333–3343.

[34] Drechsler, P. and Federle, W. (2006) Biomechanics of smooth adhesive pads in insects: Influence of tarsal secretion on attachment performance. *J. Comp. Physiol. A,* **192**(11), 1213–1222.

[35] Labonte, D. and Federle, W. (2015) Rate-dependence of 'wet' biological adhesives and the function of the pad secretion in insects. *Soft Matter,* **11**(44), 8661–8673.

[36] DeFusco, A. J., Sehgal, K. C., and Bassett, D. R. (1997) Overview of Uses of Polymer Latexes, Springer Netherlands, Dordrecht.

[37] Toikka, G., Spinks, G. M., and Brown, H. R. (2001) Fine Particle Adhesion Measured at Elevated Temperatures Using a Dedicated Force Rig. *Langmuir,* **17**(20), 6207–6212.

[38] Tiarks, F., Frechen, T., Kirsch, S., Leuninger, J., Melan, M., Pfau, A., Richter, F., Schuler, B., and Zhao, C.-L. (2003) Formulation effects on the distribution of pigment particles in paints. *Prog. Org. Coatings,* **48**(2-4), 140–152.

[39] Ding, T., Daniels, E. S., El-Aasser, M. S., and Klein, A. (2005) Film Formation from Pigmented Latex Systems: Mechanical and Surface Properties of Ground Calcium Carbonate/Functionalized Poly (*n*-butyl methacrylate-*co-n*-butyl acrylate) Latex Blend Films. *J. Appl. Polym. Sci.,* **100**(6), 4550–4560.

[40] Ding, T., Daniels, E. S., El-Aasser, M. S., and Klein, A. (2006) Film Formation from Pigmented Latex Systems: Drying Kinetics and Bulk Morphologies of Ground Calcium Carbonate/Functionalized Poly (*n*-butyl methacrylate-*co-n*-butyl acrylate) Blend Films. *J. Appl. Polym. Sci.,* **100**(3), 2267–2277.

[41] Farrokhpay, S., Morris, G. E., Fornasiero, D., and Self, P. (2004) Effects of chemical functional groups on the polymer adsorption behavior onto titania pigment particles. *J. Colloid Interface Sci.,* **274**(1), 33–40.

[42] Farrokhpay, S., Morris, G., Fornasiero, D., and Self, P. (2004) Role of polymeric dispersant functional groups in the dispersion behaviour of titania pigment particles. *Prog. Colloid Polym. Sci.,* **128**, 216–220.

[43] Farrokhpay, S., Morris, G. E., Fornasiero, D., and Self, P. (2005) Influence of polymer functional group architecture on titania pigment dispersion. *Colloids Surfaces A Physicochem. Eng. Asp.,* **253**(1-3), 183–191.

[44] Perera, D. Y. (2004) Effect of pigmentation on organic coating characteristics. *Prog. Org. Coatings,* **50**(4), 247–262.

[45] Segmentation - ImageJ. https://imagej.net/Segmentation (accessed 18.11.2018).

[46] Haeri, M. and Haeri, M. (2015) ImageJ Plugin for Analysis of Porous Scaffolds used in Tissue Engineering. *J. Open Res. Softw.,* **3**, 500–512.

[47] Morris, G. E., Skinner, W. A., Self, P. G., and Smart, R. S. C. (1999) Surface chemistry and rheological behaviour of titania pigment suspensions. *Colloids Surfaces A Physicochem. Eng. Asp.,* **155**(1), 27–41.

[48] Oliveira, C. M., Auad, A. M., Mendes, S. M., and Frizzas, M. R. (2014) Crop losses and the economic impact of insect pests on Brazilian agriculture. *Crop Prot.,* **56**, 50–54.

[49] Geurts, J., Bouman, J., and Overbeek, A. (2008) New waterborne acrylic binders for zero VOC paints. *J. Coatings Technol. Res.,* **5**(1), 57–63.

[50] Goetzke, H. H., Pattrick, J. G., and Federle, W. (2019) Froghoppers jump from smooth plant surfaces by piercing them with sharp spines. *Proc. Natl. Acad. Sci.,* **116**(8), 3012–3017.

[51] Voigt, D., Schuppert, J. M., Dattinger, S., and Gorb, S. N. (2008) Sexual dimorphism in the attachment ability of the Colorado potato beetle *Leptinotarsa decemlineata* (Coleoptera: Chrysomelidae) to rough substrates. *J. Insect Physiol.,* **54**(5), 765–776.

[52] Graf, C., Kesel, A. B., Gorb, E. V., Gorb, S. N., and Dirks, J.-H. H. (2018) Investigating the efficiency of a bio-inspired insect repellent surface structure. *Bioinspir. Biomim.,* **13**(5), 56010.

[53] Grohmann, C., Blankenstein, A., Koops, S., and Gorb, S. N. (2014) Attachment of *Galerucella nymphaeae* (Coleoptera, Chrysomelidae) to surfaces with different surface energy. *J. Exp. Biol.,* **217**(23), 4213–4220.

[54] Prüm, B., Florian Bohn, H., Seidel, R., Rubach, S., and Speck, T. (2013) Plant surfaces with cuticular folds and their replicas: Influence of microstructuring and surface chemistry on the attachment of a leaf beetle. *Acta Biomater.,* **9**(5), 6360–6368.

[55] England, M. W., Sato, T., Yagihashi, M., Hozumi, A., Gorb, S. N., and Gorb, E. V. (2016) Surface roughness rather than surface chemistry essentially affects insect adhesion. *Beilstein J. Nanotechnol.,* **7**(1), 1471–1479.

[56] Gorb, E. and Gorb, S. (2009) Effects of surface topography and chemistry of *Rumex obtusifolius* leaves on the attachment of the beetle *Gastrophysa viridula*. *Entomol. Exp. Appl.,* **130**(3), 222–228.

[57] Tang, J., Daniels, E. S., Dimonie, V. L., Klein, A., and El-Aasser, M. S. (2002) Influence of particle surface properties on film formation from precipitated calcium carbonate/latex blends. *J. Appl. Polym. Sci.,* **86**(4), 891–900.

[58] Balik, C. M. and Xu, J. R. (1994) Simultaneous measurement of water diffusion, swelling, and calcium carbonate removal in a latex paint using FTIR-ATR. *J. Appl. Polym. Sci.,* **52**(7), 975–983.

[59] Broad, R., Power, G., and Sonego, A. (1993) Extender Pigments, Springer Netherlands, Dordrecht.

[60] Hölldobler, B. and Wilson, E. (1990) The Ants, Harvard University Press, Cambridge.

[61] Otterstedt, J.-E. and Brandreth, D. A. (1998) Various applications of small particles, Springer US, New York.

[62] Bauer, U. and Federle, W. (2009) The insect-trapping rim of *Nepenthes* pitchers. *Plant Signal. Behav.,* **4**(11), 1019–1023.

[63] DeOng, E. R., Knight, H., and Chamberlin, J. C. (1927) A preliminary study of petroleum oil as an insecticide for citrus trees. *Hilgardia,* **2**(9), 351–386.

[64] Agnello, A. M. (2002) Petroleum-derived spray oils: chemistry, history, refining and formulation, University of Western Sydney, .

[65] Shogren, R. L., Petrovic, Z., Liu, Z., and Erhan, S. Z. (2004) Biodegradation behavior of some vegetable oil-based polymers. *J. Polym. Environ.,* **12**(3), 173–178.

[66] Puri, S., Butler, G. J., and Henneberry, T. (1991) Plant-derived oils and soap solutions as control agents for the whitefly on cotton. *J. Appl. Zool. Res.,* **2**(1), 1–5.

[67] Glas, J. J., Schimmel, B. C., Alba, J. M., Escobar-Bravo, R., Schuurink, R. C., and Kant, M. R. (2012) Plant glandular trichomes as targets for breeding or engineering of resistance to herbivores. *Int. J. Mol. Sci.,* **13**(12), 17077–17103.

[68] Favi, P. M., Zhang, M., Yi, S., Lenaghan, S. C., and Xia, L. (2012) Inspiration from the natural world: from bio-adhesives to bio-inspired adhesives. *J. Adhes. Sci. Technol.,* **28**(3-4), 290–319.

[69] Lazzari, M. and Chiantore, O. (1999) Drying and oxidative degradation of linseed oil. *Polym. Degrad. Stab.,* **65**(2), 303–313.

[70] Juita, Dlugogorski, B. Z., Kennedy, E. M., and Mackie, J. C. (2012) Low temperature oxidation of linseed oil: a review. *Fire Sci. Rev.,* **1**(1), 3.

[71] McClements, D. J. (2015) Food Emulsions, CRC Press, Boca Raton.

[72] Decoteau, D., Kasperbauer, M., Daniels, D., and Hunt, P. (1988) Plastic mulch color effects on reflected light and tomato plant growth. *Sci. Hortic. (Amsterdam).,* **34**(3-4), 169–175.

[73] Scott, M. J. and Jones, M. N. (2000) The biodegradation of surfactants in the environment. *Biochim. Biophys. Acta - Biomembr.,* **1508**(1-2), 235–251.

[74] Oyman, Z. O., Ming, W., and van der Linde, R. (2003) Oxidation of model compound emulsions for alkyd paints under the influence of cobalt drier. *Prog. Org. Coatings,* **48**(1), 80–91.

[75] Stenberg, C., Svensson, M., and Johansson, M. (2005) A study of the drying of linseed oils with different fatty acid patterns using RTIR-spectroscopy and chemiluminescence (CL). *Ind. Crops Prod.,* **21**(2), 263–272.

[76] Masschelein-Kleiner, L. (1995) Ancient binding media, varnishes and adhesives, ICCROM, Rome.

[77] Friedemann, K., Spangenberg, R., Yoshizawa, K., and Beutel, R. G. (2014) Evolution of attachment structures in the highly diverse Acercaria (Hexapoda). *Cladistics,* **30**(2), 170–201.

[78] Federle, W., Brainerd, E. L., McMahon, T. A., and Hölldobler, B. (2001) Biomechanics of the movable pretarsal adhesive organ in ants and bees. *Proc. Natl. Acad. Sci.,* **98**(11), 6215–6220.

[79] Greimel, K. J., Perz, V., Koren, K., Feola, R., Temel, A., Sohar, C., Herrero Acero, E., Klimant, I., and Guebitz, G. M. (2013) Banning toxic heavy-metal catalysts from paints: Enzymatic cross-linking of alkyd resins. *Green Chem.,* **15**(2), 381–388.

[80] Koschier, E. H. (2008) Essential oil compounds for thrips control - A review. *Nat. Prod. Commun.,* **3**(7), 1171–1182.

[81] Egger, B. and Koschier, E. H. (2014) Behavioural responses of *Frankliniella occidentalis* Pergande larvae to methyl jasmonate and *cis*-jasmone. *J. Pest Sci. (2004).,* **87**(1), 53–59.

Summary

In this thesis, we presented novel, eco-friendlier alternatives to insecticides inspired from plant surfaces for use in buildings and agriculture, namely, paints slippery to *Atta cephalotes* ants and spray emulsions that protect plants against *Frankliniella occidentalis* thrips.

In **Chapter 2**, we first reviewed the issues related to insect pests and to the use of pesticides to control pest populations. Coatings where insect attachment is minimised is thought to be a promising alternative to insecticides and insecticidal paints in the building industry. Understanding the locomotion behaviour of insects (both hairy and smooth pads) on both synthetic and natural surfaces is of importance to formulate such coatings and was hence reviewed. We then discussed some of the most promising state-of-the art coatings which could be used to this end, such as the SLIPS or particle film technologies.

We presented in **Chapter 3** the fabrication of model paints slippery to insects (*A. cephalotes* ants). The paints' slipperiness for *A. cephalotes* ants was evaluated in climbing tests on vertical paint panels by recording the percentage of fallen ants. These paints only contained water, an acrylic polymer binder, TiO_2, $CaCO_3$ and a coalescent. The Pigment Volume Concentration > Critical Pigment Volume Concentration (PVC > CPVC) condition was found to provide good slipperiness to ants as pigment and extender particles detach from the coating to adhere to the tacky attachment pads of insects due to lack of polymer binding the particles. Attachment was minimised when using $CaCO_3$ rather than TiO_2 particles, likely owing to their larger size and platelet shape.

In **Chapter 4**, we studied the particle detachment properties of the paints from **Chapter 3**. To this end, we assessed the feasibility of JKR-type experiments by using polydimethylsiloxane

(PDMS) hemispheres to mimic ants' smooth adhesive pads. We measured the adhesive stress of PDMS after repeated pull-offs of paints on PDMS and the number of contaminating particles present on PDMS resulting from the test. We found that the contamination level increased with load and that even paints formulated at PVC < CPVC presented detachable particles for high loads (> 40 mN). Although the results could not directly be compared to insect climbing tests, this experiment opens the field for future research as an alternative to mechanical analysis AFM for larger probes and could replace the hassle of performing climbing tests experiments.

Chapter 5 extends the work presented in **Chapter 3**. We studied the influence of the polymer binder size and pigment extender ($CaCO_3$) diameter. Large polymer binders (> 250 nm) reduce the coatings' CPVC and lead to more porous coatings. Very slippery surfaces were hence produced, due to a likely synergistic effect between particle detachment and ants' adhesive fluid absorption by the pores. Extender pigments sized between 1 μm and 10 μm impede the insects' self-cleaning mechanism and hence lead to more slippery surfaces in combination with increased porosity and reduced surface roughness. In particular, the slipperiness continuously decreased before the surface roughness average reached the threshold value of $R_a \approx 5$ μm, corresponding to the claw tip diameter of *A. cephalotes* workers.

Chapter 6 describes the formulation of bio-degradable bio-compatible linseed oil-in-water emulsion sprays for use in agriculture. Emphasis was given on the protection of crops against *F. occidentalis* thrips by trapping thrips through adhesion at the surface of leaves. Sticky coatings and crosslinked droplets successfully reduced the damage to *Chrysanthemum baltica* leaves incurred by thrips. This work opens research for novel vegetable oil-based alternatives to pesticides. Further work is needed to improve the appearance and size of the oil droplets once sprayed.

Finally, the general discussion (**Chapter 7**) summarises our findings, preliminary studies and outlines what further research can be done to improve the results discussed in the other sections. Preliminary results discussed the impact on the slipperiness to *A. cephalotes* of binders with varying glass transition temperature and chemistry; as well as pigment extenders of different shapes and chemistries. Overall, the results discussed in this thesis and particularly in **Chapter 7** can be used as a guide to formulators seeking to produce paints slippery to insects.

List of publications

This thesis

Féat, A., Federle W., Kamperman, M. and van der Gucht, J. (2019) Coatings preventing insect adhesion: An overview. *Prog. Org. Coatings*, **134**, 349-359.

Féat, A., Federle W., Kamperman, M., Murray, M. W., van der Gucht, J. and Taylor, P. L. (2019) Slippery paints: eco-friendly coatings that cause ants to slip. *Prog. Org. Coatings*, **135**, 331-344.

Other work

Vleugels, L. F. W., Féat, A., Voets, I. K. and Tuinier R. (2017) Toluidine blue-sodium lauryl ether sulfate complexes: Influence of ethylene oxide length. *Dyes and Pigments*, **141**, 420–427.

Acknowledgements

I have come a long way since September 2016, back when I did not know anything about paints or insects. Without the people who supported me over the past three years, this PhD journey would have been very different. Having worked in three different locations, there are a lot of people that I wish to thank in the following passage. I apologise if did not mention your name!

First of all, my deepest gratitude goes to my supervisors. Phil, you are the epitome of the British gentleman. Thank you for your silly jokes, your guidance, appreciating my independence and also, for making polymers with me to save time! Martin, thank you so much for taking over the job when Phil retired. You have been perfect for the task and have been very supportive during this past year. Walter, I am so grateful for the fruitful discussions and collaborations we have had during this project. It is odd to think that we might not have worked together if we had not decided to first work on insect-repellent paints during our meeting in Patras. Marleen, this work would look very different without your countless advice. Your kind words in Wageningen definitely helped cheer me up in my "down" moments when I did not get good results. I also thank you for thinking about me regarding the work on thrips as this has proven to be a great addition to this thesis. I am very glad you got the professorship in Groningen! Jasper, thank you for your guidance and continuous encouragements. Thank you for believing in me and believing that this work could be done in three years, and for allowing me to do a secondment in Wageningen. I hope that someday I will have the chance to speak French with you!

I am grateful to have been part of the great BioSmart network: Justine, Vaishali, Maria, Francisco, Mehdi, Marco, Victor, Ugo and Dimitris, you are all fantastic scientists, I've enjoyed

working alongside you and I am looking forward to seeing what the future holds for us. The conferences and the weekends spent with you are some of my best PhD memories! Sandra, you have been a great and very diligent coordinator - what I would expect from a German lady! I enjoyed our discussions and hope we can all go hiking around Dresden before the next conference. Alla, you've done a great job as a scientific coordinator. Thinking back to the conference in Paris and you not understanding how we students could not be nervous still makes me smile. I am also grateful to René and Costantino with whom I had helpful discussions. I had a "super", as Matthias would say, time with all other BioSmart supervisors too, and I hope we will meet again for possible collaborations.

Having spent 2.5 years in AkzoNobel, there are many people I wish to thank. I appreciate all of you for making me forget about the dull, detestable Slough. As one would expect, I must thank Paloma first - my cycling, gym going, traveling, political discussion, foodie partner and probably many other things I'm forgetting! At the time I was writing these lines down you were enjoying yourself in Argentina and I hope next time we travel together it will be part of *Race across the world*! Special thanks to my workmates Kate (looking forward to seeing your newborn baby), Meera, Marion, Varthika, Raquel, Bryony (who kindly proofread some chapters) and Decheng (who's also responsible for providing me with a considerable source of enjoyment, my PS4!). You all may not realise how your good mood, jokes and humour helped cheer me up throughout the years. I feel grateful for having shared these moments with you, which kept me motivated. I will certainly miss our conversations and our time outside work.

Next, I would like to thank my current and former teammates, especially the former MatSci team: Fraser, Bogdan, Radek, David and Ron for helpful discussions and welcoming me into the team in my second year. And the polymer team, Simon, Stephen, Dee, Mark I. and Neil are particularly appreciated for their help with technical support, and Neal for the helpful discussions on linseed oil. Lina, Nina, Mark A. (a.k.a. my English dictionary!) and Dorian, though I'm aware I've been very quiet in the past years, it's been a pleasure to have had you as officemates. Dorian, not to worry, I will bring in some cake when I leave!

I am grateful to my informal side microscopy team: Ann, John J. and Suraj. It has been such a pleasure to work with you. I really appreciate how you shared your passion for microscopy with me. Suraj, you did a great job at taking up the position and I am grateful for the mentoring

and advice. In no particular order, I wish to thank John S. for his constant support with data analysis, Francis – keep up the good mood, James (bonjour!). Carol, Raj and Chris, thank you for the efficient financial and admin support, this has been much helpful. Special thanks to Pete for designing the cover, because "3D modelling is easier than Photoshop".

Moving onto my labmates at the (German-dominated) Insect Biomechanics group at the University of Cambridge where I had the chance to spend three months: Marie-Yon, Manase, Simon, Caroline and Tadzio. Thank you all for the warm welcome into the group and for sharing your passion and knowledge of insects and showing me these creatures are not scary but actually fascinating! Caroline (and Victor), thank you for collecting some data on my behalf. Marie-Yon, thanks for helping me out with stick insects and the adhesion force set-up, although I did not use the data in this thesis I appreciated your help. I hope we can meet in South Korea soon, but need to work on my spice threshold in the meantime! My special thanks also go to Andrea, my housemate with whom I've shared many enjoyable moments during these two months together. Thank you for letting me play Zelda and I hope you finish your book soon!

I carried out a 4-month secondment at the Physical Chemistry and Soft Matter group at Wageningen University. There are many people I am indebted to here, notably, Sven and Tom for, in short, their assistance on the adhesion set-up and the linseed oil project. Tom, I feel grateful for your informal supervision while I was at PCC, and your constant help when I returned to Slough. Remco and Diana, thank you for the technical assistance. Ilse, Hanne and Jochem (Jochou), Aljosha (Aljochou), and others I may have forgotten, it's been a pleasure meeting with you. Aljosha, I am so impressed by your French and especially your knowledge of French literature! Thanks to the so-called Cooking Mama group, Lione, Nicolò, Raoul (looking forward to dancing salsa again!), Jessica and Simone for the enjoyable lunchtimes. Xiufeng and Hui, you are the perfect examples of how just a smile can be so motivating and completely change my mood. I would have loved to have joined the PhD trip together with all of PCC again. Mara, thank you for the administrative support. Keep on accumulating nice shoes!

There are also three gentlemen who are worth to be mentioned as I might not have considered doing a PhD without their guidance and advice during my master's degree: Leo Vleugels from DSM, Fabrice Cuoq from SABIC and Huub van Aert from Agfa.

Moving away from my workmates, it is high time I thanked my closest friends. Camille, Julie, Paloma (again) and Robin, many thanks for your motivational support. I really enjoyed our time out together and am looking forward to the next ones. I hope that someday we can reform the Agfamily in Antwerp! Thérèse, it's been great meeting up again in Germany and I'm sure that someday, we can all meet up with peeps from Rennes! Boris and Michelle, my great housemates, thanks for all the moments together. I'm sorry I couldn't make it to Bulgaria to see you running the marathon, but I'm confident we'll be able to spend some time in Plovdiv someday.

Enfin, j'aimerais terminer ces remerciements avec ma famille (déb. . .). La qualité de mon Français à l'écrit ayant fort baissé ces dernières années, j'ai bien peur de ne pas trouver les bonnes tournures. Merci pour les messages presque quotidiens, même insignifiants, qui m'ont motivée ou fait rire, notamment aux Pays-Bas où j'en avais bien besoin ! Désolée de ne pas être venue très souvent, transports oblige, mais j'espère me rattraper là où le futur m'attend. J'ai aussi hâte de rencontrer mes futurs neveux/nièces !

About the author

Aurélie Féat was born on 21/03/1993 in Mont-Saint-Aignan, France. She obtained her master's degree in formulation chemistry (*diplôme d'ingénieur*) from the National Graduate School of Chemistry of Rennes, a French *grande école* in 2016. She did three internships as part of her studies: two months at Brock University (Canada) in 2014, four months at DSM (The Netherlands) in 2015 and six months at Agfa (Belgium) in 2016. She started her PhD in 2016 as an Early Stage Researcher in the European project BioSmart Trainee. She carried out her research in three laboratories: AkzoNobel Decorative Paints (United Kingdom), the group of insect biomechanics at the University of Cambridge (United Kingdom) and in the Physical Chemistry and Soft Matter department at Wageningen University (The Netherlands). During these three years, she was supervised by Phil Taylor, Martin Murray, Walter Federle, Marleen Kamperman and Jasper van der Gucht. This thesis presents the most important results of this research project.

Overview of completed training activities

General activities

BioSmart Trainee training school 1†	Patras, Greece	2016
Adhesion science	Patras, Greece	2016
Polymer synthesis	Slough, UK	2016
Paint formulation	Slough, UK	2016
BioSmart Trainee training school 2†	Dresden, Germany	2017
BioSmart Trainee training school 3†	Paris, France	2017
Han-sur-Lesse Winter School	Han-sur-Lesse, Belgium	2018
ChemCys - Chemistry Conference for Young Scientists*	Blankerberge, Belgium	2018
BioSmart Trainee training school 4†	Ludwigshafen, Germany	2018
International Association of Colloid and Interface Scientists*	Rotterdam, The Netherlands	2018
European Technical Coatings Congress*	Amsterdam, The Netherlands	2018
International Symposium on Polyelectrolytes	Wageningen, The Netherlands	2018
BioSmart UK Joint Event†	Cambridge, UK	2019
Coatings Science International Conference†	Noordwijk, The Netherlands	2019
Adhesion in Aqueous Media: From Biology to Synthetic Materials†	Dresden, Germany	2019

† Oral presentation, * Poster presentation

General courses

Scientific writing	Dresden, Germany	2017
Making a good presentation	Dresden, Germany	2017
Patenting and Licensing	Dresden, Germany	2017
Excel course	Slough, UK	2017
Starting your own company	Paris, France	2017
Fundamentals about IP protection	Paris, France	2017
Introduction to funding in academia	Paris, France	2017
Innovation management and market needs	Ludwigshafen, Germany	2018
Diversity & Inclusion	Ludwigshafen, Germany	2018
Career assessment	Wageningen, The Netherlands	2018
Competence Assessment	Wageningen, The Netherlands	2018
Brain training	Wageningen, The Netherlands	2018
Research Data Management	Wageningen, The Netherlands	2018

Optional

Group meetings	UK/Netherlands	2016-2019
Seminars	UK/Netherlands	2016-2019
Research proposal	Wageningen, The Netherlands	2017